

**Cellular and Molecular Mechanisms regulating Cell Proliferation
during the Forebrain Development of the Mouse**

Dissertation

Zur Erlangung des Doktorgrades
der Naturwissenschaften (Dr. rer. nat.)
der Fakultät für Biologie
der Ludwig-Maximilians Universität München

Angefertigt am Max-Planck-Institut für Neurobiologie
in der Arbeitsgruppe Neuronale Spezifizierung
und an der GSF
im Institut für Stammzellforschung

Nicole Haubst
München, im Juli 2005

1. Gutachter: Prof. Dr. Magdalena Götz
2. Gutachter: Prof. Dr. Charles N. David

eingereicht am 07.07.2005

Tag der mündlichen Prüfung: 13.10.2005

1 Table of content

1	Table of content	2
2	Abstract	6
3	Zusammenfassung	7
4	Introduction	9
4.1	CNS development	9
4.2	Patterning and regionalisation	10
4.3	The transcription factor Pax6	11
4.3.1	DNA binding domains	11
4.3.1.1	The paired domain	11
4.3.1.2	The paired-type homeodomain	12
4.3.2	Pax6 expression	13
4.3.3	The role of Pax6 in the boundary formation and regionalisation	13
4.3.4	The role of Pax6 in the regulation of neurogenesis	14
4.3.5	Pax6 and cell proliferation	15
4.4	Neuroepithelial features	15
4.4.1	Interkinetic nuclear migration	15
4.4.2	Proliferative zones in the developing telencephalon	16
4.4.3	Mode of cell division	17
4.4.4	Radial glia cells	17
4.4.5	Cell polarity	18
5	Abbreviations	21
6	Material and Methods	23
6.1	Animals	23
6.2	Genotyping of transgenic mice	23
6.2.1	Genotyping of perlecan ^{-/-} mice	24
6.3	Histology	24
6.3.1	BrdU Labelling in vivo	24
6.3.2	Cryosections	25
6.3.3	Vibratome sections	25
6.4	Tissue culture	25
6.4.1	Viral infection of cortical cell cultures	26
6.5	Immunohistochemistry	26
6.5.1	Primary and secondary antibodies	26
6.5.1.1	Table Primary antibodies	27

6.5.1.2	Table Secondary antibodies	29
6.5.2	Visualisation of cell nuclei	30
6.6	Retrovirus preparation	30
6.6.1	Cloning strategy of generated Pax6 viruses	30
6.6.1.1	PD-less Pax6 virus	30
6.6.1.2	Cloning of a virus with point mutation in HelixIII of HD at nucleotide position 776 (PM776 virus).....	31
6.6.2	Ligation	31
6.6.3	Transformation	31
6.6.4	Mini-PCR screening	32
6.6.5	GPG Retrovirus preparation	32
6.6.6	Pax6 and Pax6(5a) retrovirus preparation	33
6.7	In situ hybridization	34
6.7.1	Plasmid linearization	34
6.7.2	In vitro transcription	34
6.7.3	In situ hybridization	35
6.8	In vitro electroporation of mouse embryonic brains	35
6.8.1	RNA extraction	36
6.9	RT-PCR.....	36
6.9.1	Sample preparation for RT-PCR.....	36
6.9.2	cDNA synthesis.....	37
6.9.3	RT-PCR.....	37
6.10	Quantification of neurons and proliferating cells.....	39
6.11	Statistics	39
6.12	Material	41
6.12.1	Microscopy	41
6.12.2	Complex media, buffers and solutions	42
6.12.3	Product list.....	46
6.12.4	Consumables	49
6.12.5	Instruments	50
7	Results	52
7.1	The influence of BM contact on radial glia cell fate and proliferation	52
7.1.1	Neurogenesis in the absence of basal cell attachment/polarity	52
7.1.2	Proliferation in the absence of basal cell attachment/polarity:	53
7.1.2.1	Ectopic cell clusters.....	53
7.1.2.2	Reelin signalling.....	54

7.1.2.3	Interkinetic nuclear migration in absence of radial glia endfeet attachment	54
7.1.2.4	Orientation of cell division in the absence of basal radial glia cell attachment	55
7.2	The influence of the distinct Pax6 DNA-binding domains on cell fate, proliferation and patterning in the telencephalon	56
7.2.1	The role of the different Pax6 DNA-binding domains in the regulation of neurogenesis	57
7.2.1.1	The generation of upper layer neurons in the different Pax6 mutant alleles: Tbr2 and Svet1 expression	57
7.2.2	The role of the different Pax6 DNA-binding domains in the regulation of cell proliferation	58
7.2.2.1	Interkinetic nuclear migration	59
7.2.3	The role of the different Pax6 DNA binding domains in telencephalic patterning	60
7.2.4	Role of the Pax6(5a) isoform in vivo	61
7.2.4.1	Relative expression levels of Pax6(5a), canonical Pax6 and PD-less Pax6	62
7.2.4.2	Neurogenesis and cell proliferation in Pax6(5a) ^{-/-} during development	62
7.2.4.3	Radial glia morphology and changes in gliogenesis in the Pax6(5a) ^{-/-}	63
7.3	The role of the different Pax6 DNA binding domains in patterning of the diencephalon	64
7.4	The role of the different Pax6 DNA-binding domains in eye development	64
7.4.1	The influence of the different Pax6 DNA-binding domains on neurogenesis in the eye	65
7.4.2	The role of the different Pax6 DNA-binding domains in the regulation of cell proliferation in the eye	66
7.4.2.1	Interkinetic nuclear migration in the eye	66
7.4.3	The influence of the Pax6 DNA binding domains on regionalisation -boundary formation between the optic stalk and the neuroretina	67
7.5	The role of the PD and PD5a in regard to cell proliferation and differentiation	68
7.6	The effect of Pax6 overexpression on proliferation and cell cycle length	69
7.7	Loss of functional Pax6 and the effect on cell proliferation in vitro	71
7.8	Loss of a functional PD and the effect on neurogenesis in vitro	71
7.9	Determination of the apoptosis rate in retrovirus infected cell cultures	72
7.10	Construction of Pax6 retroviral vectors	72
7.10.1.1	PD-less Pax6 virus	72
7.10.1.2	Pax6 containing a mutation in the HD (PM776)	73
7.11	Approach for the analysis of Pax6 target genes	73
8	Figures and Tables	74

9	Discussion.....	139
9.1	The role of Pax6 in the regulation of cell proliferation in the cerebral cortex	140
9.2	The role of Pax6 in the regulation of neurogenesis.....	143
9.3	The influence of the different Pax6 DNA-binding domains on the regionalisation of the telencephalon.....	145
9.4	The role of the PD5a in the developing telencephalon	146
9.5	The different DNA-binding domains of Pax6 act region-specifically in the developing telencephalon and the eye.....	147
9.6	Other mechanisms that could explain the region-specific differences of Pax6 functions.....	148
9.7	The influence of the basal cell attachment on neurogenesis and cell proliferation	150
9.8	Neurogenesis in absence of basement membrane attachment	151
9.9	Basement membrane attachment of radial glia processes and cell proliferation ...	151
10	References	155
11	Thanks and acknowledgements	164
12	Curriculum vitae	165

2 Abstract

The predominant precursor cell type during cortical neurogenesis are radial glia cells, which receive extrinsic and intrinsic signals that might influence cell proliferation and neurogenesis. These radial glia cells have direct contact to the growth factor rich basement membrane throughout cell division. However, it is not known, how the signals received from the basal cell attachment influence the behavior of radial glia cells in regard to the regulation of cell proliferation and neurogenesis. Therefore, I examined the laminin γ 1 (LN γ 1) mutant, lacking the contact of radial glial endfeet to the basement membrane, and the α 6 integrin $^{-/-}$ with a disturbed assembly of the basement membrane. The analysis of the LN γ 1 mutant and the α 6 integrin $^{-/-}$, showed no defects in the radial glia progeny, cell proliferation or their orientation of cell division. Thus, these results strongly suggest that the direct contact of radial glia cells to the basement membrane is not required for these aspects. Radial glia cells of the dorsal telencephalon are also known to be specified by the expression of the transcription factor Pax6, which plays a pivotal role in the regulation of cell proliferation, neurogenesis and regionalisation during development of the telencephalon. In order to understand how Pax6 coordinates these diverse functions at the molecular level, the roles of the different DNA-binding domains of Pax6, the paired domain (PD), the splice variant of the paired domain (PD5a) and the homeodomain (HD) were analyzed in loss- and gain-of-function approaches. The analysis of the specific paired domain mutant Pax6^{Aey18} $^{-/-}$, that lacks large parts of the paired domain, but contains an intact homeodomain and transactivating domain (TAD), showed that the paired domain is required for the regulation of neurogenesis, cell proliferation and regionalisation in the developing telencephalon and eye. The homeodomain plays only a minor role during telencephalic development, in contrast to its function in the eye, as shown by the analysis of Pax6^{4Neu} $^{-/-}$ mice, which have a point mutation in the DNA-binding domain of the homeodomain, while paired domain and transactivating domain are still functional. Moreover retrovirus-mediated overexpression of Pax6 and Pax6(5a) in cortical cells showed that splicing of the paired domain regulates between a Pax6 form that affects neurogenesis, and cell proliferation, while the other Pax6 form, containing exon5a, regulates exclusively cell proliferation.

3 Zusammenfassung

Die Mehrzahl der proliferierenden Zellen während der Neurogenese im zerebralen Cortex am Embryonaltag 14 (E14) sind radiale Gliazellen, aus denen in asymmetrischer Zellteilung Neurone hervorgehen. Die Zellproliferation und Zelldifferenzierung können einerseits durch extrinsische Faktoren, wie zum Beispiel Wachstumsfaktoren, und andererseits durch zell-intrinsische Faktoren, wie beispielsweise Transkriptionsfaktoren reguliert werden. Während der Zellteilung haben radiale Gliazellen des dorsalen Telencephalons direkten Kontakt zur Basalmembran. Die Basalmembran enthält eine Vielzahl von Faktoren, die möglicherweise das Zellteilungs- und Differenzierungsverhalten der radialen Gliazellen beeinflussen könnten. Bisher war unklar, inwiefern der direkte Kontakt zwischen den Endfüßchen der radialen Gliazellen und der Basalmembran einen Einfluß auf Zellteilung und Differenzierung hat. Deshalb wurde in dieser Arbeit anhand von zwei verschiedenen Mausmutanten dieser Einfluß untersucht. Die Laminin γ 1 Mutante (LN γ 1) zeichnet sich durch den Verlust des Kontaktes zwischen den Endfüßchen der radialen Gliazellen und der Basalmembran aus, während bei der α 6 Integrin $^{-/-}$ die Basalmembran-Zusammenlagerung gestört ist. Die Analyse dieser Mutanten zeigte, daß der Verlust des direkten Kontaktes zwischen radialen Gliazellen und der Basalmembran keinen Einfluß auf die Zellproliferation und -differenzierung hat.

Ein weiteres Charakteristikum der radialen Gliazellen des dorsalen Telencephalons ist die Expression des Transkriptionsfaktors Pax6, der eine zentrale Rolle in der Regulation der Zellproliferation, Neurogenese und Regionalisierung während der Entwicklung des Telencephalons spielt. Um zu verstehen, wie Pax6 diese verschiedenen Funktionen auf molekularer Ebene koordiniert, wurde die Rolle der verschiedenen Pax6 DNA Bindedomänen, d.h. der Pairedomäne (PD), der alternativen Spleißvariante der Pairedomäne (PD5a) und der Homeodomäne (HD), in Funktionsverlust- und Funktionsgewinnanalysen untersucht. Die Analyse der Pax6^{Aey18} $^{-/-}$ Mutante, die eine große Deletion in der PD aufweist, während Homeodomäne und Transaktivierungsdomäne noch intakt sind, zeigte die zentrale Rolle der Pairedomäne für die Regulation der Zellproliferation, Neurogenese und Regionalisierung während der Telencephalon- und Augenentwicklung auf. Im Gegensatz dazu spielt die Homeodomäne nur eine untergeordnete Rolle während der Entwicklung des Telencephalons, ist aber wichtig für die Regulation von Neurogenese, Zellproliferation und Regionalisierung während der Augenentwicklung. Dies zeigte sich in der Analyse der Pax6^{4Neu} $^{-/-}$ Mutante, deren HD keine DNA-Bindung mehr eingehen kann, während PD und TAD noch intakt sind. Außerdem konnte mittels retroviraler

Überexpression von Pax6 und Pax6(5a) in corticalen Zellen gezeigt werden, daß durch unterschiedliches Spleißen der Paired-Domäne einerseits eine Pax6 Form entsteht, die sowohl Neurogenese als auch Zellproliferation regulieren kann (kanonisches Pax6), während die alternative Spleißvariante (Pax6(5a)) ausschließlich Zellproliferation reguliert.

4 Introduction

In the developing embryo, cell proliferation is required, but it has to be well in balance with cell differentiation and regulated in time and region specific manner. Precursor cells in the central nervous system have to be specified correctly in order to acquire their neuronal identity and subtype differentiation. A first step for cell specification is the regionalisation of the brain, meaning that transcription factors are expressed in region specific patterns (Lumsden and Krumlauf, 1996; Tanabe and Jessell, 1996). One important region-specific expressed transcription factor is Pax6 (Stoykova and Gruss, 1994; Stoykova et al., 1996; Walther and Gruss, 1991). This gene is involved in the regulation of cell proliferation, neurogenesis and regionalisation. However, not only transcription factors influence these key developmental processes but also extrinsic cues, as for example growth factors, which are enriched in the basement membrane that covers the outer surface of the brain, also play an important role in the regulation of cell proliferation and differentiation.

In this thesis I studied the influence of the basement membrane in the regulation of cell proliferation and neurogenesis in the developing telencephalon, as well as the role the transcription factor Pax6 in the regulation of cell proliferation, neurogenesis and regionalisation of the developing forebrain.

4.1 CNS development

Very briefly, the mammalian central nervous system (CNS) originates from the neural plate, a portion of the dorsal ectoderm, induced by mesodermal signalling. First the neural plate proliferates and invaginates, leading to the formation of edges that finally fuse and thereby lead to the generation of the neural tube which segregates then from the surface (Fig. 1). Medial regions of the neural plate stage are now located ventrally and give rise to a ventral signalling center that secretes ventralising signals as sonic hedgehog (Shh) which then induce or regulate the expression of ventrally expressed transcription factors as Mash1, Dlx-genes, Nkx-genes (Lumsden and Krumlauf, 1996; Tanabe and Jessell, 1996). Lateral regions are now located dorsally and give rise to the dorsally located signalling centers of the roof plate which are secreting for example the bone morphogenic proteins (BMPs) (Tanabe and Jessell, 1996) fibroblast growth factors (Fgfs) (Bottcher and Niehrs, 2005; Dono, 2003; Ford-Perriss et al.,

2001) and wingless-int proteins (Wnts) (Cadigan and Nusse, 1997; Nelson and Nusse, 2004) that have been suggested to play a role in the regulation of gene expression and proliferation. The neural plate contains three types of cells: (i) Cells located in the inner area give rise to the brain and spinal cord, (ii) cells positioned externally will give rise to the neural crest cells and (iii) to the epidermis of the skin (see Fig. 1a). The formation of the neural tube occurs in an anterior to posterior gradient. Even before the posterior neural tube is completely closed, the formation of three primary vesicles (prosencephalon, mesencephalon and rhombencephalon) occurs anteriorly (Fig. 2). By the time of neural tube closure at the posterior regions, the optic vesicles have extended laterally from each side of the developing forebrain. The prosencephalon gives rise to the most anterior telencephalon and the more caudal situated diencephalon. The telencephalon forms two cerebral hemispheres which are separated by midline structures and subdivided into the dorsal cerebral cortex (ctx) and the ventral ganglionic eminences (GE). The GE are themselves subdivided into the lateral ganglionic eminence (LGE) and medial ganglionic eminence (MGE) (see Fig. 3B). The diencephalon forms dorsally thalamic and ventrally hypothalamic brain regions. It receives input from the retina, which is a derivative of the diencephalon.

4.2 Patterning and regionalisation

The development of the CNS along the anterior/posterior (A/P) and the dorso/ventral (D/V) axis is controlled by organizing signals, which are secreted molecules of the Bone morphogenetic protein (BMP), Sonic hedgehog (Shh), Fibroblast growth factor (Fgf) and Wingless-Int protein families (Jessell, 2000; Lumsden and Krumlauf, 1996; Rubenstein et al., 1998). The secretion of the signalling molecules occurs in a strict spatio-temporal pattern, assuring the proper development and specification of the different brain regions. Signalling from these organizing centers induces a specific expression pattern of different transcription factors, specifying certain regions of the brain or certain cell populations. Characteristic transcription factors expressed in the developing dorsal telencephalon are for example Pax6 which is expressed in a lateral-rostral^{high} and caudal-medial^{low} gradient (Fig. 3B), Neurogenin2, a direct downstream target gene of Pax6 (Scardigli et al., 2003) or Emx1/2 which are expressed in a lateral-rostral^{low} and caudal-medial^{high} gradient opposing to the gradient of Pax6 expression (Bishop et al., 2000; 2002; Muzio et al., 2002; 2003). In the ventral telencephalon, beside others, the basic helix-loop-helix proteins Mash1 and Olig2 and

the homeobox containing transcription factor Gsh2 are expressed (Fig. 8) (Guillemot et al., 1993; Sommer et al., 1996; Toresson et al., 2000; Zhou et al., 2000). Pax6 was shown to play a particularly crucial role in a variety of aspects in forebrain development such as in the regulation of cell proliferation, cell fate decisions and patterning (Estivill-Torrus et al., 2002; Götz et al., 1998; Grindley et al., 1997; Heins et al., 2002; Stoykova et al., 1996; Torresson et al., 2001; Warren and Price, 1997; Yun et al., 2000). However, it was not clear yet, how the regulation of these multiple functions is coordinated at the molecular level, thus the role of the different Pax6 DNA-binding domains (see below) in these key developmental aspects were analyzed in this work.

4.3 The transcription factor Pax6

4.3.1 DNA binding domains

4.3.1.1 The paired domain

Pax6 contains two DNA binding domains, the paired domain (PD) (128 amino acids (AA)) connected via a glycine rich linker region to a paired-type homodomain (HD) (60 AA), followed by a prolin-serine-thronine rich (PST-rich) transactivating domain (TAD) (Fig. 9A; for review see: Bouchard et al., 2003). The PD of Pax6 is a bipartite DNA binding domain consisting of the N-terminal 'PAI' and the C-terminal 'RED' ('PAI-RED') (Fig. 9C) (Czerny et al., 1993; Epstein et al., 1994a; Epstein et al., 1994b; Jun and Desplan, 1996; Xu et al., 1999) and both domains, PAI and RED, bind to specific DNA-binding sites. The N-terminal PAI subdomain is critical for DNA binding to Pax6 consensus sites (P6CON; 5'-ANNTTCAGCa/tTc/gANTt/ga/cAt/c-3'; Epstein et al., 1994a), while the C-terminal RED contributes to DNA binding by contacting adjacent nucleotides (Epstein et al., 1994b) (Fig. 9C).

Upon alternative splicing 14 AA (exon5a) are inserted in the N-terminal PAI domain (Fig. 9A) (Walther et al., 1991) and thus DNA binding of the PAI domain is abolished and occurs via the RED domain (Fig. 9C) (Epstein et al., 1994b). This alternative splice form of Pax6, containing exon5a, is termed Pax6(5a) in contrast to the canonical Pax6, which lacks exon5a. Pax6(5a) binds specifically to the Pax6(5a) consensus site 5aCON (5aCON: 5'-ATGCTCAGTGA|ATGTTCATTGA-3', Epstein et al., 1994b). However, the canonical Pax6 form is also able to bind to the 5aCON site and activate transcription in vitro (Epstein et al.,

1994b), while Pax6(5a) is not able to bind to P6CON sites. The Pax6(5a) form plays an important role in the eye (Azuma et al., 1996; Azuma et al., 2005; Singh et al., 2002) of vertebrates and interestingly the same modification of PD DNA-binding was recently discovered in the developing compound eye of *Drosophila* (Dominguez et al., 2004). Due to gene duplication during evolution in *Drosophila* two homologs of the canonical Pax6 form, eyeless (*ey*) (Quiring et al., 1994) and its paralog twin of eyeless (*toy*), exist (Czerny et al., 1999). The *Drosophila* homologs of the murine Pax6(5a) isoform are the two paralogs eyegone (*eyg*) and twin of eyegone (*toe*) (Jang et al., 2003; Jun et al., 1998). *Eyg* and *toe* are lacking the N-terminal part of the PD and are able to bind to 5aCON sites (Jun et al., 1998). The ratio between the canonical Pax6 and Pax6(5a) seems to be critical during eye development (Chauhan et al., 2004).

Further Pax6 isoforms lacking the PD (PD-less) have been found in mouse brain (Mishra et al., 2002), in the quail neuroretina (Carriere et al., 1993) and in *C. elegans* (Zhang and Emmons, 1995). The murine PD-less Pax6 form is generated by alternative splicing and is present in brain, eye and pancreas (Mishra et al., 2002). Intron 7 harbours a CpG island which can act as transcription initiation site for a transcript comparable to the PD-less Pax6 isolated from quail neuroretina (Kleinjan et al., 2004; Carriere et al., 1993) or to the truncated Pax6 form in *C. elegans* (Zhang and Emmons, 1995). The PD-less form binds to HD P2 consensus site but is not able to activate transcription *in vitro* (Mishra et al., 2002). Thus, transcriptional activation might depend on both DNA-binding domains, PD and HD. Interaction of the PD-less form with the full length Pax6 lead to an enhancement of transcription *in vitro* (Mikkola et al., 2001).

4.3.1.2 The paired-type homeodomain

The paired-type HD of Pax6 is similar to other HDs with a globular domain consisting of 3 α helices (60 AA). The critical AA residue for DNA binding is a serine located in helix3 at position 50 (position 9 in helix 3). Changes in this AA can abolish DNA-binding (Favor et al., 2001; Hanes and Brent, 1989; Percival-Smith et al., 1990; Schier and Gehring, 1992; Treisman et al., 1989). The HD of Pax6 binds preferentially to P3 consensus sites (5'-TAAT(N)₃ATTA-3') (Czerny and Busslinger, 1995; Wilson et al., 1993). Loss of HD DNA-binding leads to defects in eye formation (Favor et al., 2001) and further, the HD is involved in the regulation of rhodopsins (Kozmik et al., 2003).

4.3.2 Pax6 expression

Pax6 expression in the mouse embryo starts at E8 in the anterior surface ectoderm and in the neuroepithelium of the presumptive spinal cord, hindbrain and forebrain, before telencephalon and diencephalon develop (Stoykova and Gruss, 1994; Walther et al., 1991). In the developing forebrain Pax6 expression becomes restricted to the VZ cells of the dorsal telencephalon (Fig. 3B, Fig. 8B), where it persists during neurogenesis, and certain regions of the diencephalon (Grindley et al., 1995; Mastick et al., 1997; Stoykova et al., 1996; Stoykova and Gruss, 1994; Walther et al., 1991; Warren and Price, 1997) (Fig. 3A). No Pax6 expression has been detected in the second proliferative population of the telencephalon, the subventricular zone (SVZ) cells (Englund et al., 2005; Götz et al., 1998), which are located above the VZ (Smart, 1976). The Pax6 expression extends to the dorsal lateral ganglionic eminence (dLGE), whereas in the ventral telencephalon almost no Pax6 expression is detectable, except in a small stripe in the cells along the pallial-subpallial boundary (PSB) (Stoykova et al., 1996; Stoykova and Gruss, 1994), which mainly separates the dorsal from the ventral telencephalon (Fig. 3B).

4.3.3 The role of Pax6 in the boundary formation and regionalisation

Loss of Pax6 function has been extensively studied in the *Small eye* mice ($Pax6^{Sey-/-}$), a mouse strain characterized by the natural occurrence of a point mutation leading to a stop-codon prior to the HD and thus to a truncated protein lacking the homeodomain and the transactivating domain (TAD) (Hill et al., 1991). In $Pax6^{Sey-/-}$ mice the PSB is severely disrupted (Stoykova et al., 1997) and a strong increase in cell migration between the GE and the cerebral cortex has been detected (Chapouton et al., 1999). Loss of functional Pax6 leads to the loss of the border specific expression of SFRP-2, Nrg1, Tgfa and Wnt-7b in the $Pax6^{Sey-/-}$ mice (Assimacopoulos et al., 2003; Kim et al., 2001). As described above, Pax6 expression is restricted to the dorsal telencephalon and thus misspecification due to changes in patterning occurs in the $Pax6^{Sey-/-}$ mutant telencephalon such that ventral transcription factors expand dorsally (Heins et al., 2002; Stoykova et al., 1996; Stoykova et al., 1997; Stoykova and Gruss, 1994; Toresson et al., 2000; Yun et al., 2001) and the expression of Ngn2 (Scardigli et al., 2003) is lost in the regions of Pax6 expression (Stoykova et al., 2000; Toresson et al., 2000; Yun et al., 2001).

Not only the specification of dorsal versus ventral regions in the telencephalon depends on Pax6, but also arealisation of the cerebral cortex (Bishop et al., 2002; Muzio et al., 2002; 2003). Pax6 expression in the dorsal telencephalon occurs as mentioned above in a gradient (rostral^{high}-caudal^{low}, lateral^{high}-medial^{low}) opposed to the expression of Emx1 and Emx2. Loss of functional Pax6 leads to the expansion of Emx2 and in turn to the anterior expansion of the primary visual area, while loss of functional Emx2 leads to the caudal expansion of Pax6 and the domains containing somatosensory neurons and motor neurons expand (Bishop et al., 2002; Muzio et al., 2002; Muzio and Mallamaci, 2003).

Changes in regionalisation due to loss of functional Pax6 have also been observed in other regions of the CNS, as in the ventral diencephalon, hindbrain and spinal cord (Briscoe et al., 1999; Grindley et al., 1997; Osumi, 2001; Stoykova et al., 1996).

4.3.4 The role of Pax6 in the regulation of neurogenesis

Loss- and gain of function studies showed that Pax6 is involved in the regulation of neurogenesis in the developing forebrain. In the dorsal telencephalon of Pax6^{Sev}-/- mice neurogenesis is strongly impaired (Heins et al., 2002; Schmahl et al., 1993), whereas no alterations have been detected in the ventral telencephalon. In the diencephalon and spinal cord, subpopulations of neurons are lacking (Ericson et al., 1997; Mastick and Andrews, 2001) and during embryonic eye development leads the loss of functional Pax6 protein to precocious neurogenesis followed by massive cell death (Philips et al., 2005). At midneurogenesis the vast majority (80%) of the VZ precursor cells in the dorsal telencephalon are radial glia cells (Hartfuss et al., 2001) which express Pax6 (Götz et al., 1998). Loss of functional Pax6 protein in the Pax6^{Sev}-/- mice leads to a decrease in the neurogenic potential of the VZ cells (Heins et al., 2002), whereas the SVZ cells (Haubensak et al., 2004; Miyata et al., 2004; Noctor et al., 2004) seem less affected in that regard. Retrovirally mediated overexpression of Pax6 showed the strong neurogenic potential in astrocyte cultures in vitro (Heins et al., 2002).

In the adult brain, Pax6 expression in the dentate gyrus has been associated with the generation of neurons after ischemia (Nakatomi et al., 2002) and loss- and gain-of-function approaches in cells of the adult SVZ showed that Pax6 is necessary and sufficient for adult neurogenesis in the olfactory bulb, in addition Pax6 is required for neuronal subtype specification, i.e. the generation of tyrosine hydroxylase positive (TH+) neurons in the adult olfactory bulb (Hack et al., 2005).

4.3.5 Pax6 and cell proliferation

Besides its potent role in the regulation of neurogenesis Pax6 is also involved in the regulation of proliferation. Increased cell proliferation has been described in the dorsal telencephalon of the functional null allele *Pax6^{Sey}* (Estivill-Torrus et al., 2002; Götz et al., 1998).

Also other Pax6 expressing regions of the CNS exhibit changes in cell proliferation due to the loss of functional Pax6 protein, as it is the case in the diencephalon (Warren and Price, 1997), the developing eye (Marquardt et al., 2001) and in the cerebellum (Engelkamp et al., 1999). The role of Pax6 in the regulation of cell proliferation seems to be region specific, since loss of functional Pax6 in the telencephalon leads to an increase in cell proliferation (Estivill-Torrus et al., 2002; Götz et al., 1998), whereas it leads to a decreased cell proliferation in the diencephalon (Warren and Price, 1997). In the developing eye, Pax6 regulates positively cell proliferation, since the loss of Pax6 decreases the number of cells generated (Marquardt et al., 2001). In the cerebellum no changes in cell proliferation have been detected in the *Pax6^{Sey}* mice (Engelkamp et al., 1999).

As described above, Pax6 is involved in the regulation of many developmental processes, as the regulation of cell proliferation, neurogenesis and regionalisation. Interestingly, Pax6 seems to act region-specific on cell proliferation, since it promotes cell proliferation in the developing eye, while it rather suppresses cell proliferation in the developing telencephalon. Pax6 contains different DNA binding domains (PD, PD5a, HD). In order to understand how Pax6 coordinates the regulation of these multiple functions at the molecular level, the role of the different DNA-binding domains (PD, PD5a, HD) has been analyzed in loss- and gain-of-function approaches in different regions of the brain.

4.4 Neuroepithelial features

4.4.1 Interkinetic nuclear migration

As described above, the telencephalon initially develops from the neural tube which consists of a single layer of proliferating neuroepithelial cells, forming a pseudostratified epithelium. Neuroepithelial cells undergo interkinetic nuclear migration (Sauer, 1935). This term describes the intracellular translocation of the nucleus, while the proliferating cell progresses through the different cell cycle phases (Sauer, 1935; Takahashi et al., 1995) (Fig. 4). Cells progressing through M-phase are localized at the apical ventricular surface (VS). After the termination of cell division, the nuclei migrate during G1-phase outwards to reach the basal most

proliferative zone during S-phase, from where they migrate again in G2-phase towards the apical ventricular surface (VS), where the next cell division takes place. Thus, the pseudostratification of the neuroepithelium results from the movement of the nuclei along the apical-basal axis of the epithelium.

In this thesis I analyzed different mouse mutants in order to identify factors that might act as regulators of the interkinetic nuclear migration as part of the proliferative behaviour of cells in the telencephalon.

4.4.2 Proliferative zones in the developing telencephalon

Together with the beginning of neurogenesis at E11/12, the pseudostratified character of the neuroepithelium and also some epithelial features are lost (Aaku-Saraste et al., 1996). Instead, stratification/layering starts. The proliferating cells located at the apical side of the cerebral cortex, adjacent to the lateral ventricle, are termed ventricular zone (VZ) cells, the second proliferative cell population, the subventricular zone (SVZ) cells, originates from the VZ and starts to develop above the VZ (Noctor et al., 2004; Smart, 1976 and this work) at E12. As development proceeds, the VZ cells lose more and more their neuroepithelial character and achieve more glial properties. The transformation from neuroepithelial cells into radial glia cells is reflected by the appearance of astroglial markers, as for example BLBP (brain lipid-binding protein; Feng et al., 1994; Kurtz et al., 1994), RC2 (radial cell 2; Misson et al., 1988), GLAST (glutamate astrocyte specific transporter; Storck et al., 1992) and the appearance of glycogen granules (present E14 but not yet at E12). Radial glia cells are characterized by a long radial process extending towards the pial surface and attaching via their endfeet to the basement membrane (Brittis et al., 1995; Marin and Rubenstein, 2003; Miyata et al., 2001; Nadarajah et al., 2001). The vast majority (80%) of cells present in the VZ at midneurogenesis are radial glia cells (Hartfuss et al., 2001). VZ cells still undergo interkinetic nuclear migration, which means that they divide at the apical surface, but in contrast to the early neuroepithelial cells the translocation of the nucleus remains restricted to the VZ and does not occur all over the cell soma, which would include the entire cerebral wall since they extend their processes to the pial surface (for review see: Götz and Huttner, 2005). So far, it has not been described that SVZ cells undergo interkinetic nuclear migration, thus one important characteristic feature of SVZ cells is that they undergo mitosis at non-surface positions.

4.4.3 Mode of cell division

Two different types of cell divisions occur in the developing CNS. Prior to neurogenesis cells divide predominantly symmetrically and give rise to two identical daughter cells (two proliferating precursor cells). Thus the pool of precursor cells increases (Fig. 7A). Symmetric cell division is associated with the lateral expansion of the tissue and is thus correlated with the expansion of the areas in the developing cortex. At midneurogenesis symmetric cell divisions can also give rise to two postmitotic neurons (Shen et al., 2002), as it has been described for SVZ cells (abventricular cell divisions) (Noctor et al., 2004). Asymmetric cell divisions give rise to two different daughter cells, for example one precursor cell and one postmitotic neuron (Fig. 7A). The asymmetric mode of cell division leads to the radial expansion of the cortex. As mentioned above VZ precursor cells divide at the ventricular surface (VS). Different cleavage planes have been observed in cells dividing at the ventricular surface (VS) (Fig. 7B). The cleavage plane occurred either along the apical-basal axis perpendicular with respect to the VS, or parallel to the VS or in an oblique manner (Fig. 7C). On account of the apico-basal polarity of neuroepithelial/radial glia cells it has been proposed that the cleavage plane of a cell division and thus the asymmetric or symmetric distribution of cellular components is associated with cell fate (Huttner and Brand, 1997). Based on previous time lapse studies in ferret it has been proposed that a cell division with a plane perpendicular with respect to the ventricular surface (VS) is a symmetric cell division giving rise to two identical precursor cells, whereas a cell division with a horizontal plane with respect to the VS has been considered to be an asymmetric cell division. The apical daughter cell remained in the proliferative zone, whereas the basal daughter cell became a postmitotic migratory neuron and has been specified by the asymmetric inheritance of the Notch protein (Chenn and McConnell, 1995). This model has been revised by studies in the mouse cerebral cortex showing that perpendicular cell divisions can also be asymmetric by the unequal distribution of the apical membrane patch (Kosodo et al., 2004).

4.4.4 Radial glia cells

It was believed for long time that radial glia are basically support cells for migrating neurons, but recently it has been proven that they are also the main source for new born neurons (Malatesta et al., 2003; 2000; Miyata et al., 2001; Noctor et al., 2001). For the period of neurogenesis (E11-E17) in the cerebral cortex an overall number of 11 cell cycles has been

determined (Takahashi et al., 1996) and the number of cell cycle has been correlated to the laminar identity of the neurons. Neurons generated in the cell cycles 1-8 are located in layers 6 and 5, whereas neurons of layers 4 and 3/2 arise in cell cycles 9-11 in the mouse cerebral cortex (Takahashi et al., 1996). The layers of the cerebral cortex are formed in an inside-first, outside-last manner, which means that late born neurons migrate through the early born neurons and settle on top. At E11/E12 young postmitotic neurons migrate predominantly via somal translocation (Nadarajah et al., 2001). In this process the contacts to the neighbouring cells of the VZ are lost and the soma is pulled up under preservation of the basal attachment towards the pial surface (Nadarajah et al., 2001) and thus the preplate (PP) builds underneath. Neurons which are born at E14-E18 possess a small leading process and migrate along the radial processes of the radial glia cells basally, splitting the preplate into the marginal zone (MZ) and the subplate (SP) (Rakic et al., 2003; Miyata et al., 2001; Nadarajah et al., 2001; Noctor et al., 2001). Neurons are either born in the VZ or in the SVZ (Noctor et al., 2004). SVZ cells arise in an asymmetric cell division in the VZ, undergo one or more cell divisions at SVZ position and then generate neurons (Haubensak et al., 2004; Miyata et al., 2004; Noctor et al., 2004).

4.4.5 Cell polarity

Neuroepithelial cells and radial glia cells are characterized by epithelial features, as for example an apico-basal polarity (Fig. 5). Until E8.5 neuroepithelial cells are linked at the apical surface via tight junctions, whereas later on adherens junctions are present (Aakusaraste et al., 1996). Adherens junctions are in close contact to protein complexes, as the apical complex containing atypical Protein Kinase C (aPKC), the Par proteins, the small Rho-GTPase Cdc42 (for review see e.g. Schneeberger and Lynch, 2004) and the membrane bound protein Prominin-1 (Weigmann et al., 1997). The apical side of the neuroepithelial and radial glia cells is exposed cerebrospinal fluid (CSF), which contains a variety of factors and is secreted by the cells of the choroid plexus, a medial structure close to the cortical hem.

At the basal side of cerebral cortex neuroepithelial and radial glia cells attach via their endfeet to the basement membrane (BM) (Fig. 5B), which is a sheet-like layer of extracellular matrix (ECM). The BM is composed of glycoproteins and proteoglycans. The main basement membrane components are laminins, type IV collagens, nidogens and heparan sulphate proteoglycans (HSPGs) (Paulsson, 1992; Yurchenco and O'Rear, 1994) (Fig. 6A). Laminins are heterotrimeric proteins, each trimer composed of an α , β and γ chain. So far five α , three β

and three γ chains are known, combining together and generating fifteen different laminin isoforms (for review see: Quondamatteo, 2002). Type IV collagens are trimers. Each trimer is composed of three α (IV) chains in triple helix formation. Six α (IV) are known yet ($\alpha 1$ - $\alpha 6$ (IV) (for review see: Quondamatteo, 2002; Tunggal et al., 2000). Nidogens/entocins are small glycoproteins that belong to two families (for review see: Tunggal et al., 2000). Perlecan is a basement membrane associated heparan sulphate proteoglycan that can also be cell membrane associated in contrast other heparan sulphate proteoglycans. Laminins and type IV collagens form sheet like structures which are linked by perlecan and nidogen (Fig. 6B). The exact mechanism of basement membrane assembly and maintenance in vivo is not yet clear. Basement membrane assembly in vivo occurs under the mediation of different receptors as for example integrins (reviewed in Quondamatteo, 2002). Integrins are heteromeric transmembrane proteins composed of an α - and β -subunit. 18 α and 8 β integrin subunits are known so far and give rise to 24 different integrin heteromers (Bouvard et al., 2001). Meningeal cells secrete the components of the ECM, which assemble into a basement membrane underneath the meningeal cells and the neural tissue (Sievers et al., 1994). The conditional deletion of $\beta 1$ integrin under the control of the nestin promoter leads to defects in the basement membrane (Graus-Porta et al., 2001). Also other receptors, as for example dystroglycan, have been discussed as key players in basement membrane formation (reviewed in Quondamatteo, 2002). Basement membranes provide structural support for cells, separate compartments (Martinez-Hernandez and Amenta, 1983) and influence cellular behaviour as migration, differentiation and proliferation, since they contain a variety of other factors such as the Fibroblast growth factors (Fgfs) (Dono, 2003; Ford-Perriss et al., 2001) and Wingless-Int proteins (Wnts) (for review see e.g. Cadigan and Nusse, 1997; Nelson and Nusse, 2004; Nusse, 2005). Previous studies showed that heparan sulphate proteoglycans (HSPGs) bind Fgfs (for review see: Dono, 2003; Ornitz, 2000). Captured growth factors in the ECM constituting the BM might influence the proliferative behaviour of radial glia cells. Previously it has been shown that the radial process remains attached to the BM during cell division of a radial glia cell (Miyata et al., 2001) and it has been speculated that this attachment might influence the cell fate (Fishell and Kriegstein, 2003). Not only cell fate might be concerned by the attachment of RG endfeet to the BM but also cytoskeletal dynamics.

In order to answer the question how the basal polarity, achieved by radial glia endfeet attachment at the pial surface, might influence the proliferative behaviour of the radial glia cells and their cell fate, I analyzed in this work several basement membrane mutants. First, I analyzed the laminin $\gamma 1$ mutant mice, which are characterized by a targeted deletion of the

nidogen binding site in the $\gamma 1$ chain of laminin (Willem et al., 2002). The BM in this mutant forms, as detectable in laminin (LN) and fibronectin (FN) immunohistochemistry, but the components are not properly linked. Radial glia endfeet are detached from the BM at E14 and not radially arranged as it is the case in the cerebral cortex of the corresponding WT littermates. Second, I analyzed the $\alpha 6$ integrin $^{-/-}$ mice which lack the laminin receptor $\alpha 6\beta 1$ integrin. Thus the BM can not properly assemble, as shown in EM pictures (Georges-Labouesse et al., 1998). As a third mutant I analyzed the perlecan $^{-/-}$ mice, characterized by the targeted deletion of perlecan causing disassembly and disruption of the BM (Costell et al., 1999).

5 Abbreviations

Ab	antibody	FACS	fluorescence activated cell sorting
Abs	Absorption		
bHLH	basic helix-loop-helix	FCS	fetal calf serum
BLBP	brain lipid-binding protein	Fig.	figure
BMP	bone morphogenic protein	FN	fibronectin
BrdU	5-bromo-2-desoxy-uridine	G1	G1-phase of cell cycle
bp	base pair	G2	G2-phase of cell cycle
Cb	cerebellum	GAPDH	Glyceraldehyde-3-phosphate dehydrogenase
Cad	cadherin		
cDNA	complementary DNA	GE	ganglionic eminence
CDS	coding sequence	GF	growth fraction
Cfr	frontal cortex	GFAP	glial fibrillary acidic protein
ChP	choroid plexus	GFP	green fluorescent protein
CNS	central nervous system	GLAST	glutamate astrocyte-specific transporter
CP	cortical plate		
CSF	cerebrospinal fluid	GS	glutamine synthase
DAPI	4'-6'-diamidino-2-phenylindole	h	hour
		hrs	hours
DCX	doublecortin	HC	hippocampus
DNA	desoxyribonucleic acid	HD	homeodomain
DNase	desoxyribonuclease	HPRT	hypoxanthine guanine phosphoribosyl transferase
dNTP	desoxynucleotides		
CTX	cortex	HRP	horse radish peroxidase
Di	diencephalon	Ig	immunoglobulin
div	days in vitro	IRES	internal ribosomal entry site
DNA	desoxyribonucleic acid	IZ	intermediate zone
DT	dorsal thalamus	ko	knock-out
E	embryonic day	LGE	lateral ganglionic eminence
ECM	extracellular matrix	LI	labelling index
egl	external granular layer	LN	laminin
Em	emission	LTR	long terminal repeat
ET	epithalamus	LV	lateral ventricle

mAB	monoclonal antibody	P/S	penicillin-streptomycin
Ms	mesencephalon	PSB	pallial-subpallial boundary
MGE	medial ganglionic eminence	PT	pretectum
MI	maximum intensity	RNA	ribonucleic acid
min	minute	RNase	ribonuclease
M-phase	mitosis phase of the cell cycle	RC2	radial cell 2
		rln	reelin
My	myelencephalon	rpm	rounds per minute
MZ	marginal zone	RMS	rostral migratory stream
n	sample number	RT	room temperature
NE	neuroepithelium	RPE	retinal pigmented epithelium
Ngn	neurogenin		
NGS	normal goat serum	RT-PCR	real time-polymerase chain reaction
OB	olfactory bulb		
OC	optic cup	Sc	spinal cord
ORE	optic recess	SE	septum
OV	optic vesicle	SP	subplate
P	postnatal day	SEM	standard error of the mean
pAB	polyclonal antibody	SFRP	secreted frizzled related protein
PBS	phosphate buffered saline		
pBS KS	bluescript KS	Shh	sonic hedgehog
PC	posterior commissure	S-phase	DNA-synthesis phase of the cell cycle
PCR	polymerase chain reaction		
PD	paired domain	s.d.	standard deviation
PD5a	paired domain containing exon5a	SVZ	subventricular zone
		TAD	transactivating domain
PDL	poly-D-lysine	T _c	total cell cycle length
PFA	paraformaldehyde	T _s	s- phase length
PH3	phosphorylated histone H3	TF	transcription factor
Pfu	DNA-polymerase with proofreading activity	TH	thyrosine hydroxylase
		VZ	ventricular zone
Pn	pons	WT	wildtype
PP	preplate	4V	fourth ventricle
pRB	retinoblastoma protein	v	volume

6 Material and Methods

6.1 Animals

The wildtype mice used in this work are C57/Bl/6J mice obtained from Charles River.

The *Pax6*^{Sey} mice are characterized by a naturally occurring point mutation in the Pax6 gene, leading to the expression of a truncated non-functional protein (Hill et al., 1991). *Pax6*^{Sey} mice were maintained as heterozygotes on a mixed C57BL/6JxDBA/2J background. Heterozygous *Pax6*^{Sey} mice were recognized by their eye phenotype (Hill et al., 1991) and crossed in order to obtain homozygous *Pax6*^{Sey} mutant embryos. Embryos were characterized with the help of a binocular on account of their eye phenotype: homozygous *Pax6*^{Sey} mutant embryos are lacking any eye.

The *Pax6*^{Aey18} mice (Haubst et al., 2004) were maintained on a C3HeB/FeJ background. Homozygous *Pax6*^{Aey18} mutant embryos were identified by their eye phenotype. *Pax6*^{4Neu} (Favor et al., 2001) mice were maintained on a C3HeB/FeJ background. Homozygous *Pax6*^{4Neu} mutant embryos were identified by their eye phenotype and by the identification of the point mutation at position 776 in sequence analysis.

Pax6^{tm1Gfs} mice, here referred to as *Pax6(5a)*^{-/-} mice (Singh et al., 2002), are characterized by the targeted deletion of exon5a of Pax6 and were maintained as homozygotes on a C57BL/6 background.

$\alpha 6$ integrin^{-/-} embryos (Georges-Labouesse et al., 1998) and the respective WT littermates (129Sv/ C57BL/6 mixed background) were obtained from Elisabeth Georges-Labouesse.

Laminin1 mutant embryos (Willem et al., 2002) and the respective WT littermates (Sv129/ C57BL/6 background) were obtained from Ulrike Mayer.

Perlecan^{-/-} embryos (Costell et al., 1999) and the respective WT littermates (C57BL/6 background) were obtained from Reinhard Fässler.

The day of vaginal plug was considered as embryonic day 0 (E0), the day of birth as postnatal day 0 (P0). In this study we used only WT and homozygous mutant littermates.

6.2 Genotyping of transgenic mice

Genotyping of transgenic mice was performed according to a protocol of Larid et al. 1991. Tail biopsies of embryos or adult mice or were transferred into 250-500 μ l lysis buffer and incubated over night rotating at 55°C. Bones and hairs were removed by centrifugation (10

minutes at 13000 rpm) after tissue lysis was completed. The supernatant was transferred into 250-500µl isopropanol, incubated at RT for 10 minutes and then mixed. DNA precipitates were transferred with the help of a pipette tip into 250µl H₂O. DNA was dissolved at 55°C for several hours.

6.2.1 Genotyping of perlecan^{-/-} mice

To evaluate the genotypes of WT and perlecan mutants three primers were used (Perlecan sense: 5'-AAC CAG AAG GGG TGG CAA GAA-3' (Intron5); WT antisense: 5'-GCA GCA CCT CTT GAA TCT GAG-3' (Exon 6 Rev); perlecan^{-/-} antisense: 5'-TAC TGA GGC AGA GTC TCT CTC-3' (Intron 6 Rev1)). Two separate PCR reactions were performed containing as primers either perlecan sense and perlecan^{-/-} antisense or perlecan sense and WT antisense. The PCR was carried out a total volume of 20µl using 2µl DNA; 2µl 10x PCR buffer (1x final); 2µl 2mM dNTPs (100nM final); 2µl 10pmol/µl forward primer (1pmol/µl final); 2µl 10pmol/µl reverse primer (1pmol/µl final); 2µl 10pmol/µl reverse primer (1pmol/µl final); 0.8µl 50mM MgCl₂ (2mM final); 1µl Q-Solution; 0.2µl Taq-Polymerase; 8µl H₂O under the following cycling conditions: 1 cycle 95°C/180sec; 42 cycles (94°C/30sec; 55°C/30sec; 72°C/45sec); 1 cycle 72°C/180sec. The genotype of the WT gives rise to a PCR product of approximately 280bp length, the perlecan^{-/-} PCR product is 510bp long.

6.3 Histology

Time pregnant mice were sacrificed with diethylether or increasing CO₂ concentrations followed by cervical dislocation. Embryos were removed by hysterectomy and transferred into Hanks buffered salt solution (HBSS) with 10mM HEPES. Either embryonic brains were removed with the help of two dissection forceps from posterior to anterior or the entire head was taken.

6.3.1 BrdU Labelling in vivo

For the detection of the interkinetic nuclear migration during embryonic development, time pregnant mice were injected intraperitoneally (5mg BrdU/100 g body weight). The mouse was sacrificed either 0.5h or 6h after the injection.

6.3.2 Cryosections

Embryonic brains or heads were fixed in 4% paraformaldehyde (PFA) (in phosphate buffered saline (PBS)) for the following times: E12 whole head: 2hrs; E14 brain: 2hrs; E14 whole head: 3.5hrs; E16 brain: 3hrs; E16 whole head: 5hrs, E18 brain: 4hrs; E18 whole head: 7-8 hrs; P2 whole head: 8-9 hrs at 4°C. After a brief washing step with PBS, tissue was incubated at 4°C in 30% sucrose solution (in PBS) over night. After cryoprotection was completed, the tissue was embedded in a tissue-tek containing embedding mold and sections (12µm) were cut with a cryostat. Sections were collected on SuperFrost microscope slides and stored at -20°C.

6.3.3 Vibratome sections

E14 and E16 brains were fixed for 6hrs in 2% PFA at 4°C. Brains were embedded in 3% agarose (in PBS) and sections (150µm) were cut with a vibratome.

6.4 Tissue culture

Embryonic brains were isolated from E14 time pregnant mice as described above. The hemispheres were separated and the meninges were removed. After the removal of the hippocampus and the olfactory bulbs, the cortex was separated from the ganglionic eminence and transferred into HEPES containing HBSS on ice. After a brief centrifugation step in order to remove the HEPES, 1 ml trypsin containing EDTA solution was added to digest the tissue for 15 minutes at 37°C. Trypsin activity was stopped by adding 2ml DMEM (10% FCS, 1% P/S (for further details see table: 6.12.2)). Cells were mechanically dissociated with a firepolished and medium coated Pasteur-pipette. The cells were twice washed by centrifugating for 5 minutes at 1000rpm (172x g), followed by resuspending in 3ml DMEM (10% FCS, 1% P/S). Cells were counted with the help of a Neubauer-chamber and plated at a density of 5×10^5 cells per well of a 24-well plate on poly-D-lysine (PDL) coated glass coverslips. Cells were incubated at 37°C and 5% CO₂. Two hours after plating viral infection was performed. The next day 0.5ml SATO (Bottenstein and Sato, 1979) medium was added. Every second day 0.5ml of medium was replaced with 0.5ml fresh SATO medium. Prior to

fixation cells were briefly washed with PBS and then fixed for 15 minutes in 4% PFA. After 3 washes with PBS at RT, cells were processed for immunohistochemistry.

6.4.1 Viral infection of cortical cell cultures

Primary cells from E14 cerebral cortex were isolated and cultured as described above and infected with the respective retrovirus 2 hours after plating at a concentration resulting in not more than 50 clones per coverslip.

6.5 Immunohistochemistry

In general immunohistochemical pretreatments were performed for specific antibodies in increasing stringency. This means that pretreatments with NP40 were performed before Triton-X100 (Tx) treatment, acetic acid-ethanol treatment and citrate buffer treatment before HCl treatment for BrdU immunohistochemistry.

To detect BrdU that has been incorporated into the DNA, sections were pre-treated for 30 minutes in 2N HCl, followed by 2x 15 minutes incubation in 0.1M Sodium-tetraborate (pH8.5) and 3x washed for 10 minutes in PBS.

6.5.1 Primary and secondary antibodies

Cryosections were defrosted at RT and rehydrated for 10 minutes with PBS. The primary antibodies used in this work are listed in table 6.5.1.1.

Sections or coverslips were incubated with the primary antibody over night at 4°C in a humid chamber. The respective fluorescence labelled secondary antibodies were used from Jackson Immunoresearch, Inc. and Southern Biotechnology Associates, Inc. to visualize the antigen (table 6.5.1.2).

Sections or coverslips were incubated in secondary antibody solution for 1h at RT, followed by 3 washes for 10 minutes in PBS. In order to confirm the specificity of the primary

antibody, the respective secondary antibodies were incubated without previous primary antibody incubation.

6.5.1.1 Table Primary antibodies

Name	Host-animal/ working dilution	Pretreatment	Marker	Supplier	Reference
Anti- β -Galactosidase	Rabbit (1:300, 0.5% Tx, 10% NGS)	30 min in 0.5% Tx, 10% NGS	Enzyme used as marker gene	Cappel (55976)	(Williams and Price, 1995)
Anti- β -Galactosidase	Mouse (IgG1, 1:1000, 0.5% Tx, 10% NGS)	30 min in 0.5% Tx, 10% NGS	Enzyme used as marker gene	Sigma (G6282)	
Anti- β -Galactosidase	Mouse (IgG2a, 1:500, 0.5% Tx, 10% NGS)	30 min in 0.5% Tx, 10% NGS	Enzyme used as marker gene	Promega (Z3783)	
Anti- β III-Tubulin	Mouse (IgG2a; 0.5% Tx, 10% NGS)	8 min boiling in 0.01M Sodium-Citrate buffer, pH6.0 at max in microwave on sections or 15 min Acid-EtOH at -20°C on coverslips	Postmitotic neurons	Sigma (T8660)	(Lee, 1995)
Anti-BLBP	Rabbit (1:1500, 0.5% Tx, 10% NGS)	8 min boiling in 0.01M Sodium-Citrate buffer	Lipid Binding Protein, precursor cell subtypes	Nathaniel Heintz, Howard Hughes Medical Institute, Rockefeller University, New York, USA	(Feng et al., 1994; Kurtz et al., 1994)
Anti-BrdU	Mouse (IgG1, 1:10)	1h 0.5% Tx, 30 min 2N HCl, 2x 15 min Borate buffer pH8.5	S-Phase marker	Bio-Science Products (010198)	(Götz et al., 1998)
Anti-BrdU	Rat (1:100)	1h 0.5% Tx, 30 min 2N HCl, 2x15 min Borate buffer pH8.5	S-Phase marker	Abcam (ab6326)	
Anti-Brn3a	Mouse (IgG1, 1:500)		Retinal ganglion cell marker	Chemicon (MAB1585)	(Philips et al., 2005)
Anti-Fibronectin	Rabbit (1:40; 0.5% Tx, 10% NGS)	0.5% Tx, 10% NGS	Extracellular matrix component	Chemicon (AB 2033)	
Anti-GFAP	Mouse (IgG1, 1:100, 0.5% Tx, 10% NGS)	0.5% Tx, 10% NGS	Astroglialmarker	Sigma (G3893)	

Anti-Gsh2	Rabbit (1:1000, 0.5% Tx, 10% NGS)	15min in 0.5% Tx, 10% NGS	TF expressed in precursor cells of subpallium	Kenneth Campbell, Division of Developmental Biology, Cincinnati Children's Hospital Medical Center, Cincinnati, USA	(Toresson et al., 2000)
Anti-Glutamine synthase	Mouse (IgG2a, 0.5% Tx, 10% NGS)	0.5% Tx, 10% NGS	Marker for glial cells	BD Biosciences (610517)	
Anti-Islet1	Mouse (IgG2b, 1:10, 0.5% Tx, 10% NGS)	8 min boiling in 0.01M Sodium-Citrate buffer	Marker for retinal ganglion cells	Developmental Hybridoma Bank (39.4D5)	
Anti-Ki67 (Tec-3)	Rat (1:50, 0.5% Tx, 10% NGS)	8 min boiling in 0.01M Sodium-Citrate buffer	Marker for proliferating cells	Dako (dia 333-67)	
Anti-Laminin	Rabbit (1:40, 0.5% Tx, 10% NGS)		Component of the ECM	Chemicon (AB 2034)	
Anti-Mash1	Mouse (IgG1, 1:2; 0.5%Tx, 10% NGS)	8 min boiling in 0.01M Sodium-Citrate buffer	bHLH TF expressed in precursor cells of subpallium	kindly provided by F.Guillemot	
Anti-NeuN	Mouse (IgG1, 1:50, 0.5% Tx, 10% NGS)	30min 0.5% Tx, 10% NGS	Neuronal marker	Chemicon (MAB377)	(Mullen et al., 1992)
Anti-nestin	Mouse (IgG1, 1:4, 0.5% Tx, 10% NGS)			Developmental Hybridoma Bank (rat-401)	
Anti-Ngn2	Mouse (IgG2a, 1:10, 0.5% Tx, 10% NGS)	8 min boiling in 0.01M Sodium-Citrate buffer	TF expressed in precursor cells of pallium	kindly provided by D.Anderson	
Anti-Olig2	Rabbit (1:1000, 0.5% Tx, 10% NGS)		TF expressed in precursor cells of subpallium	kindly provided by D.Rowitch	Takebayashi et al. 2000
Anti-O4	Mouse (IgM, 1:1000)		Marker for oligodendrocytes	Kindly provided by J.Price	
Anti-Pax2	Rabbit (1:100, 0.5% Tx, 10% NGS)	8 min boiling in 0.01M Sodium-Citrate buffer	Marker for optic stalk	Covance (PRB-276P)	Dressler et al., 1992
Anti-Pax6	Mouse (IgG1, 1:50, 0.5% Tx, 10% NGS)	8 min boiling in 0.01M Sodium-Citrate buffer	TF expressed in VZ cells of pallium	Developmental Hybridoma Bank (chick pax6a.a. 1-223)	
Anti-Pax6	Rabbit (1:300, 0.5% Tx, 10% NGS)	8 min boiling in 0.01M Sodium-Citrate buffer	TF expressed in VZ cells of pallium	Babco (PRB-278P)	

Anti-Pax6	Rabbit (1:1000, 0.5% Tx, 10% NGS)	8 min boiling in 0.01M Sodium-Citrate buffer	TF expressed in VZ cells of pallium	Chemicon (AB 5409)	
Anti-PH3	Rabbit (1:200, 0.5% Tx, 10% NGS)	8 min boiling in 0.01M Sodium-Citrate buffer	M-Phase marker	Upstate Biotech (06-570)	(Hendzel et al., 1997)
Anti-RC2	Mouse (IgM, 1:500, 0.5% Tx, 10% NGS)	8 min boiling in 0.01M Sodium-Citrate buffer	Precursor cell subtype	kindly provided by P. Leprince	
Anti-Reelin (142 and E4)	Mouse IgG1 (1:500, 0.5% Tx, 10% NGS)		Cajal-Retzius cells in the cerebral cortex	André Goffinet, University of Louvain, Medical School, Brussels, Belgium	(de Bergueyck et al., 1998)
Anti-reticulon-1	Rat (9-4, 1:10, 0.5% Tx, 10% NGS)		Marker for PSB	kindly provided by T. Hirata	
Anti-Tbr2	Rabbit (1:2000; 0.5% Tx, 10% NGS)	8 min boiling in 0.01M Sodium-Citrate buffer and 1h 0.5% Tx, 30min 2N HCl, 2x15 min Borate buffer pH8.5	Transcription factor in SVZ cells of dorsal pallium	Kindly provided by R. Hevner	

6.5.1.2 Table Secondary antibodies

Name	Supplier
Anti-rabbit Ig FITC / TRIC / biotinylated	Jackson ImmunoResearch / Dianova
Anti-rabbit Ig Cy2	
Streptavidin AMCA	Vector Laboratories
Anti-guinea pig Ig Cy2	Dianova Immundiagnosics
Anti-rat FITC / TRIC	(Jackson ImmunoResearch)
Anti-mouse IgG1 FITC / TRIC / biotinylated	EuroPath Ltd.
Anti-mouse IgG2b FITC / TRIC / biotinylated	(Southern Biotechnology Associates)
Anti-mouse IgM FITC / TRIC / biotinylated	

6.5.2 Visualisation of cell nuclei

Cell nuclei were counterstained with DAPI (4'-6'-diamidino-2-phenylindole) (Stock 2mg/ml) diluted 1:100 in PBS for 10 minutes at RT followed by 3x 10 minutes washes in PBS. (DAPI forms fluorescent complexes with the DNA, attaching to AT-rich sequences, which can be visualized at 460 nm). To analyse the orientation of cell divisions at the ventricular surface, cell nuclei were visualized with propidium-iodide (PI). The PI staining solution contained 0.5mg/ml PI (in PBS) and 25U/ml RNase. Sections were incubated for 15 minutes at RT, followed by 3x 10 minutes washes in PBS. PI binds to double stranded DNA (Abs: 482 nm, Em: 636 nm).

Specimen were mounted in Aqua Poly/Mount (Polysciences, Northampton, UK) and analyzed at a Confocal Microscope (Leica TCS 4NT, Leica Microsystems; Olympus FV1000; Zeiss LSM510).

6.6 Retrovirus preparation

6.6.1 Cloning strategy of generated Pax6 viruses

6.6.1.1 PD-less Pax6 virus

In order to generate a viral vector containing the natural occurring splice variant of Pax6, lacking the PD (Mishra et al., 2002), linker PCR was performed. In this technique the primers contain already the restriction sites required for the ligation into the plasmid. The PCR was performed in a total volume of 100µl with 10µl 10x buffer, 2µl dNTPs, 8µl MgCl₂ (50mM), 2µl PD-less fl (10µM), 2µl PD-less r1 (10µM), 0.2µl template (Pax6 CDS in pBS KS) (1µg/µl), 1,5µl Pfu-Polymerase, 74,3µl H₂O, under the following cycling conditions: 1 cycle 95°C/5 min; 30 cycles (95°C/30sec; 58°C/30sec; 72°C/45sec); 1 cycle 72°C/7min. A product of 665bp was generated, loaded on a 1% agarose gel and after running the gel the band of interest was isolated and the DNA was extracted using a Gelextraktion kit (Qiagen) according to the instructions of the manufacturer. For directional cloning, the PCR product and the viral backbone vector (pMXIG; Nosaka et al., 1999) underwent a restriction digest with BamHI and SacII (2hrs at 37°C). The products were cleaned using a Gelextraction kit and the appropriate amount of fragment and vector were used for the ligation (see below).

6.6.1.2 Cloning of a virus with point mutation in HelixIII of HD at nucleotide position 776 (PM776 virus)

In order to construct a retrovirus containing the Pax6 CDS with a point mutation at position 776 (PM 776) identical to the mutation in the Pax6 gene of the Pax6^{4Neu}^{-/-} mice (Favor et al., 2001) two different Linker-PCRs were performed. The primers PM776f and PM776r are containing a point mutation at nucleotide position 776 and are complementary to each other. PCR reaction 1 was performed in a total volume of 100µl (for reaction mix and PCR conditions see: 2.5.3.1) using Delh3 f1 and PM776r as primers. PCR reaction 2 was performed under the same conditions using the primers PM776f and PDless r1. The two products were used as templates for PCR reaction 3, where all 4 primers were added to the reaction mix (for reaction mix and PCR conditions see: 2.5.3.1). This gave rise to a 1269bp product containing a point mutation at nucleotide position 776. The PCR product was extracted with the Gelextraction kit (Qiagen) as described above. Restriction digest with BamHI and SacII was followed by another step of Gelextraction. The cleaned product was used for ligation to the pMXIG vector.

Linker-Primer list:

Delh3f1: CGGGATCCATGCAGAACAGTCACAGC

PM 776 f: TGTCCATACCAAAGGATTAGCTTC

PM 776 r: ACAGGTATGGTTTCCTAATCGAAG

PD-less f1: CGGGATCCGAGATGCGACTTCAGC

PD-less r1: TCCCCGCGGTTACTGTAATCGAGG

6.6.2 Ligation

The ligation was performed with the ratio 1:1, 1:3 and 1:5 of vector to insert. 20ng pMXIG (cut with BamHI and SacII) were used in a total volume of 20µl ligation reaction containing 4µl 5x T4 ligase-buffer, 0.1µl T4 ligase together with the corresponding amount of insert, add H₂O. The reaction was incubated for 2 hrs at RT. Then the transformation to top10 cells has been performed.

6.6.3 Transformation

10ng of Plasmid or 1µl ligation-mix were added to 25µl of top10 cells (chemical competent cells) and incubated for 30 minutes on ice. After a head shock of 45 seconds at 42°C in a

waterbath, cells were incubated for 10 minutes on ice, then 1ml of LB medium without any antibiotics was added and cells were incubated for 1 hour at 37°C in a bacterial shaker (225rpm). 50-100µl of the cell suspension was plated on LB-agar plates containing the respective selective antibiotic (e.g. Ampicillin 50mg/ml) depending on the resistance gene of the transformed plasmid. LB-agar plates were incubated over night at 37°C. The next day colonies were picked with an autoclaved pipette tip and transferred into 3ml of antibiotic containing LB-Medium and cultured for 3-4 hours. 1ml of this preculture was transferred into 200ml antibiotic containing LB-medium and incubated over night in a bacterial shaker at 37°C, 225rpm. 1ml of the bacterial culture was mixed with 1ml of 100% glycerol, vortexed and stored at -80°C (glycerol stock). Then the bacteria were harvested and the plasmid DNA was purified following the Qiagen Midiprep protocol using a Midi Tip100 column per 100ml of bacterial culture. The DNA pellet was dissolved in 200µl of H₂O_{bidest.} The concentration was measured with a photometer at 260nm.

6.6.4 Mini-PCR screening

In order to screen for clones containing plasmid with the expected insert, clones were picked with an autoclaved pipette tip and inoculated on a new antibiotic containing LB-agar plate (for re-identification clones were numbered). Then respective clones were transferred into 20µl H₂O, followed by the addition of the PCR mastermix, containing the appropriate primers, and the PCR reaction. Clones containing the right size of insert were sequenced (Seqlab, Göttingen) and the sequences were aligned against the gene of interest.

6.6.5 GPG Retrovirus preparation

Gpg packaging cells (Ory et al., 1996) allow the production of high titer amphotropic retrovirus. In contrast to many other retrovirus packaging cell lines, which often lose their efficiency over time in culture due to the gradual loss of the packaging genes, contain the packaging plasmids of the gpg cells different selection markers (gentamycin (G418), puromycin). Thus the expression of the packaging genes is better maintained over long periods of culturing in presence of the corresponding antibiotics. Since the protein of the vesicular stomatitis virus G (VSV-G) is toxic for gpg293 cells, the expression of this gene is controlled by tetracycline. Therefore these cells are cultured in presence of tetracycline,

puromycin and G418. Retroviral vectors pseudotyped with VSV-G have a broad tropism and can be concentrated by ultracentrifugation without loss of activity (Galipeau et al., 1999). GPG cells were cultured in DMEM (10% (v/v) FCS (heat inactivated for 30 minutes at 56°C), 1% (v/v) P/S, 1µg/ml tetracycline, 2µg/ml puromycin and 0.3mg/ml G418) Cells were passaged with PBS and trypsin containing 1µg/ml tetracycline. For the viral production, gpg helper-free packaging cells were used. 90-95% confluent gpg cells were transfected with the below described viral plasmids (PD-less Pax6, PM776 and the CMMP-GFP respectively) using lipofectamine 2000 and Opti-MEM I reduced-serum medium. The medium was replaced 8-10 hours post transfection and cells were cultured in DMEM (10% FCS, 1% P/S, see table 6.12.2). The virus containing medium was harvested after 48 hrs, filtered through a 0.45µm filter and centrifuged at 50.000x g for 1.5 hrs at 4°C. The supernatant was carefully removed and the pellet was resuspended in TNE over night at 4°C, aliquoted and stored at -80°C. The titer of the virus (viral particles/ml) was determined by transduction of E14 primary cell cultures in serial dilution. After 2 div, cells were fixed and the number of clones was quantified after immunohistochemical detection of GFP. The number of GFP positive clones corresponds to the number of viral particles transduced. Typically viral titers of 10⁶-10⁷ viral particles/ml were obtained. GFP was detectable after 2 div.

6.6.6 Pax6 and Pax6(5a) retrovirus preparation

The entire coding sequence of Pax6 (1873bp fragment) (Heins et al., 2002) and Pax6(5a) (Haubst et al., 2004) (1915 bp fragment) was cloned in sense orientation into the BglII unique restriction site of the retroviral vector 1704 between the upstream LTR and the EMC IRES sequence (gift of J.E.Majors; Ghattas et al., 1991). BOSC23 helper-free packaging cells (Pear et al., 1993) were cultured in DMEM (10% FCS, 1% P/S; see also 6.12.2) and transiently transfected with the respective viral plasmid. This resulted in a viral titer of 1x 10⁵/ml.

BOSC23 cells were split 3x prior to transfection in a ratio of 1:3. One day prior to transfection, 6x 10⁶ cells were plated on a 10 cm dish, in order to achieve 80% confluence.

For the transfection 20µg DNA were mixed with CaCl₂ in 500µl (final CaCl₂ concentration 0.125M) followed by the addition of 500µl 2x HBS (per 10 cm dish). The transfection mix was incubated for 20 minutes at RT. Meanwhile the medium of the BOSC23 cells was changed to DMEM (10% FCS, 1%P/S) containing 25µM Chloroquine (9ml medium/10 cm dish). 1ml of transfection mix was added to each plate, after 8-10 hours the

DMEM/Chloroquine was replaced by DMEM (1% FCS, 1% P/S). The virus containing medium was collected after 24-48 hrs, briefly centrifuged (1000 rpm at 4°C) to remove dead cells and filtrated (0.45µm filter) on ice. The virus was concentrated at least 10fold by using centriprep YM-50 columns (amicon) in several centrifugation steps at 1500x g, 4°C according to the manufactors instructions, aliquoted and stored at -80°C.

6.7 In situ hybridization

6.7.1 Plasmid linearization

20µg of plasmid were linearized with the appropriate enzyme (40U) in a total volume of 50µl for 2.5 hours at 37°C. To remove the restriction enzyme, phenol-chloroform extraction was performed. The volume was increased to 200µl by adding sterile water (RNase free). 200µl of Phenol-Chloroform were added and strongly mixed for 1 minute, followed by a centrifugation step of 5 minutes at 13000 rpm in a table centrifuge. The upper DNA containing water phase was recovered, mixed with 200µl isoamylalcohol by means of a vortex for 1 minute and centrifuged for 5 minutes at 13000 rpm. The upper phase was recovered and 1/10 volume (20µl) of 3M sodium acetate and 0.7 volumes of 100% ethanol (RNase free) were added to precipitate DNA. The sample was centrifuged (10 minutes at RT, 13000 rpm). The supernatant was removed and the pellet was washed with 70% ethanol. After air drying, the pellet was resuspended in 18µl H₂O (RNase free), pH8.

The in situ plasmid for the generation of the Svet1 cRNA probe (plasmid from V. Tarabykin) was cut with XhoI and transcribed with T7 polymerase. The plasmid for the generation of the SFRP2 cRNA probes (plasmid from S. Pleasure) was cut with EcoRI and transcribed with T7 polymerase.

6.7.2 In vitro transcription

The following components were mixed accordingly to the manufactors protocol (Roche) in a total volume of 20µl: 1µg of linearized plasmid, 2µl NTP mix (containing digoxigenin labeled UTP; DIG-UTP), 2µl 10x transcription buffer, 1µl RNase inhibitor, 1µl T3, SP6 or T7 RNA-polymerase and H₂O (RNase free). The reaction was incubated for 2 hours at 37°C. The yield of transcript was increased by adding 1µl T3, SP6 or T7 RNA-polymerase after 1 hour.

Addition of 2µl 0.2 M EDTA (RNase free) stopped the reaction. In order to precipitate the RNA 2.5µl 4M LiCl and 75µl 100% ethanol were added. The mix was incubated at -20°C over night or for 2 hours at -80°C, then centrifuged for 7 minutes at 4°C. The pellet was washed with 70% ethanol and air dried before resuspending in 20µl RNase free H₂O, then 200µl Hybridisation buffer were added.

6.7.3 In situ hybridization

5-7µl RNA-antisense probe (corresponding to 0.5-1.0µg RNA) were diluted in 150µl hybridisation buffer and denatured for 5 minutes at 70°C, applied onto the microscope slides carrying the sections of interest and sealed with a clean coverslip. Slides were incubated overnight at 65°C in a sealed box with Whatman paper, soaked with 1x SSC in 50% formamide, in a hybridisation oven. Slides were washed for 10 minutes in pre-warmed (65°C) washing solution at 65°C and the coverslip was removed. Further 2-3 washes at 65°C for 30 minutes were done, followed by 2 washes in MABT for 30 minutes at RT. Sections were blocked in 2% blocking-solution for 1 hour at RT. Anti-digoxigenin Fab fragments coupled to alkaline phosphatase were diluted 1:2500 in blocking-solution and 150µl of this antibody-solution were applied per slide. Sections were covered with parafilm. The antibody incubation was performed in a humid chamber overnight at RT. Slides were washed 4-5 times in MABT for 20 minutes at RT, and rinsed twice in Alkaline-phosphatase (AP) staining buffer for 10 minutes at RT. 150µl NBT/BCIP-containing staining solution was added per slide and covered with parafilm. Slides were incubated 12 to 24 hours (occasionally up to 3 days) at RT. When the staining was strong enough, the reaction was stopped by rinsing the slides in AP staining buffer and shortly in water. Slides were dried for several hours at RT and mounted in AquaPoly/Mount.

6.8 In vitro electroporation of mouse embryonic brains

E13 mouse embryos were removed from the uterus (see above), the amniotic cavity was separated from the embryo, leaving the umbilical chord connection to the placenta intact. The embryos were stored on ice in PBS prior to electroporation. DNA was mixed with fast green and injected by means of a glass capillary into the lateral ventricle of the forebrain. Electrodes (diameter: 5mm) were placed at both sides of the embryonic head coming from the anterior

end of the head and the head was squeezed between the electrodes with slight pressure. 5 pulses of specific settings were applied (15ms, voltage x100: 0.7, width x10: 5, delay x100: 0.5, mode1: manual; frequency x10: 0.5). The electroporation was performed in a petridish without PBS. After electroporation embryos were transferred into PBS. The cortex was isolated and placed on a 3 cm Millicell CM filter (0.4µm pore) in a 6-well plate containing 1ml DMEM (supplemented with 10% (v/v) FCS and 1% (v/v) P/S) per well. One day after electroporation the first GFP positive cells were visible. After three days the tissue was harvested under UV light after three days by sub dissecting with a small knife (piece of a razorblade in a blade holder). The GFP positive tissue was transferred into 100µl RNAlater on ice in order to prevent that the samples are destroyed by RNAases. Samples were briefly centrifuged and RNA was extracted using the Trizol-reagent.

6.8.1 RNA extraction

For RNA extraction with Trizol-reagent 1 ml Trizol was added to the tissue that was stored in 100µl RNAlater. The tissue was homogenized with a syringe (1ml, 26G needle). RNA was extracted following the instructions of the manufacturer.

Alternatively RNA was extracted with the RNeasy Kit (Qiagen) according to the instructions of the manufacturer.

6.9 RT-PCR

6.9.1 Sample preparation for RT-PCR

Brains were isolated from the embryos as described above. To exclude contamination of the cortical tissue with ventral telencephalic tissue and vice versa, cortex and ganglionic eminence were separated at the sulcus with a special knife. Total RNA was extracted either by using the RNeasy-kit (Qiagen) or Trizol (see above) according to the instructions of the manufacturer.

6.9.2 cDNA synthesis

1µg of purified RNA was reverse transcribed with the SuperScript First Strand Synthesis System for RT-PCR (Invitrogen Life Technologies; Cat. No: 11904-018). For this 1µg RNA, 1µl 10mM dNTP-Mix, 1µl random hexamers (50ng/µl), DEPC-treated water up to 10µl were mixed, incubated at 65°C for 5 min, chilled on ice for 1 min. Meanwhile the following reaction mixture was prepared for each reaction: 2µl 10x RT buffer, 4µl 25mM MgCl₂, 2µl 0.1M DTT, 1µl RNaseOUT (Recombinant RNase Inhibitor). 9µl of this mixture was added to each RNA/primer mixture, gently mixed and briefly collected by centrifugation. Samples were incubated at 42°C for 2 min. Then 1µl of SuperScriptII RT (MoMLV reverse transcriptase) was added to each mix, samples were incubated at 42°C for 50 min. The reaction was terminated by incubating the samples at 70°C for 15 min and chilling on ice. The reactions were collected by brief centrifugation. 1µl of RNase H was added and incubated for 20 min at 37°C. cDNA samples were purified by using the Qiagen QIAquick PCR Purification Kit Protocol following the instructions of the manufacturer.

6.9.3 RT-PCR

RT-PCR was done with the LightCycler-System (Roche). For each reaction 2µl cDNA (40ng), 1µl of forward and reverse primer (see below), 2,4µl MgCl₂, 2µl reaction mix (containing SYBR Green 1 (1x) and light cycler RT-PCR enzyme mix) and 11,6µl H₂O were pipetted in a glass capillary, briefly centrifuged and the PCR was started. After an initial denaturation step at 95°C for 5 min up to 45 cycles PCR cycles (15 seconds denaturation at 95°C, 8 seconds of primer annealing at 55°C, 25 seconds of extension at 72°C) were done.

In this system relative expression levels of a gene of interest are determined by comparison to the expression levels of a housekeeper gene (GAPDH or HPRT). Samples were used undiluted, 1:10 and 1:100, as negative control a PCR reaction with H₂O instead of template was used. The lightcycler software analyses (i) the amplification of cDNA and (ii) the melting curve of the product. Each PCR cycle is followed by a quantification step obtained by measuring the fluorescence obtained by intercalation of SYBR Green I into the products generated. Each curve of amplification is characterized by 3 phases: an early background phase, a phase of exponential growth (log linear, where $N = N_0 \times (E_{\text{const}})^n$; N = number of amplified molecules, n = number of amplification cycles) and a plateau phase. The background phase lasts until the fluorescence signal from the PCR product is greater than the

background fluorescence of the probe system and the exponential phase begins when sufficient product has accumulated to be detected above the background and ends when the reaction efficiency begins to fall (plateau phase). The software of the lightcycler system plots the SYBR Green I signal of each sample against the number of cycles and the background fluorescence is removed by setting a noise band. This fluorescence threshold is used to determine cycle numbers that correlate inversely with the log of the initial template concentration. To this end the log-linear portions of the amplification curves are identified and best fit lines calculated. The crossing points (CP) are the intersections between the best-fit lines of the log-linear region and the noise band. These CPs correlate inversely with the log of the initial template concentration (LightCycler Operator's Manual, Version 3.3, April 2000, Roche). The CP determined for the candidate mRNA was normalized to those of GAPDH and HPRT to compensate for variability in RNA amount and for exclusion of general transcriptional effects. I calculated fold reduction (FR): $FR = 2^{(CP1-CP2)}$ with CP1 as the CP of the GAPDH or HPRT and CP2 as the CP of the gene of interest. The mRNA levels of GAPDH and HPRT in each tissue sample were set to 1. The expression levels of HPRT were compared to the expression levels of GAPDH in order to certify that the expression levels of GAPDH remain constant. The melting curve analysis of the lightcycler software was used to identify the product.

RT-PCR Primer

Paired forward: 5' CAGCTTGGTGGTGTCTTTGT

Paired reverse: 5' GCAGAATTCGGGAAATGTCG

Splice forward: 5' GCAGATGCAAAAAGTCCAGGT

Splice reverse: 5' CTCGTAATACCTGCCAGAA

Homeo forward: 5' TCTAATCGAAAGGGCCAAATG

Homeo reverse: 5' AGGAGGAGACAGGTGTGGTG

GAPDH forward: 5' ATTCAACGGCACAGTCAAGG

GAPDH reverse: 5' TGGATGCAGGGATGATGTTT

HPRT forward: 5' GTTGGATACAGGCCAGACTTTGT

HPRT reverse: 5' CCACAGGACTAGAACACCTGCTA

eGFP forward: 5' CGTAAACGGCCACAAGTTCAGCGTG

eGFP reverse: 5' ACTGGGTGCTCAGGTAGTGGTTGTC

Ngn2 forward: 5' ACCGCATGCACAACCTAAAC

Ngn2 reverse: 5' AGCGCCAGATGTAATTGTG

6.10 Quantification of neurons and proliferating cells

The quantification of neurons was performed in sections of the cerebral cortex at E14 from WT and homozygous mutants (Pax6^{Sey}-/-, Pax6^{Aey18}-/-, Pax6^{4Neu}-/- and Pax6(5a)-/-) at corresponding rostral, intermediate and caudal levels stained for NeuN. The thickness of the NeuN-positive cortical plate was measured in confocal pictures taken in a defined (lateral) area of the cortex by first drawing a line at right angle to the ventricular surface (VS) from the VS to the pial surface. The length of this line was determined by the ImageJ program and served as measure of the total cortical thickness. A second line was drawn from the apical to the basal side of the NeuN-positive band, and its length served as a measure for the thickness of the band of neurons, the cortical plate. The width of the cortical plate was calculated as the proportion of the overall thickness of the cerebral cortex (see table 2).

The quantification of PH3 positive cells was performed by placing a 150µm wide square, covering the entire cortical thickness parallel to the VS. All PH3 positive cells in this square were counted separately for cells lining the ventricle (VZ cells) and cells at abventricular positions (SVZ cells defined as PH3 positive cells 5 or more cell diameters away from the VS; see Smart, 1976; table 2).

The quantification of PH3 positive cells in the E14 WT, α6 integrin-/-, LNγ1 mutant hemispheres were quantified using the neuroLucida system. The hemispheres were outlined, thus with the help of the perimeter the size of the area of quantification was determined. In this area, the numbers of PH3 positive cells at the ventricular surface and at abventricular positions were quantified.

For the clonal analysis in vitro, all clones per coverslip were assessed for their cell type or size and the mean was calculated per coverslip (excluding coverslips with more than 50 clones).

6.11 Statistics

For all data sets, the arithmetic average, the standard deviation and the standard error of the mean was calculated as follows:

the arithmetic average:
$$\bar{x} = \frac{1}{n} \sum_{i=1}^n x_i$$

the standard deviation (s.d) :

$$s = \sqrt{\frac{\sum_{i=1}^n (x_i - \bar{x})^2}{n-1}}$$

the standard error of the mean (SEM):

$$SEM = \frac{s}{\sqrt{n}}$$

Error bars depict in the histograms either standard deviated (s.d.) or standard error of the mean (s.e.m.). Group comparisons were made with the unpaired t-test and p-values smaller than 0.05 were considered significant (*), p-values smaller than 0.01 were considered highly significant (***) . Calculations of the arithmetic average, the standard deviation, the standard error of the mean were performed with Microsoft Excel. The significance of the obtained data was tested using the program Stats.

6.12 Material

6.12.1 Microscopy

Fluorescent microscope	
AxioPhot microscope	Zeiss
HBO 100W fluorescent lamp	Zeiss
AxioCam HRc camera	Zeiss
Apo Tome	Zeiss
AxioVision 3.1.1.1 and 4.1 program	Zeiss
Objective Plan Neofluar 5x/0,15 (Phase 1)	Zeiss
Objective Plan Neofluar 10x/0,30 (Phase 1)	Zeiss
Objective Plan Neofluar 20x/0,50 (Phase 2)	Zeiss
Objective Plan Neofluar 40x/0,75 (Phase 2)	Zeiss
Objektive Plan-Apochromat 40x/1,30 Oil	Zeiss
Objektive Plan-Apochromat 63x/1,40 Oil (Phase 3)	Zeiss

Fluorescent stereomicroscope	
SZX 12 microscope	Olympus
U-RFL-T fluorescent lamp	Olympus
U-CMAD3 incl. U-TV1 X camera	Olympus
AnalySIS 3.1 program	Soft Imaging Systems

Confocal microscope	
Leitz DM RBE microscope	Leitz
Leica TCS NT confocal	Leica
HBO 50W fluorescent lamp	Leica
TCS NT Vers.1.6.587 program	Leica
Objective HC PL APO 10x/0.40 IMM	Leica
Objective HC PL APO 20x/0.70 IMM CORR	Leica
Objective PL APO 40x/1.25 oil Ph3	Leica
Objective PL APO 63x/1.32 oil Ph3	Leica

Confocal microscope	Olympus
Olympus FV1000	
HBO 100W fluorescent lamp	Olympus
Objective 10x	Olympus
Objective 20xW	Olympus
Objective 40x	Olympus
Objective 63x	Olympus

Confocal microscope Zeiss LSM 510	Zeiss
HBO 100W fluorescent lamp	Zeiss
Objective 10x	Zeiss
Objective 20xW	Zeiss
Objective 20x	Zeiss
Objective 40x	Zeiss
Objective 40xW	Zeiss
Objective 63x	Zeiss

6.12.2 Complex media, buffers and solutions

Name	Protocol
Alkaline-phosphatase staining buffer (AP-buffer) ISH)	100mM NaCl 50mM MgCl ₂ 100mM Tris pH9.5 0.1% tween-20 1mM levamisole in dd H ₂ O
AP - NBT/BCIP (ISH)	AP 350µg/ml NBT 175µg/ml BCIP
2x HBS	50mM HEPES, pH 7.05 50mM KCl 12mM dextrose 280mM NaCl 1.5mM Na ₂ HPO ₄
Blocking-solution (ISH)	MABT 2% blocking reagent 20% heat inactivated sheep serum
BrdU-Solution for cell culture	1mM BrdU in ddH ₂ O

BrdU-Solution for i.p.-Injection	5mg/ml (w/v) BrdU in 1x PBS
Di-sodium-tetraborate-buffer (0.1M) pH 8.5	0.1 M Na ₂ B ₄ O ₇ · H ₂ O in dd H ₂ O
Cell culture medium for primary cells and BOSC23helper free packaging cells	10% (v/v) FCS (heat inactivated 30 min at 56°C) , 1% (v/v) Penicillin-Streptomycin in DMEM (Gibco)
Cell culture medium for gpg cells	10% (v/v) FCS (heat inactivated 30 min at 56°C) , 1% (v/v) Penicillin-Streptomycin in DMEM (Gibco), 1µg/ml tetracycline, 2µg/ml puromycin and 0.3mg/ml G418
Ethanol-glacial acetic acid	20% (v/v) glacial acetic acid in ethanol absolute
FCS-PS-Medium	10% (v/v) FCS (heat inactivated 30 min. at 56°C) 1% (v/v) Penicillin-Streptomycin in DMEM
Fast Green	1% in H ₂ O
HCl (2.4 N)	2.4 N HCl (37 % (w/v)) in dd H ₂ O
HEPES-HBSS-Medium	10 mM HEPES in HBSS
Hybridisation buffer (ISH)	1x salt solution 50% formamide 10% dextran sulfate 1mg/ml wheat germ tRNA 1x Denhardt's solution ddH ₂ O
LB (Luria-Bertani) medium PH 7.0	20g/l LB broth base in ddH ₂ O
LB-agar	LB-medium 15g/l agar

LiCl (4M) (ISH)	4M LiCl ddH ₂ O
Lysis buffer pH 8.5	100mM TrisHCl 5mM EDTA 0.2% SDS 200mM NaCl 100µg/ml proteinase K
MABT (5x) (ISH) pH 7.5	500mM maleic acid 750mM NaCl 0.1% tween-20 ddH ₂ O
NaN ₃ -PBS (0.05%)	0.05% (w/v) NaN ₃ in 1x PBS
NP40 (0.1%)	0.1% NP40 (v/v) in 1x PBS
PBS (Phosphate buffered salt solution, 1x) pH 7.4	137 mM NaCl 2.7 mM KCl 80.9 mM Na ₂ HPO ₄ 1.5 mM KH ₂ PO ₄ in ddH ₂ O
PFA (2%)	2% (w/v) paraformaldehyde in 1x PBS
PFA (4%)	4% (w/v) paraformaldehyde in 1x PBS
Poly-D-lysine-hydrobromide solution	1% (v/v) PDLsolved (1mg/ml PDL in ddH ₂ O o/n solved) in 0.1M sodium-tetraborate buffer
Propidium iodide (PI) Stock-solution	10mg/ml in PBS
RNase Stock-solution	500U/ml in H ₂ O

Saline	0.9% (w/v) NaCl in ddH ₂ O
Salt solution (10x) (ISH)	2M NaCl 90mM Tris HCl, pH7.5 10mM Tris base 70mM NaH ₂ PO ₄ 50mM Na ₂ H PO ₄ 50mM EDTA ddH ₂ O
SATO-medium for primary cell culture	DMEM 1g/l Glucose 2mM Glutamine 10µg/ml Insulin (bovine) 100µg/ml Transferrin (human) 0.0286% BSA-pathocyte 0.2µM Progesterone 0.1mM Putrescine 0.45µM Thyroxine 0.224µM Selenite 0.5µM Tri-iodo-thyronine
Sodium-Citrate buffer	10x 0.1M Sodium-Citrate, pH6.0 in ddH ₂ O
SSC (20x) (ISH)	3M NaCl 0.3M sodium citrate in ddH ₂ O
Sucrose-PBS-solution (30%)	30% (w/v) sucrose in 1x PBS
TBE (10x)	450mM Tris base 440mM boric acid 10mM EDTA in ddH ₂ O
TE pH 8.0	10mM TrisHCl 1mM EDTA in ddH ₂ O

TE-buffer pH 7.5	10mM TrisHCl 0.1mM EDTA in ddH ₂ O
TNE	50mM Tris-HCl (pH7.8) 130mM NaCl 1mM EDTA
Triton X-100 10%	10% (v/v) Triton X-100 in 1x PBS
Tween-20 (0.1% / 0.5%) (ISH)	0.1% / 0.5% (v/v) Tween-20 in 1x PBS
Washing solution (ISH)	1xSSC 50% formamide 0.1% tween-20

6.12.3 Product list

Name	Supplier
Agarose (electrophoresis)	Biozym
Agarose high EEO	Biomol
Ampicillin	Sigma
Anti-DIG-FAB-fragments alkaline phosphatase	Roche
Aqua Poly/Mount mounting medium	Polysciences
Bacto-Agar	DIFCO Laboratories
BCIP (5-bromo-4-chloro-3-indolyl-phosphate, 4-toluidine salt)	Roche
beta-mercaptoethanol	Merck
Blocking reagent	Roche
Boric acid	Merck
BrdU (5-Bromo-2-desoxyuridin)	Sigma
Bromphenol blue	Merck
BSA	Sigma
CaCl ₂	Sigma
cDNA-Synthesis Kit	Invitrogen
CO ₂ -Gas	Air Liquide
DAPI	Pierce

Denhardt's solution	Sigma
Dextran sulfate	Sigma
Diethylether for anesthesia	Hoechst
DIG-RNA labelling mix (10x; DIG-UTP)	Roche
Di-Sodiumhydrogenphosphate Na ₂ HPO ₄	Merck
dNTP (for PCR)	Pharmacia Biotech
Dulbecco's modified Eagle Medium (DMEM) (with Glutamax-1 (L-Alanyl-L-Glutamin) without Natriumpyruvate with Glucose with Pyridoxin)	Gibco
EDTA (Titrplex)	Merck
Ethanol absolute (EtOH)	Riedel-deHaën
Fast Green FCF	Sigma
Fetal Calf Serum (FCS)	Sigma
Formamide	Merck
Geneticin (G418-sulfate)	Gibco
Gentamycin	Gibco
Glucose (d-glucose)	Merck
Glycerol (87%)	Merck
Glycin	Sigma
Hank's buffered salt solution (HBSS)	Gibco
Heat inactivated sheep serum	Sigma
HEPES-Buffer solution 1 M, pH 7,2 - 7,5	Gibco
Hydrochloric acid (37 %) HCl	Merck
Immersion oil 518N	Zeiss
Insulin	Sigma
Isopropanol	Merck
Kaliumchloride KCl	Merck
Kaliumdihydrogenphosphate KH ₂ PO ₄	Merck
LB broth base	Gibco
Levamisole	Sigma
Lightcycler Kit	Roche
Lipofectamine 2000	Invitrogen
l-glutamine (200mM)	Gibco
LiCl	Merck
Maleic acid	Fluka
Methanol absolut (MeOH)	Merck
MgCl ₂	Merck
MgSO ₄ ·7H ₂ O	Merck
MidiPrep-Kit	Qiagen
MidiTip 100 column	Qiagen

Molecular weight marker (1kb-ladder)	Gibco
MoMLV reverse transcriptase	Roche
NaCl	Merck
NaH ₂ PO ₄	Merck
NaHCO ₃	Merck
NaN ₃ (pure)	Merck
Natriumtetraborate (Borax) Na ₂ B ₄ O ₇ -H ₂ O	Sigma
NBT (Nitroblue tetrazolium chloride)	Roche
Normal goat serum (NGS)	Vector Laboratories
NP40 – Igepal	Sigma
Oligo(dT)12-18 primers	Roche
Opti-MEM I reduced serum Medium	Invitrogen
Paraformaldehyde (PFA)	Merck
PCR-buffer (10x)	Qiagen
Penicillin/Streptomycin-Solution 10 000 E Penicillin, 10 0000 µg/ml Streptomycin, as PenicillinG (Sodiumsalt) & Streptomycinsulfate	Gibco
Pfu-Polymerase	MBI
Phenol-chloroform-isoamylalcohol (50:49:1)	Gibco
Poly-D-Lysine Hydrobromide (PDL)	Sigma
Polyoxyethylenesorbitanmonolaurate (Tween-20)	Biorad
Progesterone	Sigma
Propidium-iodide (PI)	Sigma
Proteinase K	Roche
Putrescine	Sigma
Q-Solution (5x)	Qiagen
Red fluorescent RetroBeads™ (Beads)	Lumafluor
Restriction enzymes	New England Biolabs
RNAlater	Ambion
RNA polymerase 50U/µl (T3, T7, SP6)	Stratagene, MBI
RNase A	Qiagen
RNase inhibitor	Boehringer Mannheim
RNeasy Kit	Qiagen
RT-PCR Enzyme Mix	Roche
RT-PCR Reaction Mix SYBR green	Roche
SDS	Roth
Selenite	Sigma
Sodium citrate	Merck
Sodium selenite	Merck
Sodium acetate	Merck

Sucrose	Merck
Taq-DNA-Polymerase	Qiagen
Thyraxine	Sigma
Top10 cells	Invitrogen
Transcription buffer (5x) (ISH)	Stratagene
Transferrin	Sigma
Tri-iodo-thyronine	Sigma
TrisBase	Merck
TrisHCl	Merck
Triton X-100	Roth
Trizol	Gibco
Trypsin Type XII, 9000 BASF units/mg	Sigma
Trypsin-EDTA (1x) 0,05 % (w/v) Trypsin in HBSS without Ca ²⁺ , Mg ²⁺ with 0,02 % (w/v) EDTA (4Na)	Gibco
Wheat germ tRNA	Sigma

6.12.4 Consumables

Name	Supplier
Borosilicate glass capillaries 1.5mmO.D. x 0.86mm I.D. GC1500F-10	Havard Apparatus
Cell culture dishes, sterile (100-, 200 mm)	Falcon
Cell culture flasks (75-, 175 cm ²)	Falcon
Cell culture tubes, sterile (15-, 50 ml)	Falcon
Centriprep YM-50 (4311)	Amicon
Coverslips 24 x 24 mm	Marienfeld
Coverslips 24 x 50 mm	Marienfeld
Coverslips Ø 13 mm, autoclaved	BDH
Eppendorf tubes (0.5-, 1.5, 2.0 ml)	Eppendorf
Glass slides 76 x 26 mm, frosted end	Menzel Gläser
Glass slides Superfrost®-Plus 76 x 26mm	Menzel Gläser
Multi-well cell culture-plates, sterile (6-, 24-, 48-wells)	Nunc
Parafilm	American National can
Pasteur pipettes, autoclaved	Volac
PCR-tubes (0.2ml)	Roth
Permeable filtermembrane inserts Millicell-CM (0,4µm pore, 30mm diameter)	Millipore
Pipettes, sterile (5-, 10-, 25 ml)	Falcon

Polyallomer Centrifuge tubes 1x3 ½ in (25x 89mm)	Beckman
Razor blades, extra thin	Gillette
Superglue	UHU
Syringe filters 0.45µm	Renner
Syringe needles (Neolus, 0,4mm)	Terumo
Syringe - fine dosage (1ml)	Braun
Syringes (10-50ml)	Becton Dickinson
Whatman chromatography paper	Whatman

6.12.5 Instruments

Name	Supplier
Agarose gel chambers	MPI-workshop, Neolab
Bakterial incubator	Heraeus
Bakterial shaker Innova 4000	New Brunswick Scientific
Blade holder	FST
Bench centrifuge 5415 C	Eppendorf
Cell culture incubator	Heraeus, Binder
Centrifuge Rotana 460R	Hettich
Cooling centrifuge Sepatech Omnifuge 2.0 RS	Heraeus
Cryostate CM 3050, Cryostate CM 3050S	Leica
Electroporation tweezer platinum electrode round, 5mm, CUY650P5	Protech
Forceps Dumont #5 'Biologie' (0,05 x 0,01) mm	Fine Science Tools
Grinder Model EG-44	Narishige
Heating block	Liebisch, Eppendorf
Holder for glass capillary WP1	Protech
Hybridisation oven	Memmert
Hybridisation oven HB-1000 Hybridizer (for DNA lysis)	UVP Laboratory Products
Lightcycler	Roche
Neubauer-counting chamber improved bright-line (depth 0,100 mm/0,0025 mm ²)	Superior
Orbital shaker KS 500,	Janke & Kunkel
PCR mashine My cycler	BioRad
PCR mashine GeneAmp PCRSytem 9700	Applied Biosystems
Phase contrast microscope Diavert	Leitz
pH-meter inolab pH720	WTW
Power supply	Biorad
Preparation lights KL1500 electronic	Leica

Puller for capillaries Model PC-10	Narishige
Sorvall RC-5B refrigerated superspeed centrifuge	DuPont Instruments
Spectrophotometer, Ultrospec 3000	Pharmacia Biotech
Stereomicroscope, Wild M3Z	Heerbrugg
Stereomicroscope, Wild M8,	Leica
Steril hood "Edge Gard Hood"	The Baker Company
Steril hood Class II Typ A/B3	Nuair Biological Safety Instruments
Steril hood Herasafe	Kendro
Stimulator (TSS 10) for electroporation	Intracell
Tissue chopper	Mickle Laboratory Engineering
Ultracentrifuge Avanti J-301	Beckman Coulter
Vibratome Vibraslice 752M	Campden Instruments
Vortex	Scientific Industries
Waterbath	GFL
Waterbath for in-situ	GFL

7 Results

7.1 The influence of BM contact on radial glia cell fate and proliferation

In order to address the question whether the basal cell attachment of radial glia cells at the basement membrane has an influence on the regulation of cell proliferation and neurogenesis specific mouse mutants lacking the basal cell attachment of radial glia cells were analyzed. The laminin $\gamma 1$ mutant is characterized by the targeted deletion of the nidogen-binding site in the γ -chain, thus the BM is formed but the components are not properly linked (Halfter et al., 2002). This leads to a detachment of radial glia endfeet from the basement membrane (Fig. 10B,D,F). A second basement membrane mutant that has been analyzed to answer this question is the $\alpha 6$ integrin $^{-/-}$ mouse. $\alpha 6$ integrin forms together with $\beta 1$ integrin a heterodimer and thus acts as a ligand for laminin. Due to the loss of the laminin receptor no proper BM assembly occurs (Fig. 11D; (Georges-Labouesse et al., 1998). Despite the improper assembly of the BM radial glia morphology did not seem to be severely abnormal (Fig. 12B,D,F).

7.1.1 Neurogenesis in the absence of basal cell attachment/polarity

Neurogenesis was examined by immunohistochemistry against the neuronal marker β III-Tubulin. Youngborn neurons accumulate underneath the pial surface and thus form the cortical plate (CP). Immunohistochemistry against β III-Tubulin in the laminin $\gamma 1$ mutant (LN $\gamma 1$ mutant) (Fig. 13B) and in the $\alpha 6$ integrin $^{-/-}$ (Fig. 14B) revealed no obvious changes in the degree of neurogenesis due the basal detachment of radial glia endfeet. In WT and $\alpha 6$ integrin $^{-/-}$ frontal sections a clear band of densely packed neurons was detectable at E14 in DAPI nuclear staining, whereas in the LN $\gamma 1$ mutant the CP seemed less compact and organized (see also Halfter et al., 2002), thus the overall number of neurons could be changed and therefore additional quantification is required in both mutants, especially since both mutants develop neuronal ectopias outside the BM in the subarachnoidal space (Georges-Labouesse et al., 1998; Halfter et al., 2002). According to the results obtained so far, it seems that the basal detachment of radial glia endfeet does not influence the rate of neurogenesis.

7.1.2 Proliferation in the absence of basal cell attachment/polarity:

Not only the rate of neurogenesis but also cell proliferation might be affected due to the loss of basal cell polarity especially since the BM concentrates growth factors, that might be supplied to the radial glia endfeet contacting the BM. Previously it has been shown that a radial glia cell retains the process attached to the BM during cell division (Miyata et al., 2001). Thus it has been speculated that attachment could act on the cell behaviour in regard to cell fate (Fishell and Kriegstein, 2003). Since no changes in neurogenesis were detected, cell proliferation has been analyzed in the LN γ 1 mutant and the α 6 integrin $^{-/-}$. As mentioned above two proliferative cell populations are present in the telencephalon VZ and SVZ. Dividing precursor cells in VZ and SVZ were visualized by immunohistochemistry against phospho-Histone H3 (PH3), a marker for cells in M-phase (Hendzel et al., 1997) and quantified per area in frontal sections of rostral, intermediate and caudal levels of the telencephalon with the neuroLucida system. Since VZ cells divide at the VS and SVZ cells at abventricular positions the proliferative behavior of both populations can be analyzed separately by immunohistochemistry against PH3. No significant changes in the number of PH3 $^{+}$ cells at the VS or at non-surface positions were detectable in the LN γ 1 mutant (n= 2 litter; total number of quantified hemispheres WT n= 43; LN γ 1 mut n= 51) and α 6 integrin $^{-/-}$ (n= 3 litter, total number of quantified hemispheres WT n= 39; α 6 integrin $^{-/-}$ n= 50) due to loss of basal cell process attachment (see Fig. 15 or table 1). Thus it seems that the basal attachment is not required for the regulation of cell proliferation.

7.1.2.1 Ectopic cell clusters

However, in the dorsal and ventral telencephalon of the LN γ 1 mutant mice, ectopic clusters of proliferating Ki67 $^{+}$ and PH3 $^{+}$ cells were detected inside the cortical plate. The ectopic clusters of proliferating cells were visible for the first time at E13/E14 when the first neurons were generated, since before the entire wall of the dorsal telencephalon contained only proliferating neuroepithelial cells. The clusters of proliferating cells were detectable until E18 in the telencephalon, although they became smaller correlated to the overall decrease in proliferation. In order to check whether due to the aberrant formation of the basement membrane cells, as for example fibroblasts, have migrated into the parenchyma immunohistochemistry against fibronectin (FN) and Ki67 has been performed, but no double positive cells were detected (Fig. 16), thus we could exclude that proliferating cells migrated

into the cortex. Anti-nestin immunostaining revealed the neural origin of these cells (Fig. 16) that were in addition RC2- and BLBP-immunopositive (Fig. 17). Since SVZ precursors normally do not contain RC2 (Hartfuss et al., 2001), these data suggest that the ectopic precursors may originate from radial glia. In order to examine whether these cells generate prematurely astroglia, immunohistochemistry against GFAP has been performed, but no GFAP positive cells were detectable at E18 in these ectopic clusters.

7.1.2.2 Reelin signalling

The neurons of the marginal zone (MZ) secrete reelin, a large (385kDa) extracellular matrix protein, which is important for the neuronal migrational behaviour. The reelin expression in the LN γ 1 mutant showed alterations that might lead to changes in the neuronal migration since these mice develop ectopias (Halfter et al., 2002), which are protrusions of neurons at the brain outside. In order to see whether the formation of ectopic proliferating cell clusters is related to the altered reelin signalling immunohistochemistry against reelin and Ki67 has been performed. The band of reelin positive cells is discontinuously in the cortex of the LN γ 1 mutant. Thus one possibility could be that in regions where reelin is missing, the ectopic clusters are forming, but this was not the case. Occasionally reelin positive cells and ectopic proliferating clusters were located close to each other (yellow circles in Fig. 18) or the clusters occurred where reelin positive cells were lacking (yellow square in Fig. 18). Thus no clear correlation between the lack or presence of reelin and the formation of ectopic proliferating cell clusters has been observed (Fig. 18). The reelin expression in the α 6Integrin $-/-$ mice was not altered (Fig. 19) and no ectopic cell clusters have been detected in this mutant.

7.1.2.3 Interkinetic nuclear migration in absence of radial glia endfeet attachment

Stable apical and basal cell attachment of radial glia may be a prerequisite for interkinetic nuclear migration. The mechanism of the nuclear translocation during the interkinetic nuclear migration in proliferating VZ cells is not known yet, however interkinetic nuclear migration was disturbed upon loss of Lis1 a microtubule associated protein (Gambello et al., 2003), thus the microtubule cytoskeleton could be involved here. A 0.5 and a 6 hour BrdU pulse has been performed in the LN γ 1 mutant in order to analyze the interkinetic nuclear migration when the

cells lack the basal endfeet attachment. Surprisingly no severe alterations were detected in the interkinetic nuclear migration (Fig. 20). No changes were detectable after a 0.5h BrdU pulse and 6.0 hour BrdU pulse in the cortex of the LN γ 1 mutant (Fig. 20B) compared to the WT (Fig. 20A). Thus, the basal attachment of radial glia endfeet seems not to be important for the mechanism of interkinetic nuclear migration.

7.1.2.4 Orientation of cell division in the absence of basal radial glia cell attachment

Detachment of radial glia endfeet might lead to changes in the cytoskeleton and might thus influence the angle of cell division (and thereby maybe even cell fate). The chromatin was counterstained by propidium-iodide (PI, dye intercalating in the major groove of the DNA) and angles of cell divisions were measured in ana- and telophase of M-phase, since the spindle apparatus is rotating until the cell enters anaphase (Haydar et al., 2003), by imageJ program. Cell divisions were classified into three groups: horizontal cell divisions in an angle of 0-30° with respect to the VS, oblique cell division (30-60°) and perpendicular cell divisions (60-90°) with respect to the VS. This analysis has been performed in frontal sections of rostral, intermediate and caudal levels of WT and LN γ 1 mutant, WT and α 6 integrin $^{-/-}$ and in a third basement membrane mutant, the perlecan $^{-/-}$ and the corresponding WT. The perlecan $^{-/-}$ lacks the heparan sulphate protoglycan perlecan, which is a linker molecule that connects laminin and collagen. The homozygous perlecan $^{-/-}$ develops almost always an exencephalic brain at E14, which means that the brain is severely malformed (Fig. 21). In total more than 20 litters of E14 perlecan $^{-/-}$ mice have been prepared and only one of these contained a homozygous perlecan $^{-/-}$ that developed an exencephalus at one hemisphere whereas the other hemisphere remained closed (Fig. 21). Since the intact hemisphere was nevertheless malformed, it was only possible to determine the percentages of dividing cells at the VS. In all three basement membrane mutants the same percentages of cells dividing in a perpendicular, horizontal or oblique plane of division were detected (Fig. 22A,B,C). No significant changes in the orientation cell divisions were detected between WT (Fig. 22A; n= 103 mitosis) and LN γ 1 mutant (Fig. 22A; 2 litter analyzed; n= 110 mitosis), WT (Fig. 22B; n= 89 mitosis) and α 6 integrin $^{-/-}$ (Fig. 22B; 2 litter analyzed; n= 150 mitosis) and in WT (Fig. 22C; n= 53 mitosis) and the perlecan $^{-/-}$ (Fig. 22C; 1 litter analyzed; n= 41 mitosis). Taken together it seems that the basal detachment of radial glia endfeet at the basement membrane does not affect the orientation of cell division.

7.2 The influence of the distinct Pax6 DNA-binding domains on cell fate, proliferation and patterning in the telencephalon

Not only extrinsic cues can influence the behavior of a cell in regard of cell proliferation and differentiation, but also intrinsic factors as for example transcription factors play a role.

As detailed above, the paired box transcription factor Pax6 plays an important role in the developing forebrain. Pax6 is involved in the regulation of neurogenesis in the dorsal telencephalon (see for example: Heins et al., 2002; Schmahl et al., 1993), in the regulation of cell proliferation (Estivill-Torrus et al., 2002; Götz et al., 1998) and in the regionalisation of the telencephalon coupled with the formation of the pallial-subpallial boundary (Chapouton et al., 1999; Heins et al., 2002; Stoykova et al., 1996; Stoykova et al., 1997; Stoykova et al., 2000; Toresson et al., 2000; Yun et al., 2001). One intriguing question that arises in this context is: How are all these diverse functions coordinated at the molecular level? As described above, Pax6 consists of a paired DNA-binding domain, which is subdivided in the N-terminal PAI subdomain and the C-terminal RED subdomain and a paired-type HD. In order to examine the role of the different DNA binding domains in vivo I took advantage of different mutant Pax6 alleles affecting specifically the different DNA-binding domains. The role of the PD was assessed by the analysis of the *Pax6^{Aey18}* mutant mice, which are characterized by the loss of a splice acceptor site in front of exon 5a such that exon 5a and exon 6 are deleted. Thus a large part of the PD is missing, whereas the HD and TA remain unaffected (Fig. 23B; Haubst et al., 2004). The *Pax6^{tm1Gfs}* mice (here referred to as *Pax6(5a)*^{-/-}; Singh et al., 2002), are specified by the targeted deletion of exon 5a, thus the specific function of exon 5a has been assessed by the analysis these mutants (Fig. 23C). The role of the HD was analyzed by means of the *Pax6^{4Neu}* mutant mice, carrying a pointmutation in the third helix of the HD leading to a change in the aminoacid at the critical position 50. Thus DNA-binding of the HD is abolished, but the PD and TAD are retained (Fig. 23D; Favor et al., 2001). The results obtained from the analysis of the different Pax6 alleles was compared to WT littermates and the phenotype of the functional null allele *Pax6^{Sey}*^{-/-} (Fig. 23E; Hill et al., 1991).

7.2.1 The role of the different Pax6 DNA-binding domains in the regulation of neurogenesis

Neurogenesis was analysed by immunohistochemistry against the neuronal marker proteins NeuN and β III-Tubulin. As described above, postmitotic neurons migrate from the proliferative zones in the dorsal telencephalon towards the pial surface and settle below, forming the cortical plate (CP). Immunohistochemistry against NeuN in $Pax6^{Aey18-/-}$ mutant mice compared to WT littermates (Fig. 24A) showed that the thickness of the CP is strongly decreased (Fig. 24B), whereas the specific loss of the HD in the $Pax6^{4Neu-/-}$ mice had no effects on the thickness of the CP, i.e. the degree of neurogenesis (Fig. 24D). The analysis of the $Pax6(5a-/-)$ mice revealed no obvious changes in the degree of neurogenesis compared to WT (Fig. 24C). The quantification of the thickness of the CP in comparison to the overall thickness of the cerebral cortex revealed that neurogenesis in the $Pax6^{Aey18-/-}$ mice is significantly decreased to the same extent ($p < 0.001$) as in the $Pax6^{Sey-/-}$ mice (table 2). Thus even though $Pax6^{Aey18-/-}$ is not a truncation mutant and still has an intact HD and TAD it exhibits the full neurogenesis phenotype, suggesting a key role of the paired domain in this process. The quantification analysis of neurogenesis (ratio of thickness CP to thickness of the cortex) confirmed the findings of the immunohistochemical analysis in the HD mutant mice $Pax6^{4Neu-/-}$ and also the targeted deletion of exon5a in the $Pax(5a-/-)$ mice, where no changes were detectable (see table 2). Thus, the PD, but not the HD of Pax6 is required for the regulation of neurogenesis in the cerebral cortex.

7.2.1.1 The generation of upper layer neurons in the different Pax6 mutant alleles: *Tbr2* and *Svet1* expression

Recently it has been shown that the transition of radial glia cells to SVZ cells is associated with the upregulation of the T-domain transcription factor *Tbr2* (Bulfone et al., 1999) and a downregulation of Pax6 (Englund et al., 2005). *Tbr2* mRNA expression was strongly reduced in the the $Pax6^{Sey-/-}$ mice (Englund et al., 2005), consistent with the aberrant specification of SVZ cells in the $Pax6^{Sey-/-}$ mutant cortex (Nieto et al., 2004; Tarabykin et al., 2001). In order to determine which DNA-binding domains are involved in the regulation of *Tbr2* I examined its expression in the domain-specific Pax6 mutant mice. *Tbr2* expression is absent in the cortex of the PD mutant ($Pax6^{Aey18-/-}$) (Fig. 25C), whereas it was still detectable in the cortex of the $Pax6^{4Neu-/-}$ mice (Fig. 25B). Interestingly, I found *Tbr2* also expressed in the neurons in

the eye (Fig. 25D), which means that it is not only expressed in neurogenic precursors but also in neurons, as it has been described also for the early telencephalon E10-E12 by Englund (2005). Cux2 and Svet1 two further marker proteins specifying SVZ precursor cells and their progeny the upper layer neurons have been identified recently (Nieto et al., 2004; Tarabykin et al., 2001; Zimmer et al., 2004). Cux2 and Svet1 are absent in the functional null allele *Pax6^{Sey}*^{-/-}. I analyzed in this work the expression pattern of Svet1 (Tarabykin et al., 2001) by in situ hybridisation in the Pax6 alleles *Pax6^{Sey}*^{-/-} (was used as a control), *Pax6^{Aey18}*^{-/-}, *Pax6^{4Neu}*^{-/-} and *Pax6(5a)*^{-/-} at E14. Svet1 expression was absent in the SVZ of the functional null allele *Pax6^{Sey}*^{-/-} (Fig. 26A') and almost completely absent in the SVZ of the *Pax6^{Aey18}*^{-/-} (Fig. 26B'), while it was expressed normally in the SVZ of *Pax6^{4Neu}*^{-/-} and *Pax6(5a)*^{-/-} mice. Thus, it seems that the PD is required for the expression of Tbr2 and Svet1 in the SVZ, while the HD seems to play no role in that regard.

7.2.2 The role of the different Pax6 DNA-binding domains in the regulation of cell proliferation

In the functional null allele *Pax6^{Sey}* cell proliferation is increased in the dorsal telencephalon (Estivill-Torrus et al., 2002; Götz et al., 1998). In order to assess proliferating cells immunohistochemistry against Ki67 (Gerlach et al., 1997), a marker for proliferating cells in all stages of the cell cycle and against phospho-Histone H3 (PH3), a marker for cells in M-phase (Hendzel et al., 1997) was performed. Since VZ precursor cells divide at the VS and SVZ precursor cells at abventricular positions (Haubensak et al., 2004; Miyata et al., 2004; Noctor et al., 2004; Smart, 1976), PH3 was not only used for the detection of cells in M-phase but also as a marker to discriminate these two precursor populations (see for example Fig. 24A).

In a first set of experiments dividing precursor cells were quantified per hemisphere in cortex (ctx) and ganglionic eminence (GE) during development starting at E12, when the first SVZ cells become apparent until late neurogenesis at E16 in the *Pax6^{Sey}*^{-/-} mice. Loss of functional Pax6 protein in the telencephalon of the *Pax6^{Sey}*^{-/-} mice leads specifically to an increase in the percentage of abventricular dividing cells in the cerebral cortex (Fig. 27A). The proportion of cells dividing at abventricular positions in the cortex (ctx) reached levels that resemble the percentages of cells dividing at abventricular positions in the ventral telencephalon (GE) (Fig. 27B), where hardly any Pax6 protein is expressed. Thus, the cerebral cortex of *Pax6^{Sey}*^{-/-} mice seems to achieve proliferative properties of the ventral telencephalon due to the loss of the

functional Pax6 protein. In order to assess which DNA-binding domains of Pax6 are involved in the regulation of cell proliferation in the cerebral cortex, quantification of PH3 positive cells was performed at E14 in the different Pax6 mutant alleles (*Pax6^{Aey18}*^{-/-}, *Pax6^{4Neu}*^{-/-}, *Pax6(5a)*^{-/-}) and compared to the phenotype of the functional null allele *Pax6^{Sey}*^{-/-}. To standardize the quantification, proliferation was quantified per area since alterations in proliferation can affect the size of the cortical hemispheres. Cells dividing at the VS and at non-surface positions were quantified over an area of 150 µm along the VS (see material and methods). Proliferation was strongly increased in the *Pax6^{Aey18}*^{-/-} mice as can be seen in the increased number of PH3 positive cells in the cortex (Fig. 24B). Quantification of dividing precursor cells revealed that the overall number of PH3 positive cells dividing at the ventricle in the *Pax6^{Aey18}*^{-/-} mice was not changed in comparison to the WT cortex, but exclusively the number of PH3 positive cells dividing at abventricular positions was significantly increased (2.7fold, see table 2). This phenotype was very similar to the functional null allele *Pax6^{Sey}*^{-/-} (Fig. 24E), where a 2.4 fold increase in the number of the SVZ precursor cells was detected (see table 2). No changes in the number of PH3 positive cells were detectable in the HD mutant *Pax6^{4Neu}*^{-/-} (Fig. 24D) or in the *Pax6(5a)*^{-/-} mice (Fig. 24C) (table 2).

Thus, the PD not only plays an important role in the regulation of neurogenesis, but is also involved in the regulation of cell proliferation in the dorsal telencephalon, whereas the HD seems to play no role in this regard.

7.2.2.1 Interkinetic nuclear migration

In contrast to SVZ precursor cells, VZ precursor cells undergo interkinetic nuclear migration. One possibility for the increased number of cells dividing at abventricular positions in the *Pax6^{Sey}*^{-/-} cortex could be that the interkinetic nuclear migration is disturbed (Götz et al., 1998). In order to study changes in the interkinetic nuclear migration, BrdU, a DNA base analogon, which is incorporated into the DNA during S-phase of the cell cycle (Nowakowski et al., 1989), was injected intraperitoneally into time pregnant (E14) mice. BrdU is metabolized 30 minutes post injection (Packard et al., 1973) and can be detected by immunohistochemistry. A short pulse of 0.5 hour was used in order to detect cells in S-phase, which are localized at the basal side of the ventricular zone. In the WT cerebral cortex, a band of BrdU positive cells is detectable in the basal part of the ventricular zone after a BrdU pulse of 0.5 hour and the apical zone of the VZ is free of BrdU labelled nuclei (Fig. 28A). A long BrdU pulse of 6 hours was used to assess the translocation of the nuclei towards the VS. This

experiment showed that the VZ precursors have migrated from the basal to the apical end of the VZ in the WT cortex, forming a more or less compact band at the VS (Fig. 28C). Since BrdU labels all cells in S-phase (VZ and SVZ cells) the SVZ cells became apparent as a band above the basal VZ (see Fig. 29C, dashed white line). A 0.5 hour BrdU pulse in the Pax6^{Sey}^{-/-} revealed that cell nuclei are not located in a clear band as it is the case for the E14 WT cortex, but rather more spread all over the VZ with some nuclei located in the apical VZ, close to the VS (Fig. 28B). This impression persists in the 6 hour BrdU pulse (Fig. 28D). Although a certain portion of BrdU positive nuclei translocated to the VS, many BrdU labelled nuclei were displaced and spread all over the proliferative zone reaching even the pial surface (arrows in Fig. 28D) compared to WT. The analysis of the specific PD mutant Pax6^{Aey18}^{-/-} revealed similar a similar phenotype (Fig. 29B), as was detected in the functional null allele Pax6^{Sey}^{-/-} after a 0.5h and 6.0h BrdU pulse. In contrast, the HD mutant mice Pax6^{4Neu}^{-/-} mice (Fig. 30B,D) and the Pax6(5a)^{-/-} (Fig. 31B,D) did not show any changes in that regard after 0.5 hour and 6.0 hours of BrdU pulse. Thus, a 0.5 and 6.0h BrdU pulse leads to a similarly altered phenotype in regard of the location of S-phase cells in the Pax6^{Sey}^{-/-} and Pax6^{Aey18}^{-/-} cortex compared to the WT. No differences were detected in the positions of S-phase cells in the cortex of Pax6^{4Neu}^{-/-} and Pax6(5a)^{-/-} mice, compared to the WT situation. Since Pax6 acts differently on cell proliferation in different regions of the CNS, the interkinetic nuclear migration of neuroepithelium cells in the eye has been studied as well (see below).

7.2.3 The role of the different Pax6 DNA binding domains in telencephalic patterning

Next the role of the PD and HD in mediating dorso-ventral patterning in the forebrain was examined. In the Pax6^{Sey}^{-/-} cortex hardly any Neurogenin (Ngn) 2 immunoreactivity was detectable in the dorsal telencephalon (Fig. 32E), but corresponding to the graded expression of Pax6 (lateral/rostral^{high}, medial/caudal^{low}), Ngn2 was still detectable in medial and caudal regions in the cortex of Pax6^{Sey}^{-/-} and Pax6^{Aey18}^{-/-} mutants (Fig. 33). The expression domains of transcription factors expressed in the ventral telencephalon, such as Mash1, Gsh2 and Olig2, expand into the dorsally in the absence of Pax6 function (Heins et al., 2002; Stoykova et al., 2000; Toresson et al., 2000; Yun et al., 2001). Loss of a functional PD in the Pax6^{Aey18}^{-/-} mutant causes precisely the same phenotype in the lateral cortex (Fig. 32A'; Fig. 34B) as detected in the Pax6^{Sey}^{-/-} mutant mice (Fig. 32D'), while no changes in the dorso-ventral patterning were observed in the cortex of the Pax6(5a)^{-/-} (Fig. 32B') and the HD mutant

Pax6^{4Neu}*-/-* (Fig. 32C' and Fig. 34D,F). These findings further support the crucial role of the canonical PD in telencephalic development.

The region of the telencephalon where the expression domains of dorsal and ventral transcription factor abut is the pallial-subpallial boundary (PSB) (Lumsden and Krumlauf, 1996), which consists of a radial glia fascicle that is specified in the ventral most region of the Pax6 expression territory for example by the expression of secreted frizzled related protein 2 (SFRP2), a putative Wnt-inhibitor (Kim et al., 2001). SFRP2 expression is lost at the PSB of the Pax6^{Sey}*-/-* telencephalon (Kim et al., 2001; Fig. 35D'). The same phenotype was observed in Pax6^{Aey18}*-/-* (Fig. 35B') and interestingly also in the HD mutant Pax6^{4Neu}*-/-* (Fig. 35C'), while SFRP2 expression in the Pax6(5a)*-/-* telencephalon appeared normal (Fig. 35B'). The boundary specific marker reticulon-1 is specifically expressed in the radial glia fascicle of the PSB (Hirata et al., 2002) (see Fig. 36A,C), while no reticulon-1 expression is detectable in the telencephalon of the Pax6^{Sey}*-/-* (Hirata et al., 2002 and Fig. 36E). In contrast to the telencephalon of functional null allele *Pax6*^{Sey}*-/-*, reticulon-1 expression is detectable at the region of the PSB in the telencephalon of the Pax6^{Aey18}*-/-* (Fig. 36B) and Pax6^{4Neu}*-/-* mice (Fig. 36D). However, no formation of the radial glia fascicle can be observed in these two mutants.

Taken together, these results suggest that the HD and the PD cooperate in some aspects as for example the regulation of SFRP2 and reticulon-1 expression, but not all aspects of differentiation of the PSB. Other effects of Pax6 on dorso-ventral patterning, as the region-specific expression of transcription factors depend predominantly on the PD of Pax6.

7.2.4 Role of the Pax6(5a) isoform in vivo

So far it became clear that the PD is the essential DNA-binding domain for the mediation of all aspects in cortical development that involve Pax6 as transcriptional regulator, although the specific deletion of exon5a in the Pax6(5a)*-/-* had no effect on cortical development at E14. In contrast to the other Pax6 mutants (Pax6^{Sey}*-/-*, Pax6^{Aey18}*-/-*, Pax6^{4Neu}*-/-*) analyzed in this work Pax6(5a)*-/-* mice are viable and grow into adulthood. The intriguing question that arises in this context is: What is the specific role of the alternatively spliced PD5a in the telencephalon?

7.2.4.1 Relative expression levels of Pax6(5a), canonical Pax6 and PD-less Pax6

Nothing was known so far about the ratio of expression of the canonical Pax6 compared to the Pax6(5a) isoform in the developing cortex, thus expression levels were determined by RT-PCR using WT cortical RNA of different developmental stages as template. Interestingly Pax6(5a) levels are increasing over time and are expressed almost at the same level as canonical Pax6 at E18 (Fig. 37B). As described above, the PD of the canonical Pax6 is able to bind to both paired domain consensus sites (P6CON and 5aCON), thus it might well be that the specific loss of the Pax6(5a) isoform is compensated by the canonical Pax6. In order to see whether the loss of Pax6(5a) leads to changes in the expression of canonical Pax6, real time RT-PCR on RNA from the early developing (E10, E11, E12) cortex has been performed. Indeed an increase in the expression levels of canonical Pax6 protein was detected. Interestingly, Pax6 expression increased to the same extent as the Pax6(5a) isoform is contributing to the overall Pax6 levels in the WT situation (10-15%, see Fig. 37C).

As described above, alternative splicing leads not only to the generation of the Pax6(5a) isoform, but also to the generation of a PD-less Pax6 form. This isoform consists of the HD as DNA-binding domain and the TAD and has been found to be highly expressed in mouse brain (Mishra et al., 2002), but so far nothing is known about the specific expression of this isoform in the telencephalon. RT-PCR was performed in order to assess the expression levels of the PD-less Pax6 from E10–E18. Interestingly are the expression levels of the PD-less Pax6 form during the early development higher, while they are decreasing at the end of neurogenesis (Fig. 38A).

7.2.4.2 Neurogenesis and cell proliferation in Pax6(5a)^{-/-} during development

In order to see whether the compensation of the loss of the Pax6(5a) expression in the Pax6(5a)^{-/-} by canonical Pax6 at early developmental stages is also reflected in neurogenesis and the regulation of cell proliferation, immunohistochemistry against NeuN and PH3 has been performed. Indeed no differences were detectable in comparison to the WT, while in the cortex of the functional null mutant Pax6^{Sev}^{-/-}, neurogenesis was delayed and cell proliferation was not changed at E12. Thus, early in development (E12) until mid neurogenesis (E14, see above) no changes in regard to neurogenesis and cell proliferation were detected. Since the expression levels of canonical Pax6 and Pax6(5a) are almost equal at E18 it seems rather improbable that canonical Pax6 can compensate the specific loss of

Pax6(5a) at this stage. Therefore it might be possible that the Pax6(5a)^{-/-} mice show a 'late' phenotype. Thus neurogenesis and cell proliferation were analyzed at E16 (Fig. 39) and at postnatal stage P2 (Fig. 40) in the cortex of the Pax6(5a)^{-/-}, but no changes were detected.

One region of the mouse brain where Pax6 expression in the adulthood is linked to neurogenesis is the olfactory bulb (OB) (Hack et al., 2005). Pax6^{Sey}^{-/-} mice are lacking OBs (Hogan et al., 1986) and develop instead an olfactory bulb like structure (OBLS) in the ventral telencephalon (Jimenez et al., 2000; Stoykova et al., 2003). In contrast, olfactory bulbs develop normally in the Pax6(5a)^{-/-} (Fig. 41). Pax6 expression in the OB is mainly restricted to a subset of periglomerular interneurons, which are dopaminergic and located in the glomerular layer of the OB (Fig. 41E). In addition Pax6-immunoreactivity is detectable in the granular layer, where it is localized mostly in young doublecortin-immunoreactive neurons (Hack et al., 2005).

Immunohistochemistry against tyrosine hydroxylase (TH), a rate limiting enzyme in the synthesis of dopamin, was used to understand the role of the Pax6(5a) isoform in the generation of dopaminergic periglomerular interneurons at P2, but no obvious changes in the TH positive neurons of the OB were detected (Fig. 41B,D), except that they appeared less organized and more scattered than in the WT (Fig. 41A,C).

7.2.4.3 Radial glia morphology and changes in gliogenesis in the Pax6(5a)^{-/-}

The radial glia morphology in the Pax6^{Sey}^{-/-} mice that lack any functional Pax6 protein is slightly altered and seems disorganized (Fig. 42B,D,F), although the basement membrane was not altered (Fig. 42H). Possibly could the specific loss of exon5a influence the radial glia morphology, but no changes were detectable in the Pax6(5a)^{-/-} mice during mid- (Fig. 43B,D) and late neurogenesis (Fig. 44F). Interestingly, the further analysis of glial markers at P2 revealed that the glial marker BLBP is stronger expressed in the Pax6(5a)^{-/-} mice (Fig. 44B), than in the WT (Fig. 44A), whereas RC2 and Glutaminsynthase (GS) expression (Fig. 44D) and GFAP expression were not altered.

7.3 The role of the different Pax6 DNA binding domains in patterning of the diencephalon

The Ngn2 expression was also analyzed in the diencephali of the different *Pax6* mutant alleles. In the E14 WT diencephalon Ngn2 expression occurs all along the ventricle in a thin band of cells and is expressed at higher levels in the dorsal and ventral regions, where Pax6 expression occurs (Fig. 45). Ngn2 expression was detectable in the diencephali in the absence of functional Pax6 protein (*Pax6^{Sey}-/-*) (Fig. 46), in the absence of a functional PD (*Pax6^{Aey18}-/-*) (Fig. 47), in the absence of HD DNA-binding (*Pax6^{4Neu}-/-*) (Fig. 48) and in the absence of exon5a (*Pax6(5a)-/-*) (Fig. 49). Thus the loss of functional Pax6 or the loss of a specific DNA-binding domain of Pax6 does not influence the expression of Ngn2 in the diencephalon in contrast to the telencephalon.

7.4 The role of the different Pax6 DNA-binding domains in eye development

As mentioned already above Pax6 is not only an important transcription factor in the developing telencephalon but fulfils as well a pivotal role in the developing eye.

Very briefly, during eye development the optic vesicle (OV) evaginates from the presumptive ventral diencephalon and expands laterally towards the surface ectoderm (SE) in the head region at E8 (Fig. 50). A brief contact between optic vesicle and surface ectoderm is followed by the invagination of the optic vesicle and thus the formation of the two-layered optic cup (Fig. 50). Upon this, thickening of the surface ectoderm is induced and leads to the formation of the lens placode which invaginates from the SE to form the lens (Fig. 50). At these stages Pax6 is expressed in the optic vesicle and in the overlying surface ectoderm. As development proceeds, Pax6 expression becomes restricted to the inner layer of the optic cup (presumptive neuroretina), the surface ectoderm (presumptive cornea) and the lens. Upon completion of the eye development, *Pax6* expression is confined to the neural retina, the cornea and the lens epithelium. The formation and proper positioning of the developing eye depends on the interaction of Pax6 and other transcription factors. Early Pax6 and Pax2 are coexpressed in the optic vesicle (Bäumer et al., 2003), later Pax2 expression is restricted to the ventral optic cup and is finally confined to the optic stalk. The promotor region of Pax6 contains a putative binding site for Pax2 and vice versa. Both transcription factors are repressing each other and hence form the boundary between neuroretina and optic stalk (Schwarz et al., 2000). No eyes

develop in the absence of functional Pax6 protein in the Pax6^{Sey}^{-/-} mice (Grindley et al., 1995; Hill et al., 1991). The optic vesicle expands laterally in order to contact the surface ectoderm. The surface ectoderm in the homozygous Pax6 null mutants is devoid of Pax6 expression (Grindley et al., 1995) and fails to form lens placode and lens pit (Hogan et al., 1988; Hogan et al., 1986), thus no lens develops. The optic vesicle does not invaginate properly and thus no optic cup formation can be observed and no retinal pigmented epithelium (RPE) develops (Grindley et al., 1995). In the remnant eye vesicle do the first neurons develop precociously at E10, but then they die and are not detectable anymore at E14 (Philips et al., 2005).

Here I analyzed the roles of the different DNA-binding domains of Pax6 in the regulation of neurogenesis, cell proliferation and regionalisation in the developing eye at E14.

Loss of a functional PD in the Pax6^{Aey18}^{-/-} mice (Haubst et al., 2004) and loss of a functional HD in the Pax6^{4Neu}^{-/-} mice (Favor et al., 2001) leads to the absence of eye formation, whereas in case of specific loss of the Pax6(5a) isoform in the Pax6(5a)^{-/-} mice (Singh et al., 2002) eye development occurs, even though with morphological aberrations (Singh et al., 2002).

7.4.1 The influence of the different Pax6 DNA-binding domains on neurogenesis in the eye

Within the eye remnant that is detectable in the Pax6^{Sey}^{-/-}, Pax6^{Aey18}^{-/-} and Pax6^{4Neu}^{-/-} mice at E14 retinal tissue was identified by the presence of nestin positive neuroepithelial cells. The lens was not detectable in the Pax6^{Sey}^{-/-} mice, whereas some lens remnants were occasionally detected in the Pax6^{Aey18}^{-/-} and Pax6^{4Neu}^{-/-} mutants (for Pax6^{4Neu}^{-/-} see e.g. Fig. 52B). In order to assess whether any neurons are detectable at E14 in the above described mutant Pax6 alleles immunohistochemistry against β III-Tubulin as a marker for young postmitotic neurons was performed. No β III-Tubulin positive cells were detectable at E14 in the Pax6^{Sey}^{-/-} mice (Fig. 51B), while a considerable number of β III-Tubulin-immunoreactive cells were present in the Pax6^{Aey18}^{-/-} mice (PD mutant) (Fig. 52A) and less in the Pax6^{4Neu}^{-/-} mice (HD mutant) (Fig. 52B). In the Pax6(5a)^{-/-} mice no changes in neurogenesis were detectable in comparison to the WT control (compare Fig. 51A and Fig. 52C). In total 7 different cells types (six neuronal subtypes and Müller glia) are present in the eye, which are generated in a sequential time restricted manner. Among the first neuronal cells generated are the retinal ganglion cells. In order to see whether retinal ganglion cells develop in the absence of a functional PD, PD5a or HD immunohistochemistry against Islet1 and Brain3a (Brn3a) has been performed in the different Pax6 mutants. No Islet 1 or Brn3a positive cells were detectable in the eye remnant

of the Pax6^{Sey}-/- mice (Fig. 53B), while Islet 1 and Brn3a positive cells were detectable in the Pax6^{Aey18}-/- mice (Fig. 53C), Pax6^{4Neu}-/- mice (Fig. 53D) and in the Pax6(5a)-/- mice (Fig. 53E). The retinal pigment epithelium is visible in WT by the normal ‘white’ light of the microscope (Fig. 53A’). In the functional null allele *Pax6*^{Sey}-/- the development of the RPE fails (Grindley et al., 1995), while the same phenotype was observed in the Pax6^{Aey18}-/- mutant eye vesicle, occasionally some RPE was detectable at the outer surface of the eye vesicle in the Pax6^{4Neu}-/- mice (Fig. 53D’, red arrow), whereas the RPE developed normally in the Pax6(5a)-/- (Fig. 53E’).

Thus, taken together, in contrast to the developing telencephalon both DNA-binding domains, PD and HD, play a role in the regulation of neurogenesis in the developing eye. Mutants of each DNA-binding domain exhibit a phenotype with severe eye malformation and reduced neurogenesis, suggesting that the lack of each domain impairs neurogenesis. However, only if no Pax6 protein is present, neurogenesis fails completely.

7.4.2 The role of the different Pax6 DNA-binding domains in the regulation of cell proliferation in the eye

Since Pax6 is involved in the regulation of cell proliferation in the eye (Marquardt et al., 2001), cell proliferation was also analyzed in the eye of Pax6(5a)-/- and the remnant eye vesicles of Pax6^{Sey}-/-, Pax6^{Aey18}-/- and Pax6^{4Neu}-/- mutants by immunohistochemistry against PH3. In the functional null allele *Pax6*^{Sey}-/- the number of PH3 positive cells is strongly decreased in the tissue remnant of the eye (Fig. 51B). Loss of a functional PD (Pax6^{Aey18}-/-) (Fig. 52A) and HD (Pax6^{4Neu}-/-) (Fig. 52B) leads as well to a decrease in the number of PH3 positive cells, whereas no obvious alterations in the number of PH3 positive cells were detected in the eye of the Pax6(5a)-/- mice at E14 (Fig. 52C). In contrast to the developing telencephalon loss of a functional Pax6 protein leads to a decrease in cell proliferation and these results show that both DNA binding domains, PD and HD are required for the regulation of cell proliferation in the developing eye.

7.4.2.1 Interkinetic nuclear migration in the eye

Since the interkinetic nuclear migration is a general feature of neuroepithelial cells, it takes also place in the neuroepithelium of the developing eye. To detect cells in S-phase BrdU was

administered for 0.5 hour and 6 hours (see also above). Indeed after 0.5h BrdU pulse cells in S-phase were detectable at the most basal side of the neuroepithelium, close to the zone where the postmitotic neurons are located and after 6 hours cell nuclei translocated to the side of the epithelium, where cells divide (RPE side) (see arrow Fig. 54). In contrast to the telencephalon no SVZ cells or basal precursors were detectable in the retina at E14. In the functional null allele *Pax6^{Sey}*^{-/-} interkinetic nuclear migration was detectable to a certain extent, despite the general decrease in cell proliferation (Fig. 54B,D). Also in the PD mutant mice (*Pax6^{Aey18}*^{-/-}) (Fig. 55B,D) and HD mutant mice (*Pax6^{4Neu}*^{-/-}) (Fig. 56B,D) interkinetic nuclear migration occurred normally. BrdU labeled nuclei were located at the basal side of the proliferative zone after a 0.5 h BrdU pulse, in some distance to cells in M-phase (PH3 positive) cells, which are located at the most apical site of the proliferative zone. Whereas during a 6.0 hour BrdU pulse most cell nuclei migrated towards the apical surface at the positions where cells undergo M-phase. Cell proliferation was strongest decreased in the *Pax6^{Sey}*^{-/-}, followed by a less strong decrease in the PD mutant *Pax6^{Aey18}*^{-/-}. Cell proliferation in the *Pax6^{4Neu}*^{-/-} (lacking HD DNA-binding) seemed even a bit less decreased than in the *Pax6^{Aey18}*^{-/-} (compare Fig. 55 and Fig. 56).

Taken together, interkinetic nuclear migration takes place in the absence of functional Pax6 protein in the remnant eye vesicle of *Pax6^{Sey}*^{-/-} to certain extent and was clearly detectable after a 0.5h and 6.0h BrdU pulse in the remnant eye vesicle of the *Pax6^{Aey18}*^{-/-} (PD mutant) and *Pax6^{4Neu}*^{-/-} (HD mutant).

7.4.3 The influence of the Pax6 DNA binding domains on regionalisation -boundary formation between the optic stalk and the neuroretina

As described above, Pax6 and Pax2 repress each other by binding to the enhancer region of the respective other gene. Pax2 expression is restricted to the optic stalk, while Pax6 is expressed in the inner neuroretina in the E14 WT eye (see Fig. 57A). In the homozygous functional null allele *Pax6^{Sey}*^{-/-}, Pax2 expression expands in the eye vesicle at E12 (Fig. 57C). This expansion persists at E14 in the *Pax6^{Sey}*^{-/-}, however, the Pax2 expression occurs more patchy than at E12 (Fig. 57C,E). Here I analyzed which DNA-binding domains of Pax6 are required for the transcriptional repression of Pax2. In the case of loss of a functional PD (*Pax6^{Aey18}*^{-/-}) (Fig. 58B), Pax2 expression expands as well into the remnant eye tissue. In the HD mutant (*Pax6^{4Neu}*^{-/-}) only single Pax2 positive cells were detectable in the pseudo-optic cup (Fig. 58D) and in general the expansion was not as strong as in the *Pax6^{Sey}*^{-/-} mice (Fig.

57E). In contrast, the targeted deletion of exon5a in the Pax6(5a)^{-/-} mice (Fig. 58F) did not alter Pax2 expression, also not at later developmental stages (P2, see Fig. 41F,G). Taken together, both DNA-binding domains of Pax6 seem to be required for the repression of Pax2 expression in the neuroretina, however it seemed that Pax2 expansion was less strong in the Pax6^{4Neu}^{-/-}.

In summary these results show that in the developing eye, in contrast to the developing telencephalon both DNA-binding domains of Pax6 are contributing to the regulation of neurogenesis and cell proliferation. Furthermore both DNA-binding domains are required for the restriction of the Pax2 expression to the optic stalk domain.

7.5 The role of the PD and PD5a in regard to cell proliferation and differentiation

In order to separate the roles of canonical Pax6 and Pax6(5a) isoform in the regulation of neurogenesis and cell proliferation gain-of function experiments were performed. Replication-incompetent retroviruses containing either only LacZ as a marker (encoding for β -Galactosidase (β -Gal)), (BAG =control virus, Williams et al., 1991), or LacZ followed by an IRES and the Pax6 gene (Heins et al., 2002), or LacZ followed by an IRES and the Pax6(5a) gene (Haubst et al., 2004) (Fig. 59) were used. The progeny of single infected cells was analyzed after 7 days in vitro (div). Retroviruses infect dividing cells only during cell division. The virus is inherited by one daughter cell and the viral DNA integrates into the host DNA. The progeny of a single infected cell represents a cell clone and was detected by immunohistochemistry against β -Gal (Heins et al., 2001; 2002; Williams et al., 1991). This experiment allowed to assess the cell-autonomous role of the Pax6 isoforms in regulating neurogenesis and cell proliferation. After 7 div the clonal composition was assessed by immunohistochemistry against NeuN for neurons, O4 for oligodendrocytes, GFAP for astrocytes and RC2 or anti-nestin for undifferentiated precursors. Accordingly to the cell composition, clones were classified as pure neuronal clone, when only neurons were present, as mixed when the clone contained besides neurons also other cells and a pure non-neuronal when no neurons were detectable. Overexpression of Pax6 with a canonical PD in cells from E14 WT cortex led to a significant increase in the percentage of pure neuronal clones, on the expense of the glial clones (astrocytes 3% of clones, n=249; oligodendrocytes 0% of clones, n=81) (Fig. 59A,C).

In contrast, overexpression of Pax6(5a) did not influence the cell fate, since no increase in neurogenesis was detectable (Fig. 59A,C) and the percentage of glial clones generated was comparable to the control situation (astrocytes 11% of clones, n=137; oligodendrocytes 7% of clones, n=103). The proneuronal bHLH transcription factor Mash1 (Casarosa et al., 1999) is involved in patterning and cell fate decisions in the ventral telencephalon and expands dorsally in the absence of functional Pax6 protein (Fig. 32). Upon overexpression of canonical Pax6 the number of Mash1 positive cells was significantly downregulated (2% of clones compared to 14% of clones in the control), whereas no effect was detectable upon Pax6(5a) overexpression in the number of Mash1 positive cells (18% of clones).

The same set of experiments was performed on the functional null background in cortical cells from E14 Pax6^{Sey}^{-/-} mice. The control situation (BAG) showed that significantly less pure neuronal clones were generated in the absence of functional Pax6 protein. Overexpression of canonical Pax6 not only rescued, but even led to a significant increase in the percentage of pure neuronal clones generated, while the overexpression of Pax6(5a) had no effect on neurogenesis even in the absence of Pax6. Since canonical Pax6 is able to bind to both consensus sites (P6CON and 5aCON), while Pax6(5a) binds to 5aCON sites only, these results suggest that the regulation of target genes mediating the neurogenic effect of Pax6 depends on the P6CON site and that the neurogenic effect of Pax6 is mediated by the canonical PD. Besides the role of the Pax6 isoforms in the regulation of cell fate decisions, also the regulation of cell proliferation upon overexpression of canonical Pax6 and Pax6(5a) was studied. Both isoforms lead to a significant decrease in the number of cells generated per clone. Interestingly, overexpression of Pax6(5a) reduced cell proliferation, i.e. clonal size independent from the cell type (neuronal or glial) (Fig. 59D).

In summary it may be said that the Pax6(5a) isoform reduces cell proliferation independently of cell fate, while canonical Pax6 couples the reduction of cell proliferation with cell fate decisions, i.e. neurogenesis.

7.6 The effect of Pax6 overexpression on proliferation and cell cycle length

In order to assess which parameters of the cell cycle are influenced by Pax6, cell proliferation was analyzed upon Pax6 overexpression in three different sets of experiments using the cumulative BrdU labeling method (CLM) (Nowakowski et al., 1989). BrdU is incorporated into the DNA of proliferating cells during S-phase and can be detected by

immunohistochemistry. The ratio of cells in S-phase (BrdU positive) at a given timepoint to the total number of proliferating cells (Ki67 positive) gives the labeling index (LI). BrdU labeling of the proliferating cells progresses successively over time, since all proliferating cells undergo S-phase at some point and since BrdU was present in a sufficient concentration in the cell culture medium all the time (Fig. 60A). E14 WT cortical cells were infected with β -Gal (BAG) or Pax6 containing retrovirus, cultured for 2 div and BrdU was administered for 0.5, 2.0, 4.0, 8.0 hours prior to fixation. This cumulative BrdU labeling allowed the determination of the cell cycle length and the S-phase length of E14 WT cortical cells in the control situation (BAG-infected cells) and upon Pax6 overexpression in vitro. Immunohistochemistry against β -Gal has been performed in order to detect retrovirus infected cells per clone, against Ki67 to reveal the proliferating cells per clone and against BrdU to assess the cells that went through S-phase during BrdU administration. The cell proliferation upon Pax6 overexpression has been studied by calculating the growth fraction (GF= ratio of proliferating cells (Ki67 positive) to the entire pool of retrovirus infected cells (β -Gal positive)). The cell cycle and S-phase length were determined by calculating the labeling index (LI= percentage of cells in S-phase (BrdU labeled nuclei) among all proliferating cells (Ki67 positive)). As third value the ratio of BrdU labeled nuclei among all β -Gal positive cells has been determined. The shortest BrdU pulse duration was 0.5 hour prior to fixation, labeling all proliferating cells in S-phase at that time, thus the fraction of proliferating cells in the first pulse is equal to T_S/T_C . The labeling index is the proportion of cells labeled in the total population at a given time, thus i.e. the first BrdU pulse labels at $t=0$, $LI_0=T_S/T_C$. The LI was determined for the different times of BrdU exposure. The time when all proliferating (Ki67 positive) cells are BrdU labelled, gives the total cell cycle length (T_C) minus the length of S-phase (T_S) ($T_C - T_S$) (see Fig. 60A). The point where the slope crosses the x-axis gives the length of S-phase (T_S). The crossing point of the y-axis gives the LI at the time 0 ($t=0$, $LI_0=T_S/T_C$) (Fig. 60A). The slope was calculated using the equation $y= p*q+x$. $T_C - T_S$ was calculated setting $y= 100$, T_S was calculated setting $x= 0$.

The determination of the GF showed that upon Pax6 overexpression proliferation is significantly decreased ($p= 0.017$). In average 55,4% of cells per clone are proliferating in the Pax6 overexpression situation compared to 70,5% in the control situation. The value obtained for the GF of WT BAG-infected cortical cells does not significantly differ ($p= 0.05$) from the GF value obtained in WT BAG-infected cells in the analysis of the cell proliferation in vitro upon loss of functional Pax6 (see below 7.4.2).

The total cell cycle length (T_C) length upon Pax6 overexpression was 17,2 hours compared to 17,2 hours in the control situation (Fig. 60B). The T_S duration in the control situation was 4,1 hours, while Pax6 overexpression lead to a T_S of 4,4 hours. Thus the overexpression of Pax6 did not lead to significant changes in the cell cycle and S-phase length.

7.7 Loss of functional Pax6 and the effect on cell proliferation in vitro

As described above, in the absence of functional Pax6 protein more cells are proliferating at abventricular positions in the dorsal telencephalon (see Fig. 24E, 27A and table 2). In addition, the PSB does not form and increased cell migration from the ventral into the dorsal telencephalon takes place in the Pax6^{Sey}^{-/-} (Chapouton et al., 1999). In order to exclude that the increased number of cells dividing at abventricular positions in the cortex of Pax6^{Sey}^{-/-} mice originates from the ventral telencephalon, where no Pax6 is expressed, the proliferative behavior of Pax6^{Sey}^{-/-} cortical cells was analyzed in vitro. Cells from E14 WT and Pax6^{Sey}^{-/-} cortex were infected with the β -Gal containing retrovirus (BAG), cultured for 2 div and BrdU was added to the culture medium 0.5 hour prior to fixation in three different sets of experiments.

Also in vitro cell proliferation was significantly increased ($p= 7.7 \times 10^{-8}$) in the cortical cells of Pax6^{Sey}^{-/-} (GF: 88,7%), while in the WT cortical cells only 64,7% were proliferating (Fig. 61). No significant changes were detected in the LI in the cortical cells of Pax6^{Sey}^{-/-} mice (LI: BrdU/Ki67: 21,1%) compared to 17,2% in the WT cortical cells (Fig. 61 to the left; $p= 0.208$), while the ratio of BrdU labeled cells to the total cells (β -Gal positive) was significantly increased ($p= 0.00568$) in the Pax6^{Sey}^{-/-} (19,2%) compared to the WT cortical cells (11,1%), reflecting the overall increase in cell proliferation.

Thus this experiment showed that the changes in cell proliferation in the cortex of the Pax6^{Sey}^{-/-} mice arise because of cell intrinsic changes, i.e. loss of functional Pax6 protein.

7.8 Loss of a functional PD and the effect on neurogenesis in vitro

As described above, neurogenesis is impaired in the cortex of the Pax6^{Aey18}^{-/-}. In order to exclude that the impairment in neurogenesis is compensated by enhanced cell migration from the ventral into the dorsal telencephalon in the Pax6^{Aey18}^{-/-} and to test whether the changes in regard to neurogenesis are cell intrinsic, neurogenesis of the Pax6^{Aey18}^{-/-} mice was analyzed

in vitro. E14 WT and Pax6^{Aey18}^{-/-} cortical cells were infected with a control virus carrying β -Gal as a marker (BAG, Williams et al., 1991) and cultured for 7 div. Neurogenesis was assessed by immunohistochemistry against NeuN and β III-Tubulin. The in vitro data confirmed the in vivo findings. Significantly less neurons were generated from the Pax6^{Aey18}^{-/-} cortical cells (39,4% neurons among β -Gal positive cells \pm 4,3 (s.d); n= 414 cells) compared to the WT situation (56% neurons among β -Gal positive cells \pm 4,8 (s.d); n= 346 cells) (Fig. 62). This means that the changes in neurogenesis are cell autonomous due to the lack of a functional PD in the Pax6^{Aey18}^{-/-} mice.

7.9 Determination of the apoptosis rate in retrovirus infected cell cultures

In order to examine whether the retroviruses used and/or high levels of Pax6 expression have an influence on apoptosis, WT cortical cells were infected either by BAG, Pax6 or Pax6(5a) retroviruses, cultured for 2 div and immunostained against β -Gal for the detection of cells generated by one clone, against NeuN for the determination of neurons generated and chromatin was counterstained with DAPI in order to detect pyknotic nuclei for the determination of the apoptosis rate in the viral infected clones. In the control situation (BAG and 1726) only 1% of pyknotic nuclei was detected (n= 373 cells), whereas no apoptosis was detected upon overexpression of Pax6 (n= 205 cells) and Pax6(5a) (n= 125 cells).

7.10 Construction of Pax6 retroviral vectors

7.10.1.1 PD-less Pax6 virus

As mentioned already, alternative splicing leads also to the generation of the PD-less Pax6 isoform, consisting of the HD as DNA-binding domain and the TAD (Mishra et al., 2002). PD-less Pax6 expression levels are changing in the developing telencephalon from high expression levels at E10 to decreased levels at E18 (see above 7.2.4.1). So far, nothing is known about the role of this isoform during development. Thus, I constructed a replication incompetent retroviral vector, containing the coding sequence (CDS) of the PD-less Pax6, followed by an IRES and the CDS of GFP, which might provide a new tool for the examination of the role of the PD-less Pax6 protein.

7.10.1.2 Pax6 containing a mutation in the HD (PM776)

Since the loss of a functional HD had only subtle effects in the developing telencephalon (loss of SFRP2 expression, no formation of radial fascicle at the PSB), a retroviral vector lacking DNA-binding of the HD has been constructed. The Pax6 CDS contained a pointmutation in helix III at position 776bp, leading to the same mutant Pax6 form as present in the Pax6^{4Neu}^{-/-} (Favor et al., 2001). The mutated Pax6 CDS is followed by an IRES and the CDS of GFP. This viral construct might provide a new tool for the overexpression of a Pax6 containing a mutated HD, to gain further insights in the role of the HD in regard to neurogenesis and cell proliferation.

7.11 Approach for the analysis of Pax6 target genes

In order to assess genes that are directly or indirectly regulated by Pax6 in the developing telencephalon E13 embryos were co-electroporated *ex vivo* either with GFP expressing control vector or Pax6 containing vector coelectroporated with GFP expressing vector. The electroporated cortices were initially kept *in vitro* for 2 days but this time proved too short to detect upregulation of candidate genes thus it had to be increased to 3 div (Fig. 63A,B). GFP expression was already detectable after 1 div. However, when explants were cultured for 3 days, a significant increase of the known target Ngn2 was observed by RT-PCR (Fig. 63C). Further electroporations were performed to collect sufficient amounts of RNA (2-6µg) to examine expression differences upon Pax6 transduction using affymetrix microarrays.

8 Figures and Tables

Formation of the neural tube

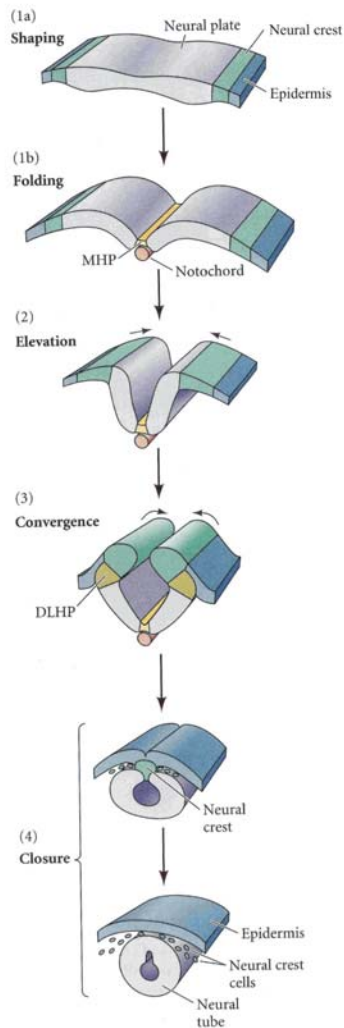


Fig. 1: Formation of the neural tube in the chick embryo

Folding of the neural plate (1a) starts at the medial neural hinge point (MHP; 1b), where cells are anchored to the notochord. Epidermal cells move towards the dorsal midline (2), the neural folds converge at the dorso/lateral hinge point (DLHP; 3) followed by the closure of the neural tube (4). Neural crest cells link the neural tube with the epidermis (4), then they disperse and the neural tube separates from the epidermis. (Drawings after Smith and Schoenwolf, 1997; taken from: Scott F. Gilbert, *Developmental Biology*, Seventh edition).

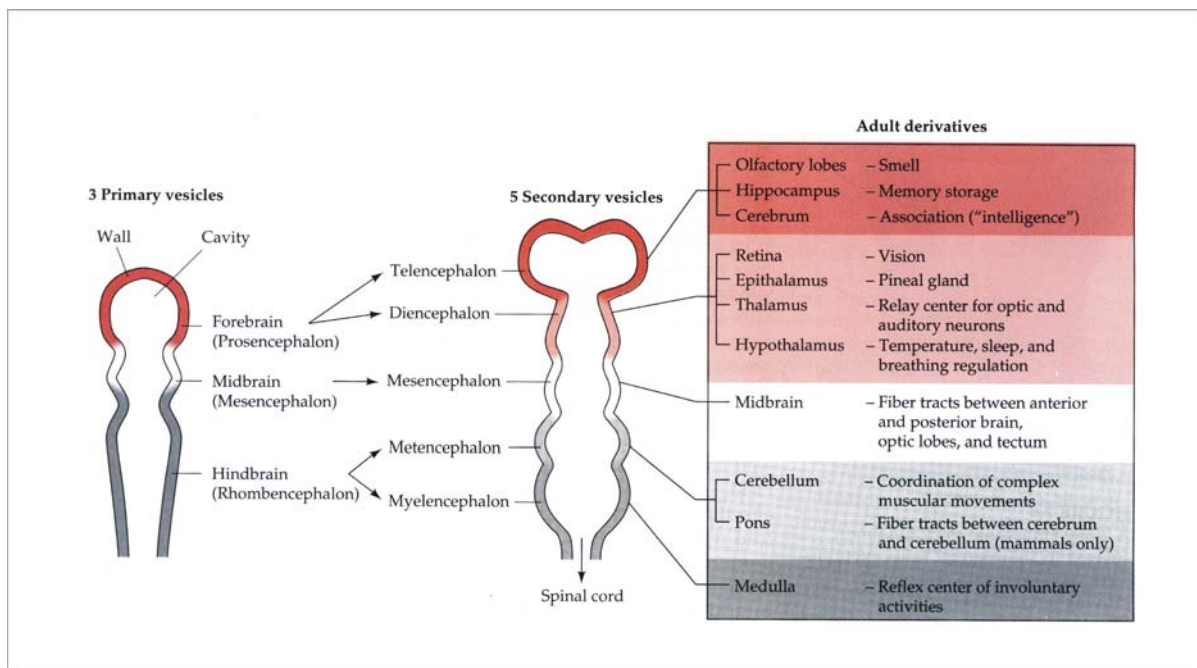


Fig. 2: Development of the early human brain

Three primary vesicles are further subdivided into five secondary vesicles during development. These secondary vesicles develop into regions with different functions, depicted in the box (after Moore and Persaud, 1993; Scott F. Gilbert, Developmental Biology, Fourth Edition).

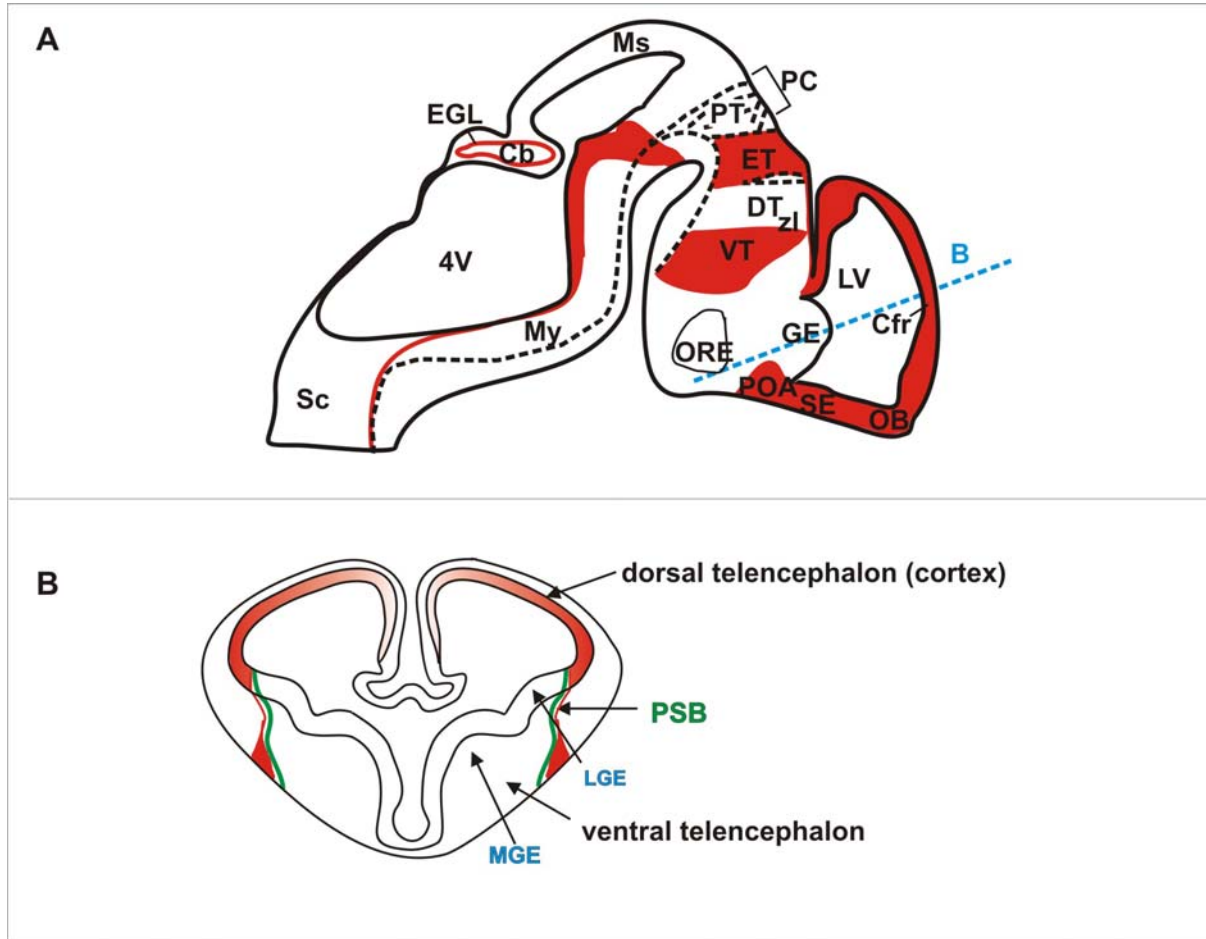


Fig. 3: Schematic drawing of E13.5 mouse brain and Pax6 expression domains

(A) Sagittal section through the E13.5 mouse brain, showing the Pax6 expression domains (red). (B) Frontal section through E13.5 mouse telencephalon at the level of the dashed blue line in (A). The dorsal telencephalon (= cortex) and ventral telencephalon abut at the pallial-subpallial boundary (PSB) (green). The ventral telencephalon is subdivided in the medial ganglionic eminence (MGE) and the lateral ganglionic eminence (LGE). Pax6 is expressed in a lateral-rostral high and medial-caudal low gradient in the telencephalon.

Abbreviations: Cb (cerebellum), Cfr (frontal cortex), DT (dorsal thalamus), egl (external granular layer of cerebellum), ET (epithalamus), GE (ganglionic eminence), LV (lateral ventricle), Ms (mesencephalon), My (myelencephalon), OB (olfactory bulb), ORE (optic recess), PC (posterior commissure), Pn (pons), POA (Anterior preoptic area), PT (pretectum), SE (septum), 4V (fourth ventricle).

((A) Modified after Stoykova and Gruss, 1994), (B) modified after Marin and Rubenstein, 1993).

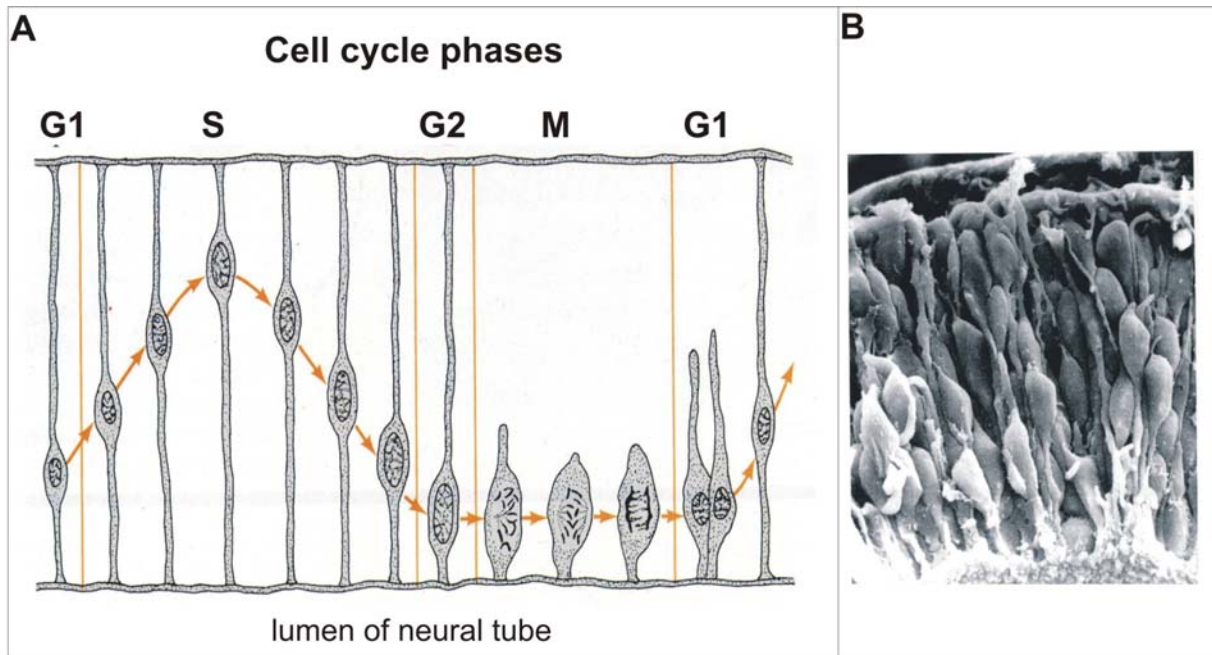


Fig. 4: Interkinetic nuclear migration

(A) Schematic drawing (after Sauer, 1935), showing the translocation of the nucleus of chick neuroepithelial cells in correlation with the progression through the different cell cycle phases. M-phase takes place at the ventricular surface close to the lumen of the neural tube. The nucleus is translocated in G1-phase to the basal neuroepithelium, where S-phase takes place. During G2-phase the nucleus reaches the ventricular surface again. (B) Scanning electron micrograph of chick neural tube, showing cells in different stages of the cell cycle.

The picture is not correct anymore since it has been shown meanwhile that one daughter cell inherits a process during cell division (Miyata et al., 2001 and Noctor et al., 2001).

(Pictures taken from Scott F. Gilbert, *Developmental Biology*, 4th edition).

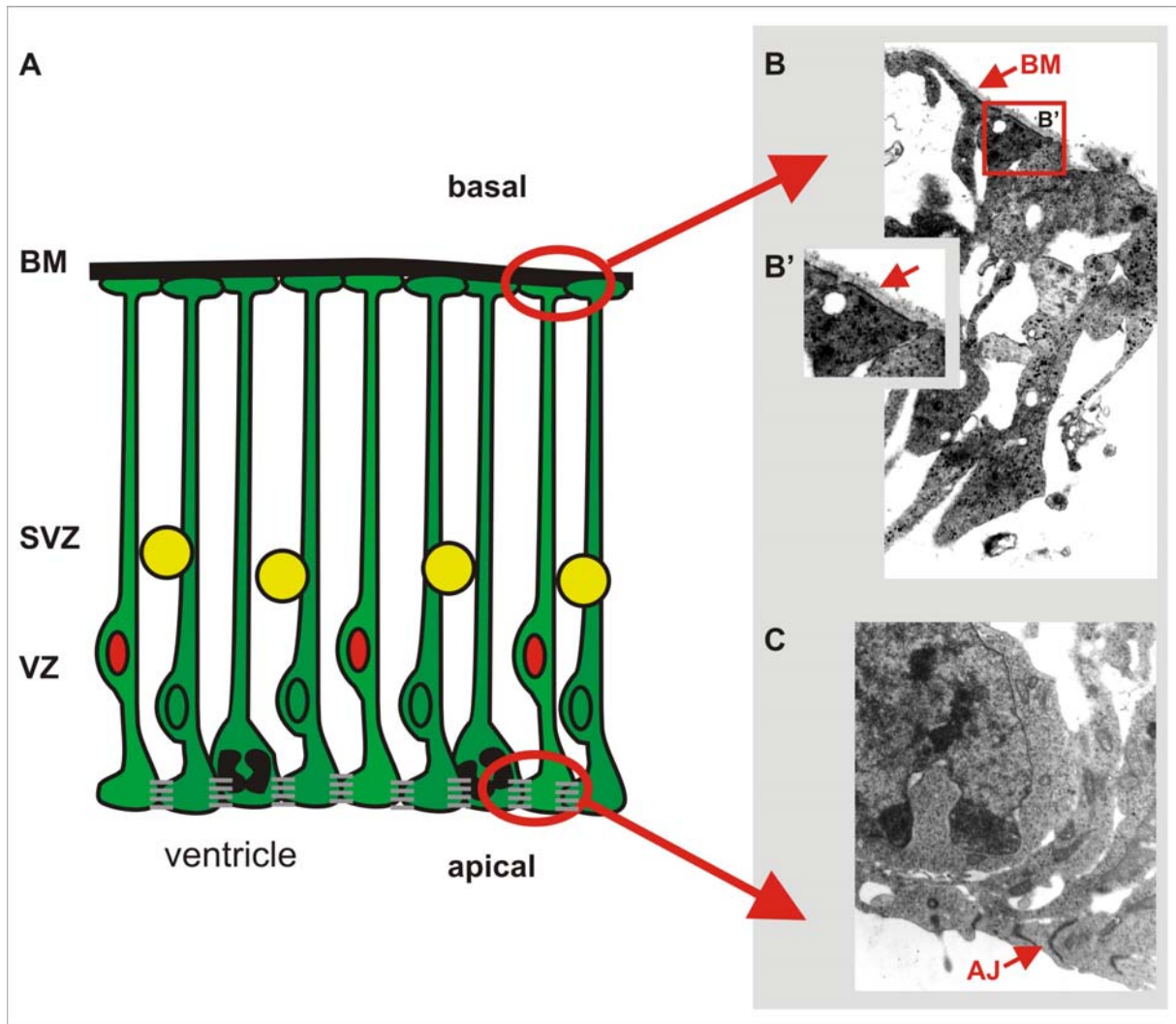


Fig. 5: Apico-basal polarity of radial glia cells

(A) Schematic drawing depicting the ventricular zone (VZ) cells (radial glia cells at E14) lining the ventricle and extending to the basement membrane and the subventricular zone (SVZ) cells located above. VZ precursor cells attach with their endfeet to the basement membrane at the pial surface (B). The arrow in B' indicates the basement membrane. Cells are linked to each other at the apical side via junctional complexes (C, indicated by AJ; see also grey bars in A).

Abbreviations: AJ= adherens junctions; BM= basement membrane; SVZ= subventricular zone; VZ= ventricular zone.

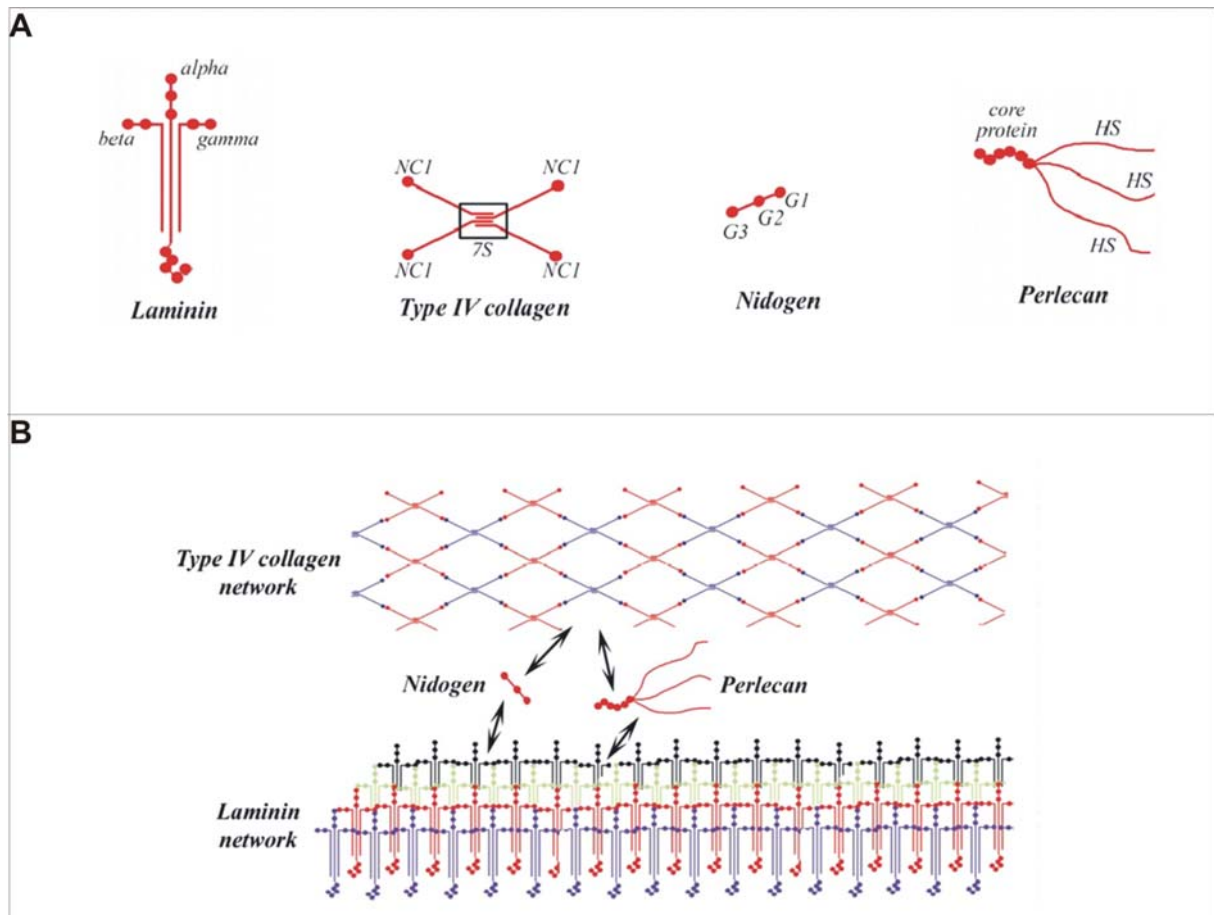


Fig. 6: Schematic drawing of the main basement membrane components and of the basement membrane architecture

(A) **Laminin** is composed of three different protein chains (alpha, beta and gamma chain). The N-terminal domains of each chain form a short arm and contain globular domains, whereas the long arm has a coiled structure, composed of all three chains. The alpha chain contains five globular domains at the C-terminal end.

Type IV collagen consists of four monomers each composed of three alpha (IV) helical chains. The four monomers interact with each other at their respective N-terminal sites. The boxed 7S region is the central region of the tetramer, termed after the sedimentation coefficient. The globular domains at the respective C-terminal end of each monomer are important for the head to head interaction, which is required for the polymerisation of type IV collagen.

Nidogen molecules consist of three globular domains, G1 at the N-terminal end, G2 and G3 at the C-terminal end.

The core protein of **Perlecan** molecules resembles a chain of pearls. Two to three heparan sulfate side chains are located at the N-terminal end.

(B) Basement membranes are networks of type IV collagens and laminins linked via nidogen or perlecan molecules.

(Picture taken from: Quondamatteo, 2002).

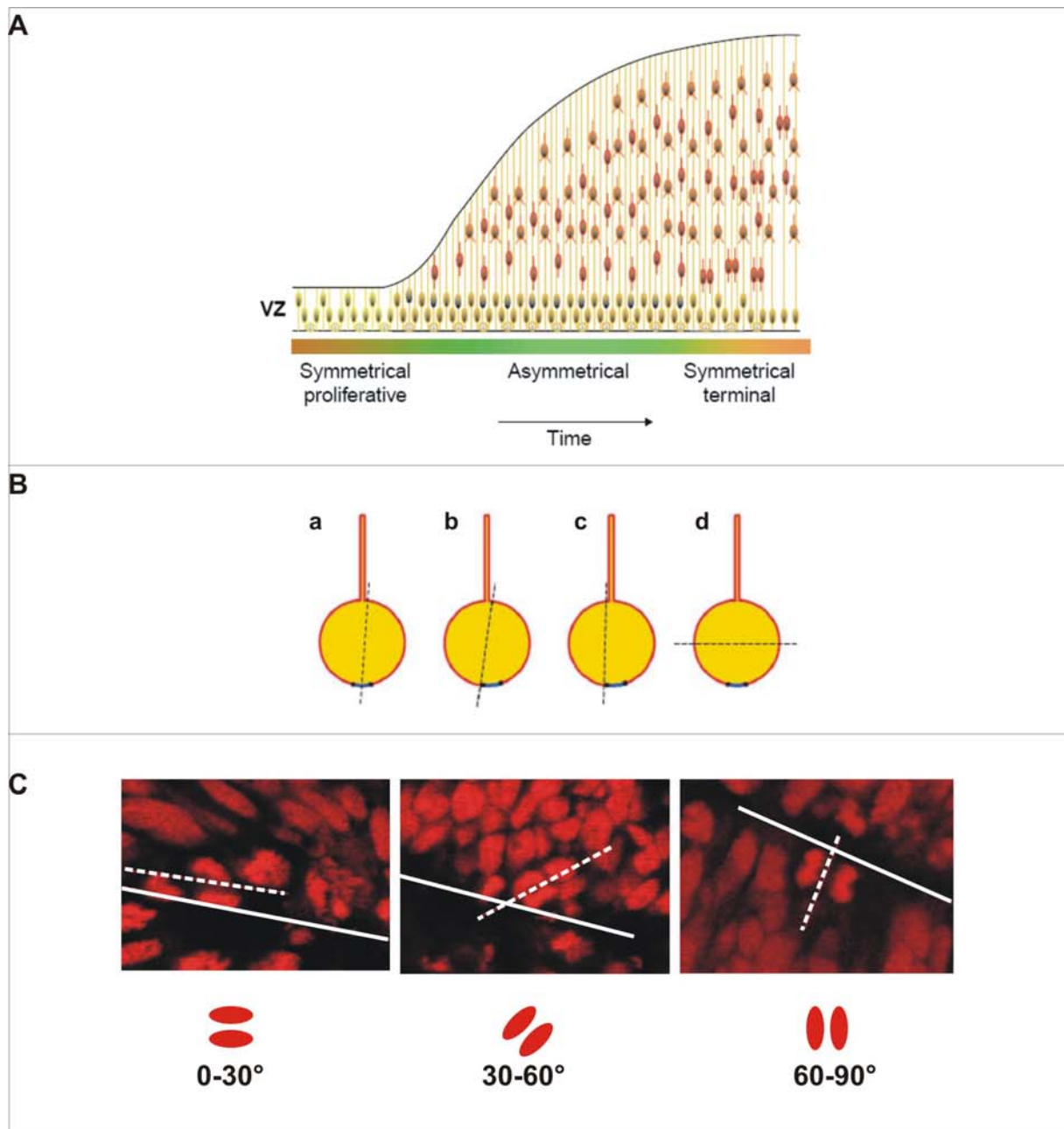


Fig. 7: Mode of cell division during development of the cerebral cortex

(A) Before the onset of neurogenesis cell divisions occur predominantly symmetric and thus increase the precursor pool. As neurogenesis starts, more and more asymmetric cell divisions take place, generating one neuron and one precursor cell. At midneurogenesis in the SVZ and at the end of neurogenesis terminal symmetric cell divisions take place.

(Picture taken from Fishell and Kriegstein, 2003).

(B) Cell divisions at the ventricular surface occur at different angles with respect to the ventricular surface (VS): perpendicular (a,b,c) or horizontal (d) with respect to the VS. The dashed line indicates the cleavage plane. All cell divisions depicted are asymmetric in regard of the distribution of cell components as the basal process, or the apical membrane portion is distributed asymmetrically (Picture taken from Wodarz and Huttner, 2003).

(C) Angles of cell division at the VS were measured and classified in three groups horizontal (0-30°), oblique (30-60°) and perpendicular (60-90°) with respect to the VS. The white line indicates the VS, the dashed white line gives the angle of cell division.

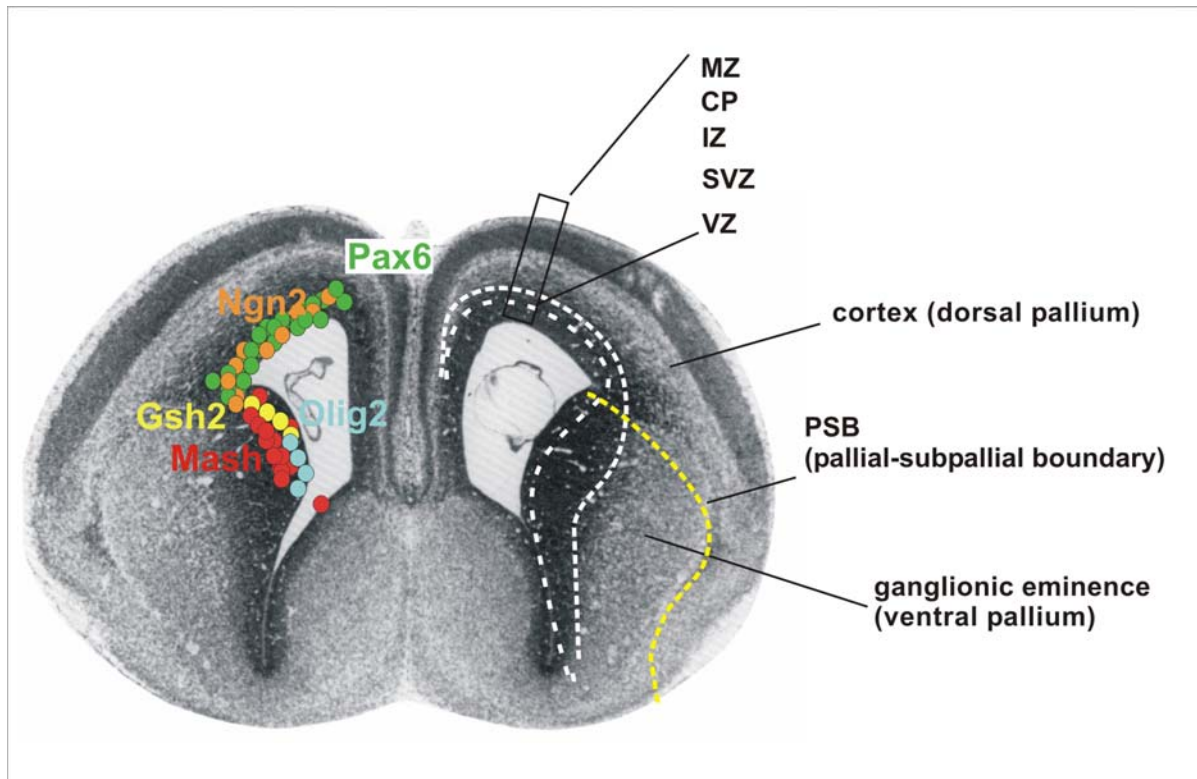


Fig. 8: Expression pattern of transcription factors in the developing telencephalon

(A) Schematic drawing of the transcription factor expression pattern that will be analyzed in this thesis. Pax6 and Ngn2 are expressed in the dorsal pallium (cortex), while Gsh2, Olig2 and Mash1 are expressed in the ventral pallium (ganglionic eminence). The expression domains of ventral and dorsal transcription factors abut at the pallial-subpallial boundary (PSB).

(Picture of mouse telencephalon, taken from Schambra et al., 1992).

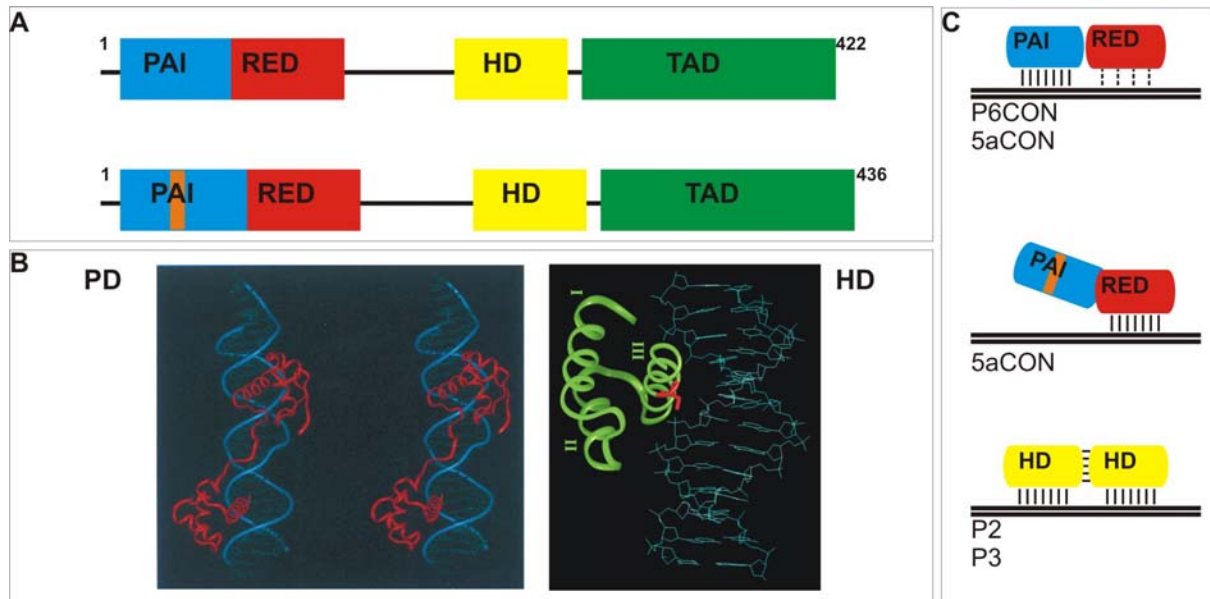


Fig. 9: Schematic drawing of Pax6

(A) The canonical Pax6 form (422 AA) consists of a PD, which is subdivided in the N-terminal 'PAI' and the C-terminal 'RED' subdomain (PAI-RED), linked to a HD followed by a TAD, whereas the Pax6(5a) isoform (436 AA) is characterized by a 14AA insert into the PAI domain and the presence of a HD and TAD. (Picture modified after Chauhan et al., 2004).

(B) Micrograph depicting DNA-binding of the PD (to the left) protein in red, DNA in blue (taken from Xu et al., 1999) and HD DNA-binding (to the right) protein in green, DNA in blue (taken from Favor et al., 2001).

(C) DNA-binding of the PD of the canonical Pax6 form occurs predominantly via the N-terminal PAI domain (blue), but also the C-terminal RED (red) domain contributes. In the Pax6(5a) isoform, DNA-binding of the PAI is abolished and occurs exclusively via the RED domain to 5aCON sites. The HD (yellow) binds preferentially as dimer to palindromic P3 sites containing TAAT as core sequence. (Modified after Epstein et al., 1994a, b; Czerny et al., 1995; Kozmik et al., 1997; Chauhan et al., 2004).

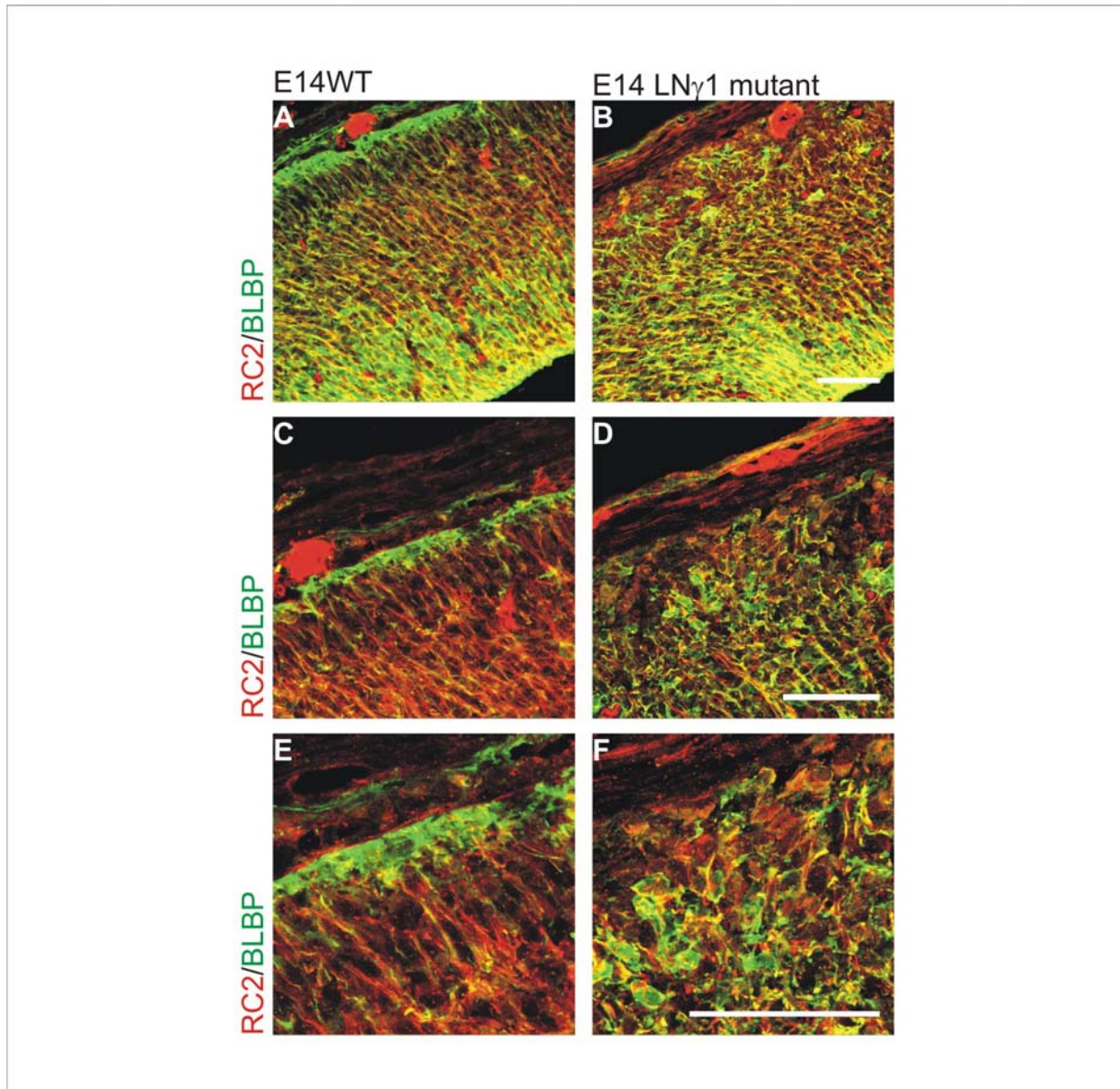


Fig. 10: Radial glia morphology in the LN γ 1 mutant

Micrographs of coronal sections of the E14 cortex in WT (A-E) and the LN γ 1 mutant (B-F). Immunohistochemistry against BLBP and RC2 revealed the morphology of radial glia cells in the cerebral cortex. In contrast to the E14 WT (A,C,E), are the endfeet of radial glia processes of the LN γ 1 mutant (B,D,F) not attachend to the basement membrane. In the WT radial glia endfeet build a 'band' underneath the pial surface, which is detectable best in the BLBP immunostaining (green) in (E), while in the LN γ 1 mutant no 'band' of endfeet can be observed (F), instead radial glia endfeet are disorganised. Scale bars: 50 μ m

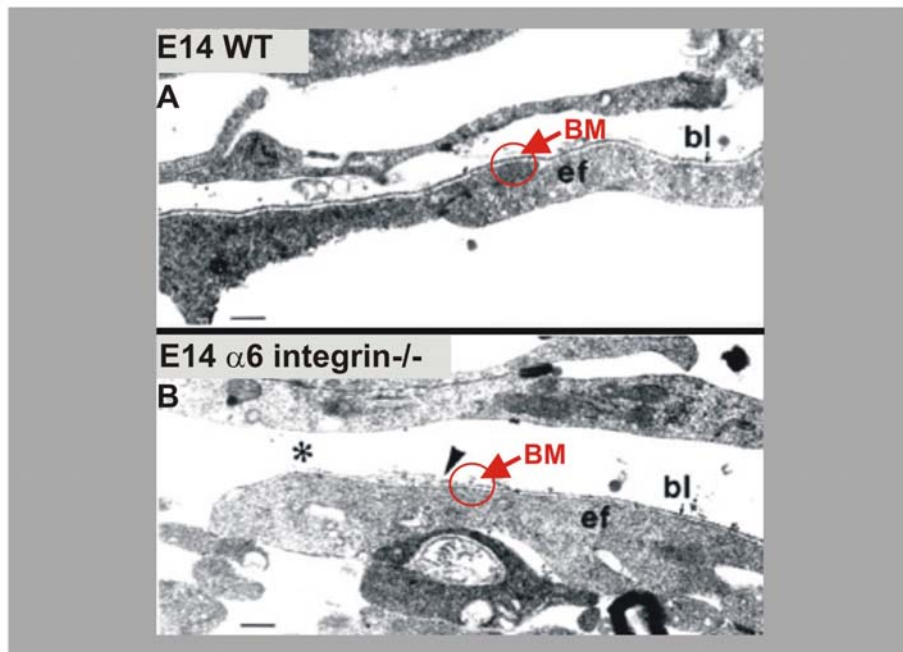


Fig. 11: Basement membrane assembly in the $\alpha 6$ integrin^{-/-}

Electronmicroscope pictures of coronal sections of the E14 cortex at the region of the pial surface, depicting radial glia endfeet (ef) and the basement membrane (BM).

The basement membrane assembly is disturbed in the $\alpha 6$ integrin^{-/-} (red circle in B) compared to the corresponding E14 WT (red circle in A).

(Picture taken from Georges-Labouesse et al., 1998).

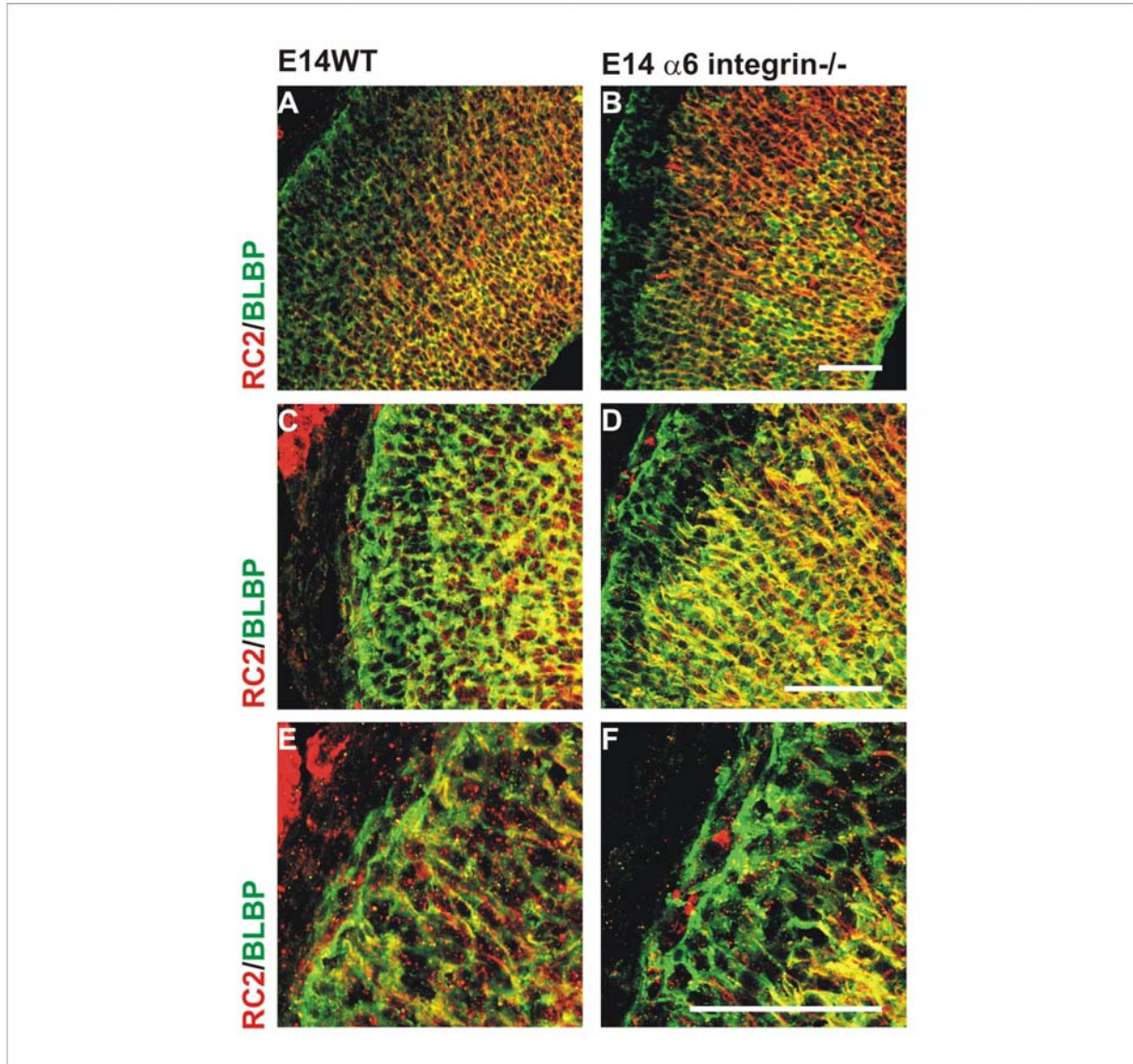


Fig. 12: Radial glia morphology in $\alpha 6$ integrin $^{-/-}$ cortex

Micrographs depicting coronal sections of the E14 cortex. Immunohistochemistry against RC2 and BLBP was used to analyse the morphology of radial glia cells.

Despite the improper basement membrane assembly, the radial glia morphology seems not severely altered in the $\alpha 6$ integrin $^{-/-}$ (B,D,F) compared to the WT cortex (A,C,E).

Scale bars: 50 μ m

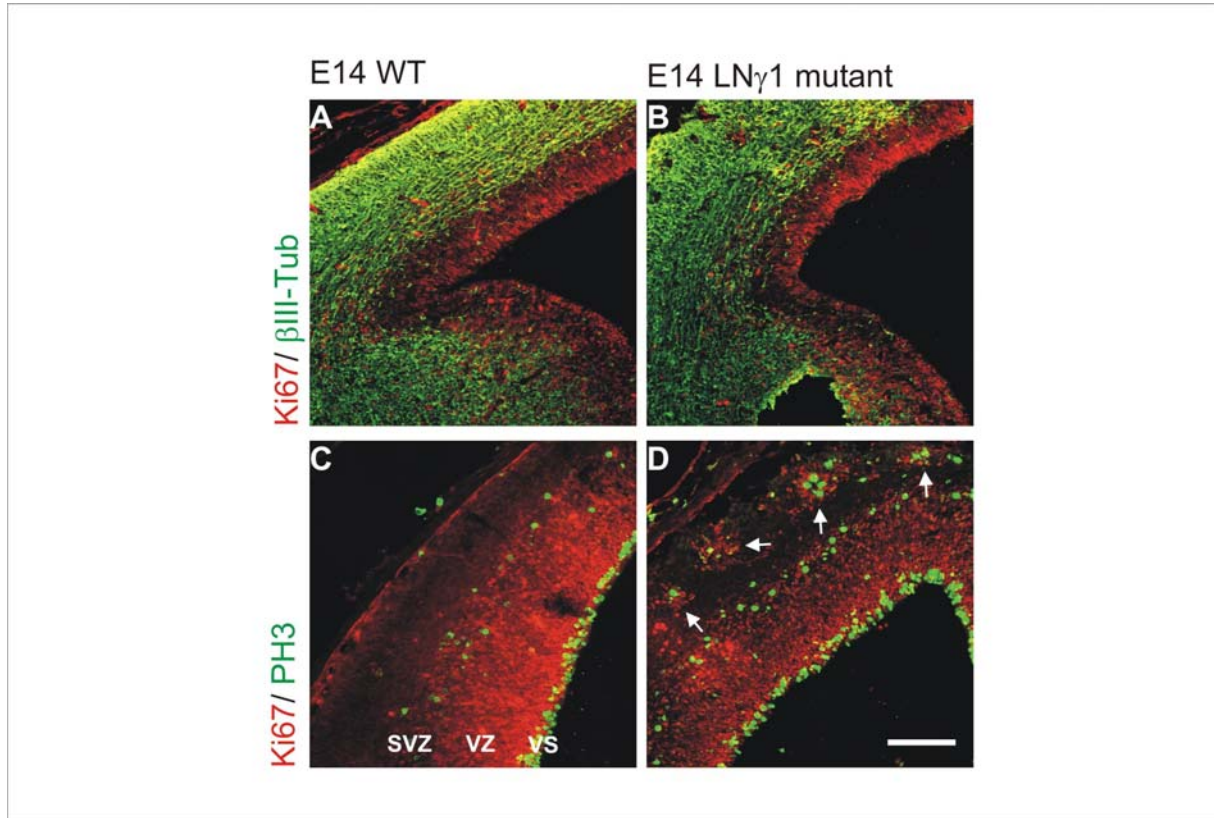


Fig. 13: Neurogenesis and cell proliferation in the LN γ 1 mutant

Micrographs depicting coronal sections of the E14 telencephalon. Neurogenesis was analyzed by immunohistochemistry against β III-Tubulin (green) and cell proliferation was assessed by immunohistochemistry against Ki67 (marker for proliferating cells, red A-D) and PH3 (marker for cells in M-phase, green C,D)..

The detachment of radial glia endfeet at the basement membrane in the telencephalon of the LN γ 1 mutant (B) seems not to alter neurogenesis (B) compared to the WT (A). Also cell proliferation seems normal in the cortex of the LN γ 1 mutant (B,D) compared to WT (A,C). The number of PH3+ cells dividing at the ventricular surface (VS, location indicated in C), which correspond to the VZ (location indicated in C) and at abventricular positions, which correspond to the subventricular zone (SVZ, indicated in C) is not altered due to loss of basal cell attachment in the LN γ 1 mutant (D), but in contrast to the WT (C) clusters of cells proliferating at ectopic positions inside the cortical plate were detected in the LN γ 1 mutant (see arrows in D).

Scale bar: 100 μ m

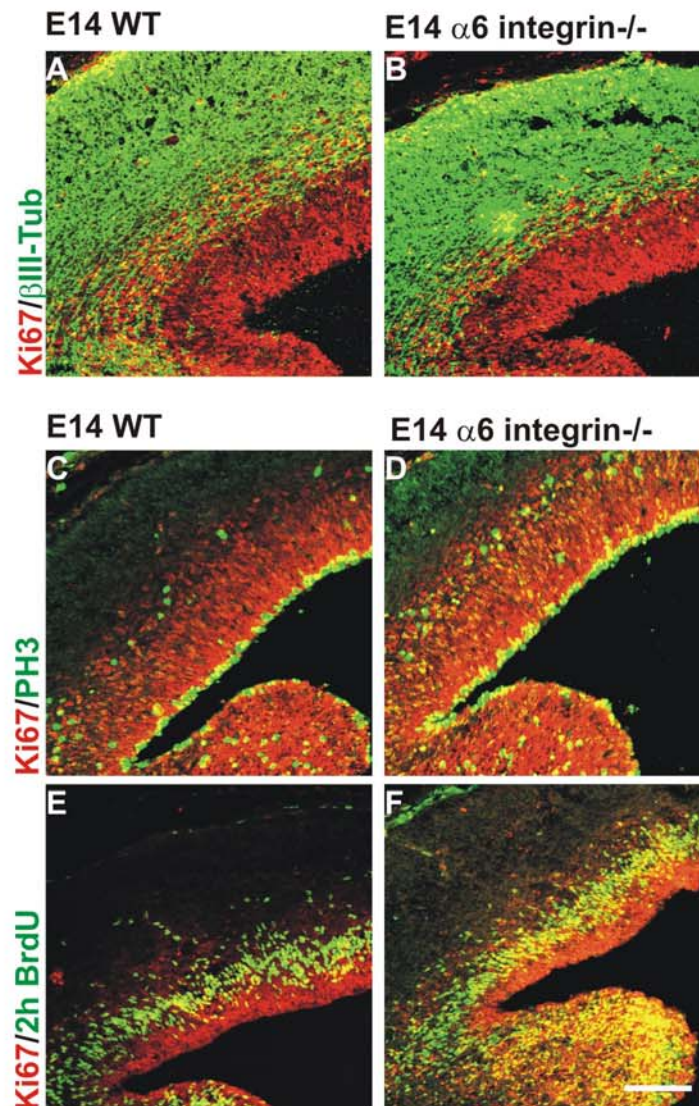


Fig. 14: Neurogenesis and cell proliferation in $\alpha 6$ integrin $^{-/-}$

Microrgraphs depicting coronal sections of the lateral cortex of WT and $\alpha 6$ integrin $^{-/-}$. Immunohistochemistry against β III-tubulin (green, in A,B) was used to detect postmitotic neurons, against Ki67 (red, A-F) was used to detect proliferating cells. Cells in M-phase were assessed by immunohistochemistry against PH3 (green, C,D) and cells in S-phase were detected by immunohistochemistry against BrdU (green). A 2h BrdU was given.

The improper basement membrane assembly in the $\alpha 6$ integrin $^{-/-}$ does not influence neurogenesis (B) compared to WT (A) and also cell proliferation was normal as detected by immunohistochemistry against Ki67 in the cerebral cortex of the $\alpha 6$ integrin $^{-/-}$ (B,D,F) compared to WT (A,C,E). The number of PH3+ cells was not altered in the cortex of the $\alpha 6$ integrin $^{-/-}$ (D) compared to the WT (C). No obvious changes in S-phase cells were detected in the $\alpha 6$ integrin $^{-/-}$ (F) compared to the WT (E).

Scale bar: 100 μ m

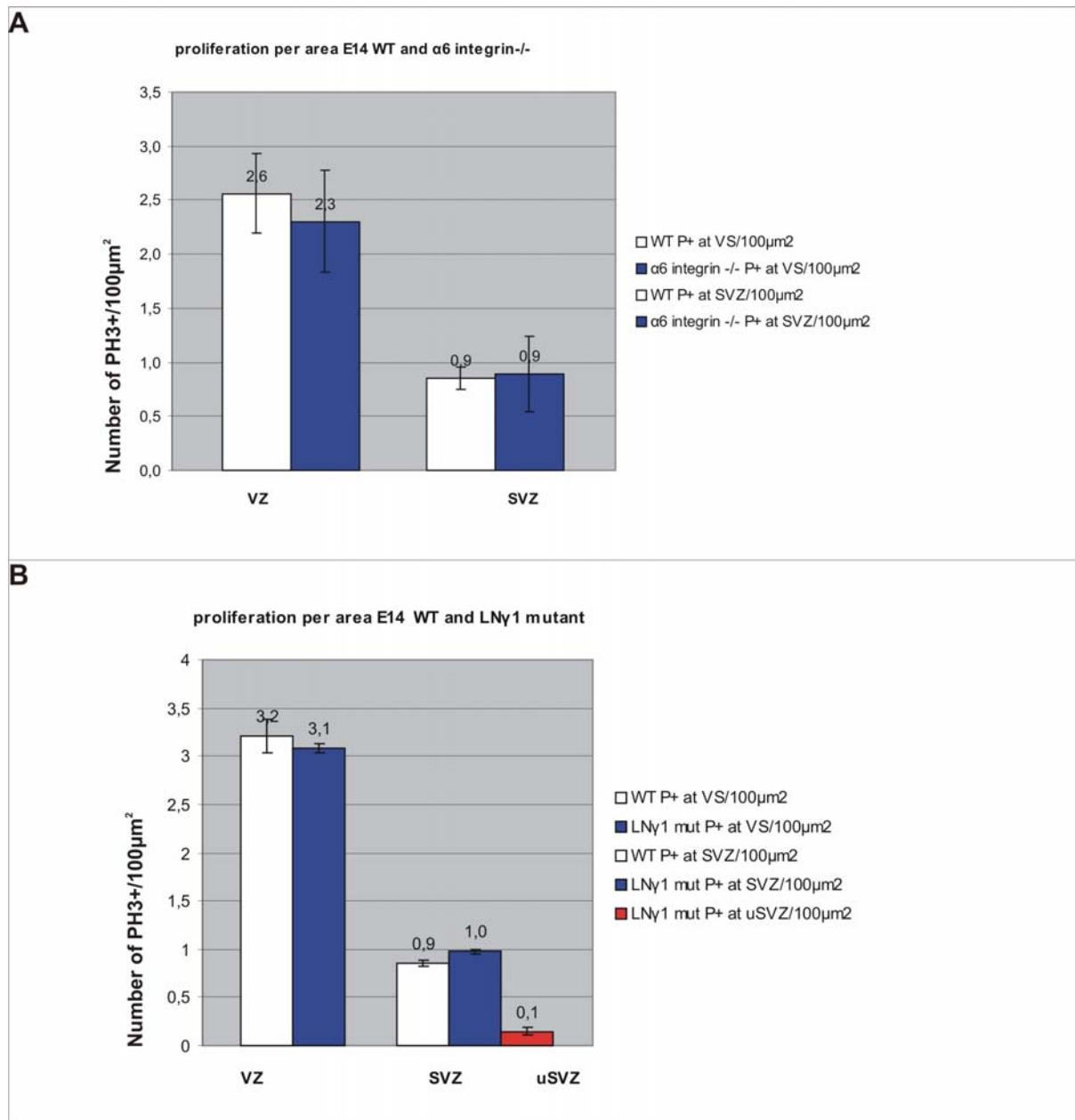


Fig. 15: Proliferation per area in basement membrane mutants, LN γ 1 mutant and $\alpha 6$ integrin $^{-/-}$
 No changes in the number of PH3⁺ cells dividing at the ventricular surface and at abventricular positions were detected in the $\alpha 6$ integrin $^{-/-}$ (blue bars) compared to the corresponding E14 WT littermate (white bars) (A) and in the LN γ 1 mutant (blue bars) compared to the corresponding E14 WT littermate (white bars) (B). As described in Fig. 13 ectopic proliferating cell clusters were detected in the telencephalon of the LN γ 1 mutant. The number of PH3⁺ cells in the ectopic proliferating cell clusters in the LN γ 1 mutant cortex is given as a third column (red) to the right. In the corresponding WT littermates and in the $\alpha 6$ integrin $^{-/-}$ cortex hardly any PH3⁺ cells at ectopic positions were detected. Error bars are given as s.d.

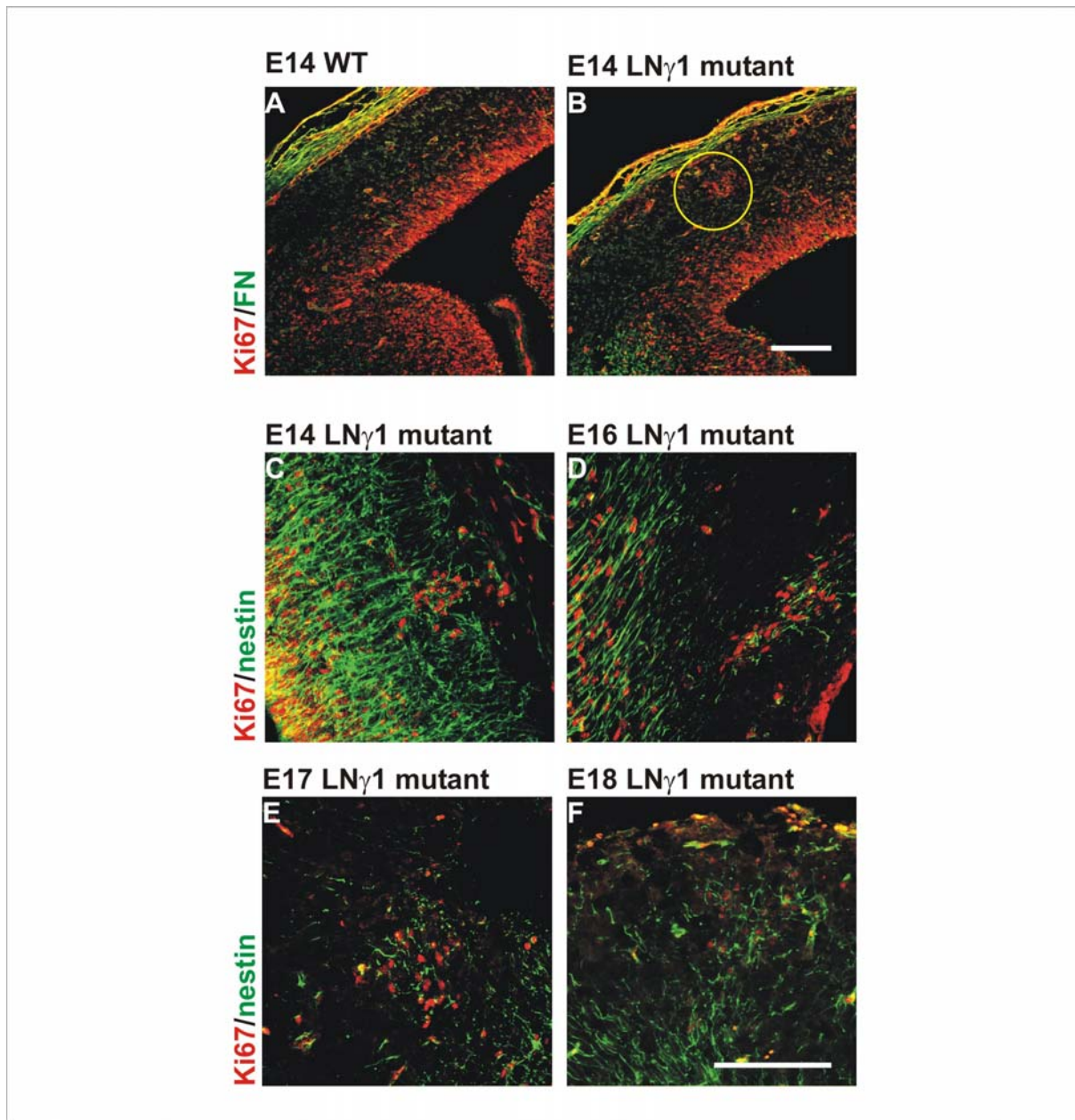


Fig. 16: Characterization of ectopic proliferating cells in the LN γ 1 mutant

Micrographs of coronal sections of the telencephalon. Immunohistochemistry against fibronectin (FN, green) a marker for fibroblasts and Ki67 (marker for proliferating cells) was performed to analyze whether fibroblasts migrated into the parenchyma. The ectopic proliferating cells in the cortex of the LN γ 1 mutant are fibronectin (FN) negative (B). The clusters of ectopic proliferating cells persist until E18 in the cortex of the LN γ 1 mutant and contain nestin positive cells (green) from E14 to E18 (C,D,E,F). Scale bars: 100 μ m

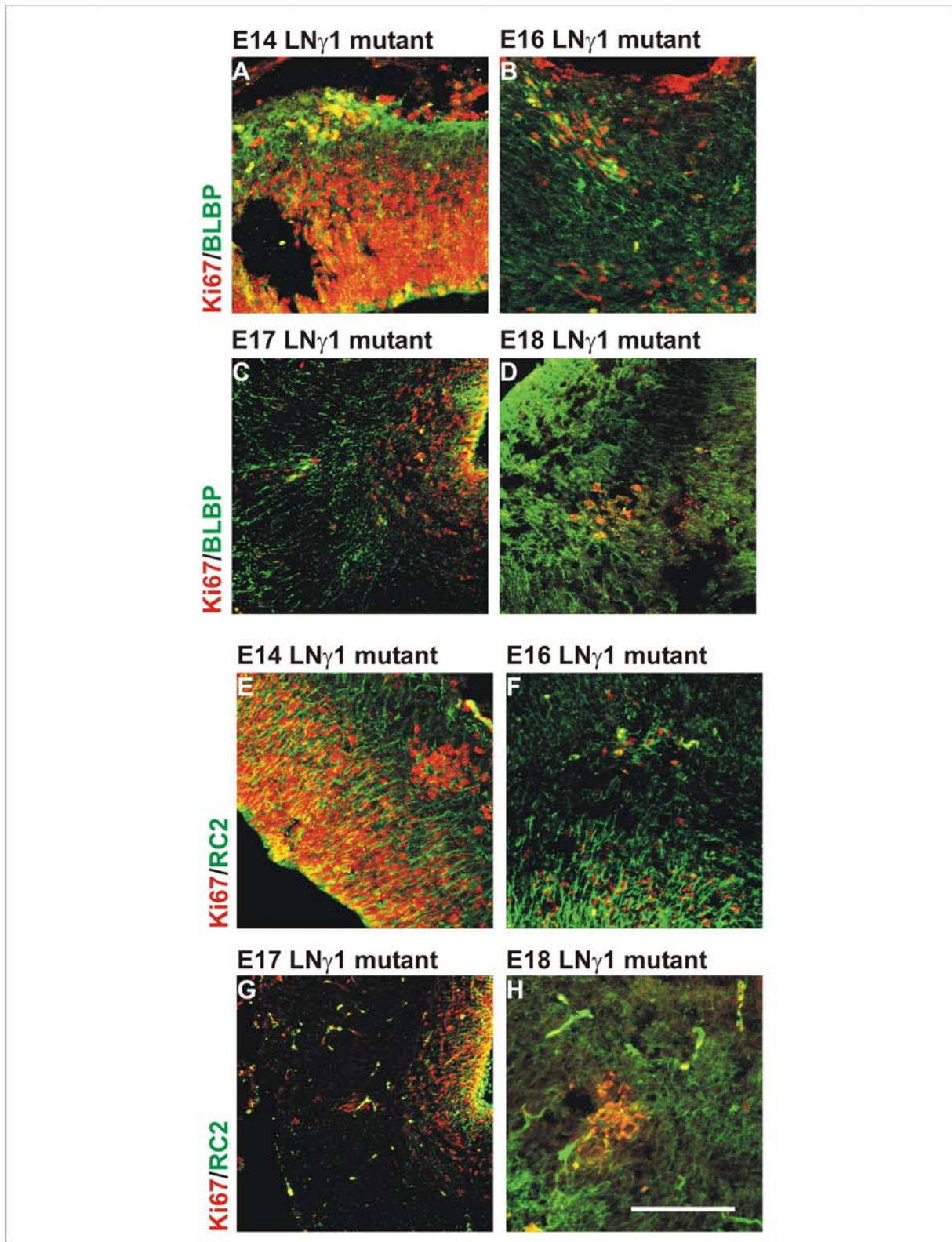


Fig. 17: Characterization of ectopic proliferating cell clusters in LN γ 1 mutant

Micrographs depicting coronal sections of E14-E18 cerebral cortex. Immunohistochemistry against Ki67 (marker for proliferating cells, red), RC2 and BLBP (marker for radial glia cells, green) was performed to determine the origin of the ectopic proliferating cells.

From E14-E18 cells proliferating in ectopic clusters in the cortex of the LN γ 1 mutant were immunoreactive for BLBP and RC2, thus they seem to be radial glia cells originating from the ventricular zone.

Scale bar: 100 μ m

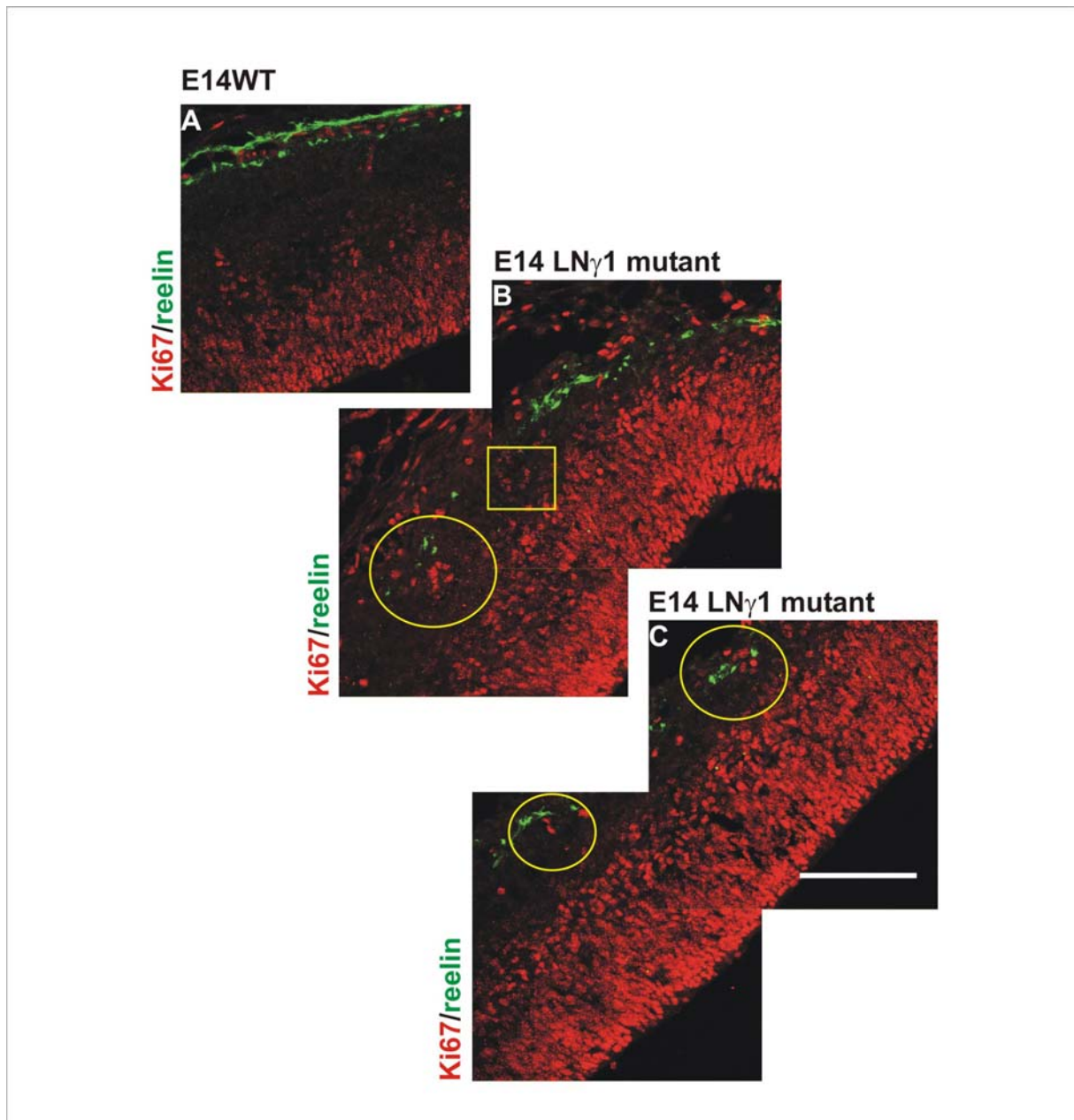


Fig. 18: Reelin expression and the formation of ectopic proliferating cell clusters in the LN γ 1 mutant
 Microrgraphs of coronal cortical sections. In order to assess why these ectopic cell clusters develop, immunohistochemistry against reelin (a signalling molecule for neurons to terminate their migration) and Ki67(marker for proliferating cells) was performed.

The reelin expression was not homogenous in the cortex of the LN γ 1 mutant (see also Halfter et al., 2002). No clear correlation was observed between the presence of reelin positive cells and the formation of ectopic cell clusters in the cortex of the LN γ 1 mutant (B,C). The yellow circles show colocalisation of proliferating Ki67 positive cells (red) and reelin positive cells (green), but occasionally clusters formed also in regions where no reelin positive cells were detectable (yellow square).

Scale bar: 100 μ m

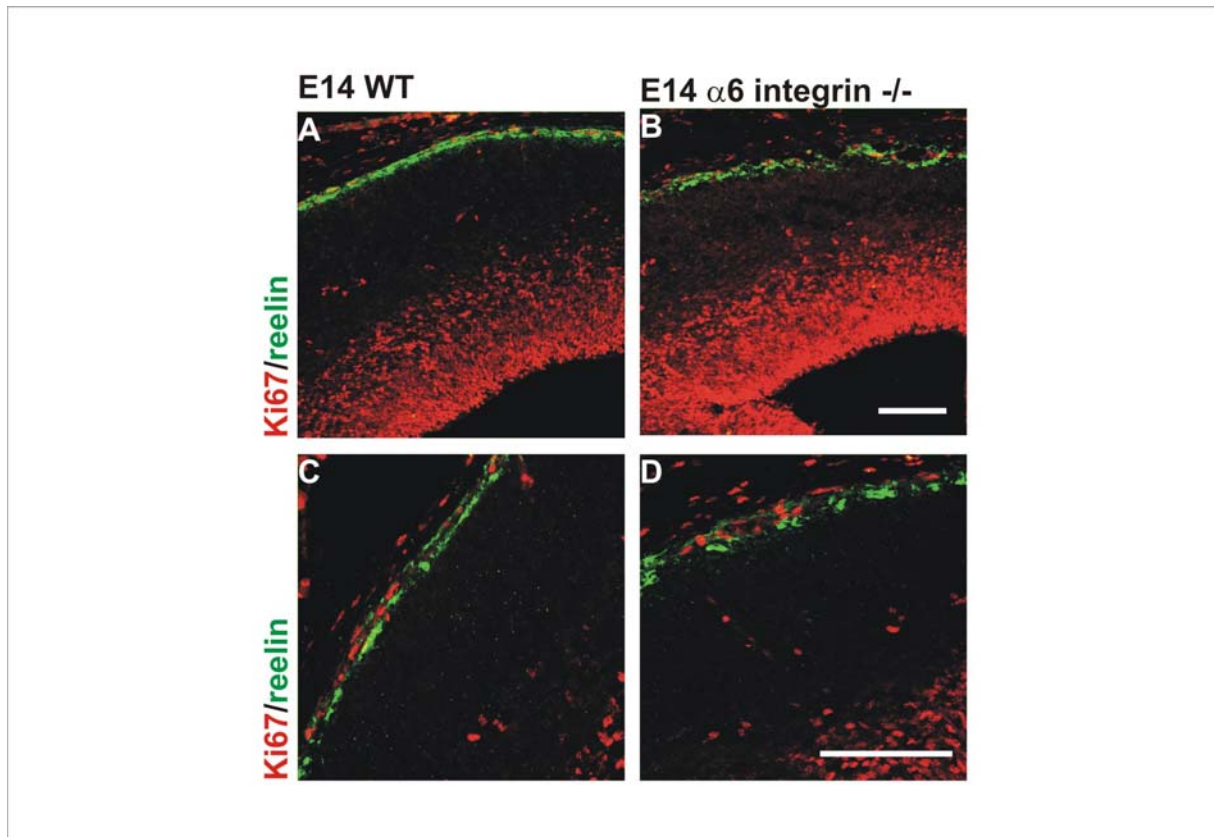


Fig. 19: Reelin expression in the $\alpha 6$ integrin $-/-$

Micrographs depicting coronal sections of E14 WT and $\alpha 6$ integrin $-/-$ cortex. Immunohistochemistry against Ki67 was performed to see whether clusters of ectopic proliferating cells develop in the cortex of $\alpha 6$ integrin $-/-$. No formation of ectopic proliferating cell clusters was observed in the $\alpha 6$ integrin $-/-$ (B,D) on account of the improper basement membrane assembly, and the reelin expression was normal in the $\alpha 6$ integrin $-/-$ (B,D) compared to WT (A,C).

Scale bars: 100 μ m

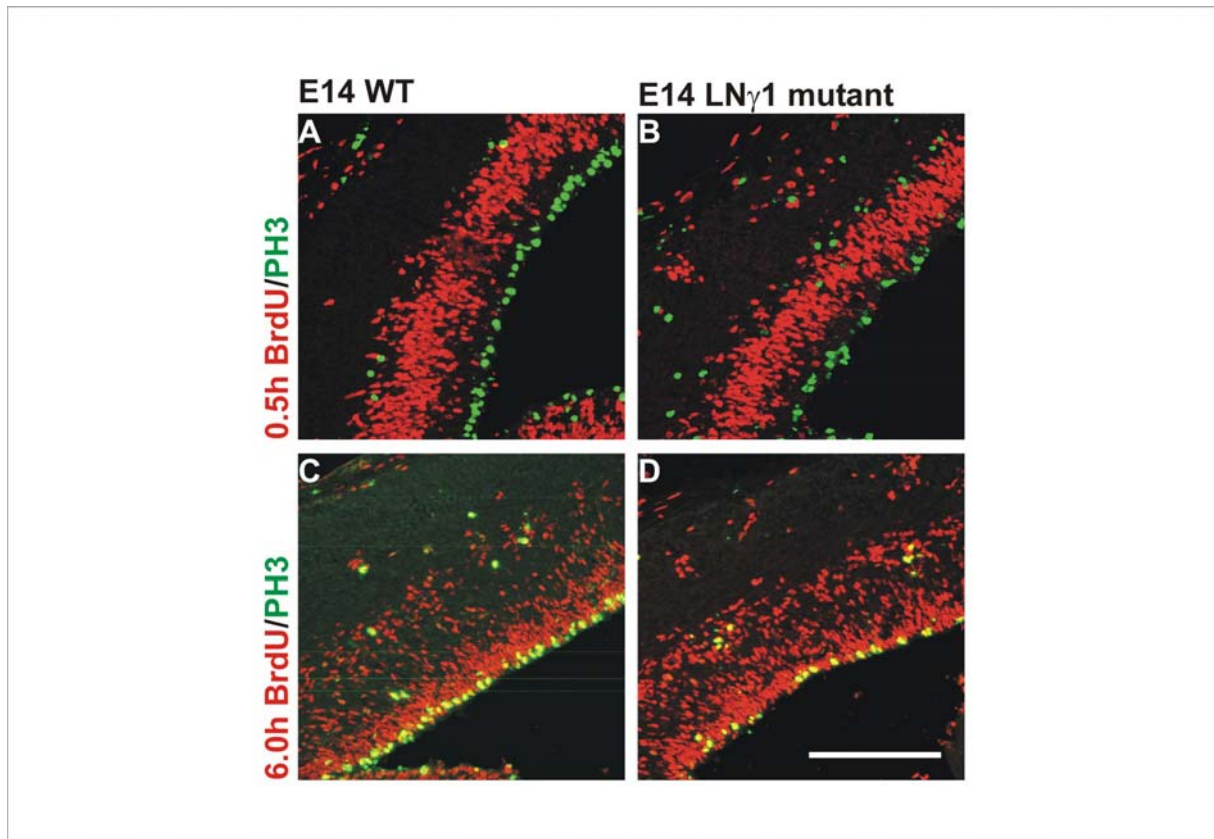


Fig. 20: Interkinetic nuclear migration in the LN γ 1 mutant

Micrographs of coronal sections of the lateral cortex at E14. Immunohistochemistry against BrdU (red) was performed to detect changes in the interkinetic nuclear migration. PH3 immunohistochemistry labels VZ and SVZ cells in M-phase (green). No obvious changes in the interkinetic nuclear migration were detected in the LN γ 1 mutant (B), which lacks the attachment of the radial glia endfeet at the basement membrane, compared to the corresponding WT littermate (A) in the 0.5h BrdU pulse and in the 6h BrdU pulse in the LN γ 1 mutant (B) compared to the WT (C).

Scale bar: 100 μ m

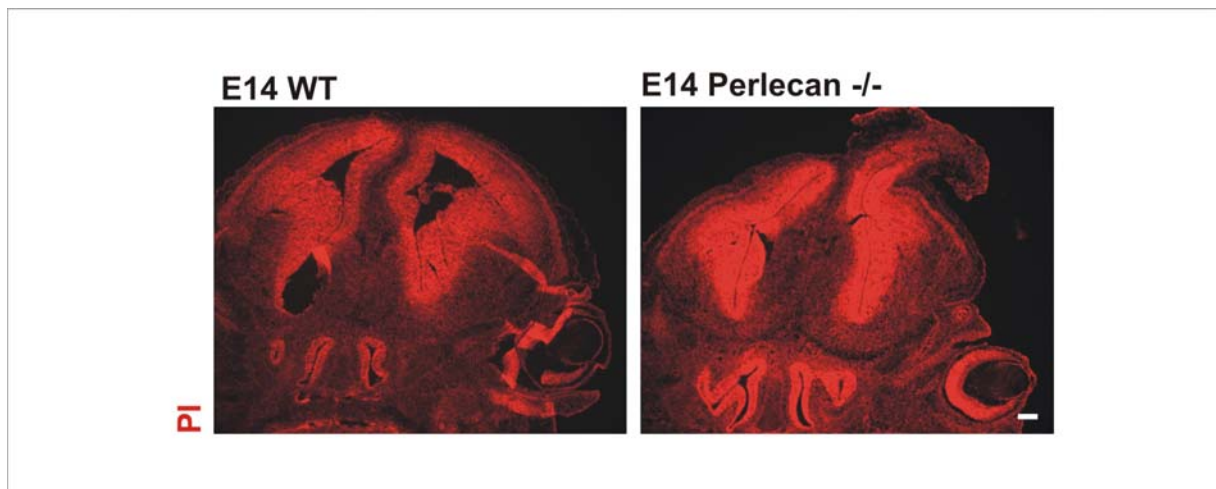


Fig. 21: E14 WT and perlecan^{-/-} brain morphology in coronal sections

Micrographs depicting coronal sections of the E14 WT and perlecan^{-/-} telencephalon assessed by propidium iodide (PI) staining, which detects the chromatin and thus labels cell nuclei.

Perlecan^{-/-} mice develop in most cases an exencephalic brain at E14. The analysis of the orientation of cell division was done on the left hemisphere of the depicted E14 perlecan^{-/-} telencephalon.

Scale bar: 100 μ m

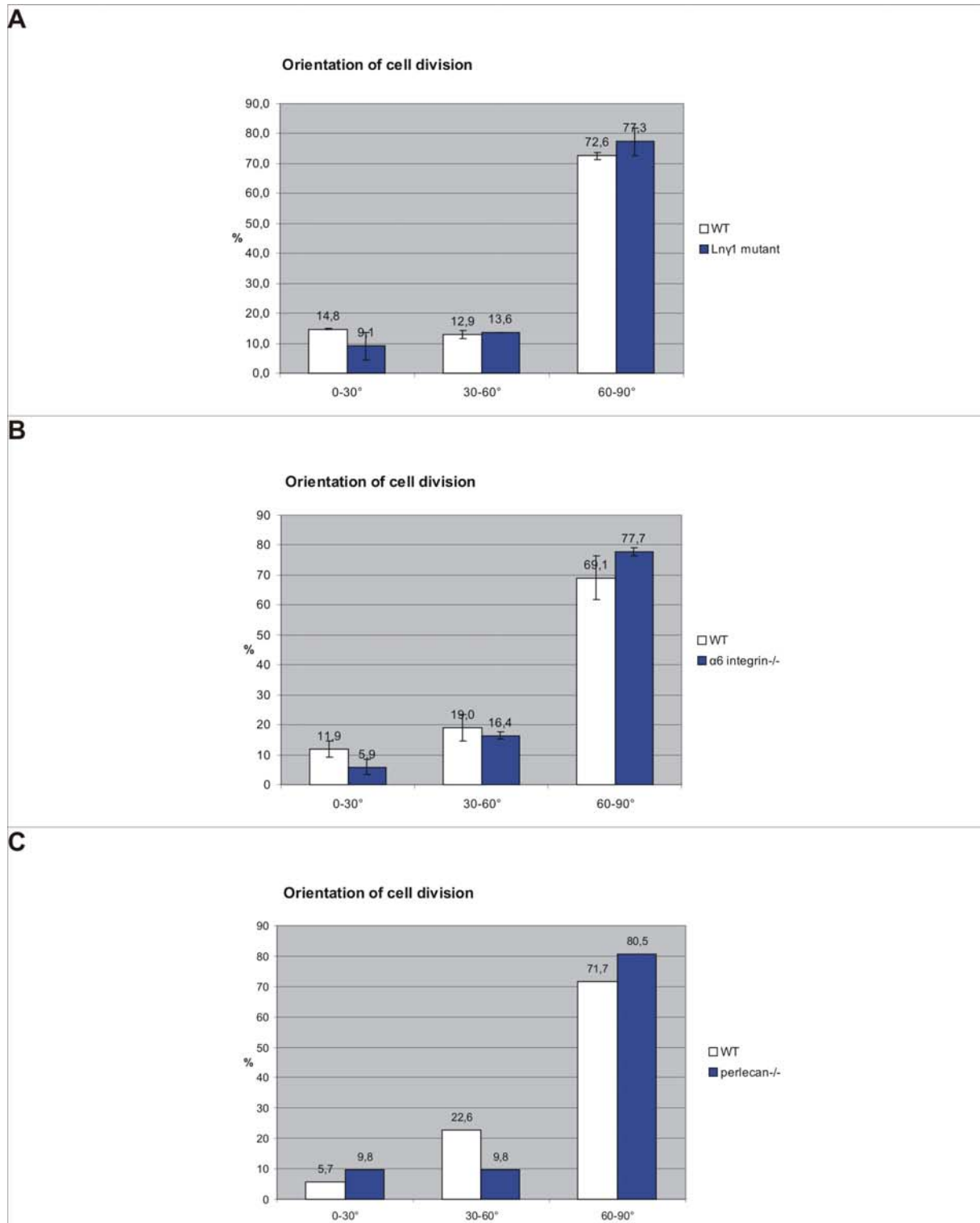


Fig. 22: Orientation of cell division in the basement membrane mutants

Histogram depicting the quantification of the orientation of cell divisions in anaphase at the ventricular surface at E14, assessed by propidium iodide staining. No significant changes in the orientation of cell division were detected in the basement membrane mutant mice LNy1 mutant (A), $\alpha 6$ integrin^{-/-} (B) and perlecan^{-/-} (C). Error bars given as s.d..

The columns in C (WT and perlecan^{-/-}) lack error bars since only one brain was analyzed.

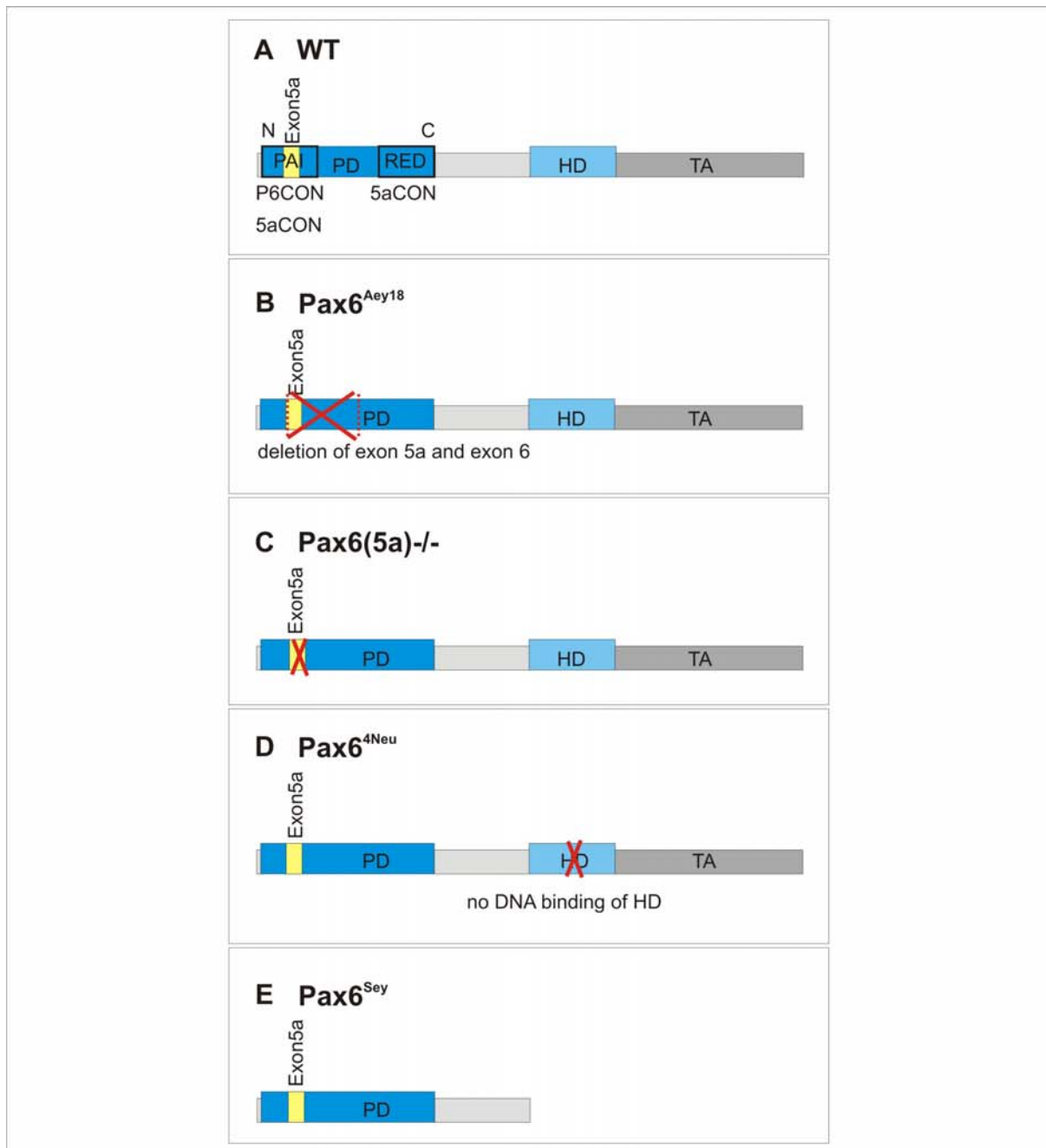


Fig. 23: Schematic drawings of the Pax6 mRNA in WT and mice harbouring mutations in the distinct DNA-binding domains of Pax6

The mRNA of Pax6 (A) consists of two DNA-binding domains, the paired domain (PD) and the homeodomain (HD). The PD is a bipartite DNA-binding domain, subdivided in the N-terminal PAI and the C-terminal RED domain. The PAI domain is able to bind to P6CON (Pax6 consensus site) and 5aCON (Pax6(5a) consensus site), whereas the RED domain binds exclusively to 5aCON. By means of alternative splicing, 14 AA are inserted into the N-terminal PAI domain (see yellow box) and thereby PAI DNA-binding is abolished. The transactivation domain (TA), important for gene activation, is located at the C-terminal end of Pax6. The *Pax6^{Aey18}* mutant (B) is characterized by a large deletion in the PD (exon 5a and exon 6), whereas the HD and TA are still present. The *Pax6(5a)^{-/-}* (C) lacks exon 5a in the PD due to gene targeting (Singh et al., 2002), while the rest of the PD, HD and TA are unaffected. *Pax6^{4Neu}* mutant mice (D) bear a point mutation in the HD that abolishes DNA binding of the HD, while PD and TA remain intact (Favor et al., 2001). The *Pax6^{Sey}* mutant mice are characterized by a truncated form of Pax6, lacking the HD and TA (E). These mutants have a comparable phenotype to the full gene deletion (*Pax6^{-/-}*) and are therefore referred to as functional null alleles.

Abbreviations: PD= paired domain; HD= homeo domain; TA= PST-rich transactivator domain; P6CON= Pax6 consensus site; 5aCON= Pax6(5a) consensus site.

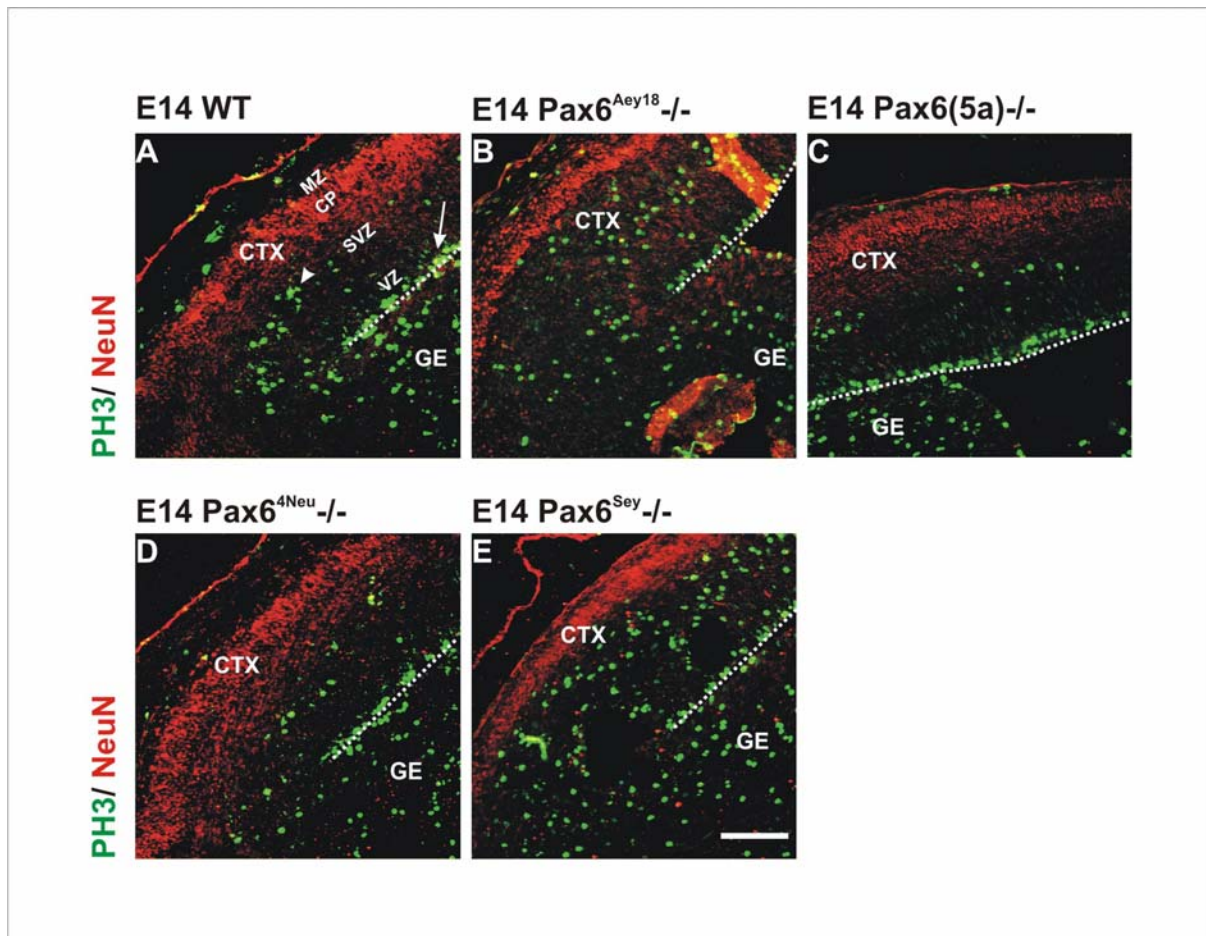


Fig. 24: Neurogenesis and cell proliferation in the cerebral cortex in different mutant Pax6 alleles

Micrographs (A-E) show coronal sections of the lateral cerebral cortex immunostained against the neuronal marker NeuN (red) and a marker for cells in M-phase, PH3 (green) at E14 in the respective mutant Pax6 alleles as indicated in the panel. The band of NeuN-positive cells is reduced in the PD mutant *Pax6^{Aey18}*^{-/-} (B) compared to WT cortex (A), indicating a reduced neurogenesis that appears comparable in extent to the phenotype in the functional null allele *Pax6^{Sey}*^{-/-} (E). In contrast, no changes in neurogenesis were observed for the cortex of *Pax6(5a)*^{-/-} (C) or the HD mutant *Pax6^{4Neu}*^{-/-} (D).

In the mutants with a decrease in neurogenesis (the PD mutant *Pax6^{Aey18}*^{-/-} and *Pax6^{Sey}*^{-/-}), an increase in the number of PH3-positive cells was observed (B,E), while no changes in comparison to WT (A) were seen in the cortex of *Pax6(5a)*^{-/-} (C) and *Pax6^{4Neu}*^{-/-} (D). Note that the PH3-positive cells were mostly increased in the subventricular zone (SVZ, arrowhead in A; increase in B and E), but not in the VZ (arrow in A). Thus, the PD of Pax6 is necessary and sufficient to mediate the effects of Pax6 on neurogenesis and cell proliferation in the cerebral cortex, while targets of the HD seems to play no role in these aspects. The dashed white line (A-E) indicates the ventricular surface of the cortex.

Abbreviations: MZ= marginal zone; CP= cortical plate, SVZ= subventricular zone; VZ= ventricular zone; CTX= cortex; GE= ganglionic eminence.

Scale bar: 100µm.

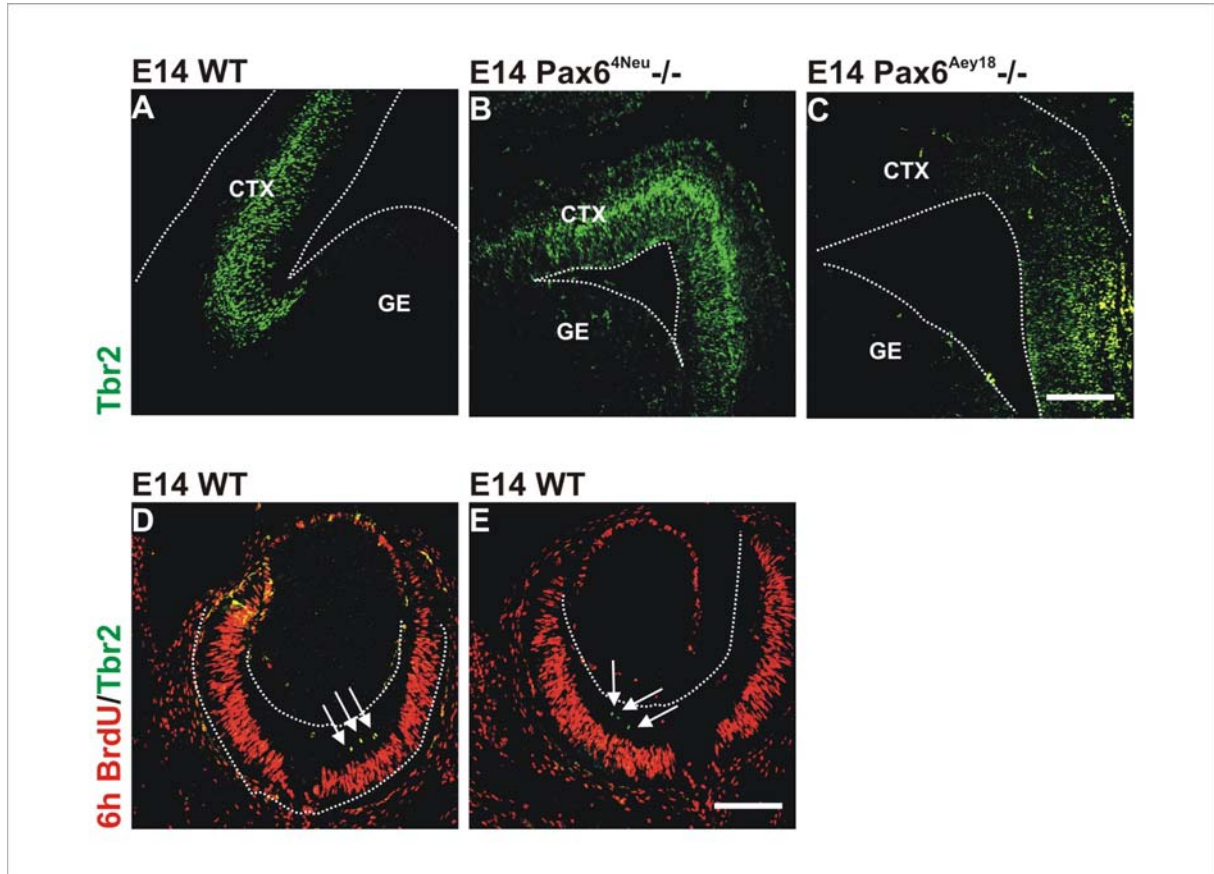


Fig. 25: Tbr2 expression in the cerebral cortex of WT, Pax6^{Aey18}-/-, in the Pax6^{4Neu}-/- and in the WT eye
 Coronal sections of E14 telencephalon immunostained against Tbr2, a transcription factor that is specifically expressed in the cells of the SVZ in the WT cerebral cortex at E14 (A). Tbr2 expression was detectable in the cerebral cortex of the Pax6^{4Neu}-/- mutant mice (lacking HD DNA-binding), while Tbr2 expression in the Pax6^{Aey18}-/- (PD mutant) was absent in the lateral cortex, but present at very medial cortical regions where also Pax6 is expressed at a very low level. Thus, the PD of Pax6 seems to be required for the regulation of Tbr2 expression in the SVZ.

Tbr2 expression was also found in some neurons in the developing eye at E14 (see arrows in D,E). In order to visualize the eye structure better, immunohistochemistry against BrdU (red) is shown, which labels proliferating cells, located at the outer surface of the optic cup, while the neurons are located at the inner surface where the Tbr2 positive cells are present. The dashed white line indicates the outline of the telencephalon (A,C) and the ventricular surface (B,C). The outline of the neuroretina is given with a dashed white line (D) and the inner surface of the neuroretina is visualized by a dashed white line (E).

Scale bar: 100µm

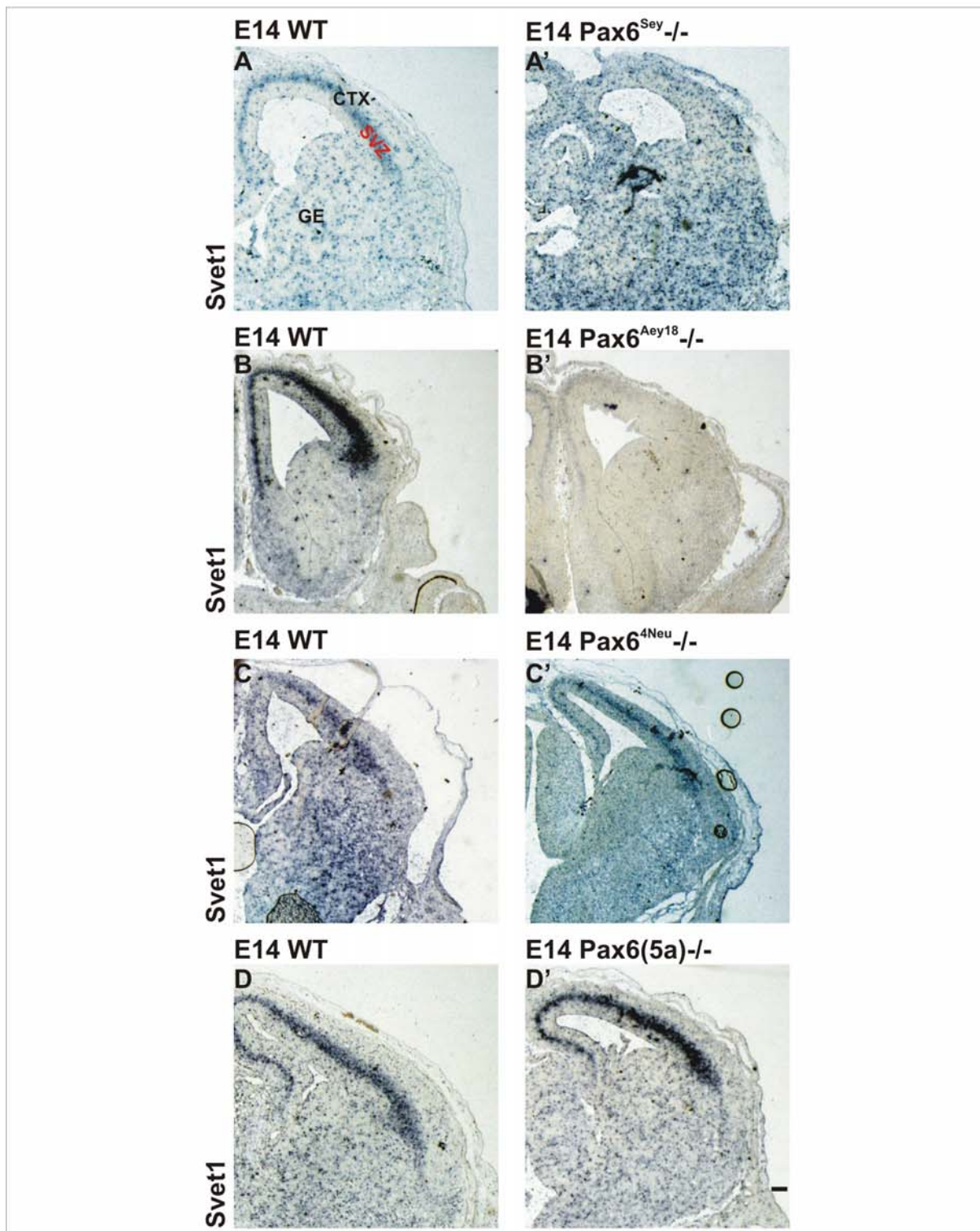


Fig. 26: *Svet1* expression in the subventricular zone of the cerebral cortex in the specific Pax6 mutant alleles

Micrographs depicting in situ hybridization for *Svet1* (subventricular tag 1) RNA in coronal sections of the telencephalon of WT and mutant littermates as indicated in the panel at E14. *Svet1* is expressed at high levels in the subventricular zone (SVZ) of the cerebral cortex of WT (A,B,C,D), Pax6^{4Neu}-/- (lacking HD DNA-binding) (C') and Pax6(5a)-/- mice (D'), while its expression is lost at this position in the telencephalon of the Pax6^{Scy}-/- (A') and almost not detectable anymore in the cortex of the Pax6^{Aey18}-/- (B') (lacking a large part of the PD). Thus, DNA binding of the PD of Pax6 seems to be required for the regulation of *Svet1* expression in the SVZ.

Abbreviations: CTX= cortex; GE= ganglionic eminence; SVZ= subventricular zone. Scale bar: 100µm

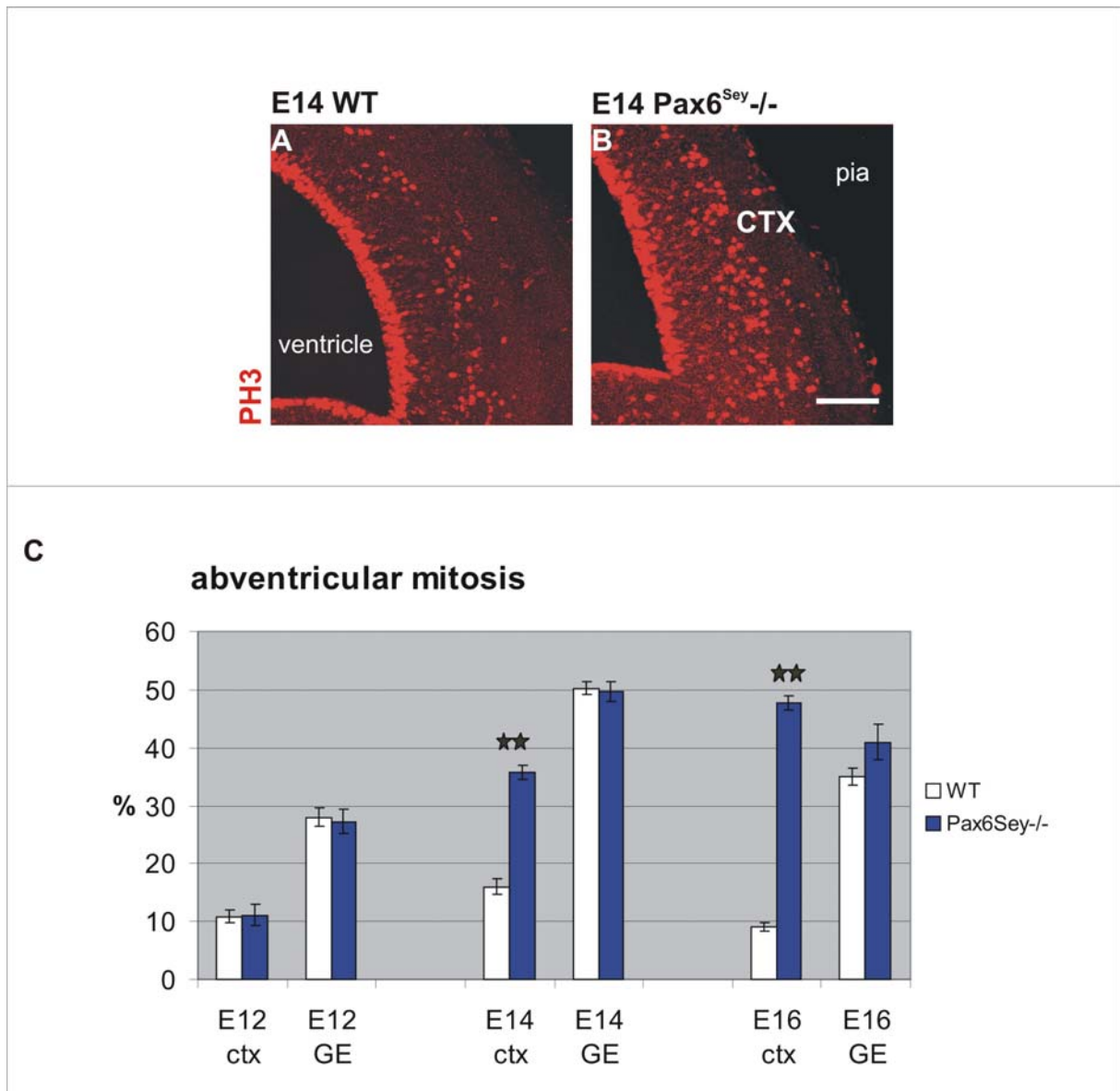


Fig. 27: Increase in cell proliferation in the Pax6^{Sey}-/- mutant mice

Microrgraphs depicting coronal cortical sections at the lateral level at E14 in WT (A) and Pax6^{Sey}-/- (B). Loss of functional Pax6 leads to a strong increase in cell proliferation in the dorsal telencephalon (ctx) of the Pax6^{Sey}-/- as detected by immunohistochemistry against PH3, a marker for cells in M-phase. Especially the number of cells dividing at abventricular positions is strongly increased and increases over time in the Pax6^{Sey}-/- mutant cortex (C, blue bars) compared to the WT (C, white bars).

Scale bar: 100µm

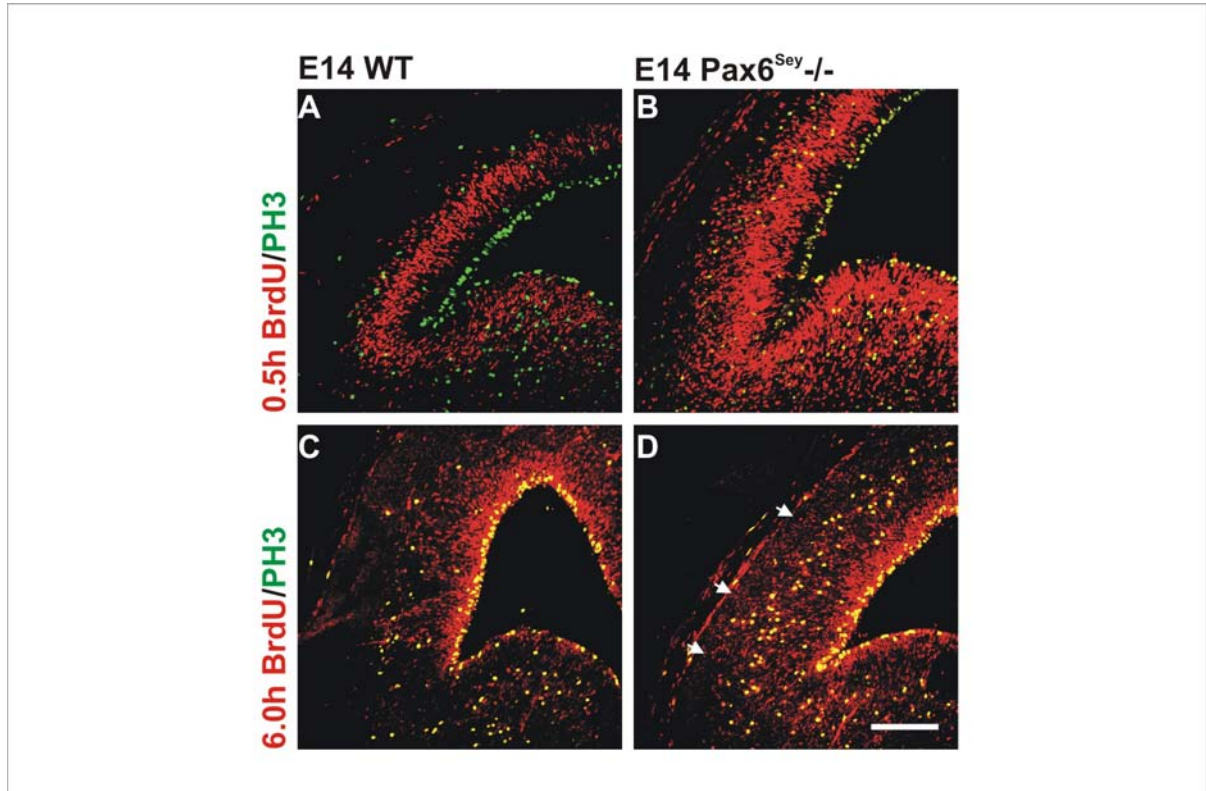


Fig. 28: Interkinetic nuclear migration in the absence of functional Pax6

Microrgraphs (A-D) depicting the lateral cortex of E14 WT and the functional null allele *Pax6*^{Scy}-/- after a 0.5h and a 6.0h BrdU pulse. The sections were immunostained against BrdU (red, a marker for cells in S-phase) and PH3 (green, a marker for cells in M-phase). Dividing PH3 positive cells were detectable at the ventricular surface (corresponding to the ventricular zone (VZ) cells) and at abventricular positions (corresponding to the subventricular zone (SVZ) cells).

In the WT cerebral cortex (A), a band of BrdU labeled cells (red) is visible in the basal part of the VZ after a 0.5h BrdU. Note that the apical zone of the VZ does not contain any BrdU labeled cells. In the cortex of the functional null allele *Pax6*^{Scy}-/- (B) much more BrdU labeled cells are detectable in the proliferative zone and they seem to be more spread than in the WT, with even some BrdU labeled cells that are located in the apical zone of the VZ close to the ventricular surface. The thickness of the apical VZ that is normally free of BrdU labeled cells is smaller in the cortex of the *Pax6*^{Scy}-/-.

After a BrdU pulse of 6.0 hours cells have translocated their nuclei towards the VS in the WT (C), which leads to the appearance of a band of BrdU positive cells at the VS. In the *Pax6*^{Scy}-/- cortex (D) cell nuclei were as well translocated to the VS, but the BrdU positive cells are still more spread all over the cerebral cortex reaching almost the pial surface (arrows in D).

Scale bar: 100µm

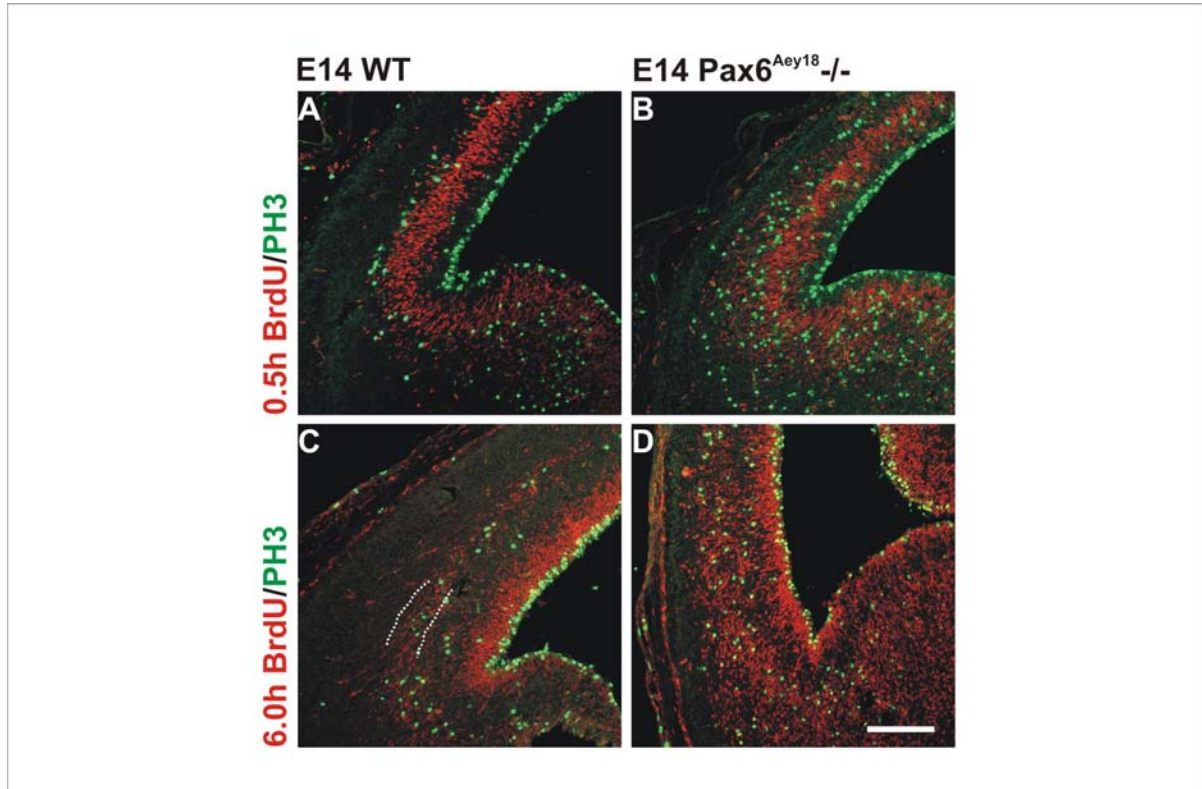


Fig. 29: Interkinetic nuclear migration in the Pax6^{Aey18}-/- mutant

Microrgraphs (A-D) depicting the lateral cortex of E14 WT and Pax6^{Aey18}-/- (lacking a functional PD) after a 0.5h and a 6.0h BrdU pulse. The sections were immunostained against BrdU (red, a marker for cells in S-phase) and PH3 (green, a marker for cells in M-phase). Dividing PH3 positive cells are detectable at the ventricular surface (corresponding to the ventricular zone (VZ) cells) and at abventricular positions (corresponding to the subventricular zone (SVZ) cells).

In the WT cerebral cortex (A), a band of BrdU labeled cells (red) is visible in the basal part of the VZ after a 0.5h BrdU. Note that the apical part of the VZ does not contain any BrdU labeled cells.

In contrast in the Pax6^{Aey18}-/- (B) more cells are BrdU positive in the proliferative zone and the width of the apical area of the VZ that does not contain BrdU labeled nuclei is decreased. After a BrdU pulse of 6.0 hours cells have translocated their nuclei towards the VS in the WT (C), which leads to the appearance of a band of BrdU positive cells at the VS. In the Pax6^{Aey18}-/- cortex (D) cell nuclei were as well translocated to the VS, but BrdU positive cells are more spread all over the cerebral cortex, very similar to the situation in the cerebral cortex of the functional null allele Pax6^{Scy}-/- (see Fig. 28). The dashed white line indicates the SVZ in the WT (C).

Scale bar: 100µm

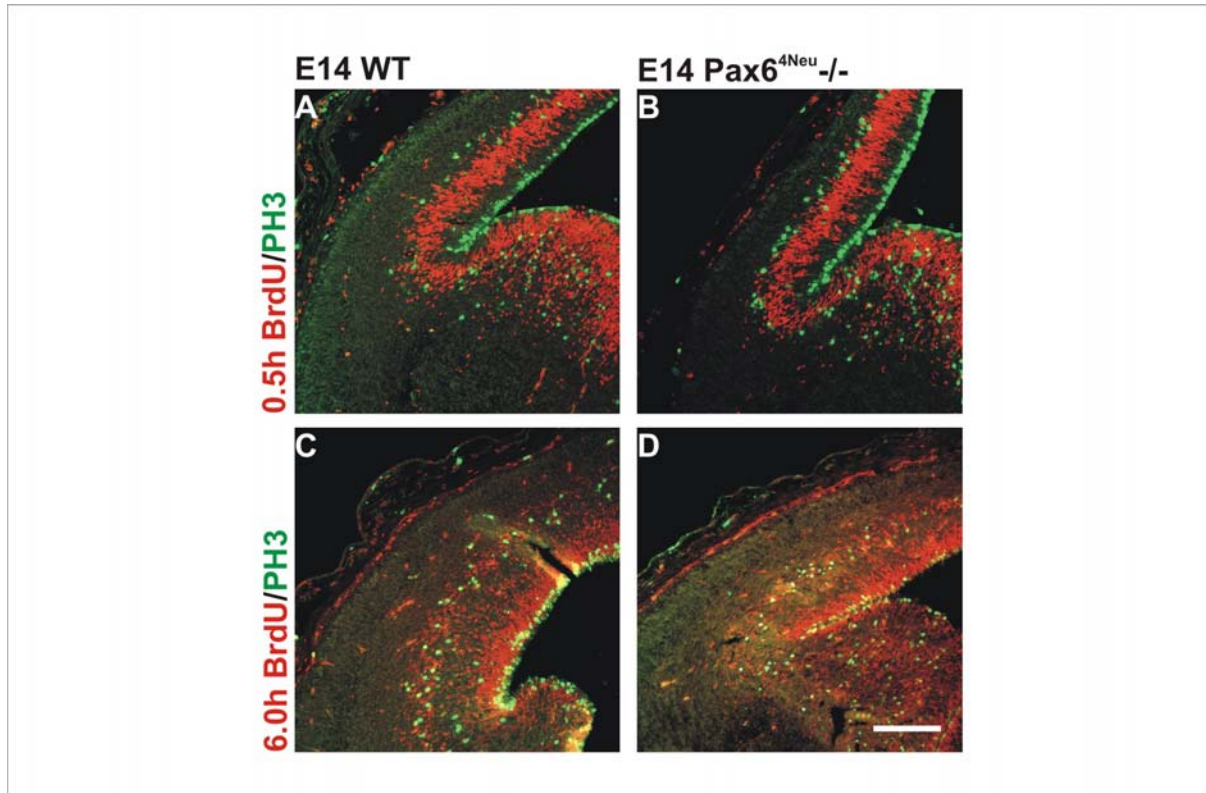


Fig. 30: Interkinetic nuclear migration in the Pax6^{4Neu}-/- mutant

Microrgraphs (A-D) depicting the lateral cortex of E14 WT and Pax6^{4Neu}-/- (lacking HD DNA-binding) after a 0.5h and a 6.0h BrdU pulse. The sections were immunostained against BrdU (red, a marker for cells in S-phase) and PH3 (green, a marker for cells in M-phase). Dividing PH3-positive cells are detectable at the ventricular surface (corresponding to the ventricular zone (VZ) cells) and at abventricular positions (corresponding to the subventricular zone (SVZ) cells).

In the WT cerebral cortex (A), a band of BrdU labeled cells (red) is visible in the basal part of the VZ after a 0.5h BrdU. Note that the apical zone of the VZ does not contain any BrdU labeled cells. The same phenotype as in the WT (A) was detected in the Pax6^{4Neu}-/- (B) cerebral cortex. In addition, the width of the band in the basal VZ containing BrdU labeled nuclei was very similar between WT and Pax6^{4Neu}-/-.

After a BrdU pulse of 6.0 hours cells have translocated their nuclei towards the VS in the WT (C), which leads to the appearance of a band of BrdU positive cells at the VS and the same phenotype was detected in the Pax6^{4Neu}-/- (D).

Scale bar: 100µm

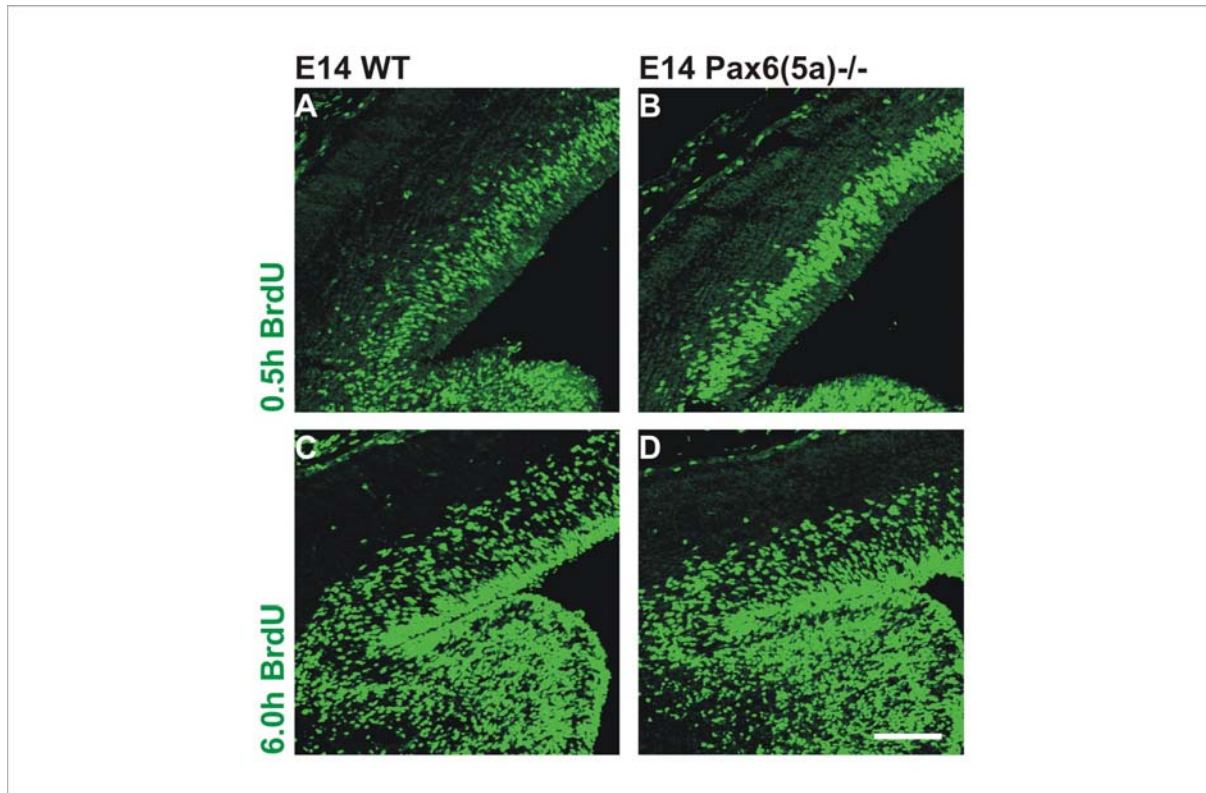


Fig. 31: Interkinetic nuclear migration in the Pax6(5a)^{-/-}

Microrgraphs (A-D) depicting the lateral cortex of E14 WT and Pax6(5a)^{-/-} (lacking specifically exon 5a) after a 0.5h and a 6.0h BrdU pulse. The sections were immunostained against BrdU (green, a marker for cells in S-phase).

In the WT cerebral cortex (A), a band of BrdU labeled cells (green) is visible in the basal part of the VZ after a 0.5h BrdU.

The same phenotype as in the WT (A) was detected in the Pax6(5a)^{-/-} (B) cerebral cortex. The width of the apical zone of the VZ, that is free of BrdU positive nuclei, is very similar in WT (A) and Pax6(5a)^{-/-} (B).

After a BrdU pulse of 6.0 hours cells have translocated their nuclei towards the VS in the WT (C), which leads to the appearance of a band of BrdU positive cells at the VS and the same phenotype was detected in the Pax6(5a)^{-/-} (D).

Scale bar: 100µm

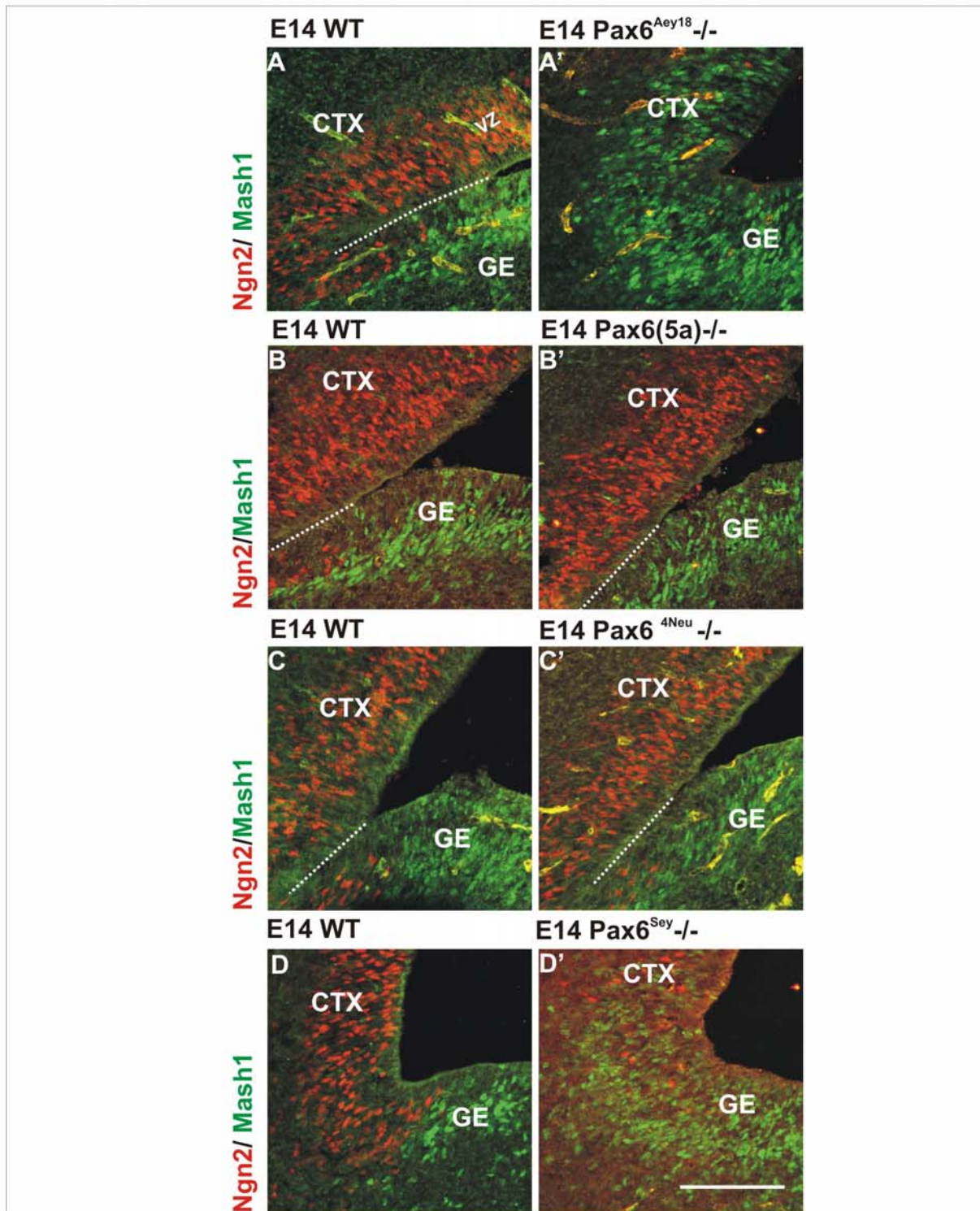


Fig. 32: Regionalisation in the telencephalon of the different mutant Pax6 alleles

Micrographs of coronal sections depicting the lateral telencephalon at E14. In WT cortex (CTX) (A-D), but not ganglionic eminence (GE) precursors are Ngn2-immunopositive (red), while precursors in the GE, but not the CTX, are Mash1-immunoreactive (green in A-D). Panels from corresponding Pax6 mutant mice are depicted in the right column (A'-D'). Note that Ngn2-immunoreactivity is not detectable in the cortex of Pax6^{Aey18}-/- (carrying a large deletion in the PD) (A') and the functional null allele Pax6^{Sey}-/- (E'), while it is unaffected in the cortices of Pax6(5a)-/- (B') and Pax6^{4Neu}-/- (lacking HD DNA-binding) (C') mice. Conversely, Mash1-immunoreactivity spreads ectopically into the cortex of Pax6^{Aey18}-/- (A') and Pax6^{Sey}-/- (D') mice, but is not changed in Pax6(5a)-/- (B') or Pax6^{4Neu}-/- (C') telencephalon. Thus, the PD of Pax6 seems to be necessary and sufficient to exert patterning of the telencephalon. The dashed white line (A,B,B',C,C') indicates the ventricular surface. Scale bar: 100µm.

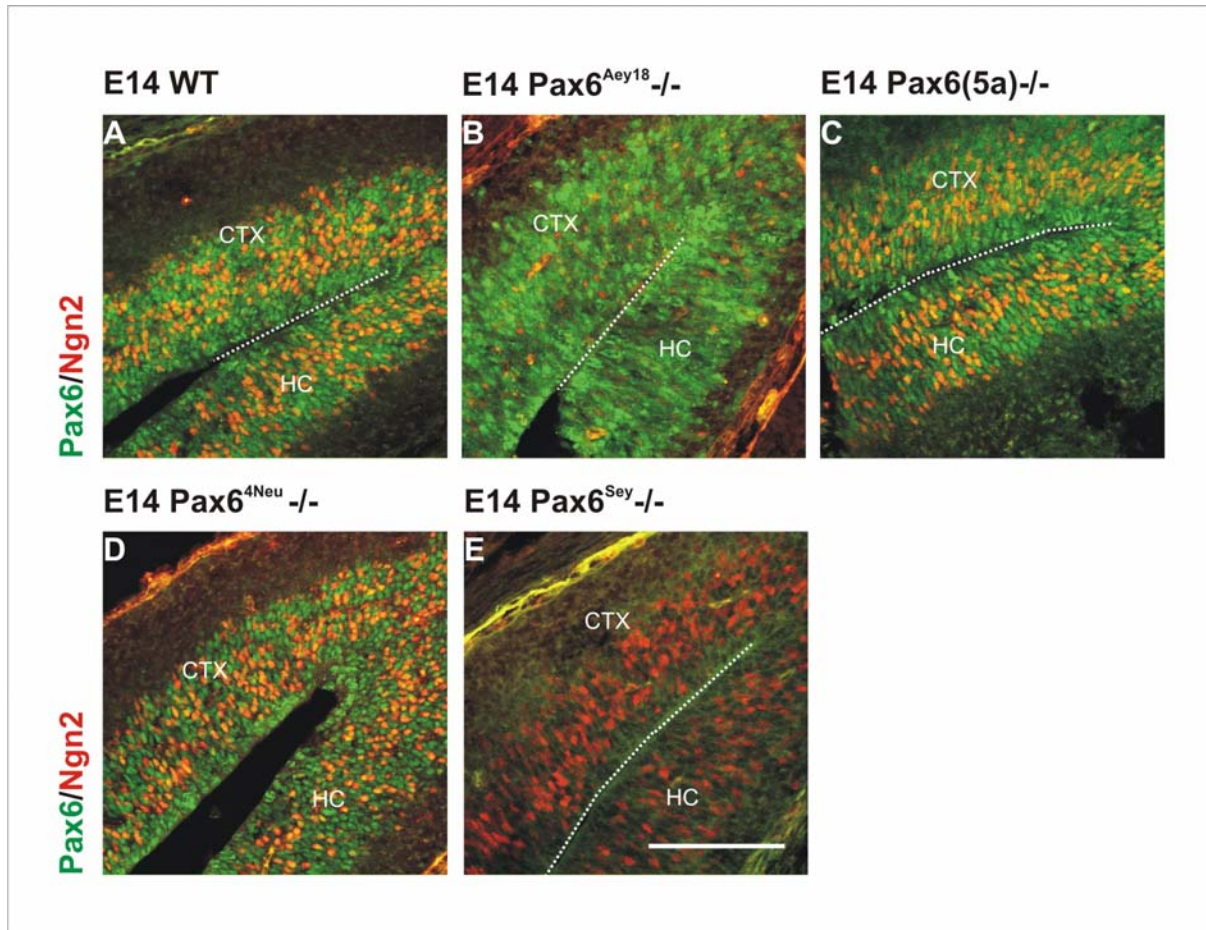


Fig. 33: Ngn2 expression in caudal/medial regions of the telencephalon in absence of specific DNA-binding domains

Micrographs of coronal sections of the caudo-medial cortex from E14 mice immunostained against Ngn2 (red) and Pax6 (green). Ngn2-immunoreactive cells are a subset of Pax6-positive cells that are severely reduced, but not completely absent in the medial cortex of the PD mutant $Pax6^{Aey18-/-}$ (B) and in the functional null allele $Pax6^{Sey-/-}$ (E) compared to WT (A). No changes in the number of Ngn2-positive cells were detectable in the cortex of $Pax6(5a)-/-$ (C) and the HD mutant $Pax6^{4Neu-/-}$ (D). The dashed white line (A,B,C,E) indicates the ventricular surface.

Abbreviations: CTX=cortex; HC=Hippocampus.

Scale bar: 100 μ m

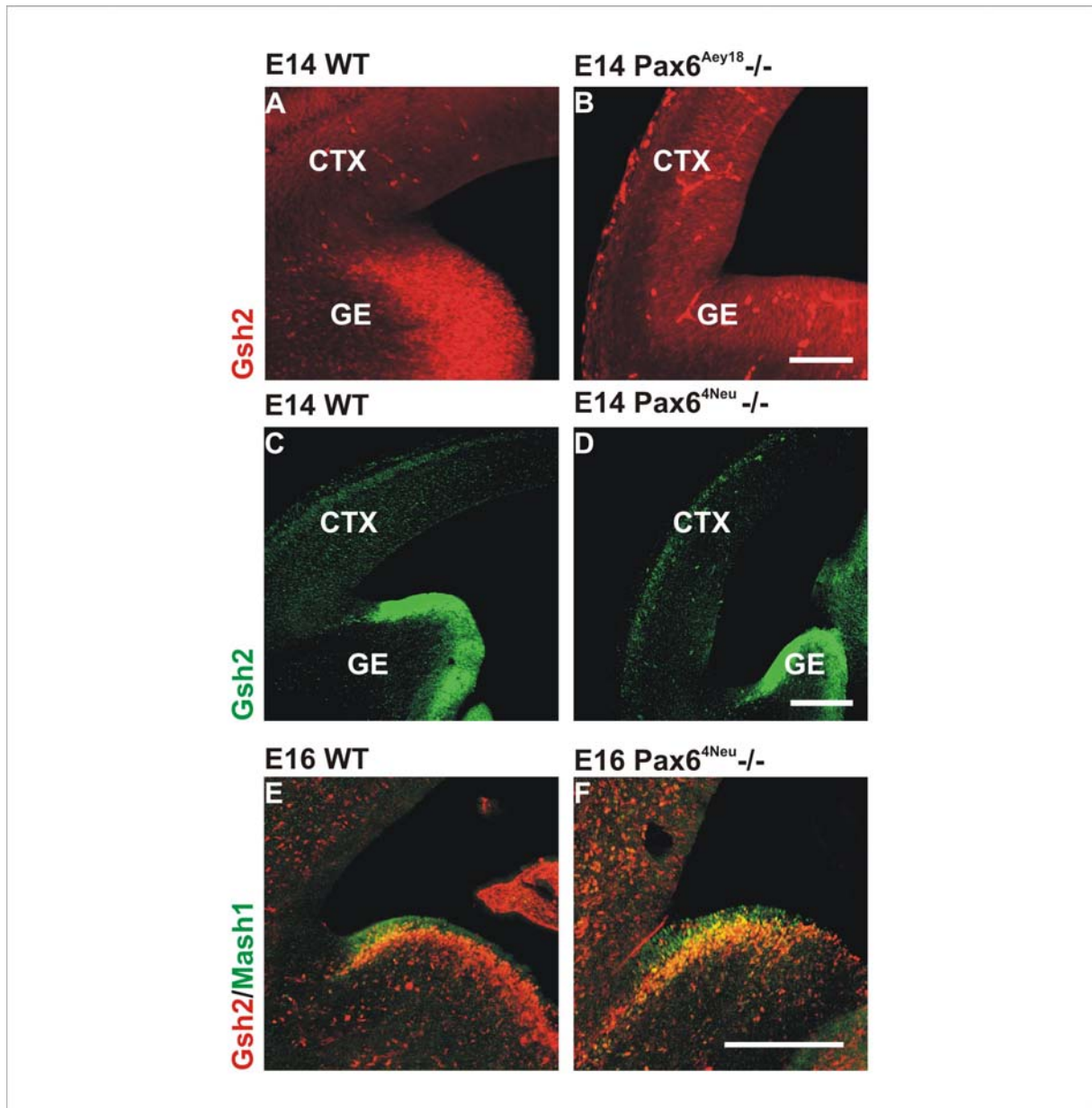


Fig. 34: Regionalisation in the absence of a functional PD and HD

Micrographs of coronal sections depicting the lateral cortex of E14 WT and E14 Pax6^{Aey18}^{-/-}, Pax6^{4Neu}^{-/-} and E16 WT and Pax6^{4Neu}^{-/-} mutants. Immunohistochemistry against Gsh2 and Mash1 was used in order to analyze regionalisation of the telencephalon.

The transcription factor Gsh2 is expressed in the ganglionic eminence (GE) in the WT telencephalon (A). In contrast, loss of a functional PD in the Pax6^{Aey18}^{-/-} (B) leads to the expansion of Gsh2 into the cortex (CTX), while no expansion of Gsh2 is detectable in the Pax6^{4Neu}^{-/-} (lacking HD DNA-binding) (D) compared to the corresponding WT (C) at E14. Also at E16 no expansion of Gsh2 was detectable in the telencephalon of Pax6^{4Neu}^{-/-} (F) compared to the WT control (E).

Scale bars: 100µm

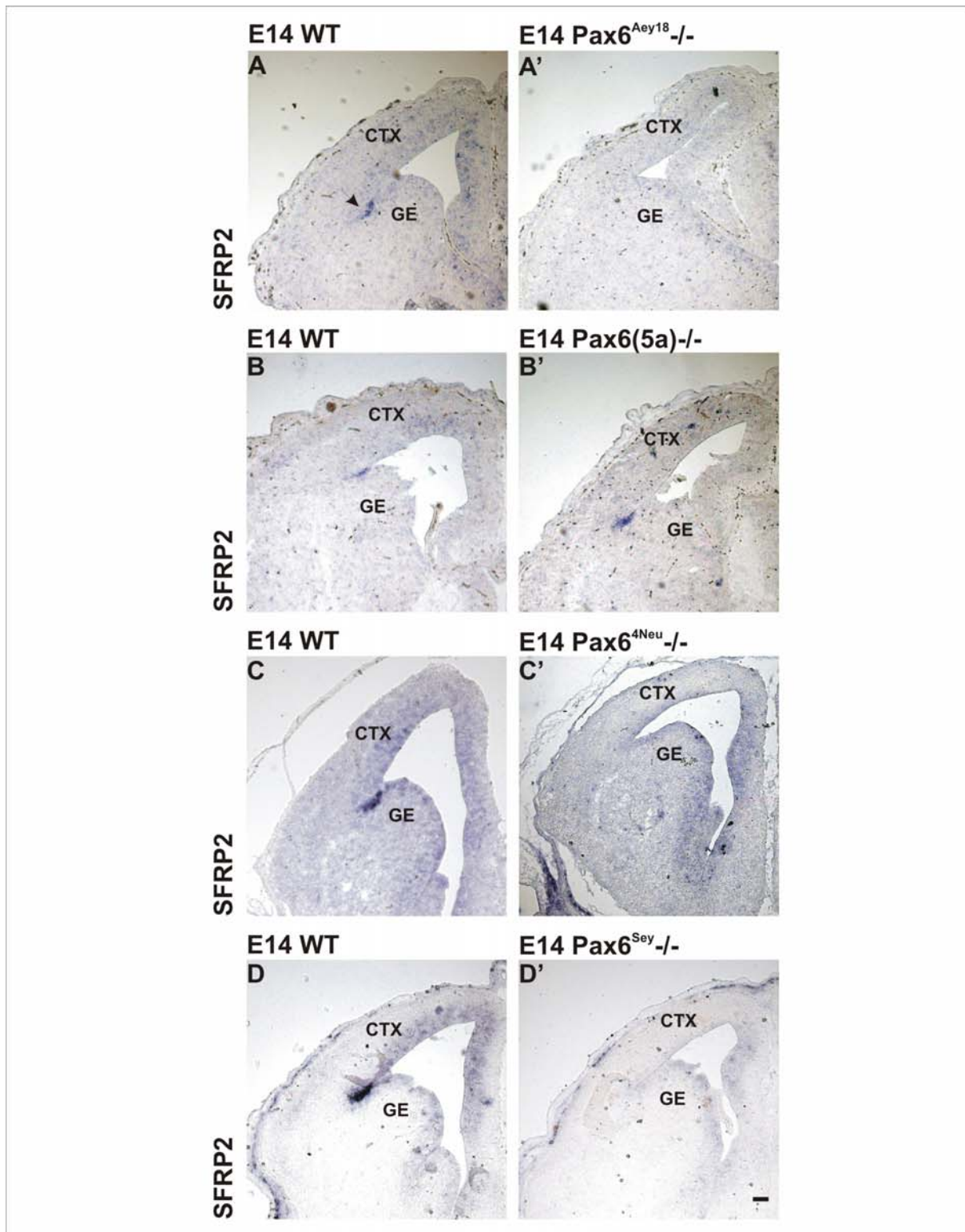


Fig. 35: SFRP2 expression at the pallial-subpallial boundary in the specific Pax6 mutant alleles
 Micrographs depicting in situ hybridization for SFRP2 (secreted frizzled related protein 2) mRNA in coronal sections of the telencephalon of WT and mutant littermates as indicated in the panel at E14. SFRP2 expression is highest in the cells of the pallial (CTX)-subpallial (GE) boundary (PSB) in the telencephalon of WT (see arrowhead in A and B-D), and Pax6(5a)-/- mice (B'), while its expression is lost at this position in the telencephalon of the Pax6^{Aey18}-/- (A') (lacking a large part of the PD), the HD Pax6^{4Neu}-/- (lacking HD DNA-binding) (C') mice and in the functional null allele Pax6^{Sey}-/- (D'). Thus, both, DNA binding of the PD and the HD of Pax6 are required for SFRP2 expression at the pallial-subpallial boundary. Abbreviations: CTX=cortex; GE= ganglionic eminence. Scale bar: 100µm

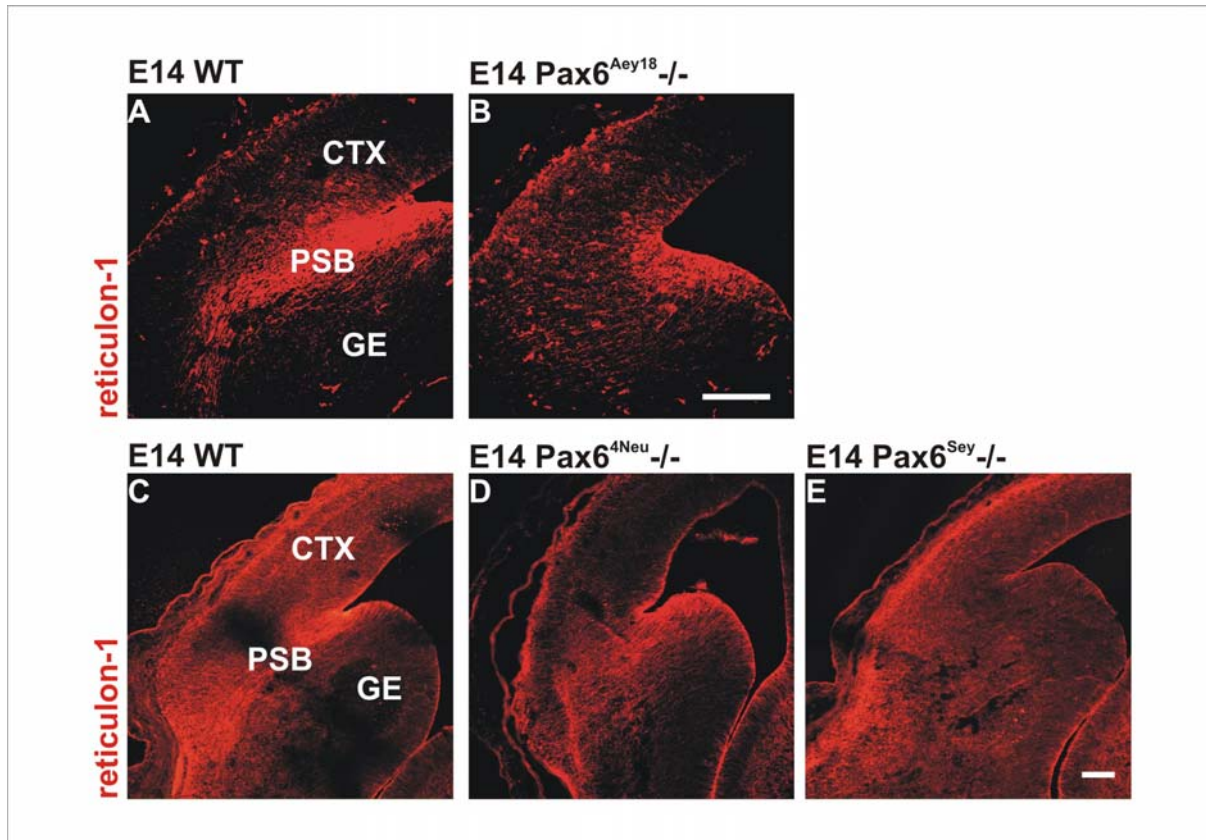


Fig. 36: Expression of reticulon-1 at the pallial-subpallial boundary

Micrographs of coronal sections depicting the telencephalon at the region of the pallial-subpallial boundary (PSB) at E14.

Reticulon-1 (red) is specifically expressed in the radial glia cells that form the radial glia fascicle at the PSB. In the WT telencephalon reticulon-1 immunohistochemistry reveals the presence of a fascicle that forms at the PSB, where cortex (ctx) and ganglionic eminence (GE) abut (A,C). Loss of functional Pax6 protein in the $Pax6^{Sey-/-}$ leads to a failure in the formation of the PSB, which is reflected in the lack of reticulon-1 expression (E). While reticulon-1 expression is still detectable in the telencephalon of the $Pax6^{Aey18-/-}$ (PD mutant) and in the $Pax6^{4Neu-/-}$ (HD mutant), no fascicle formation can be observed. Instead, radial glia cells extend more parallel in a rather broad area towards the pial surface (B,D) compared to the WT (A,C). Abbreviations: CTX= cortex; GE= ganglionic eminence; PSB= pallial-subpallial boundary.

Scale bars: 100 μ m

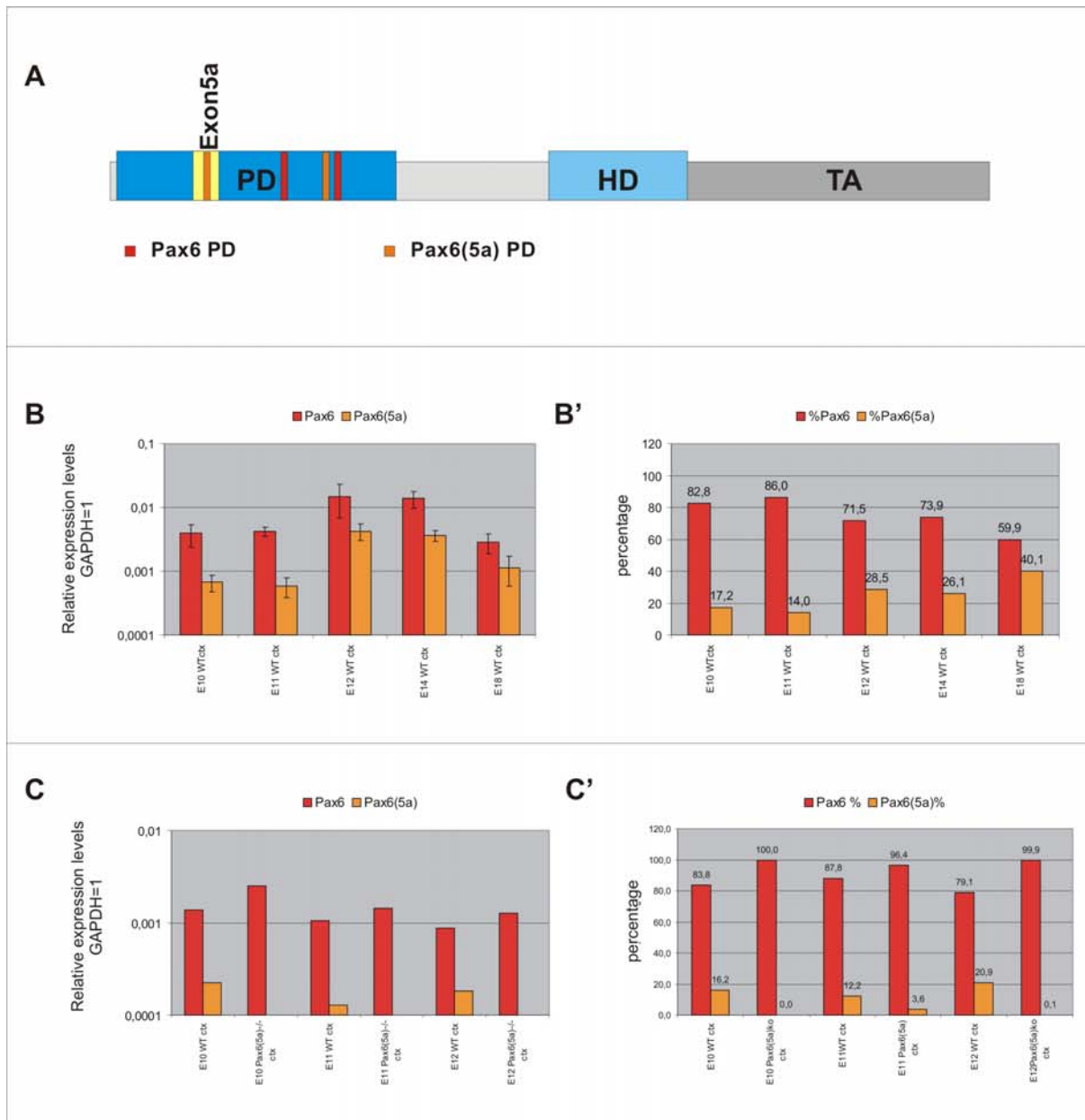


Fig. 37: Expression levels of Pax6 isoforms during embryonic development of the cerebral cortex of WT and Pax6(5a)^{-/-} embryos

(A) Schematic drawing of the Pax6 and Pax6(5a) (exon 5a= yellow insert into paired domain, PD) mRNA with the position of the primers (given as coloured stripes) used for the detection of the different Pax6 isoforms containing a PD (red), the Pax6(5a) isoform (orange).

(B) Shows the expression levels obtained by real-time RT-PCR analysis of Pax6 and Pax6(5a) mRNA relative to GAPDH in tissue isolated from cortex (ctx) of WT at E10, E11, E12, E14 and E18. Note that the expression levels of Pax6(5a) are increasing during development to almost equal levels compared to the canonical Pax6 isoform. (B') gives the calculated corresponding percentages to the expression levels in (B).

(C) Shows the expression levels obtained by real-time RT-PCR analysis of Pax6 and Pax6(5a) mRNA relative to GAPDH in tissue isolated from cortex (ctx) of WT or Pax6(5a)^{-/-} mice at E10, E11, and E12. Note that the expression of the canonical form of Pax6 (= all Pax6 isoforms containing a PD (red) minus Pax6(5a) isoform) is increased in the Pax6(5a)^{-/-} cortex compared to WT levels by 1,8 fold at E10 and by 1,4 fold at E11 and 12. This increase may therefore be sufficient to compensate the loss of Pax6(5a) mRNA that comprises only 15-20% of the total Pax6 mRNA containing a PD in WT cortex.

(C') gives the calculated percentages to the expression levels given in (C).

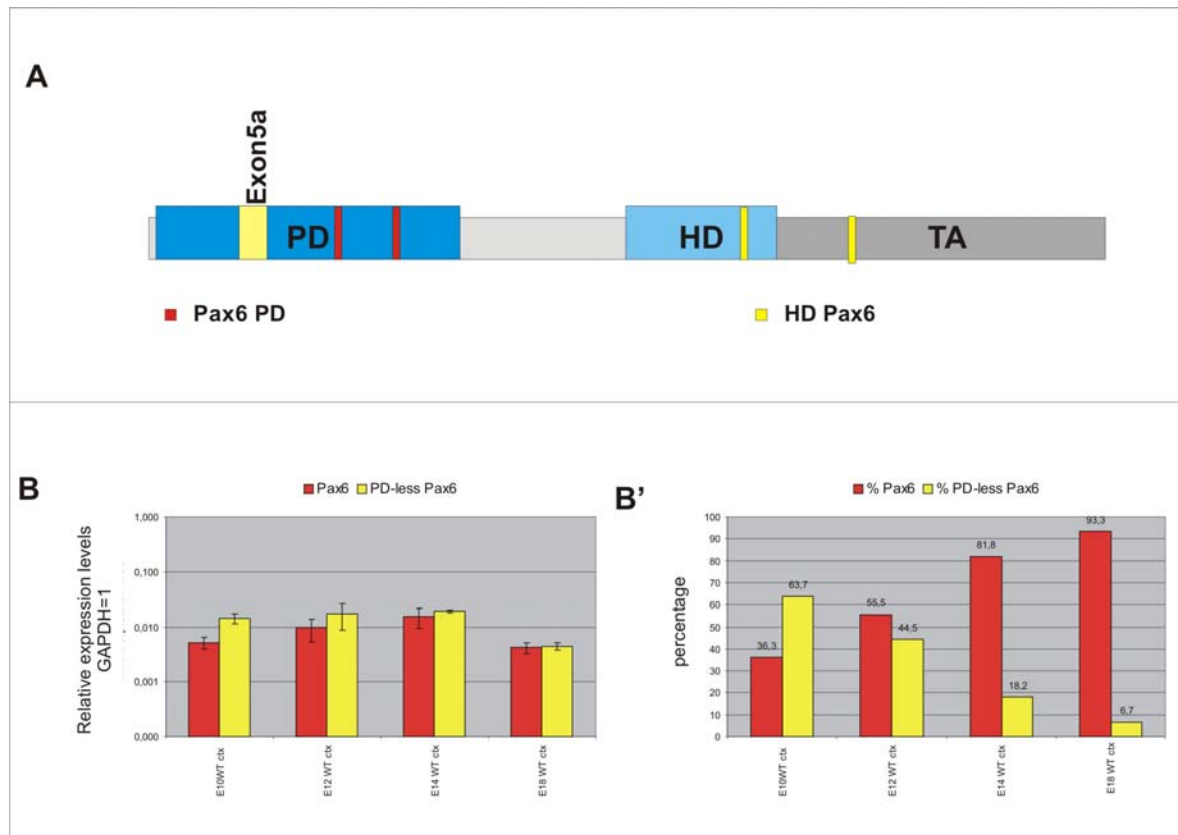


Fig. 38: Expression levels of Pax6 containing a paired domain and Pax6 containing a homeodomain in the cerebral cortex of WT embryos

(A) Schematic drawing of the Pax6 and Pax6(5a) (exon 5a= yellow insert into paired domain, PD) mRNA with the position of the primers (given as coloured stripes) used for the detection of the Pax6 isoforms containing a paired PD (red) and Pax6 containing a homeodomain (HD) (yellow).

(B) Shows the expression levels obtained by real-time RT-PCR analysis of Pax6 with a paired domain (red bars) and Pax6 mRNA containing a homeodomain (yellow bars) relative to GAPDH expression in tissue isolated from cortex (ctx) of WT at E10, E12, E14 and E18. Note that the expression levels of the Pax6 containing only a homeodomain are increased at early developmental stages (E10-E12), while they are decreased at E18. (B') gives the calculated corresponding percentages to the expression levels in (B).

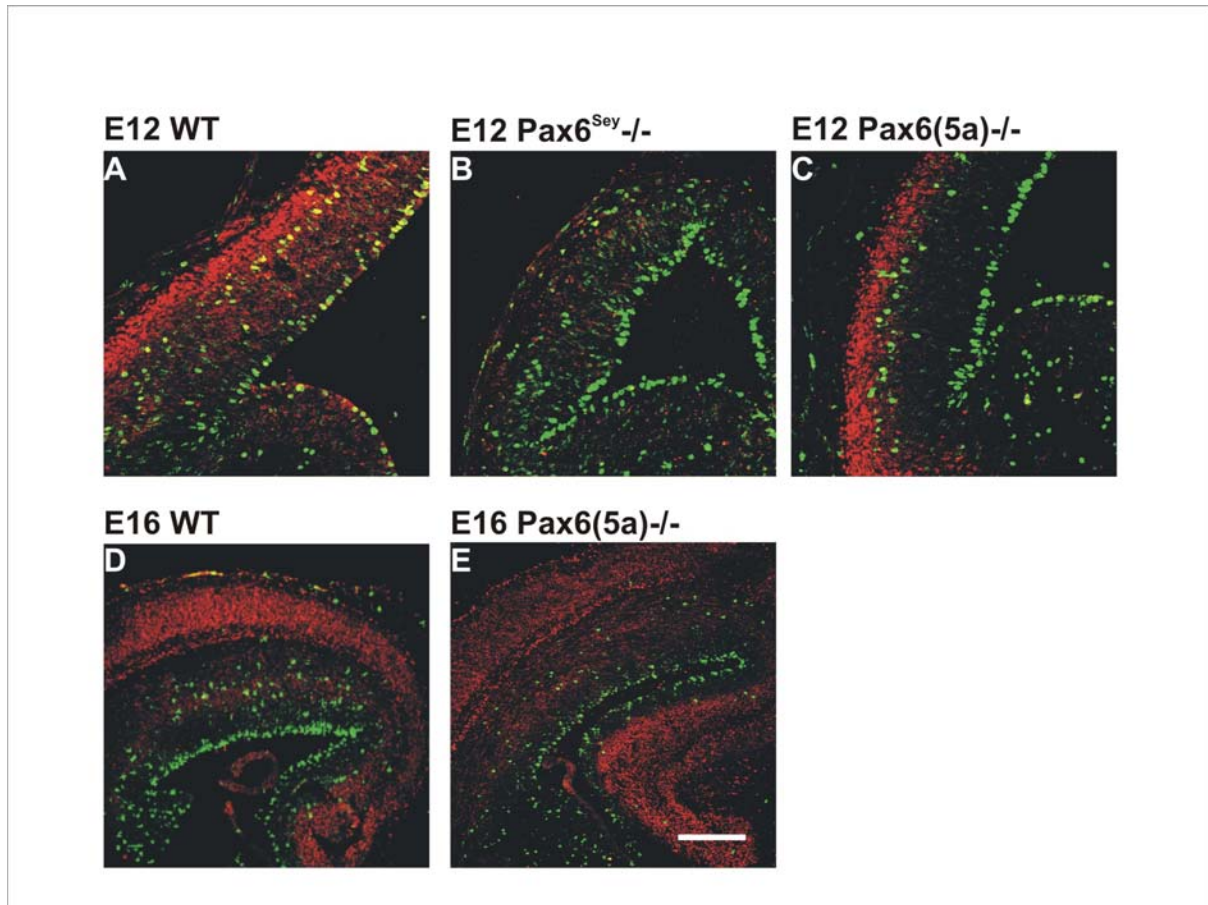


Fig. 39: Neurogenesis and cell proliferation in the cerebral cortex of Pax6^{Sey}-/- and Pax6(5a)-/- mice
 Micrographs (A-E) show coronal sections of the lateral cerebral cortex immunostained for NeuN (red; neuronal marker) and PH3 (green; marker for cells in M phase) at E12 and E16 in the respective mouse mutants as indicated in the panel. Note that no band of NeuN-positive cells is detectable in the E12 cortex of Pax6^{Sey}-/- mice (B) compared to the WT (A), while neurogenesis in the Pax6(5a)-/- (C) is normal at E12. The number of PH3positive cells dividing at the ventricular surface and at abventricular positions is not altered in the cortex of the Pax6^{Sey}-/- (B) and Pax6(5a)-/- mice (C) at E12. Neurogenesis and cell proliferation are not altered at E16 in the cortex of the Pax6(5a)-/- mice (E) compared to the E16 WT cortex (D).
 Scale bar: 100µm

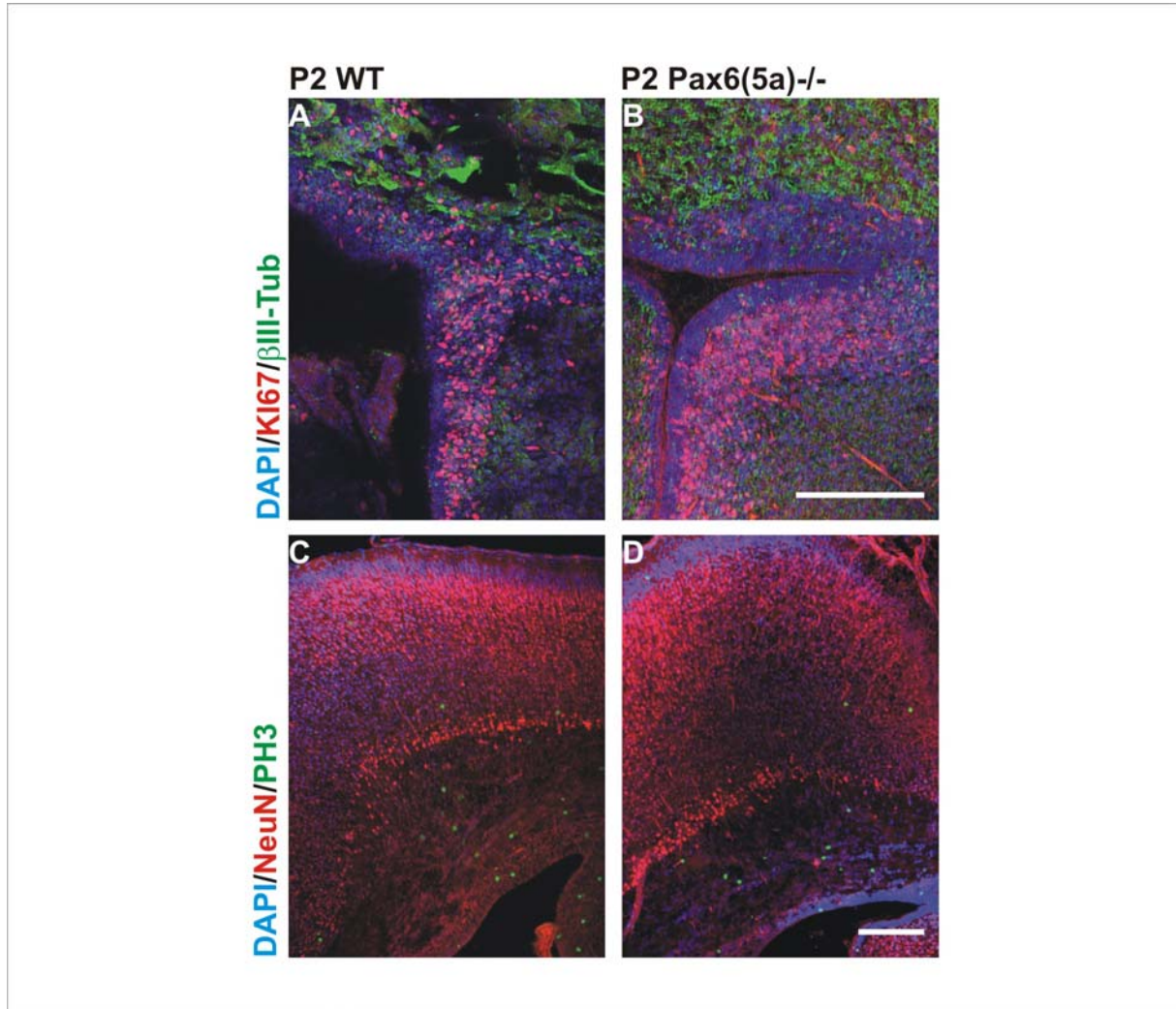


Fig. 40: Neurogenesis and cell proliferation in WT and Pax6(5a)^{-/-} at P2

Micrographs depicting coronal sections of the lateral cerebral cortex immunostained against the neuronal markers β III-Tubulin and NeuN, and against Ki67 (marker for proliferating cells) and PH3 (marker for cells in M-phase).

No changes in neurogenesis and cell proliferation were detected in the cerebral cortex of the Pax6(5a)^{-/-} (B,D,) compared to WT (A,C,) at P2.

Scale bars: 100 μ m

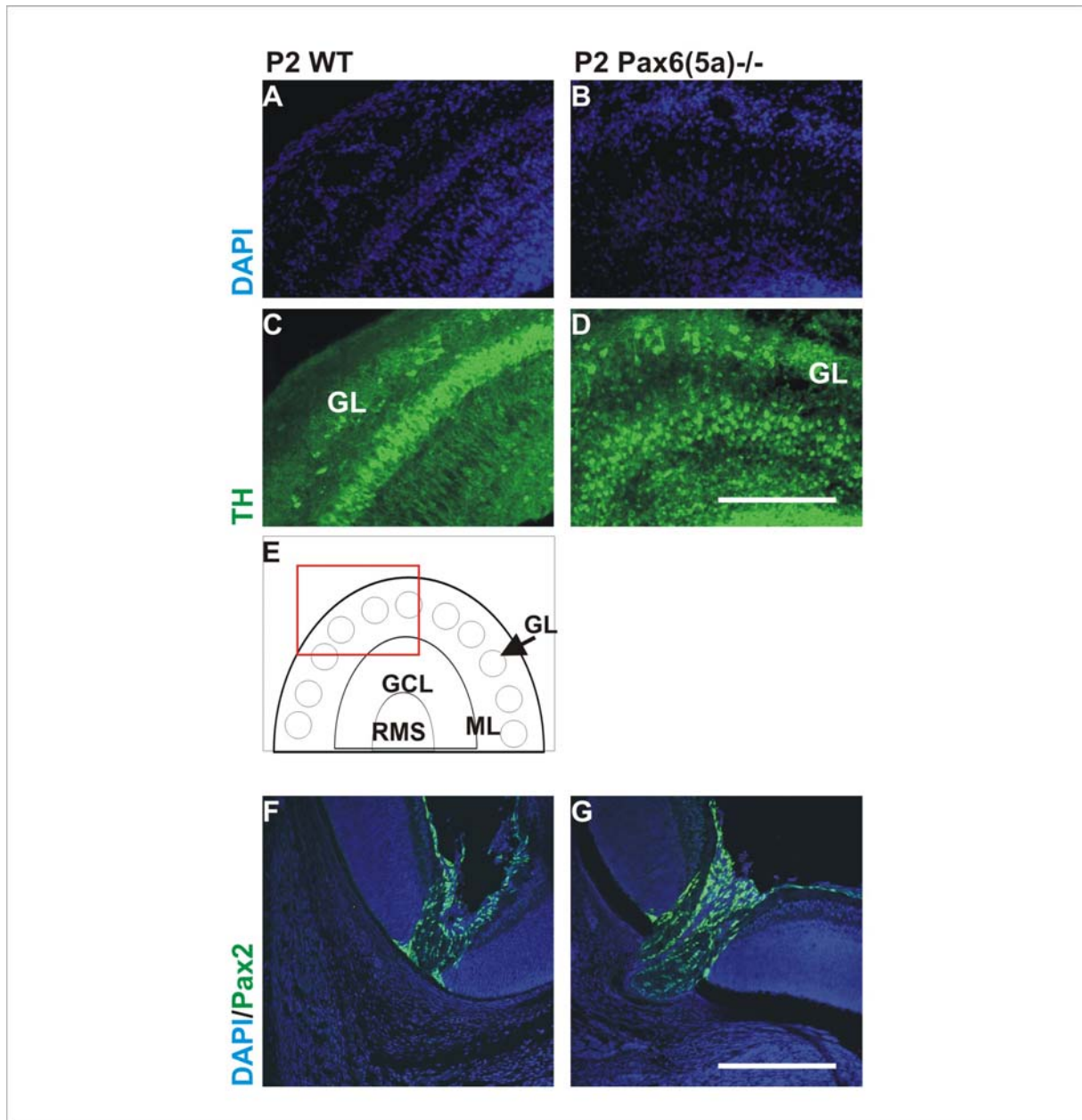


Fig. 41: Analysis of TH+ dopaminergic neurons in the olfactory bulb of Pax6(5a)-/- at P2
 Micrographs of coronal sections of the olfactory bulb at P2. Tyrosinhydroxylase positive (TH+) dopaminergic neurons are present in the glomerular layer (GL) of the olfactory bulb in the Pax6(5a)-/-. However, neurons seem less organized in the GL of Pax6(5a) (D) than in the WT (C). (E) Schematic drawing depicting the olfactory bulb of a coronal section with the glomerular layer (GL), the mitral cell layer (ML) the granular cell layer (GCL) and rostral migratory stream (RMS). The red box indicates the area depicted in A-D. No changes in the Pax2 expression (green) were detectable in the eye of P2 Pax6(5a)-/- mice compared to the WT (F). GL= glomerular layer; ML= mitral cell layer; GCL= granular cell layer. Scale bars: 100µm

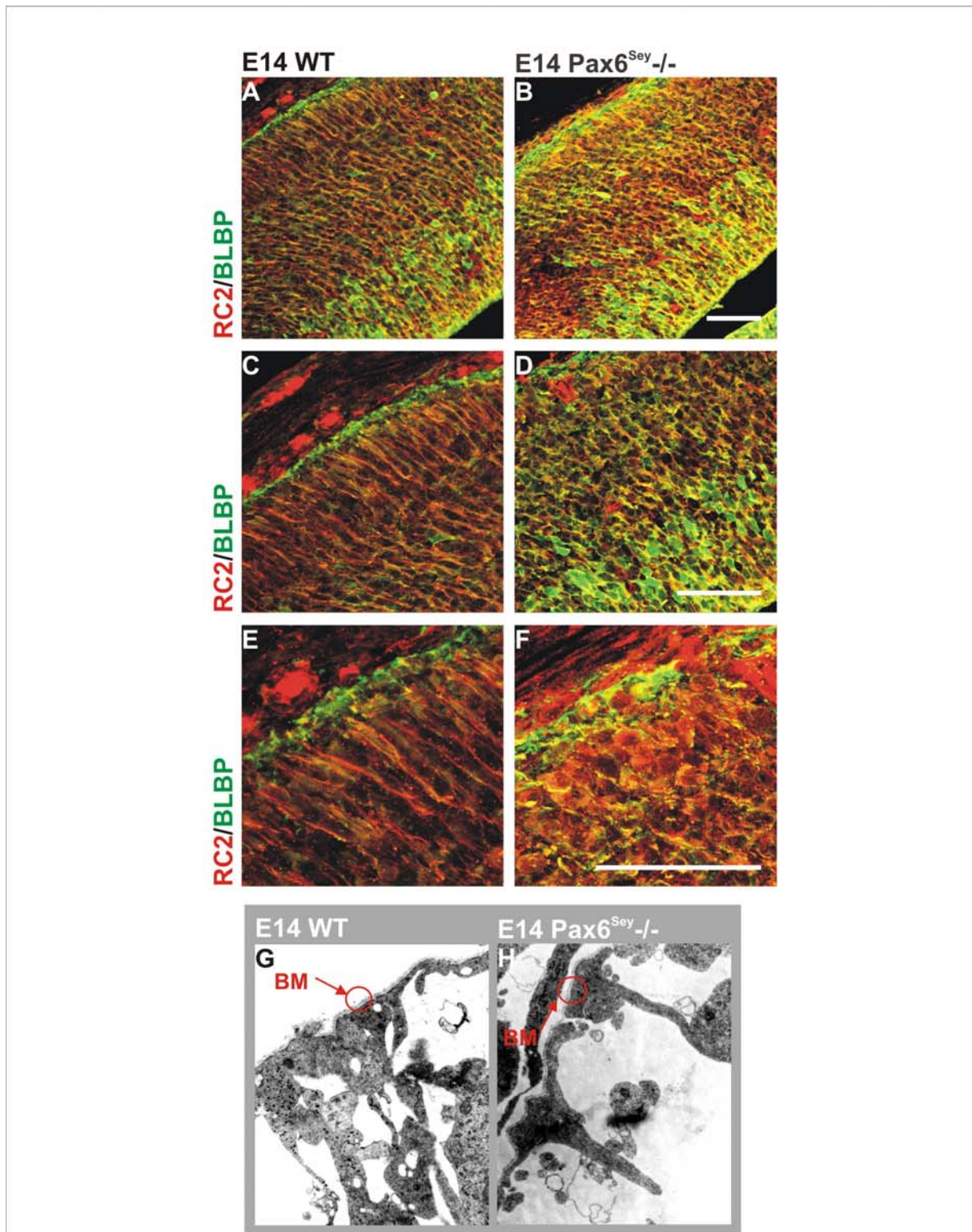


Fig. 42: Radial glia and basement membrane morphology in Pax6^{Sey} -/-

Micrographs depicting coronal sections of E14 cerebral cortex. Immunohistochemistry against RC2 and BLBP, two markers for radial glia cells in the cerebral cortex, was used for the visualisation of radial glia cells.

The radial glia morphology of Pax6^{Sey} -/- seems a bit less organized (B-F) especially at basal regions underneath the pial surface, compared to the morphology of the radial glia cells in WT (A-E).

Despite the alteration in radial glia morphology the basement membrane forms normally in the Pax6^{Sey} -/- (red circle) compared to the E14 WT (G; red circle).

Scale bars: 50µm

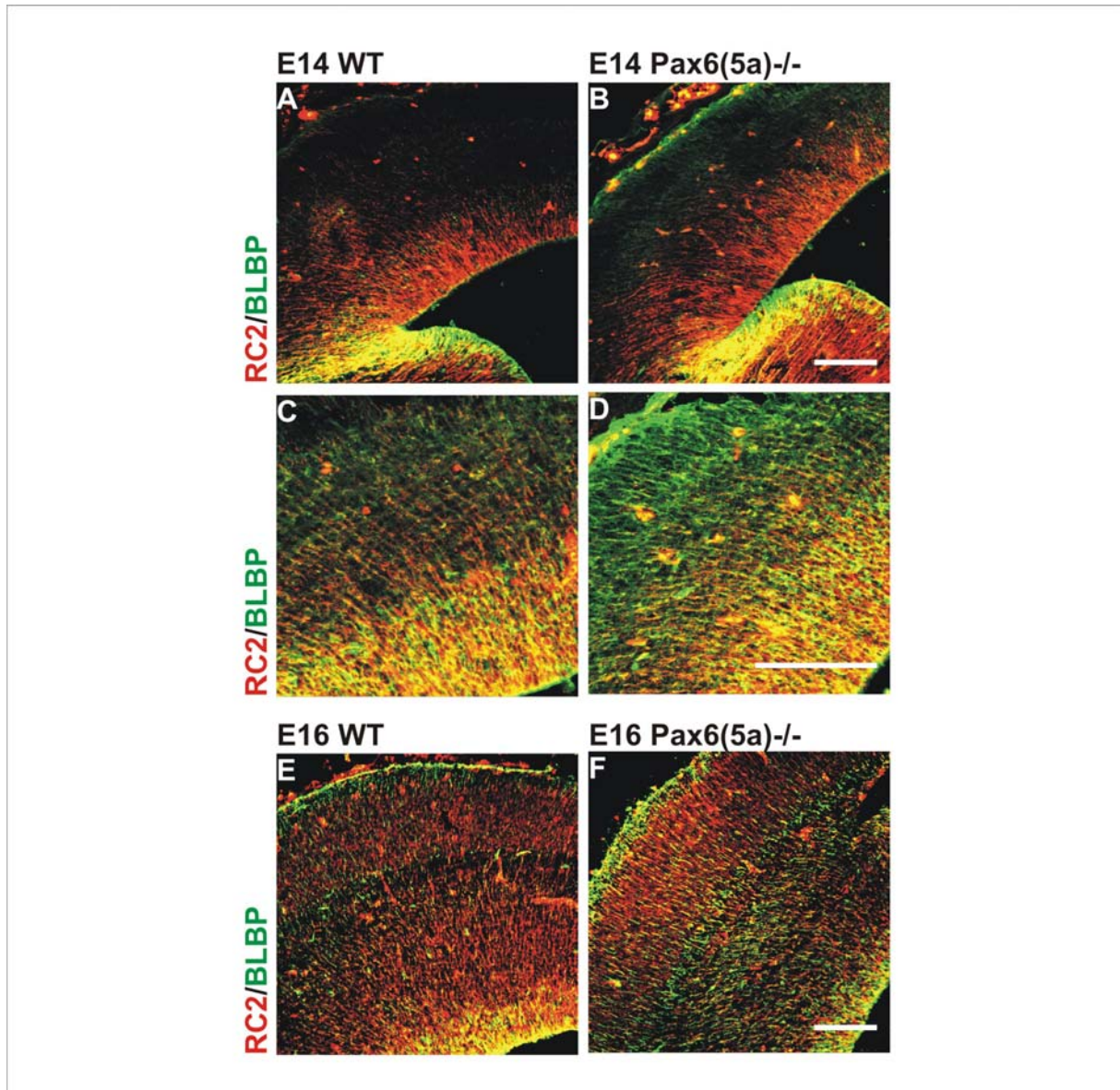


Fig. 43: Radial glia morphology at E14 and E16 in the Pax6(5a)^{-/-} cortex

Micrographs depicting coronal sections of the cortex at E14 (A,B,C,D) and at E16 (E,F).

Immunohistochemistry against RC2 and BLBP, two markers for precursor cells in the cerebral cortex in Pax6(5a)^{-/-} (B,D) revealed no changes in the radial glia morphology at E14 compared to WT (A,C). Also at E16 no changes were detected in the radial glia morphology in the cortex of the Pax6(5a)^{-/-} (F) compared to the WT (E).

Scale bars: 100µm

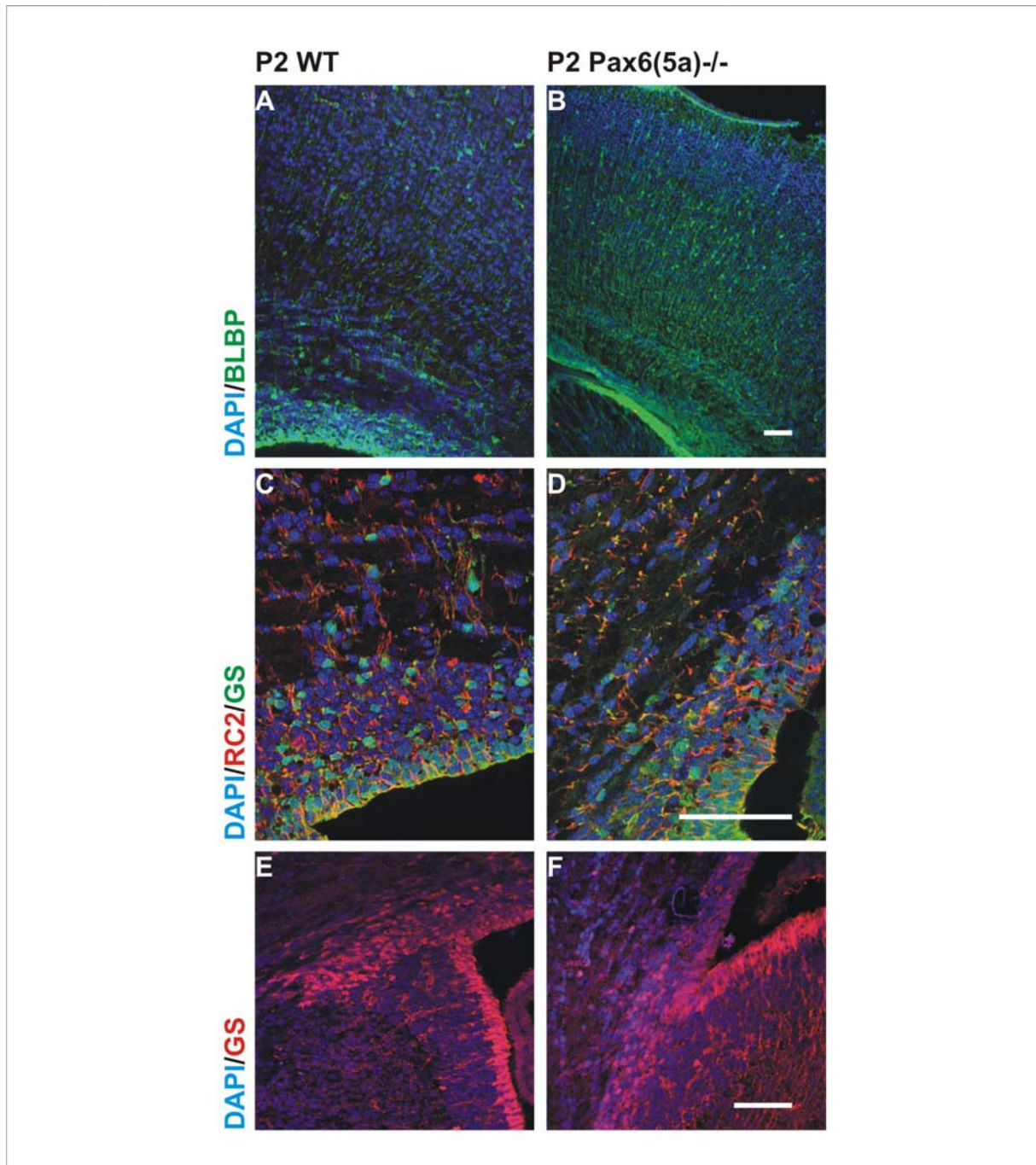


Fig. 44: Glial marker analysis in the Pax6(5a)-/- at P2

Microrgraphs depicting coronal sections of P2 WT and Pax6(5a)-/- cerebral cortex at medial levels (A,B) and at lateral levels (C-F). Immunohistochemistry against the glial marker BLBP at P2 showed a slight increase in BLBP immunoreactivity in the cortex of the Pax6(5a)-/- (B) compared to the WT (A). While no changes were detected in the expression of RC2 and GS (glutamine synthase) in the cortex of WT (C,E) and Pax6(5a)-/- (D,F).

Scale bars: 100µm

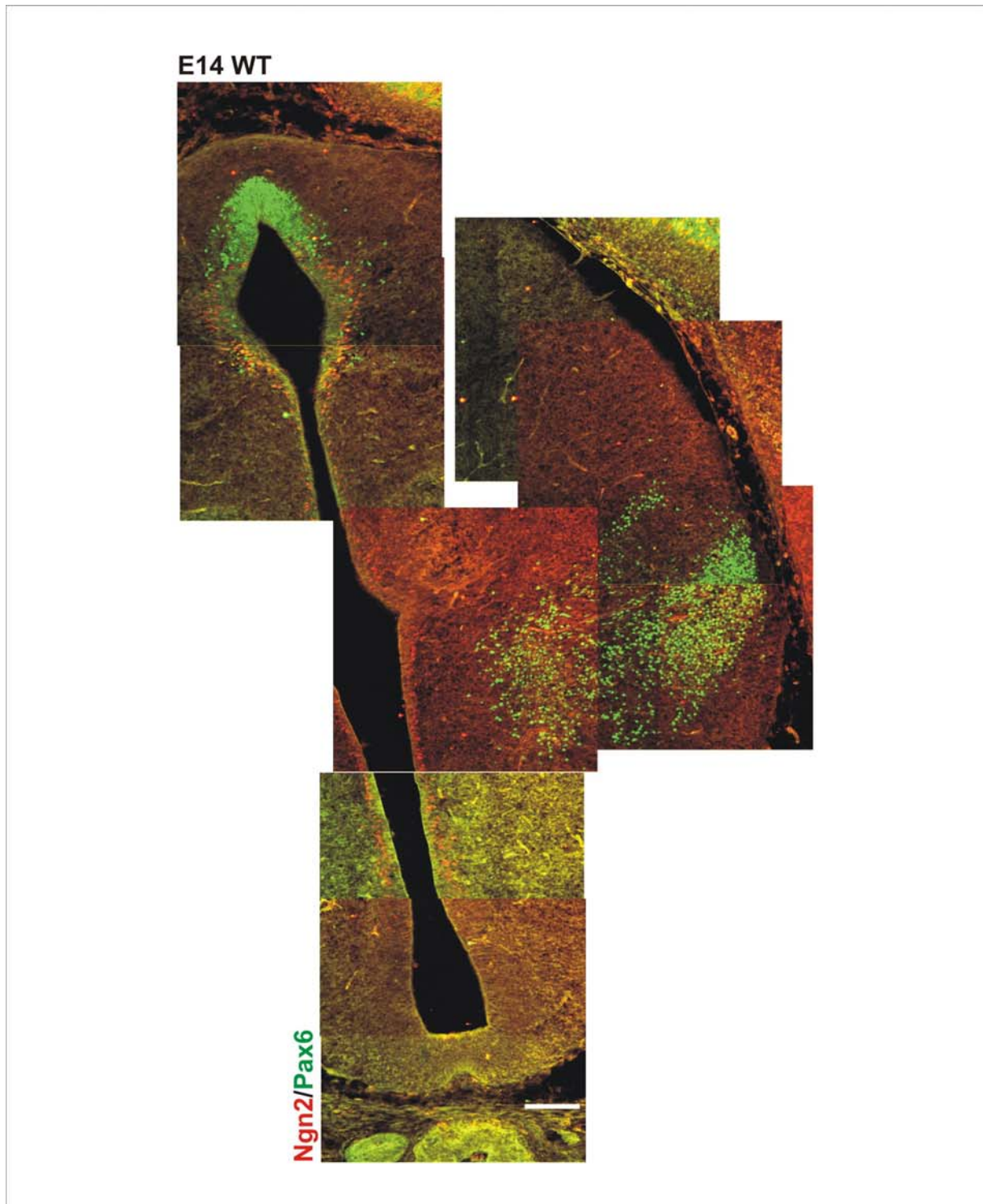


Fig. 45: Ngn2 and Pax6 expression in the E14 WT diencephalon

Coronal section of WT diencephalon at medial level at E14. In the WT, Pax6 expression is detectable the dorsal diencephalon and in the ventral diencephalon in the mantlw layer extending up to the zona limitans intrathalamica (ZLI). Ngn2 is coexpressed with Pax6 in the dorsal diencephalon. Further, Ngn2 expression was detectable along the ventricle in the proliferative zone. Depending on the plane of section Ngn2 was also detectable in the ventral diencephalon.

Scale bar: 100µm

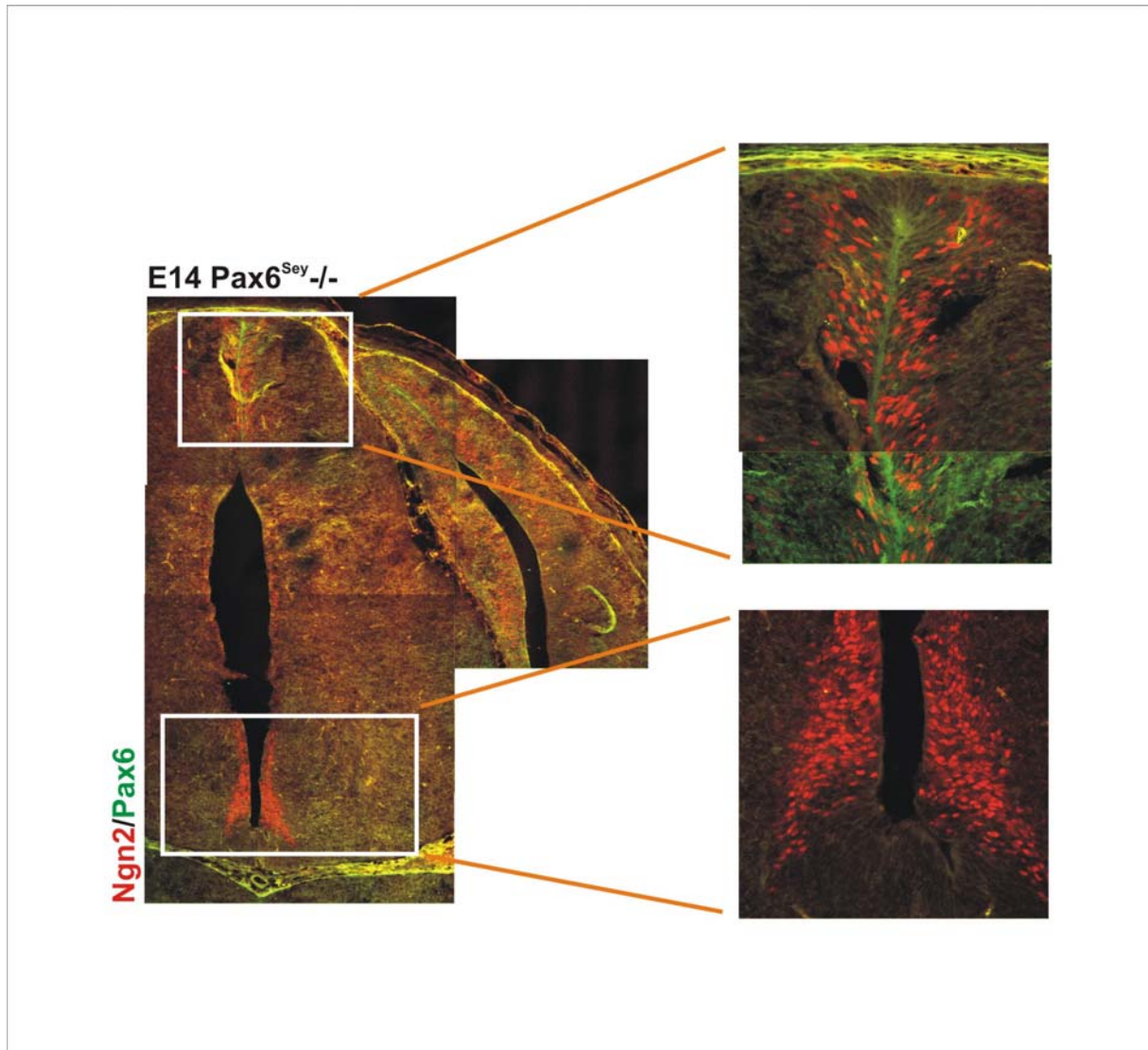


Fig. 46: Ngn2 expression in the Pax6^{Sey}-/- diencephalon

Coronal section of diencephalon at E14. No reduction in the Ngn2 expression was detectable in the absence of functional Pax6 protein in the diencephalon of the Pax6^{Sey}-/-. According to another angle of cutting, another domain of Ngn2 expression became apparent in the ventral diencephalon. This Ngn2 positive domain was not specifically detected in the case of loss of functional Pax6 but also in WT diencephali, depending on the angle of cutting.

Scale bars: 100µm

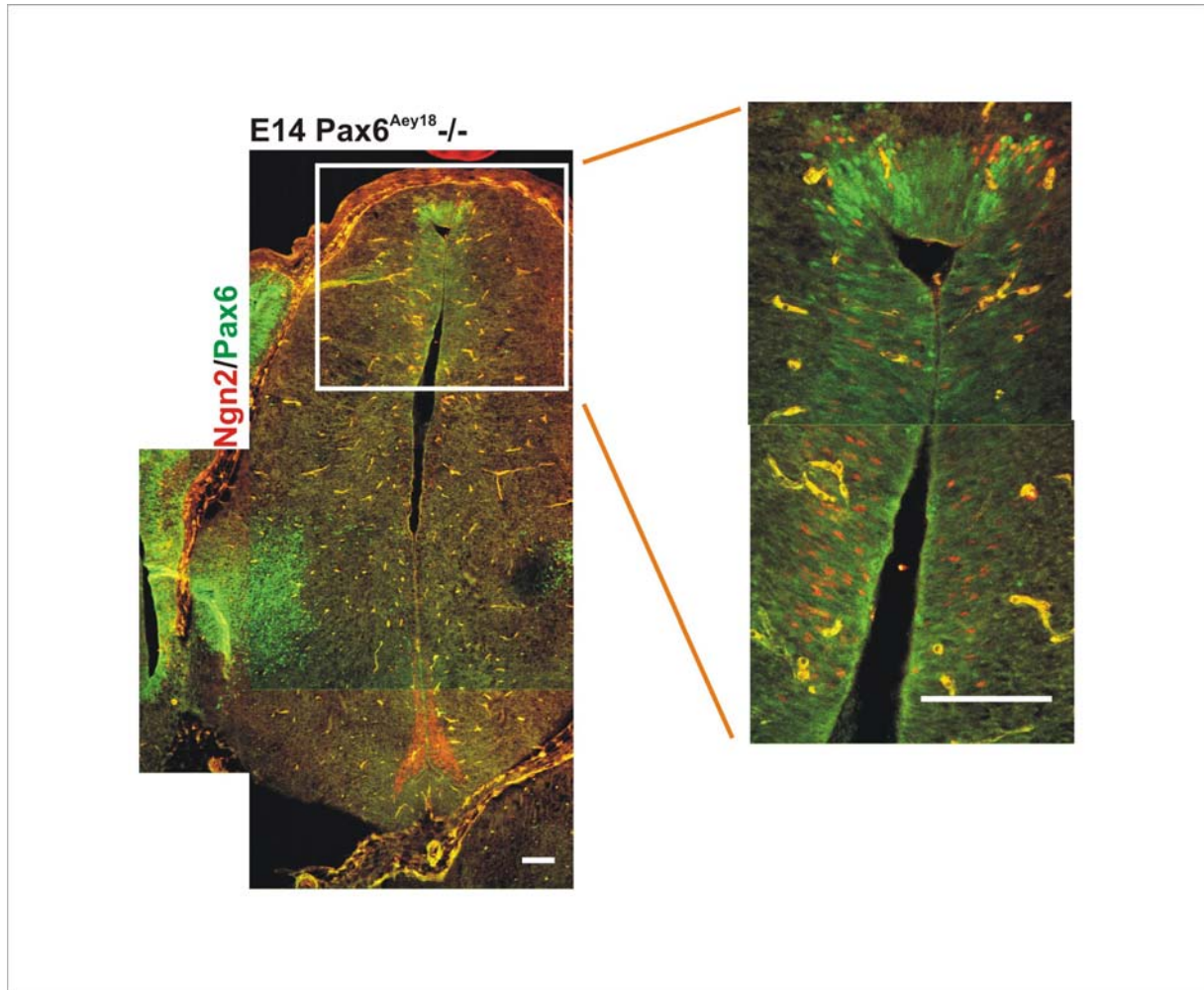


Fig. 47: Ngn2 and Pax6 expression in the E14 *Pax6^{Aey18}-/-* diencephalon

Ngn2 expression was detectable in the diencephalon (coronal section) of the *Pax6^{Aey18}-/-*. However, Ngn2 expression in the dorsal diencephalon of the *Pax6^{Aey18}-/-* seemed slightly reduced. On account of the level of cutting also in the diencephalon of the *Pax6^{Aey18}-/-* a Ngn2 expression domain in the ventral diencephalon became apparent.

Scale bars: 100µm

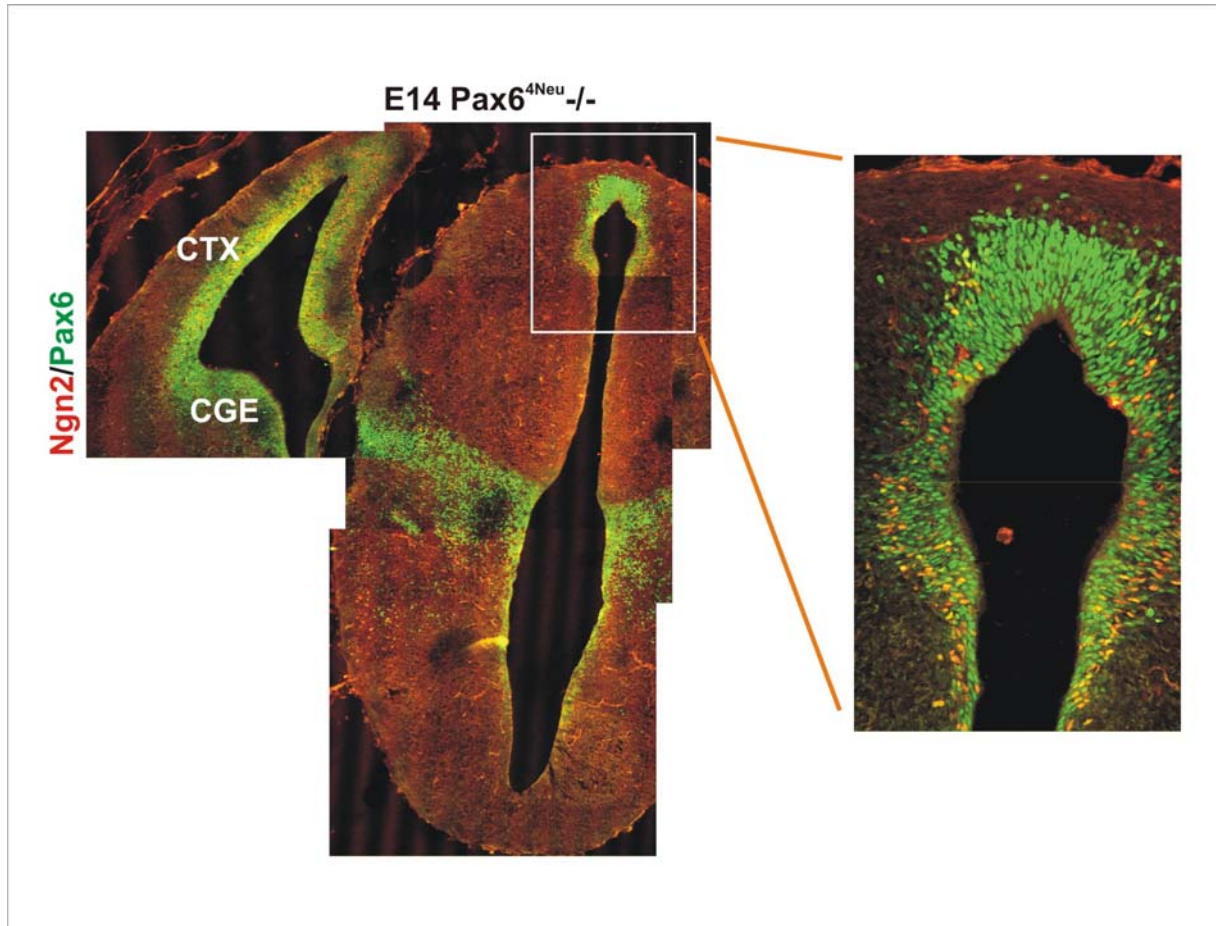


Fig. 48: Ngn2 and Pax6 expression in the E14 $Pax6^{4Neu-/-}$ diencephalon

Coronal section of E14 diencephalon. The lack of HD-DNA binding in the $Pax6^{4Neu-/-}$ did not influence the Ngn2 expression in the E14 diencephalon.

Scale bar: 100 μ m

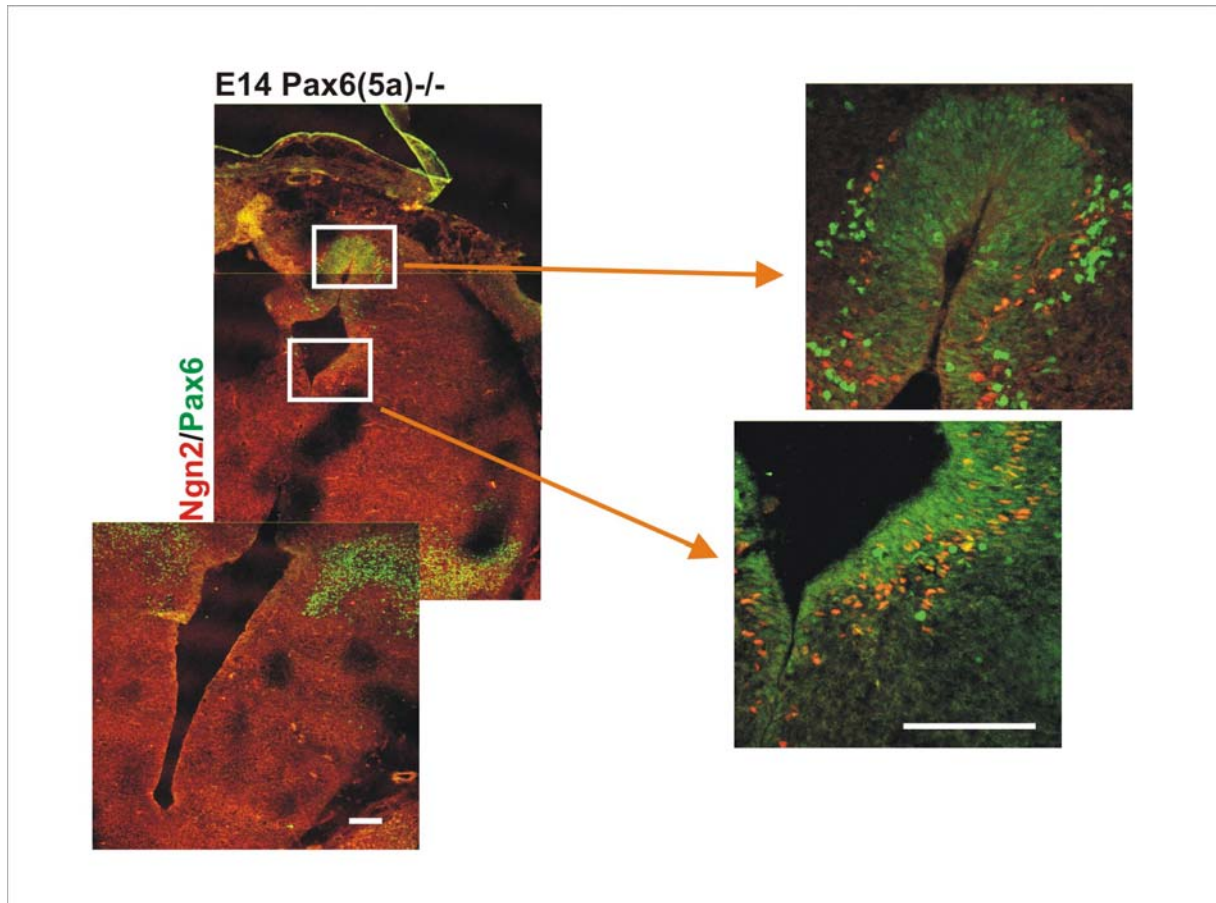


Fig. 49: Ngn2 and Pax6 expression in the E14 *Pax6(5a)*^{-/-} diencephalon

Coronal section of E14 diencephalon. No changes in the Ngn2 expression were detectable in the *Pax6(5a)*^{-/-} compared to the WT situation (Fig. 45).

Scale bar: 100µm

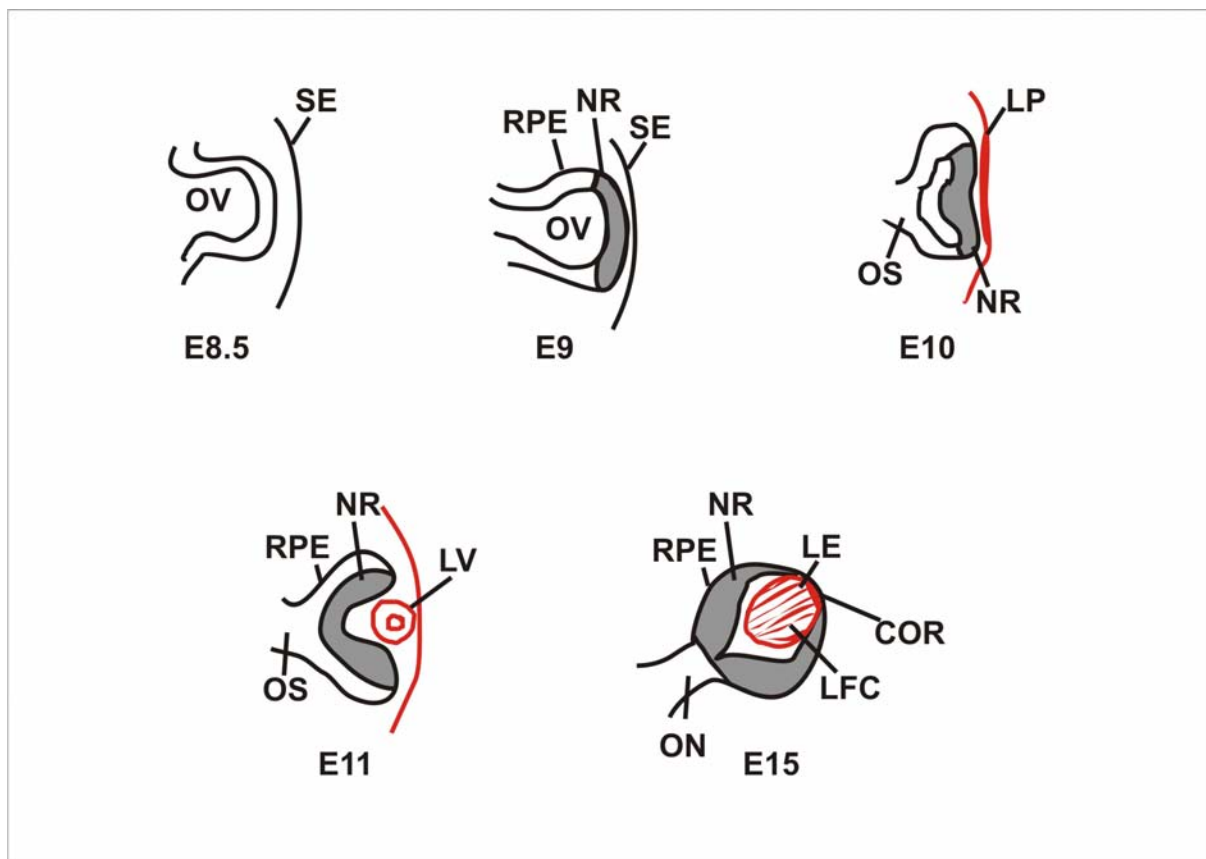


Fig. 50: Eye development

At E8.5 the optic vesicle (OV) evaginates from the ventral diencephalon towards the surface ectoderm (SE). *Pax6* is expressed in the epithelium of the OV and in the SE.

As eye development progresses (E10), *Pax6* expression becomes confined to the inner layer of the optic cup, the lens placode cells, which form the lens pit (LP), and the immediately adjacent regions of the surface ectoderm. The contact of the OV with the SE induces the formation of the lens. The OV invaginates, forming the optic cup with the inner neuroretina and the outer retinal pigmented epithelium (RPE) and the lens pinches off from the SE. At E15.5, *Pax6* expression remains in the neural retina (NR), the lens epithelium (LE) and the cornea (COR).

(Modified after Ashery-Padan, 2002).

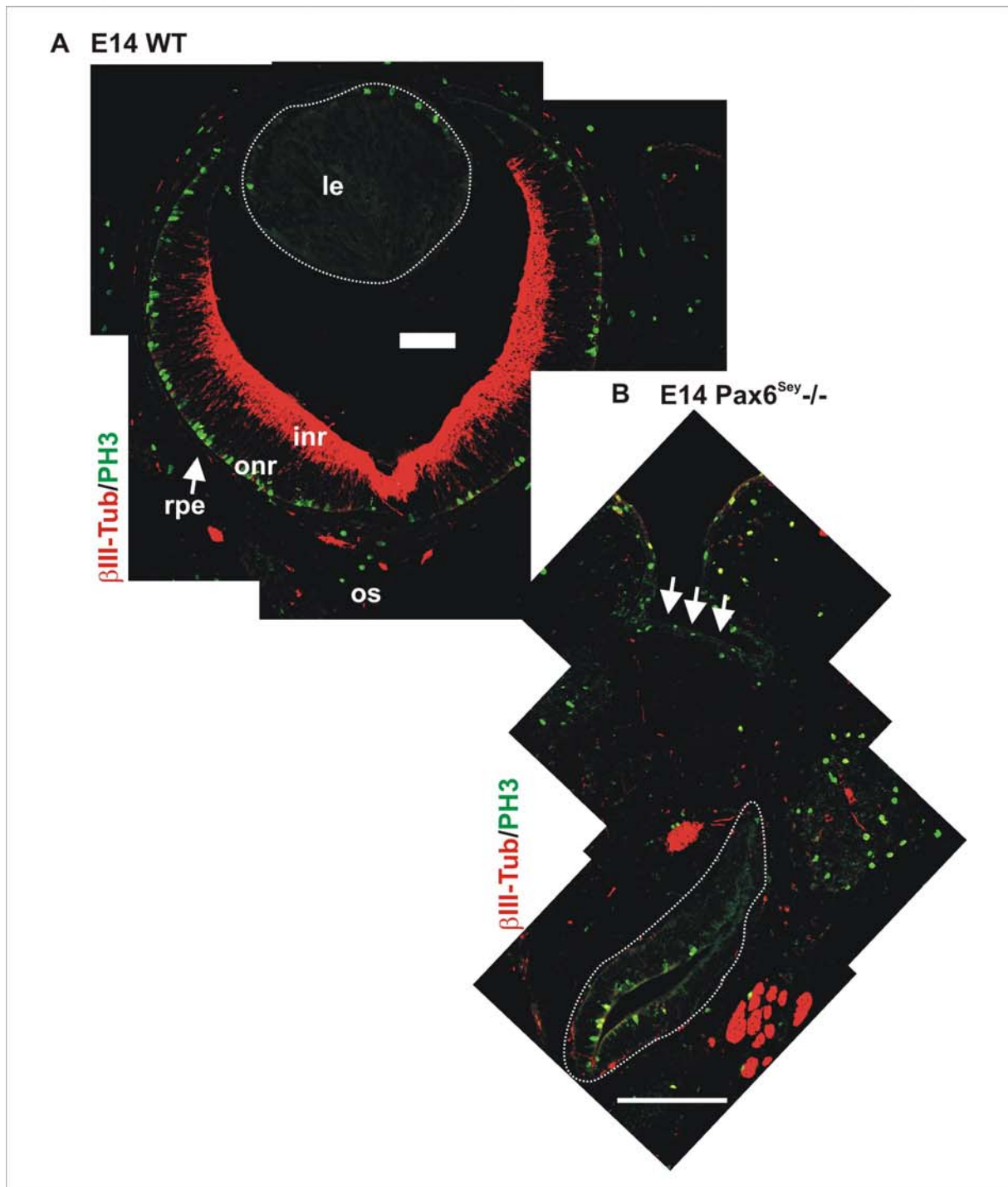


Fig. 51: Eye development in the WT and the functional null allele *Pax6*^{Sey-/-}
 Micrographs showing coronal sections of E14 embryonic heads at the level of the developing eye, the outer surface is oriented upwards. Immunohistochemistry against β III-Tubulin (red) was used to detect neurons in the inner neuroretina (inr) and against PH3 (green) was used to detect proliferating cells. In the WT E14 eye proliferating cells are located at the outer surface of the neuroretina (onr), while postmitotic neurons are located at the inner neuroretina (inr). The retinal pigmented epithelium is not visible, but would be located outside the onr, as indicated by the arrow in (A). The functional null allele *Pax6*^{Sey-/-} fails to develop eyes. Instead, only a remnant of the eye vesicle (indicated by white dashed line) is detectable at E14, located at some distance from the surface ectoderm (indicated here with arrows). No neurons are detectable in the remnant of the eye vesicle and only few proliferating cells. The dashed white line in A outlines the lens. Abbreviations: le= lens; inr= inner neuroretina; onr= outer neuroretina; rpe= retinal pigmented epithelium; os= optic stalk.
 Scale bar: 100 μ m

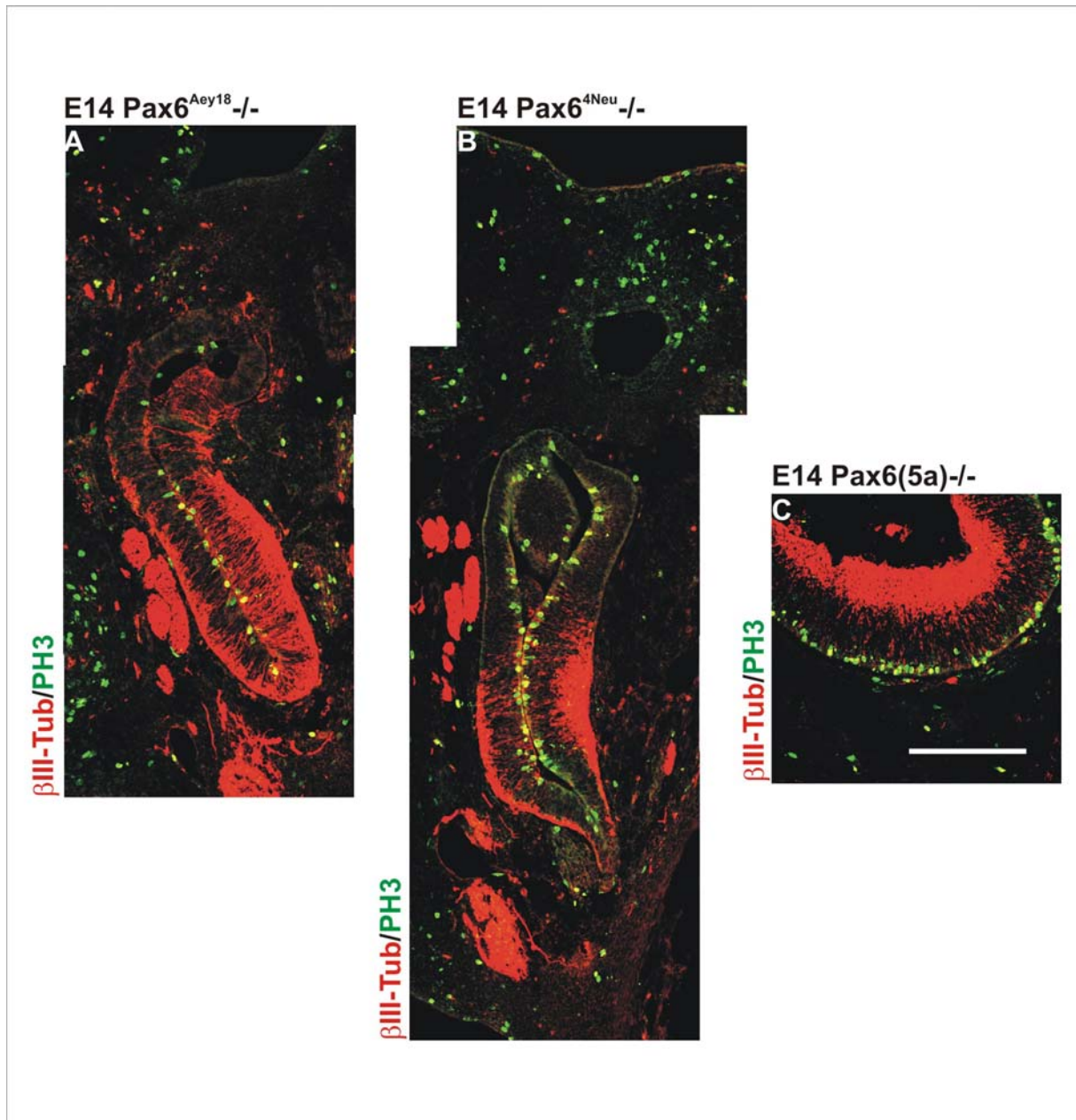


Fig. 52: Eye development in $Pax6^{Aey18-/-}$, $Pax6^{4Neu-/-}$ and $Pax6(5a)-/-$ at E14

Micrographs depicting coronal sections of E14 embryonic heads at the level of the developing eye.

Immunohistochemistry against β III-Tubulin (red) was used to detect neurons in the inner neuroretina (inr) and against PH3 (green) was used to detect proliferating cells. The $Pax6^{Aey18-/-}$ and the $Pax6^{4Neu-/-}$ fail, as the functional null allele $Pax6^{Sey-/-}$, to develop an eye. But in contrast to the $Pax6^{Sey-/-}$, neurons are generated in the remnant of the eye vesicle in the $Pax6^{Aey18-/-}$ (A) and $Pax6^{4Neu-/-}$ (B), while neurogenesis seems normal in the $Pax6(5a)-/-$ (C). Also cell proliferation in the PD mutant ($Pax6^{Aey18-/-}$) and in the HD mutant ($Pax6^{4Neu-/-}$) is less decreased than in the case of loss of functional Pax6 protein ($Pax6^{Sey-/-}$; see Fig. 51), while cell proliferation seems normal in the $Pax6(5a)-/-$.

Scale bar: 100 μ m

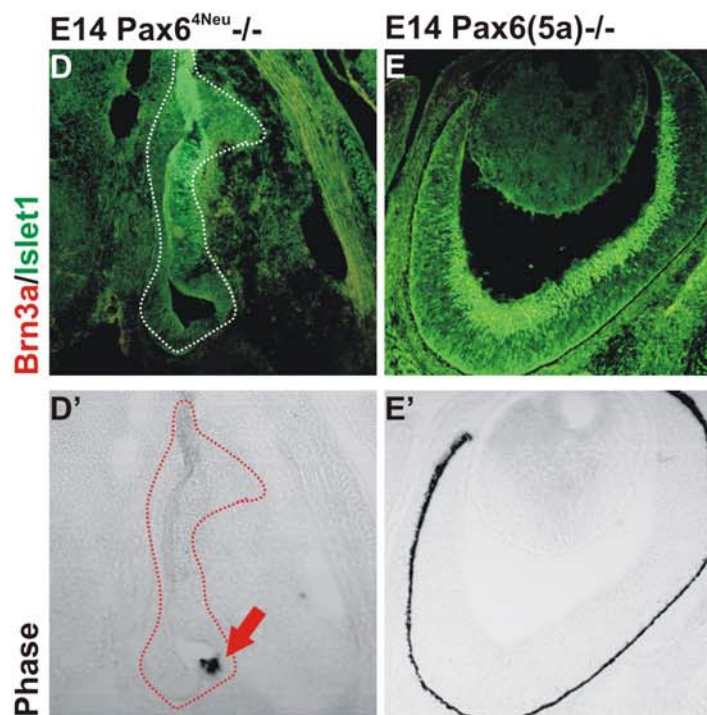
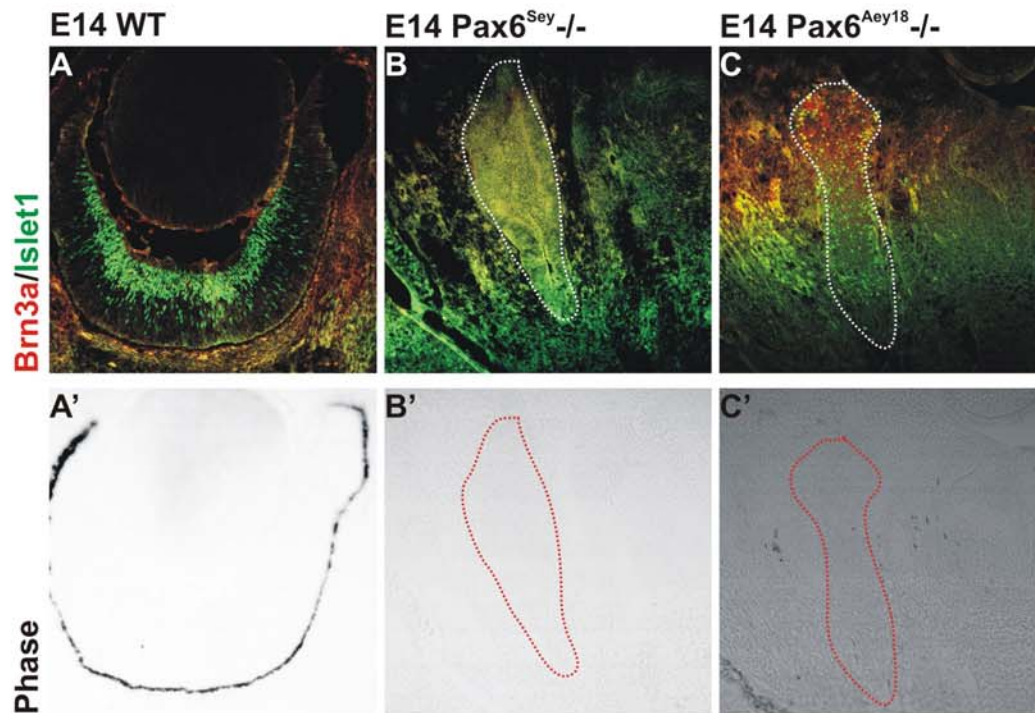


Fig. 53: Neuronal subtypes and RPE development in the specific Pax6 mutant alleles

Micrographs depicting coronal sections of E14 embryonic heads at the level of the developing eye. The outer surface of the head is oriented upwards. Immunohistochemistry against Islet 1 (green) and Brn3a (red) was used to detect the differentiation of retinal ganglion cells at E14. The RPE was visualized by normal light microscopy.

In the E14 WT neuroretina mainly Islet 1 and only few Brn3a positive retinal ganglion cells were detectable (A). The RPE was lining the outer surface of the neuroretina (A'). No Brn3a and Islet 1 positive cells were detectable in the Pax6^{Sey}-/- and also no RPE development occurred (the eye vesicle remnant is outlined in white (B) and red (B')).

In contrast, Brn3a and Islet 1 positive cells were detectable in the Pax6^{Aey18}-/- (C) and Pax6^{4Neu}-/- (D), in addition in the latter occasionally RPE remnants were detected (red arrow in D'). No changes Brn3a and Islet 1 expression and the formation of an RPE were detected in the Pax6(5a)-/- (E,E'). The dashed white or red line indicates the eye vesicle remnant.

Scale bar: 100µm

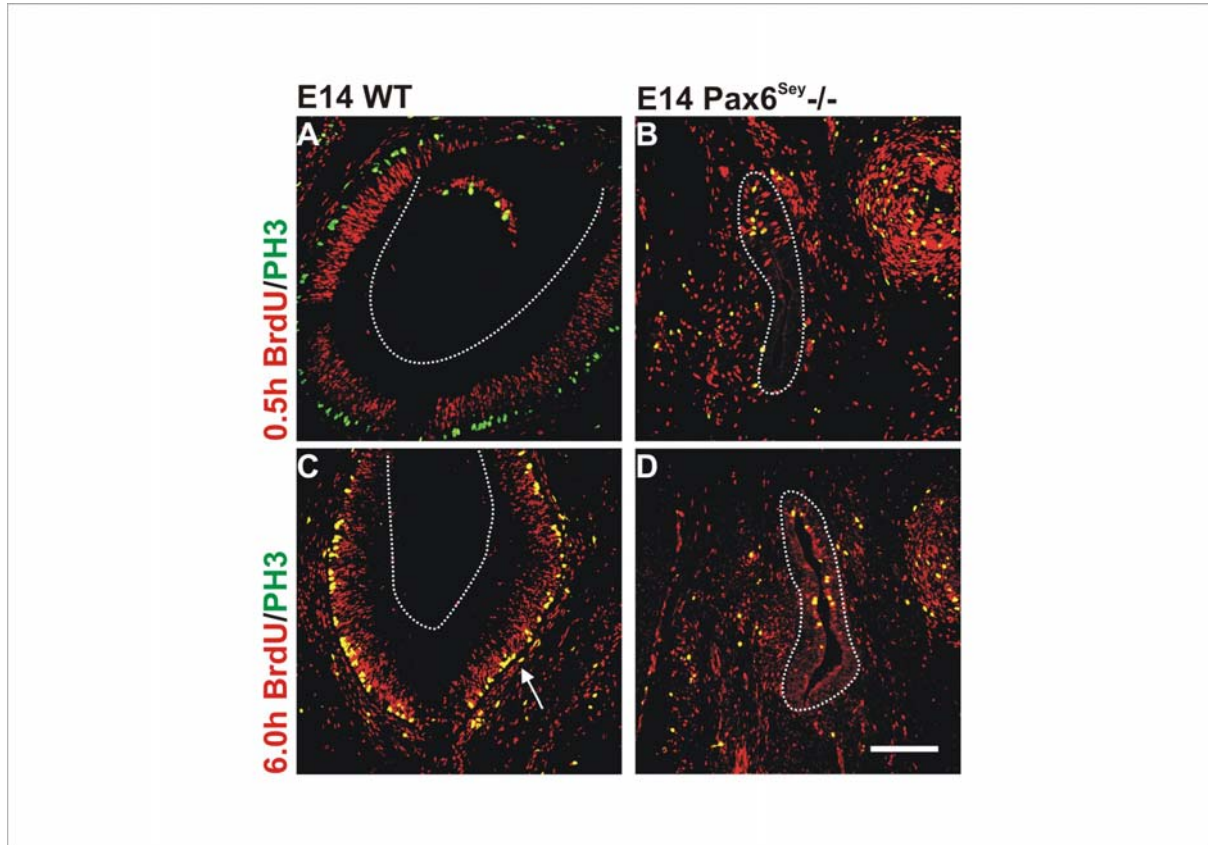


Fig. 54: Interkinetic nuclear migration in the neuroepithelial cells of the retina in WT and Pax6^{Sey}-/-
 Micrographs depicting coronal sections of E14 embryonic heads at the level of the developing eye. The outer surface of the head is oriented upwards. Immunohistochemistry against BrdU was used to detect the position of cell nuclei after a 0.5h and a 6.0h BrdU pulse in order to analyze the interkinetic nuclear migration. Immunohistochemistry against PH3 was used to recognize the orientation of the epithelium. A 0.5h BrdU pulse reveals that cells in S-phase are located at the basal side of the neuroepithelium, close to the inner neuroretina where the postmitotic neurons are located in the WT (A). Note the small zone that is free of BrdU labeled cells at the apical VZ. After 6 hours, cells have translocated their nuclei towards the apical VZ, where cell division takes place as visible by the presence of PH3 positive cells (green) in the WT (C). In the remnant eye vesicle of the Pax6^{Sey}-/- PH3 positive cells are located at the inner side of the neuroepithelium since the optic cup formation fails. In the 0.5h BrdU pulse only some BrdU positive cells are detectable mostly away from the ventricular surface, where the PH3 positive cells are located in the Pax6^{Sey}-/-(B). After 6h, almost all BrdU positive cells are mostly colocalized with the position of the PH3 positive cells (D). Thus, the cells of the remnant eye vesicle undergo interkinetic nuclear migration in the Pax6^{Sey}-/- to a certain extent in the absence of functional Pax6 protein.
 Scale bar: 100µm

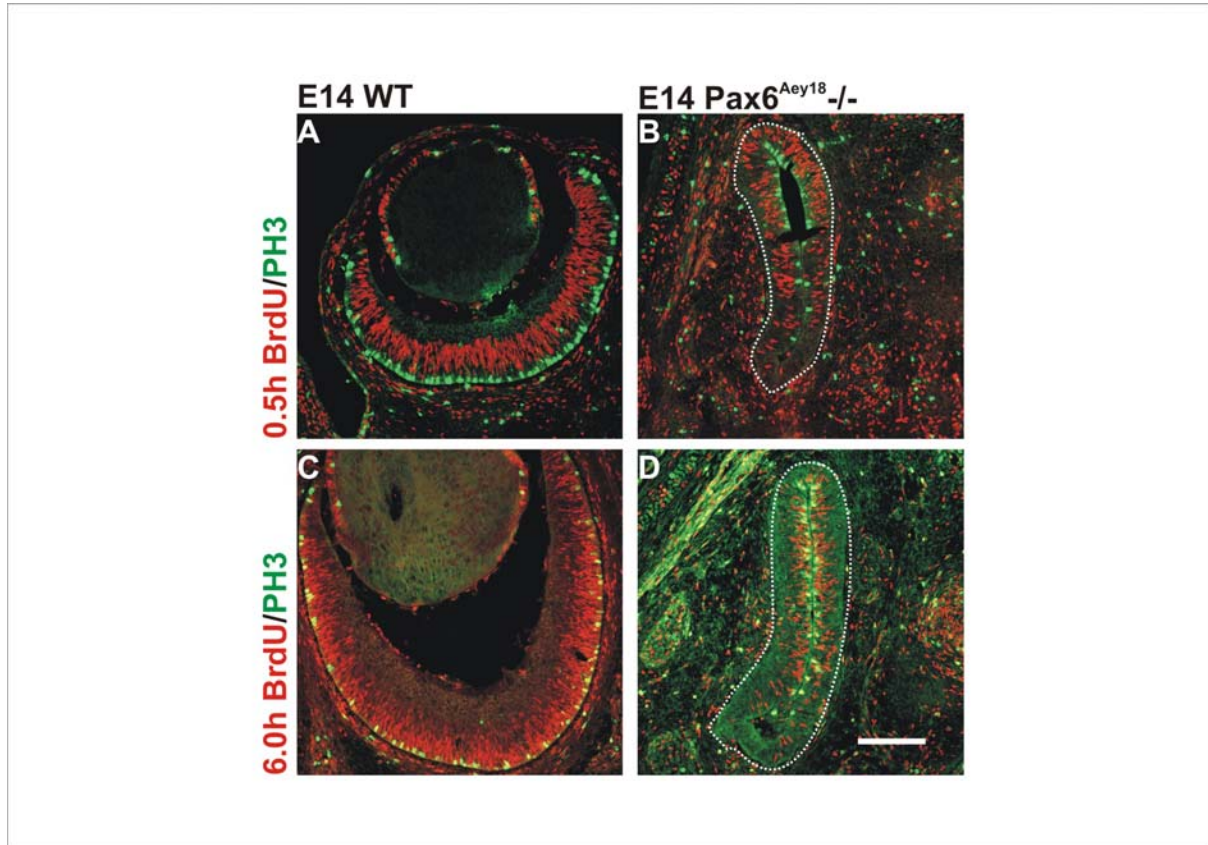


Fig. 55: Interkinetic nuclear migration in the developing eye in the absence of a functional PD ($Pax6^{Aey18-/-}$)

Micrographs showing coronal sections of E14 embryonic heads at the level of the developing eye. The outer surface of the head is oriented upwards. Immunohistochemistry against BrdU was used to detect the position of cell nuclei after a 0.5h and a 6.0h BrdU pulse in order to study the interkinetic nuclear migration. Immunohistochemistry against PH3 was used to recognize the orientation of the epithelium. For description of the interkinetic nuclear migration in the WT see Fig. 54. In the remnant eye vesicle in the $Pax6^{Aey18-/-}$ cell proliferation is decreased compared to WT, but not as much as in the $Pax6^{Sey-/-}$ (Fig. 54). Cells in S-phase (BrdU positive, red) are located in the basal side of the neuroepithelium, while cells in M-phase (PH3 positive, green) are located at the apical side. Note that a small area at the apical side is devoid of BrdU positive cells after 0.5h BrdU pulse. After 6 hours, cells have translocated their nuclei towards the apical side in the $Pax6^{Aey18-/-}$. Thus, interkinetic nuclear migration seems to occur in the absence of a functional PD in the neuroepithelium of the eye. The dashed white line marks the remnant eye vesicle in the $Pax6^{Aey18-/-}$. Scale bars: 100 μ m

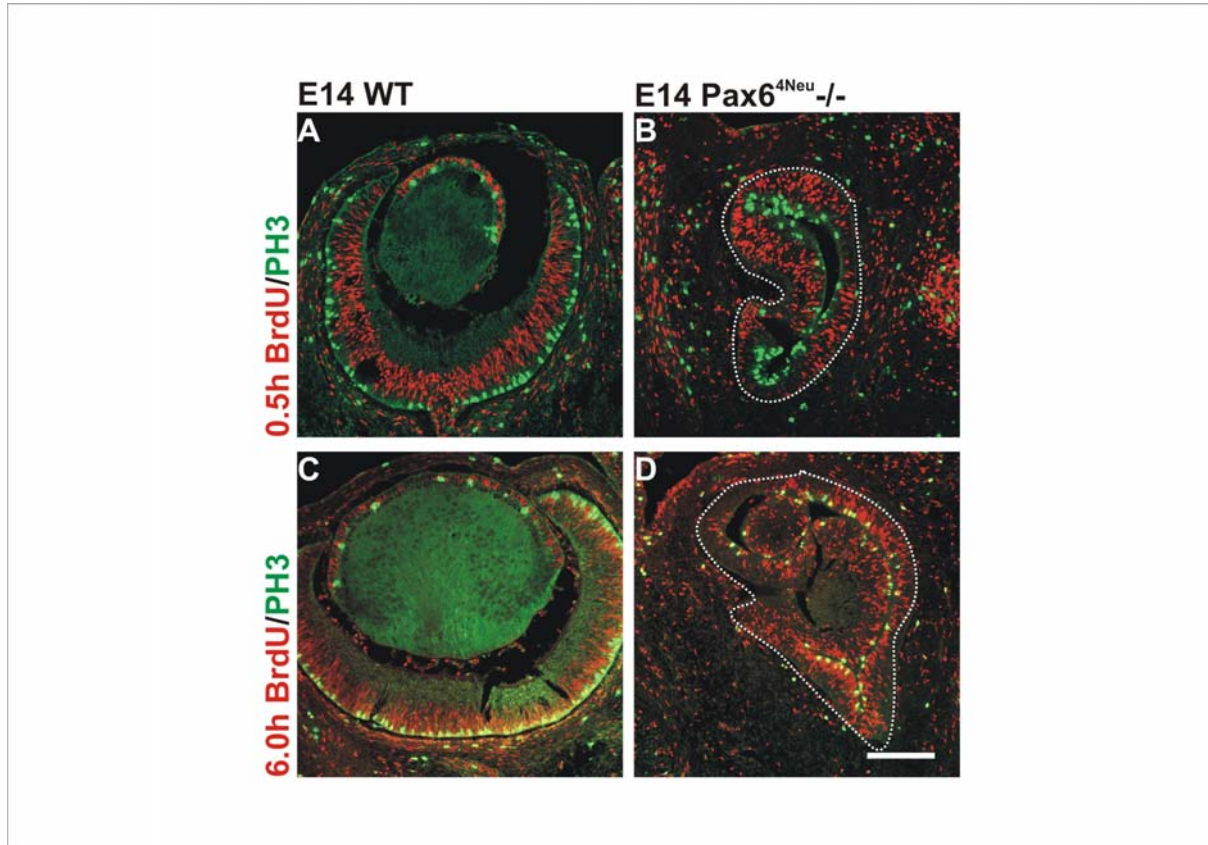


Fig. 56: Interkinetic nuclear migration in the developing eye in the absence of a functional HD ($Pax6^{4Neu-/-}$)

Micrographs depicting coronal sections of E14 embryonic heads at the level of the developing eye. The outer surface of the head is oriented upwards. Immunohistochemistry against BrdU was used to detect the position of cell nuclei after a 0.5h and a 6.0h BrdU pulse to study the interkinetic nuclear migration.

Immunohistochemistry against PH3 was used to recognize the orientation of the epithelium. Due to the failure of optic cup formation, the epithelium is inverted in the $Pax6^{4Neu-/-}$. For description of the interkinetic nuclear migration in the WT see Fig. 54. In the remnant retinal tissue in the $Pax6^{4Neu-/-}$ cell proliferation is decreased compared to WT, but not as much as in the $Pax6^{Sey-/-}$ (Fig. 54) and in the $Pax6^{Aey18-/-}$. After a 0.5h BrdU pulse cells in S-phase (BrdU positive, red) are located at the basal side of the neuroepithelium, while cells in M-phase (PH3 positive, green) are located at the apical side. After 6 hours of BrdU pulse most cells have translocated their nuclei towards the apical side in the $Pax6^{4Neu-/-}$. Thus, interkinetic nuclear migration seems to occur in the absence of a functional HD in the neuroepithelium of the eye. The dashed white line delineates the remnant eye vesicle in the $Pax6^{4Neu-/-}$.

Scale bars: 100µm

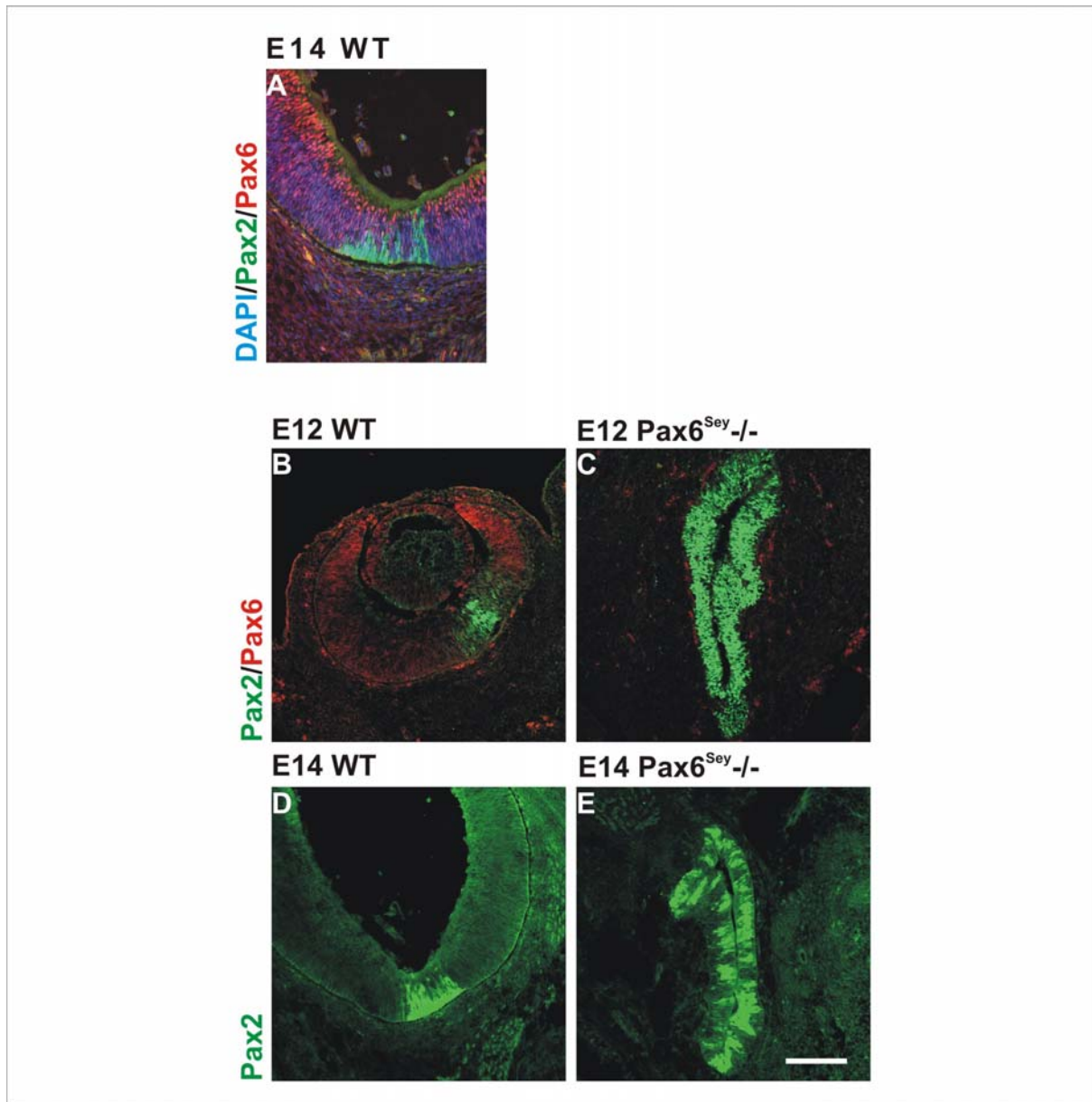


Fig. 57: Pax2 expression in the absence of functional Pax6 protein

Micrographs depicting coronal sections of the eye at E12 and E14. The outer surface of the head is oriented upwards. The expression domains of Pax2 and Pax6 establish the boundary between optic stalk and the neuroretina. Pax2 (green) is expressed in the optic stalk, while the Pax6 expression (red) is restricted to the inner neuroretina at E14 (A). Also at E12 Pax2 expression is restricted to the region of the optic stalk in the WT (B). Loss of functional Pax6 protein leads to the expansion of Pax2 into the entire remnant eye vesicle in the Pax6^{Sey-/-} (C). At E14 the expansion of Pax2 into the remnant eye vesicle remains (E), but occurs more patchy than at E12. Thus, the homozygous loss of functional Pax6 protein leads to changes in the expression domain of Pax2.

Scale bar: 100µm

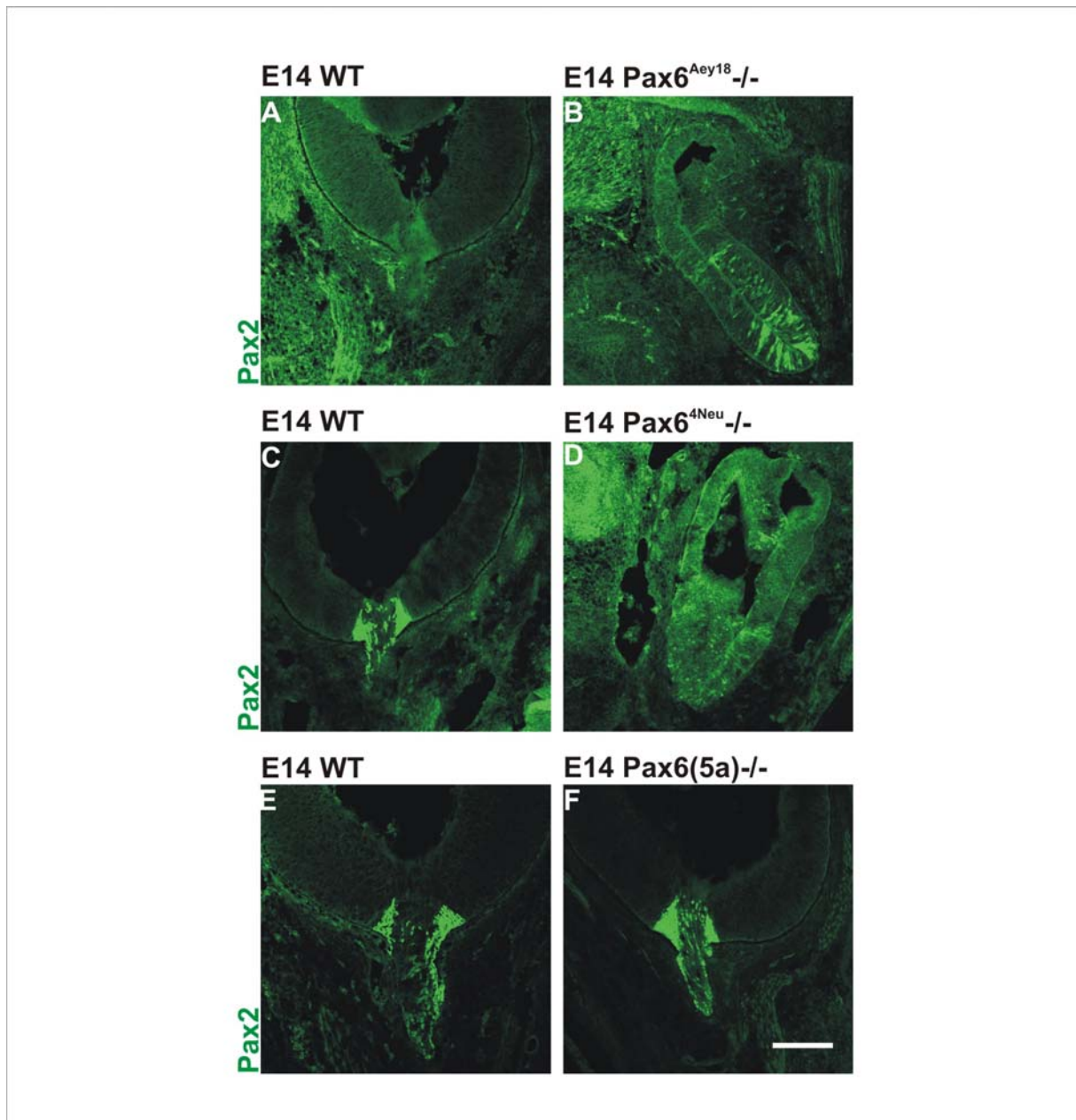


Fig. 58: Pax2 expression in mice carrying defects in PD, HD and PD5a DNA-binding

Micrographs depicting coronal sections of the eye at E14 oriented with the outer surface upwards. Regionalisation has been studied by immunohistochemistry against Pax2. As described before, Pax2 expression is restricted to the optic stalk in the WT (A,C,E), while loss of a functional PD leads to an expansion of Pax2 into the remnant eye vesicle in the $Pax6^{Aey18-/-}$ (B). Mostly single Pax2 expressing cells were detected in the 'pseudo-optic cup' of the $Pax6^{4Neu-/-}$ (lacks DNA-binding of the HD; D), while the Pax2 expression in the $Pax6(5a)-/-$ was normal. Thus, loss of PD or HD DNA-binding leads to the expansion of Pax2 expression, however the phenotype in the HD mutant seems less pronounced. Scale bar: 100 μ m

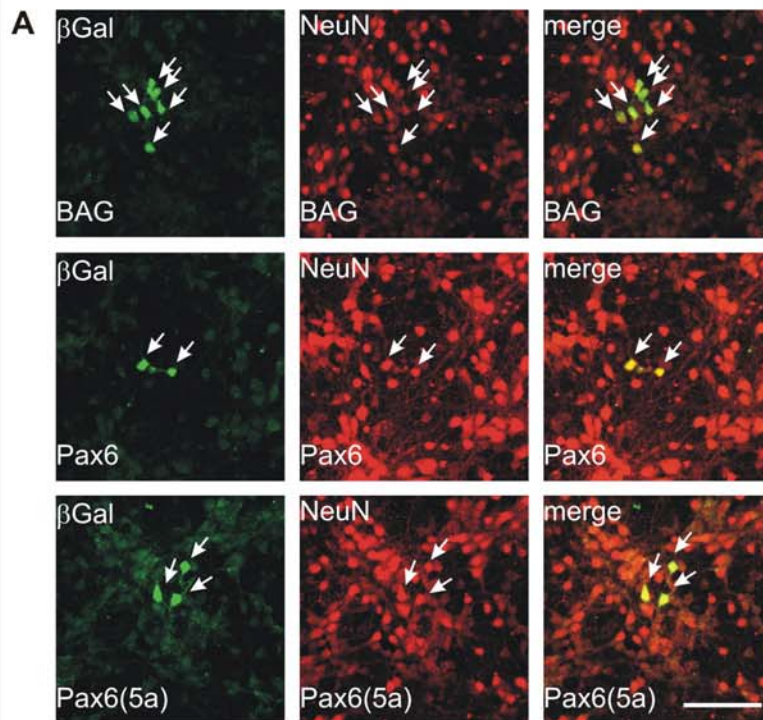


Fig. 59: Retroviral overexpression of Pax6 and Pax6(5a) showed that Pax6(5a) acts specifically on cell proliferation without affecting cell fate

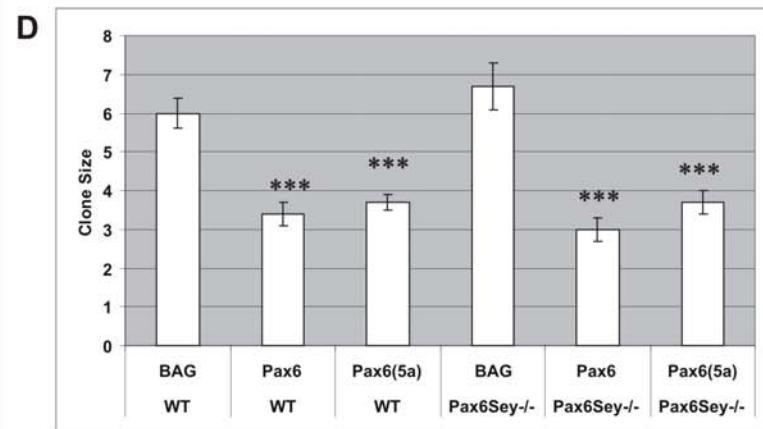
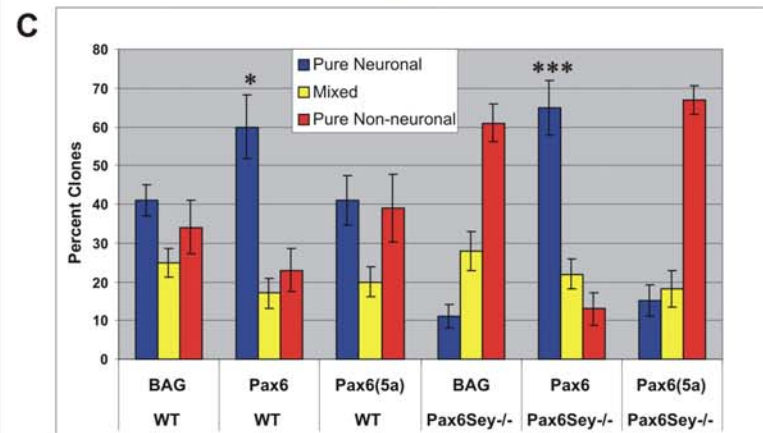
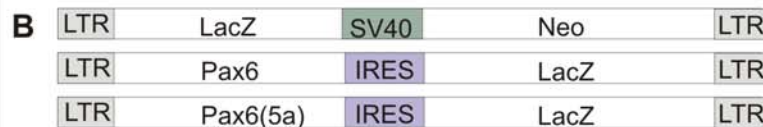
(A) Corresponding micrographs of cells in a clone, isolated from the E14 cortex, infected either with BAG control retrovirus (upper row), Pax6-containing retrovirus (middle row) and Pax6(5a)-containing virus (lower row). Cells were cultured for 7div and immunostained against β -Galactosidase (green) and NeuN (red).

Scale bar: 50 μ m.

(B) Schematic drawings of the retroviral constructs used for control (BAG), Pax6 (canonical form of PD) and Pax6(5a) (PD5a) overexpression together with the marker gene LacZ.

(C) Histogram showing the clone types of either control (BAG), Pax6 or Pax6(5a) infected cells isolated from E14 WT (bars to the left) or $Pax6^{Sey-/-}$ mutant cortex (bars to the right) after 7 div. Note that the percentage of pure neuronal clones (blue bars) increases significantly (compared to WT control, t-test, see Materials and methods) in the cells transduced with virus containing the gene for canonical Pax6, at the expense of the mixed (yellow bars) and pure non-neuronal clones (red bars). In contrast, Pax6(5a) exerted no effect on the clone type, even in the absence of functional Pax6 in $Pax6^{Sey-/-}$ cortical cells.

(D) Histogram depicting the mean size of clones (= the number of β -Galactosidase-positive cells per clone, i.e. the number of cells generated by a single infected precursor) in the cultures described in (C). Note that the clone size was reduced after transduction of cortical cells with Pax6 and Pax6(5a). Pax6(5a) was sufficient to reduce cell proliferation, suggesting that this effect is mediated by the 5aCON site. Numbers of clones analyzed: WT Ctrl: 395, WT Pax6: 243, WT Pax6(5a): 268; $Pax6^{Sey-/-}$ Ctrl: 353, $Pax6^{Sey-/-}$ Pax6: 229, $Pax6^{Sey-/-}$ Pax6(5a): 219.



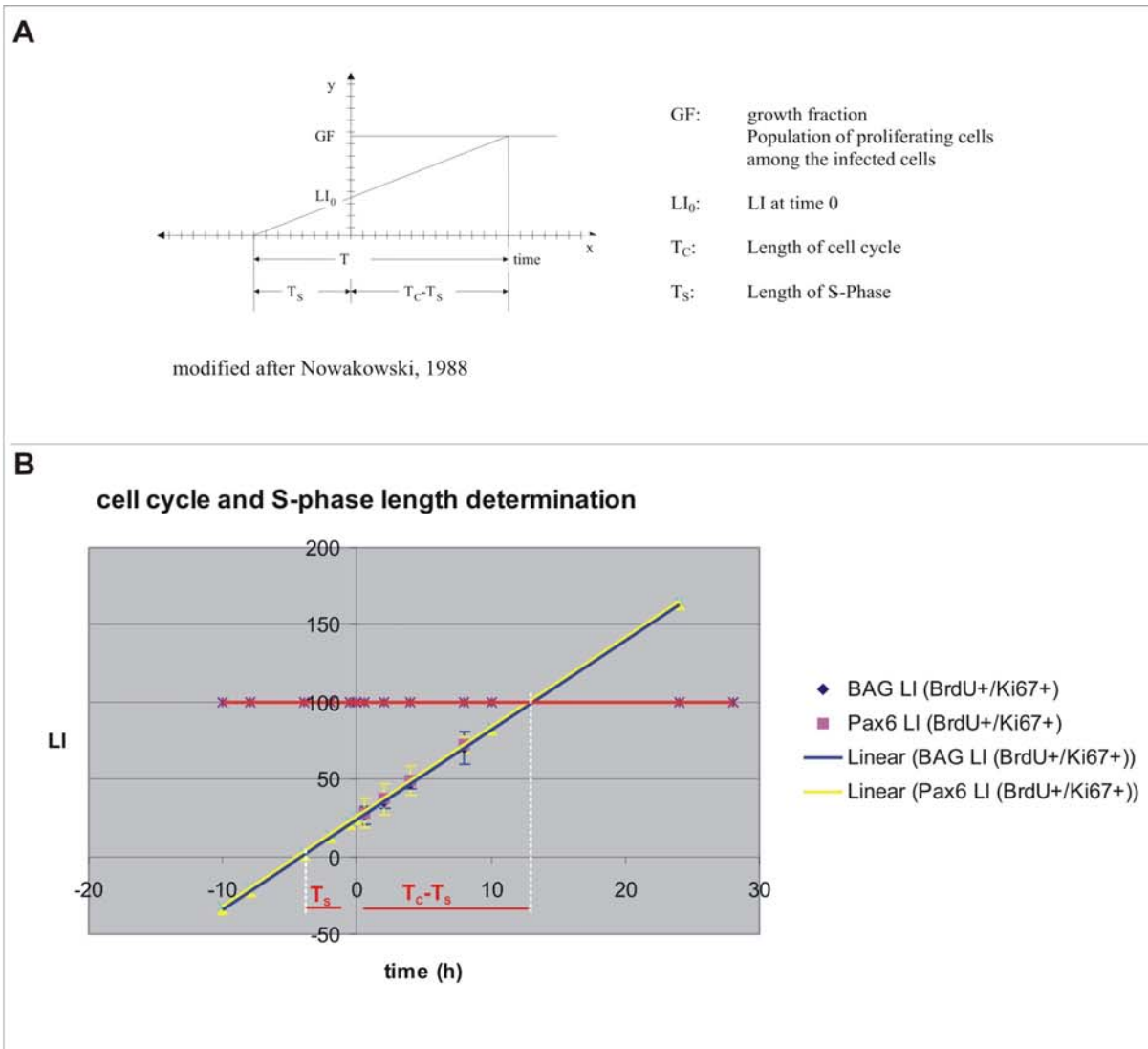


Fig. 60: Proliferation and cell cycle length determination upon Pax6 overexpression

(A) Proliferating cells incorporate the DNA-base analogon BrdU during S-phase into the DNA. The labeling index (LI) is the ratio of BrdU labeled cells to the number of proliferating cells. The timepoint t_0 gives the ratio of BrdU labeled cells at time 0 and is the crossing point of the curve at the y-axis. The longer cells are exposed to BrdU, the more proliferating cells enter S-phase and thus incorporate BrdU. Hence the LI increases over time until all proliferating cells entered S-phase and incorporated BrdU. A LI of 1 or 100% reflects that all proliferating cells went once through S-phase. The growth fraction (GF) gives the ratio of proliferating cells to the total cell number. In the experiments done in this work the total cell number is equal to the number of β -Gal positive cells. The point where the curve crosses 100% (calculated value) gives the total cell cycle length (T_c) minus the length of S-phase (T_s), the crossing point of the slope at the x-axis gives T_s .

(B) The LI-curve of the WT control (BAG) is given in blue, with the error bars given in blue. The LI-curve upon Pax6 overexpression is given in yellow with yellow error bars. The error bars are given for the experimentally determined data points. Data point without error bars are calculated. The red line indicates a LI of 100%, which means that all proliferating cells incorporated BrdU. The dashed white line to the right indicates $T_c - T_s$, the dashed white line to the left indicates T_s . Note that both curves (BAG, blue and Pax6, yellow) are parallel and cross the red line almost at identical points.

Upon Pax6 overexpression no significant changes in the cell cycle and S-phase length were detected compared to the WT control situation.

Error bars are given as s.e.m..

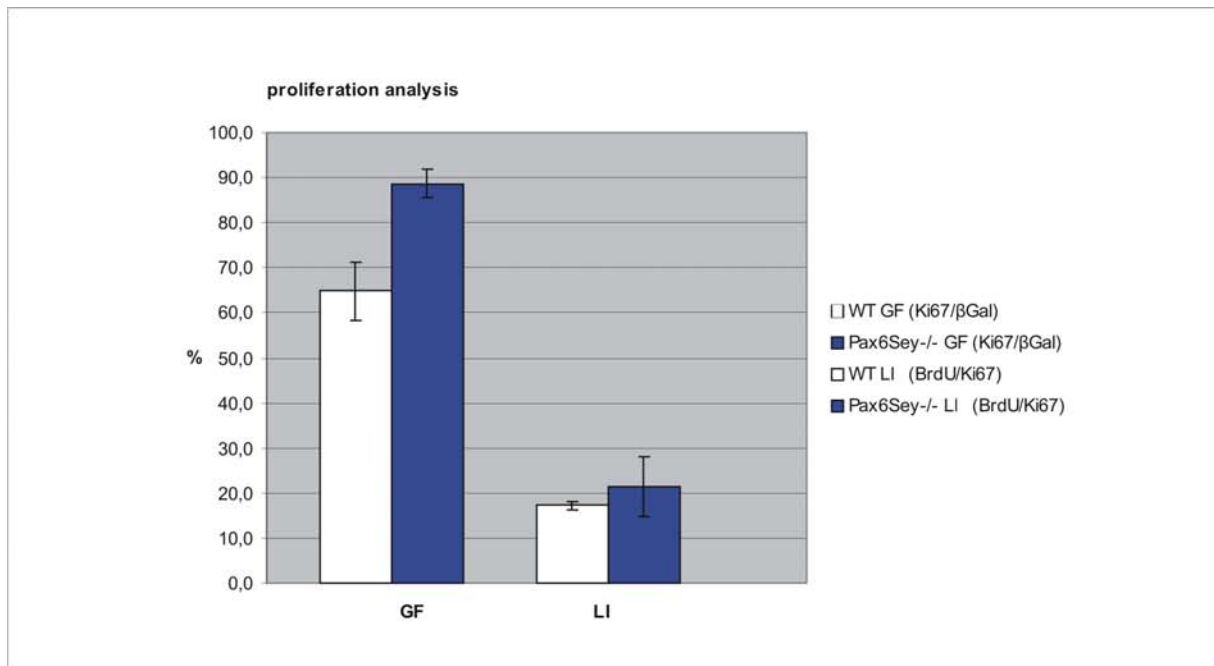


Fig. 61: Proliferation analysis of E14 WT and Pax6^{Sey}-/- cortical cells

Histogram depicting the proliferation analysis of BAG (see Fig. 59) infected E14 WT and Pax6^{Sey}-/- cortical cells after 2 div. Immunohistochemistry against β-Gal allowed the determination of cell clones. The growth fraction (GF, to the left) gives the ratio of proliferating cells to the total number of cells (β-Gal positive) analyzed. The GF was significantly increased in Pax6^{Sey}-/- cortical cells.

No significant changes were detectable in the LI (ratio of BrdU positive cells to the total number of proliferating cells (given to the right) in the Pax6^{Sey}-/- cortical cells compared to the WT.

Error bars are given as s.d..

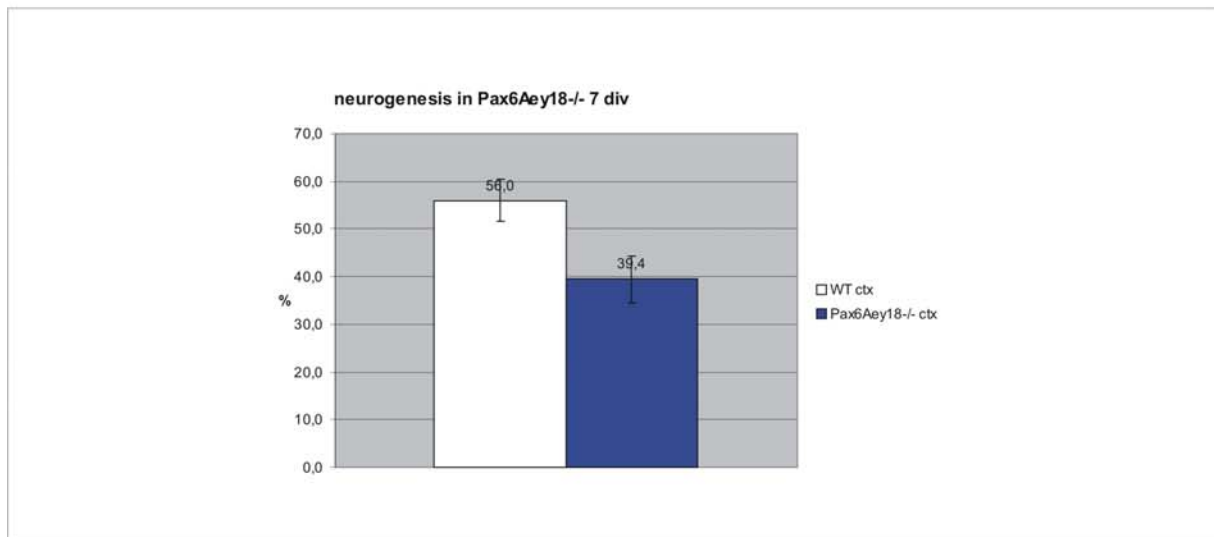
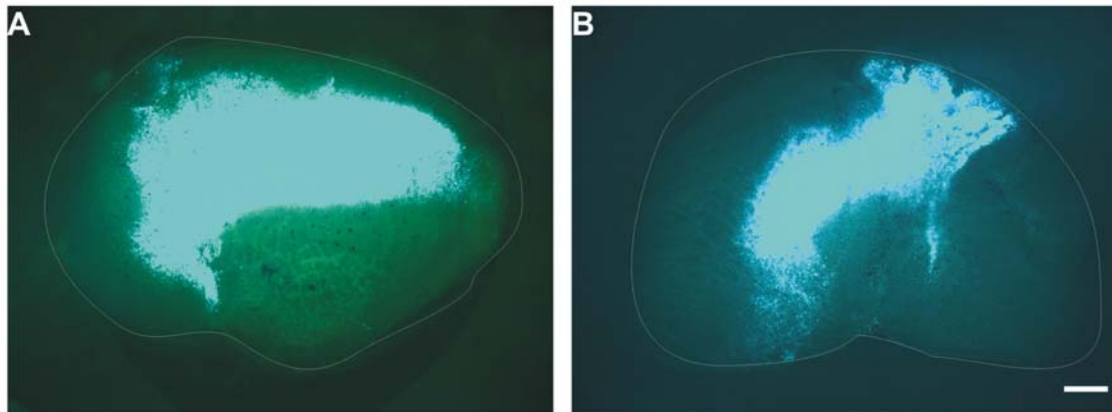


Fig. 62: Analysis of neurogenesis in E14 WT and Pax6^{Aey18}-/- cortical cells

Histogram depicting the percentage of neurons generated per total number of cells (β-Gal positive) analyzed. The number of neurons generated in the cortical cell culture of Pax6^{Aey18}-/- cells (blue bar) was significantly decreased after 7 div compared to the WT (white bar).

Error bars are given as s.d..



Pax6 overexpression 3div

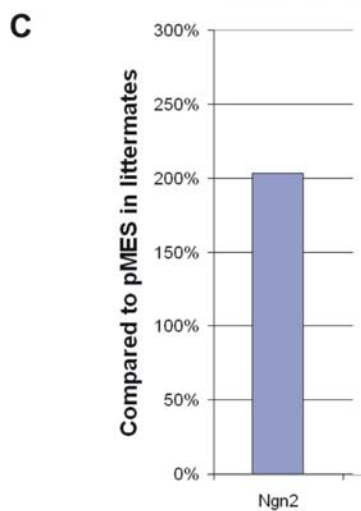


Fig. 63: Pax6 overexpression in vitro

(A,B) Micrographs depicting cortical explants electroporated with PMESGFP control and Pax6 containing plasmids, cultured for 3div. The mRNA was analyzed by real time RT-PCR for the expression of Ngn2. Upon Pax6 overexpression after 3div, the mRNA levels of the direct target gene Ngn2 were 2fold increased compared to the WT cortical tissue that has been electroporated with the GFP expressing control plasmid (PMES) only, which proved that the system worked. The white line in A and B indicates the outline of the cortex after 3 div.

Scale bar: 100µm

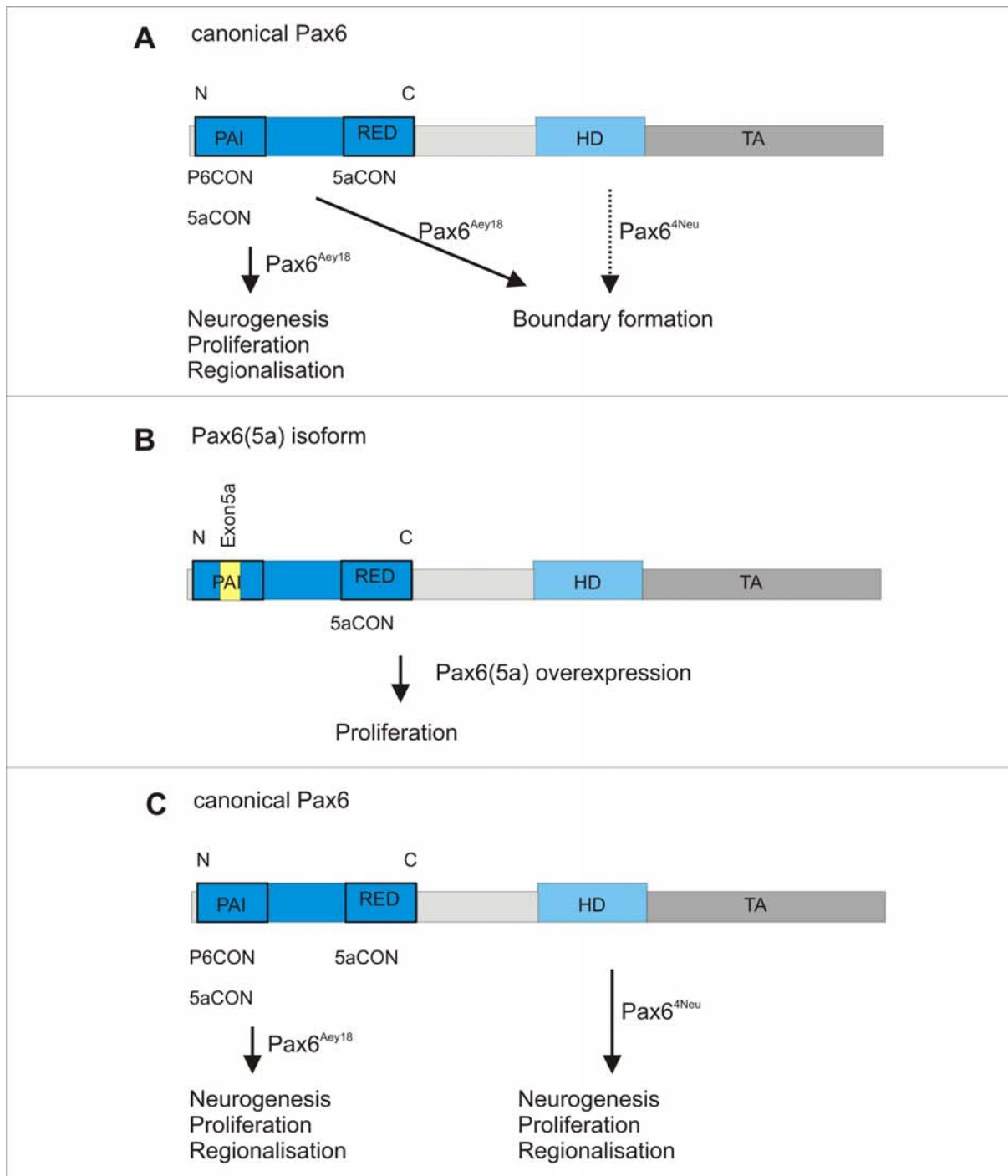


Fig. 64: Summary for the specific roles of the Pax6 DNA-binding domains in the developing telencephalon and developing eye

Analysis of the Pax6^{Aey18}^{-/-} mutant showed that the PD of Pax6 (A,B) is important for the regulation of neurogenesis, proliferation and regionalisation in the developing telencephalon and that it contributes to the formation of the pallio-subpallial boundary. The lack of a phenotype in neurogenesis and proliferation in the telencephalon of Pax6^{4Neu}^{-/-} mice showed that the HD has no role in these processes (A), but is involved in some aspects of the pallio-subpallial boundary formation (SFRP2 expression). The Pax6(5a) isoform (B) is generated by alternative splicing leading to the insertion of a 14AA insert in the N-terminal PAI subdomain of the PD, abolishing DNA binding and thereby favoring DNA binding via the RED domain. Retroviral overexpression revealed the anti-proliferative role of the Pax6(5a) isoform in cortical cells.

In contrast to the telencephalon, both Pax6 DNA-binding domains, PD and HD, contribute to the regulation of neurogenesis, cell proliferation and regionalisation in the developing eye (C), as shown by the analysis of the Pax6^{Aey18}^{-/-} and Pax6^{4Neu}^{-/-}.

Table 1: Quantitative analysis of cell proliferation in the basement membrane mutants LN γ 1 mutant and in the α 6 integrin $^{-/-}$

	Proliferation/Area (number of PH3+ cells per 100 μ m ²) at Ventricular surface	Proliferation/Area (number of PH3+ cells per 100 μ m ²) at Subventricular zone*	Proliferation/Area (total number of PH3+ cells per 100 μ m ²)	Percent abventricular PH3+ cells per 100 μ m ²
WT	3,2 \pm 0,433	0,9 \pm 0,244	4,1 \pm 0,600	20,9 \pm 4,732
LN γ 1mutant	3,1 \pm 0,580	1,1 \pm 0,362	4,2 \pm 0,849	26,2 \pm 5,499
WT	2,6 \pm 0,367	0,9 \pm 0,105	3,4 \pm 1,146	25,5 \pm 1,281
α 6 integrin $^{-/-}$	2,3 \pm 0,476	0,9 \pm 0,346	3,2 \pm 0,826	26,7 \pm 3,585

All values given as mean \pm s.d. with WT to LN γ 1mutant n= 43, LN γ 1mutant n=51; WT to α 6 integrin $^{-/-}$ n=39, α 6 integrin $^{-/-}$ n= 50

*including uSVZ in LN γ 1 mutant

Table 2. Quantitative analysis of the phenotypes of mouse mutants with specific defects in Pax6 DNA-binding domains

	Ratio of thickness of cortical plate (neurons)/ thickness of entire cortex	Proliferation/Area (number of PH3+ cells per radial stripe of 150 μ m) at Ventricular surface	Proliferation/Area (number of PH3+ cells per radial stripe of 150 μ m) at Subventricular zone	Proliferation/Area (total number of PH3+ cells per radial stripe of 150 μ m)	Percent abventricular mitosis per hemisphere
WT	0.25 \pm 0.039	13.9 \pm 4.2	4.9 \pm 2.6	18.8	24.2 \pm 5.2
Pax6 ^{Aey18} $^{-/-}$	0.21 \pm 0.0311 p<0.009	12.8 \pm 2.5 p<0.453	13.3 \pm 2.9 p<1.8*10 ⁻⁷	26.1	42.0 \pm 8.7
WT	0.25 \pm 0.070	11.8 \pm 2.0	5.9 \pm 3.1	17.7	26.1 \pm 6.0
Pax6(5a) $^{-/-}$	0.22 \pm 0.064 p<0.1	12.3 \pm 3.4 p<0.661	4.3 \pm 2.1 p<0.143	16.6	25.4 \pm 4.2
WT	0.23 \pm 0.055	15.1 \pm 5.3	6.3 \pm 4.5	21.4	29.7 \pm 7.4
Pax6 ^{4Neu} $^{-/-}$	0.23 \pm 0.029 p<0.8	13.1 \pm 3.8 p<0.311	5.9 \pm 3.8 p<0.847	19	27.2 \pm 5.5
WT	0.23 \pm 0.035	16.3 \pm 6.3	7.8 \pm 6.7	24.1	16.0 \pm 6.9
Pax6 ^{Sey} $^{-/-}$	0.17 \pm 0.041 p<0.0007	17.1 \pm 5.6 p<0.831	19.1 \pm 5.6 p<9.8*10 ⁻⁵	36.2	35.8 \pm 5.2

All values given as mean \pm s.d. with n=12

9 Discussion

In this work, intrinsic and extrinsic cues in the developing telencephalon and eye have been analyzed with respect to the regulation of cell proliferation, neurogenesis and regionalisation. The transcription factor Pax6 is a potent cell intrinsic regulator of cell proliferation, neurogenesis and regionalisation. Pax6 is expressed in the radial glia cells of the telencephalon, which constitute the majority of precursor cells in the VZ during neurogenesis. The analysis of specific mouse mutants allowed assessing the functional roles of the different DNA-binding domains of Pax6. We could show that the canonical PD is necessary and sufficient to regulate all developmental functions of Pax6 in the telencephalon, while the alternative splice variant of the PD (PD5a) specifically affects cell proliferation without affecting cell fate or patterning. In contrast, mutation of the HD affected only subtle aspects of the boundary delineating the dorsal and ventral telencephalon. The canonical PD binds to both Pax6 consensus sites (P6CON and 5aCON), whereas the PD5a binds to 5aCON sites only, thus these results suggest that neurogenesis is regulated by target genes containing P6CON sites, while cell proliferation is regulated via 5aCON target sites. In contrast to the developing telencephalon, where the HD plays only a minor role in the regulation of neurogenesis, cell proliferation and regionalisation, both Pax6 DNA-binding domains (PD and HD) contribute to the regulation of these aspects in the developing eye.

Radial glia cells do not only depend on the cell intrinsic factors, but are also exposed to extrinsic signals that might regulate the key developmental processes cell proliferation and neurogenesis. Thus, the influence achieved by the attachment of radial glia endfeet to the basement membrane on the proliferative behavior and cell differentiation has been studied. The analysis of the LN γ 1 mutant, lacking the contact of radial glia cells to the basement membrane and the α 6 integrin $^{-/-}$, characterized by the improper basement membrane assembly, let us conclude that neither the detachment of radial glia endfeet nor the improper assembly of the basement membrane affects cell proliferation and neurogenesis in the developing telencephalon.

9.1 The role of Pax6 in the regulation of cell proliferation in the cerebral cortex

Two proliferative populations are present in the developing telencephalon, the VZ originating from the early neuroepithelium, and the SVZ (Smart, 1976) that becomes apparent with the onset of neurogenesis at E12 and originates from the VZ (Noctor et al., 2004). Loss of functional Pax6 protein in the Pax6^{Sey}^{-/-} mice leads to an increase in cell proliferation in the cortex (Estivill-Torrus et al., 2002; Götz et al., 1998). The quantification of cells dividing at the ventricular surface (VS), corresponding to VZ precursor cells, versus cells dividing at abventricular positions (SVZ positions) in the cerebral cortex of Pax6^{Sey}^{-/-} mice revealed that especially the number of cells dividing at abventricular positions is increased during cortical neurogenesis. The Pax6^{Sey}^{-/-} allele leads to the generation of a non functional truncated protein, lacking the transactivating domain. So far, nothing was known about the roles of the different Pax6 DNA binding domains (PD, PD5a and HD) in the regulation of cell proliferation. Our in vivo analysis of the Pax6^{Aey18}^{-/-} allele showed that the loss of a functional PD under preservation of a functional HD and TAD in the Pax6^{Aey18}^{-/-} mutant leads to the same cell proliferation phenotype as in the functional null allele Pax6^{Sey}^{-/-}, also at the quantitative level. In contrast, no changes in cell proliferation were observed in the cortex of the Pax6^{4Neu}^{-/-}, lacking specifically HD DNA-binding and in the cortex of the Pax6(5a)^{-/-}, lacking specifically exon5a of the PD. Thus, we could demonstrate that the PD of Pax6 is required for the regulation of cell proliferation in the cerebral cortex.

What could be the reason for the increase in the number of precursors at abventricular positions? Several markers have been reported recently for the identification of neuronal SVZ precursors, as for example the homeodomain transcription factors Cux1, Cux2 (Nieto et al., 2004; Zimmer et al., 2004), the non-coding RNA Svet1 (Tarabykin et al., 2001) and the T-domain transcription factor Tbr2 (Englund et al., 2005). All these markers are lost in the SVZ cells of the functional null allele Pax6^{Sey}^{-/-} and at the same time, upper layer neurons are absent in the cortex of the Pax6^{Sey}^{-/-} mice (Englund et al., 2005; Nieto et al., 2004; Tarabykin et al., 2001; Zimmer et al., 2004). The analysis of Svet1 and Tbr2 expression in the specific mutant Pax6 alleles showed that an intact PD is required for the expression of these genes, since the loss of a functional PD in the cortex of Pax6^{Aey18}^{-/-} mice led to the absence of Svet1 and Tbr2, while both were detectable in the Pax6^{4Neu}^{-/-} (HD mutant) and the Pax6(5a)^{-/-}. The expression of Svet1, Cux2 and Tbr2 correlates with the generation of upper layer neurons (Englund et al., 2005; Nieto et al., 2004; Tarabykin et al., 2001; Zimmer et al., 2004) in the

cortex, thus it might be that their loss leads to an ongoing cell proliferation, associated with the lack of neuronal differentiation in the mutant Pax6 alleles *Pax6^{Sey}-/-* and *Pax6^{Aey18}-/-*.

Another possibility for the increased number of proliferating cells at abventricular positions in the cortex of the *Pax6^{Sey}-/-* could be that the apoptosis rate is changed due to the loss of functional Pax6 protein, but immunohistochemistry against activated caspase-3 in the cerebral cortex of WT and *Pax6^{Sey}-/-* at E14 did not show any differences in that regard.

Further, it could also be that the increased SVZ in the cortex of *Pax6^{Sey}-/-* mice develops due to changes in cell migration in the telencephalon. The pallial-subpallial boundary (PSB) is lost in the telencephalon of the *Pax6^{Sey}-/-* (Stoykova et al., 1997) and as one consequence, increased cell migration from the ventral into the dorsal telencephalon takes place (Chapouton et al., 1999). In order to determine whether the increased SVZ develops (i) on account of increased cell migration of precursor cells from the ventral telencephalon into the cerebral cortex or (ii) due to cell autonomous changes, cortical cells were isolated from WT and *Pax6^{Sey}-/-* at E14 and cultured for 2 days in vitro (div). Prior to fixation the DNA-base analogon BrdU was added to the culture medium. This enabled us to determine the labeling index (LI= ratio of BrdU positive cells to total number of proliferating cells). Cells in S-phase incorporate BrdU in the DNA, thus a short BrdU pulse reveals possible changes in S-phase of the cell cycle or changes in the proliferation rate. No significant changes in the LI were detected between cortical cells from WT and *Pax6^{Sey}-/-*, thus no changes in S-phase of the cell cycle seem to occur. However, the determination of the growth fraction (GF= ratio of proliferating cells to total cell number) showed a significant increase in the GF in cortical cells isolated from *Pax6^{Sey}-/-* compared to cortical cells of corresponding WT littermates, which means that cell proliferation is indeed increased in the cortex of *Pax6^{Sey}-/-* mice. This increase might be based on a cell autonomous effect, namely the loss of functional Pax6 protein.

In order to determine whether Pax6 acts cell autonomously on cell proliferation, gain-of-function experiments were performed. The analysis of cell proliferation in the *Pax6^{Aey18}-/-* cortex showed that the PD is the important DNA-binding domain for the regulation of cell proliferation. However, it was not yet clear, whether Pax6 with a canonical PD, or Pax6 containing the alternatively spliced PD (PD5a) is required in this regard. Hence we determined the specific roles of the PD and PD5a in the regulation of cell proliferation, using a retroviral vector containing either the canonical Pax6 or the alternative splice variant Pax6(5a). Here we could show that both isoforms, canonical Pax6 and Pax6(5a), decrease the number of cells generated per clone after 7 div in WT and even in *Pax6^{Sey}-/-* cortical cells,

which means that both isoforms of the PD are able to regulate cell proliferation. Thus, the decrease in cell proliferation upon Pax6 overexpression in individual cortical precursors together with the increase in cell proliferation in vivo and in vitro in cortical cells upon loss of functional Pax6 protein ($Pax6^{Sey-/-}$), argues strongly for a cell autonomous effect of Pax6 on cell proliferation.

The next question we asked was: How can Pax6 overexpression lead to a decrease in cell proliferation? First of all it could be that high levels of Pax6 protein are inducing apoptosis. We could exclude this possibility, since no changes in apoptosis (assessed by quantification of pyknotic nuclei in the infected clones) were detectable in cortical cells infected with control virus or Pax6 containing virus. Another possibility could be that Pax6 leads to a slower cell cycle, thus less cell divisions occur per time unit. Alternatively it could be that Pax6 overexpression leads to an increase in cell differentiation, thus more cells exit the cell cycle. In order to test for these possibilities, we analyzed the cell cycle and S-phase length in WT cortical cells upon retrovirus mediated Pax6 overexpression compared to WT cortical cells, infected with control virus. This analysis showed that increased levels of Pax6 expression do not lead to changes in cell cycle or S-phase length, which argues for the latter possibility proposed above, namely for an increased cell cycle exit rate. This result is well in line with the increase in the number of pure neuronal clones obtained upon Pax6 overexpression (see below).

A characteristic feature of proliferating VZ cells in the telencephalon is the translocation of their nuclei in correlation with the different cell cycle phases (Sauer, 1935). BrdU pulse experiments indicated that there might be changes in the interkinetic nuclear migration in the $Pax6^{Sey-/-}$ mice (Estivill-Torrus et al., 2002; Götz et al., 1998), since cells seem to translocate their nuclei in a less organized fashion. BrdU pulse experiments in the different mutant Pax6 alleles revealed in the PD mutant ($Pax6^{Aey18-/-}$) a phenotype similar as the one detected in the $Pax6^{Sey-/-}$ mice, while no changes in the interkinetic nuclear migration were detectable in the HD mutant ($Pax6^{4Neu-/-}$) or in the $Pax6(5a-/-)$ mice. This suggests a role of the PD in the regulation of the interkinetic nuclear migration. What could be the reason for the ‘picture’ that we detected in regard of the interkinetic nuclear migration? One possibility could be that G2/M-phase is shortened in the Pax6 mutant cells, and that these cells start to divide before they reach the ventricular surface. However, my results excluded this possibility since the length of G2/M phase is not changed in the $Pax6^{Sey-/-}$ mice (Haubst, diploma thesis). Another explanation could be that the interkinetic nuclear migration of the VZ cells is not altered at all in the $Pax6^{Sey-/-}$ and $Pax6^{Aey18-/-}$ mutant cortex. Since BrdU labels all cells in S-phase, also

the SVZ precursors that do not undergo interkinetic nuclear migration (Smart, 1976) are labeled. The strongly increased SVZ precursor population could expand in the ventricular zone in the Pax6^{Sey}^{-/-} and Pax6^{Aey18}^{-/-} cortex. One evidence for this scenario is that the band of abventricular mitosis detected by immunohistochemistry against PH3 is much broader in the Pax6^{Sey}^{-/-} and Pax6^{Aey18}^{-/-} cortex than in the WT (see Fig. 28, 29). Thus, the effect of the coordinated nuclear translocation of the BrdU labeled VZ cells that we detected in the WT, is blurred by the presence of an increased number of BrdU positive SVZ cells in the Pax6^{Sey}^{-/-} and Pax6^{Aey18}^{-/-} cortex (see for example Fig. 29D). Further support for this hypothesis was obtained by the analysis of the interkinetic nuclear migration in the neuroepithelial cells of the developing eye. Although cell proliferation was strongly decreased in the remnant eye vesicle of Pax6^{Sey}^{-/-}, Pax6^{Aey18}^{-/-} and Pax6^{4Neu}^{-/-}, interkinetic nuclear migration seemed to occur despite loss of wild type Pax6 protein.

Taken together, these results show clearly that cell proliferation increases in the cerebral cortex and in cortical cell culture due to the loss of functional Pax6, whereas Pax6 gain-of-function decreases cell proliferation in cortical cells. These findings argue for a cell autonomous role of Pax6 in the regulation of cell proliferation. In other regions of the CNS Pax6 is also involved in the regulation of cell proliferation, as e.g. in the diencephalon and the developing eye. However, in the Pax6^{Sey}^{-/-} diencephalon and in the targeted deletion of Pax6 in the neuroretina of the developing eye, decreased cell proliferation was detected (Marquardt et al., 2001; Warren and Price, 1997), thus Pax6 seems to act region-specifically on cell proliferation.

9.2 The role of Pax6 in the regulation of neurogenesis

Loss of functional Pax6 protein in the telencephalon does not only lead to an increase in cell proliferation, but also to a decrease in cortical neurogenesis (see e.g. Heins et al., 2002). Here we addressed the question which DNA-binding domains of Pax6 are involved in the regulation of cortical neurogenesis. The analysis of the mouse mutants harboring specific mutations in the distinct DNA-binding domains of Pax6 revealed that the PD mutant (Pax6^{Aey18}^{-/-}) shows the same phenotype as the functional null allele Pax6^{Sey}^{-/-} in regard to neurogenesis, while the HD mutant (Pax6^{4Neu}^{-/-}) and the targeted deletion of exon5a (Pax6(5a)^{-/-}) did not show aberrant phenotype in neurogenesis compared to the corresponding WT. The decrease in neurogenesis was confirmed at the quantitative level and

proved to be significant. As described above, the radial glia fascicle at the pallial-subpallial boundary (PSB) in the $Pax6^{Aey18-/-}$ telencephalon fails to form. However, the boundary specific marker protein reticulon-1 was still present in the $Pax6^{Aey18-/-}$, in contrast to the functional null allele $Pax6^{Sey-/-}$, where the loss of the PSB is correlated with the enhanced cell migration from the ventral to the dorsal telencephalon (Chapouton et al., 1999). We were concerned that the alterations of the PSB could allow increased cell migration from the ventral telencephalon into the cortex and thus compensate the decreased neurogenesis in the $Pax6^{Aey18-/-}$ cortex. In order to exclude this possibility, we analyzed neurogenesis in cortical cell culture after 7 div. Indeed, we found a significant decrease in the percentage of neurons generated from cortical cells of the $Pax6^{Aey18-/-}$ compared to the WT, indicating that the PD acts cell autonomously on the regulation of neurogenesis. Thus, we conclude that beside the regulation of cell proliferation, also the regulation of neurogenesis in the telencephalon depends on the PD of Pax6. However, since the deletion of the PD in the $Pax6^{Aey18-/-}$ mice includes also exon5a, it was not yet clear, whether Pax6 with a canonical PD, or Pax6 containing the alternatively spliced PD (PD5a) is involved in the regulation of neurogenesis. Upon specific retrovirus mediated overexpression of either canonical Pax6 or Pax6(5a) in individual precursor cells we showed that canonical Pax6 induces a significant increase in the percentage of pure neuronal clones, while the PD5a was not able to influence neurogenesis. Hence it seems that the target genes containing P6CON sites are mediating the neurogenic effect, which is well in line with the presence of the P6CON site in the direct target gene *Ngn2* (Bertrand et al., 2002). In summary we could thus show that exclusively canonical Pax6 acts on the regulation of neurogenesis in the developing telencephalon.

As mentioned above, SVZ precursors are specified by the expression of *Cux1/2*, *Tbr2* and *Svet1* and generate the upper layer neurons (II-IV) (Englund et al., 2005; Nieto et al., 2004; Tarabykin et al., 2001; Zimmer et al., 2004). The expression of these genes is lost in the functional null allele $Pax6^{Sey-/-}$. Here we could show that the expression of *Tbr2* and *Svet1* is as well lost in the PD mutant ($Pax6^{Aey18-/-}$). At the same time SVZ precursors proliferate more also at later developmental stages, and the cortical plate is decreased in thickness in the $Pax6^{Sey-/-}$ and $Pax6^{Aey18-/-}$ cortex at E18. In summary, a conclusion would be that SVZ precursor cells in the $Pax6^{Sey-/-}$ and $Pax6^{Aey18-/-}$ mutant cortex are lacking the expression of transcription factors that specify the upper layer neurons and instead of undergoing neuronal differentiation, cells continue to proliferate. In contrast to the developing telencephalon, *Tbr2* was also expressed in the neurons of the neuroretina, which means that it is not only

expressed in neurogenic precursors but also in neurons, as it has been described also for the early telencephalon E10-E12 (Englund et al., 2005).

Taken together these results showed that Pax6 regulates neurogenesis in the developing telencephalon by means of the canonical PD cell autonomously. However, the role of Pax6 in the regulation of neurogenesis is not exclusively restricted to the telencephalon, but includes also other regions of the CNS. Loss of functional Pax6 in the diencephalon, the cerebellum and the spinal cord is associated the loss of neuronal subpopulations (Briscoe et al., 1999; Engelkamp et al., 1999; Vitalis et al., 2000; Warren and Price, 1997).

9.3 The influence of the different Pax6 DNA-binding domains on the regionalisation of the telecephalon

Severe changes in regionalisation occur in the telencephalon of the Pax6^{Sey}-/- mice (Stoykova et al., 1996; Toresson et al., 2000; Yun et al., 2001). So far it was not clear which DNA-binding domains of Pax6 are involved in establishing the regionalisation of the telencephalon. Here we showed that regionalisation in the telencephalon of the PD mutant Pax6^{Aey18}-/- was altered to a similar extend as in the Pax6^{Sey}-/- mice. Ngn2 expression, a direct downstream target gene of Pax6, was almost completely absent in rostro-lateral regions, whereas it was still detectable in regions of low Pax6 and high Emx2 expression. Also other transcription factors, which are normally expressed in the ventral telencephalon, as Mash1 and Gsh2 expand dorsally in the telencephalon of the Pax6^{Aey18}-/- mice, while the loss of HD DNA-binding in the telencephalon of the Pax6^{4Neu}-/- or the specific loss of exon5a in the Pax6(5a)-/- did not lead to any changes in the regionalisation.

Interestingly, we found that the expression of the wnt-inhibitor SFRP2 at the pallial-subpallial boundary (PSB), the region where the dorsal pallium and the ventral subpallium abut, is lost in the telencephalon of the Pax6^{4Neu}-/- and Pax6^{Aey18}-/- mice. Furthermore, the formation of the radial glia fascicle at the PSB fails, although in contrast to the functional null allele Pax6^{Sey}-/-, the expression of the PSB specific marker reticulon-1 (Hirata et al., 2002) was still detectable in both mutants (Pax6^{Aey18}-/- and Pax6^{4Neu}-/-). In addition we detected in both mutants (Pax6^{Aey18}-/- and Pax6^{4Neu}-/-) high levels of BLBP expression in the reticulon-1 expressing cells. Thus it seems that multiple mechanisms contribute to the formation of the PSB, which might as well act as a signalling center in the developing telencephalon as previously proposed (Assimacopoulos et al., 2003). In summary these results showed that

both DNA-binding domains of Pax6 (PD and HD) are required to act on SFRP2 and reticulon-1 expression, which means that either both DNA-binding domains bind cooperatively to the DNA or that the PD might be required to modulate DNA-binding of the HD (Jun and Desplan, 1996; Mikkola et al., 2001; Mishra et al., 2002; Singh et al., 2000) or the HD might interact with the C-terminal RED domain of the PD as previously shown in vitro (Bruun et al., 2005).

9.4 The role of the PD5a in the developing telencephalon

We did not detect any changes in neurogenesis, cell proliferation and regionalisation in the Pax6(5a)^{-/-} telencephalon (E12- P2). However, there are several reasons why this result has to be interpreted with caution: (i) The canonical form of the PD is able to bind to both consensus sites (P6CON, 5aCON). (ii) The expression levels of canonical Pax6 increase 1.4 fold in the cortex of the Pax6(5a)^{-/-} which is a sufficient amount to compensate the loss of the normal expression levels (10-20%) of Pax6(5a). Hence as a conclusion from the in vivo analysis follows that Pax6(5a) does not fulfil any specific roles, which could not be taken over by the canonical Pax6. This has been confirmed by the overexpression experiments described above, where we showed that the overexpression of Pax6(5a) in individual precursor cells leads to a significant decrease in clonal size, while no effect on cell fate was detectable, even in cells of the Pax6^{Sey}^{-/-} mice lacking functional Pax6 protein. In contrast, overexpression of the canonical Pax6 isoform decreased the clonal size and influenced the cell fate. Since Pax6(5a) binds exclusively to 5aCON sites, the target genes involved in cell proliferation should contain 5aCON sites, while target genes involved in the regulation of neurogenesis would rather contain P6CON sites, which is already confirmed for the direct target gene of Pax6 and proneuronal gene Ngn2 (Bertrand et al., 2002; Scardigli et al., 2003).

One reason for a decreased clonal size could be an increase in the apoptosis rate, but no significant changes in apoptosis were detectable upon Pax6 or Pax6(5a) overexpression. A second cause for a small number of cells per clone could be changes in the mode of cell division, leading to more asymmetric cell divisions, which generate one precursor and one postmitotic cell. The experiment for the determination of the cell cycle length (see above) showed, that cell proliferation decreases already after 2div from 70% in the control infected cells to 55% after Pax6 overexpression, with no detectable changes in the cell cycle length. In addition, the number of pure neuronal clones was increased upon overexpression of canonical

Pax6. Thus it might be that Pax6 overexpression leads to an increased number of asymmetric cell divisions.

In summary, we conclude from our loss-of-function analysis of the PD mutant Pax6^{Aey18}^{-/-}, the functional null allele Pax6^{Sey}^{-/-}, the HD mutant Pax6^{4Neu}^{-/-}, the Pax6(5a)^{-/-} and the gain-of-function studies on the canonical Pax6 and Pax6(5a) that the PD is the most important DNA-binding domain in the telencephalon, mediating the effects of Pax6 in the regulation of neurogenesis, the cell autonomous effect of Pax6 on cell proliferation, and the influence of Pax6 on the regionalisation in the telencephalon. Further we could show by gain-of-function experiments that the PD5a acts on cell proliferation. The HD is involved together with the PD in regulation of certain aspects of the formation of the pallial-subpallial boundary in the telencephalon (for summary see Fig. 64).

9.5 The different DNA-binding domains of Pax6 act region-specifically in the developing telencephalon and the eye

Pax6 expression in the CNS is not restricted to the telencephalon but is also detectable for example in the diencephalon and the developing eye. Interestingly, Pax6 seems to regulate cell proliferation in a region dependent context. While loss of functional Pax6 in the telencephalon leads to an increase in cell proliferation (Estivill-Torrus et al., 2002; Götz et al., 1998), decreased cell proliferation occurs in the early diencephalon of the functional null allele Pax6^{Sey}^{-/-} (Warren and Price, 1997). The targeted deletion of Pax6 in the neuroretina showed that Pax6 promotes cell proliferation and is required to maintain cells in a multipotent precursor state (Marquardt et al., 2001). In the invertebrate eye of *Drosophila* cell proliferation is promoted by the Pax6(5a) homolog *eyegone* (*eyg*), while the Pax6 homologs *eyeless* (*ey*) and *twin of eyeless* (*toy*) rather promote cell specification and differentiation (Dominguez et al., 2004). The targeted deletion of Pax6(5a) in the vertebrate eye leads to a decreased number of iris and lens fiber cells (Singh et al., 2002), showing that the target genes of Pax6(5a) in vertebrates and *eyg* in invertebrates fulfil similar roles in the regulation of cell proliferation. Thus, one conclusion would be that the specific function of Pax6(5a) in the developing telencephalon in regard to the regulation of cell proliferation must have evolved later than in the eye.

The absence of functional Pax6 leads to the absence of eyes in the Pax6^{Sey}^{-/-} (Grindley et al., 1995; Hill et al., 1991). In the case of loss of a functional HD in the Pax6^{4Neu}^{-/-} mice (Favor et

al., 2001) and PD in the $Pax6^{Aey18-/-}$ mice (Haubst et al., 2004) no eye development occurs as well. In all three $Pax6$ alleles ($Pax6^{Sey-/-}$, $Pax6^{Aey18-/-}$, $Pax6^{4Neu-/-}$) a remnant of the eye vesicle can be detected. Occasionally, a lens-like remnant has been detected in the $Pax6^{4Neu-/-}$ and $Pax6^{Aey18-/-}$, but never in the $Pax6^{Sey-/-}$ mice. The $Pax6(5a-/-)$ mice develop an eye which is at postnatal stages characterized by a decrease in lens fiber cells and cells of the iris (Singh et al., 2002). Due to premature neurogenesis followed by massive apoptosis in the remnant of the eye vesicle in the functional null allele $Pax6^{Sey-/-}$ (Philips et al., 2005) no β III-Tubulin positive cells were detectable at E14 and proliferation was severely reduced, while in the PD ($Pax6^{Aey18-/-}$) and HD ($Pax6^{4Neu-/-}$) mutant neurons (β III-Tubulin positive) of different subtypes (Brn3a positive and Islet-1 positive neurons) were generated and also cell proliferation was less reduced. Neurogenesis and cell proliferation did not show severe alterations in the embryonic eye of $Pax6(5a-/-)$ mice at E14. No retinal pigmented epithelium (RPE) developed in the $Pax6^{Sey-/-}$ and $Pax6^{Aey18-/-}$ mutant mice, while occasionally little RPE residues were detectable in the HD mutant $Pax6^{4Neu-/-}$. Thus, in pronounced contrast to the developing telencephalon both DNA-binding domains PD and HD contribute to the regulation of neurogenesis and cell proliferation in the developing eye. The selective use of PD, PD5a and HD might thus contribute to the region-specific differences of $Pax6$ function in the CNS.

9.6 Other mechanisms that could explain the region-specific differences of $Pax6$ functions

Not only the selective use of different DNA-binding domains can contribute to region-specific differences of $Pax6$ function. Also different expression levels of the different $Pax6$ splice variants (canonical $Pax6$, $Pax6(5a)$ and PD-less $Pax6$) could be involved, since a specific ratio of $Pax6$ and $Pax6(5a)$ improved transcriptional activation (Chauhan et al., 2004). The region specific expression levels are also correlated with the region specific usage of promotor and enhancer elements (for review see: Morgan, 2004). Recently natural antisense transcripts (NATs) of $Pax6$ ($Pax6OS$ = $Pax6$ opposite strand) have been detected in the eye (Alfano et al., 2005), but not yet in the telencephalon. While some NATs display a sequence complementary to exonic sequences of their corresponding sense genes, the NATs of $Pax6$ and also $Pax2$ are complementary to intronic sequences. Thus, one could speculate that the $Pax6$ NATs could act on intronic enhancer elements or possible splicing sites of $Pax6$, since they occurred in six different alternative splice forms (Alfano et al., 2005). It might be possible that the binding of

Pax6 NATs to intronic sequences, as for example enhancer elements, silences distinct alternative splice forms of *Pax6*. Interestingly, the NATs described by Alfano and colleagues (2005) were discovered also for other genes that are alternatively spliced. In the *Vax2*^{-/-} is also the corresponding *Vax2OS* significantly decreased, while the overexpression of *CrxOS* lead to a reduction of *Crx* levels (Alfano et al., 2005). Thus one could speculate that NATs might be involved in the regulation of the region-specific function of *Pax6* by modulating the gene activity, especially in combination with different expression levels of the alternative *Pax6* forms, as the canonical *Pax6*, *Pax6(5a)* or the PD-less form of *Pax6*.

But maybe even different ratios of the different *Pax6* isoforms might be sufficient to specify the region-specific role of *Pax6*. For example, the PD-less *Pax6* form interacts with the PD of *Pax6* and thus enhances the transcriptional activation by *Pax6* in vitro (Mikkola et al., 2001). In this context my result concerning the expression levels of the PD-less *Pax6* is of interest. The PD-less *Pax6* form is higher expressed than the PD-containing form at E10-E12, at the onset on neurogenesis, compared to midneurogenesis at E14, while at E18 both forms are expressed at equally lower levels in the cerebral cortex. Thus it might be possible that the PD-less *Pax6* form is involved in the regulation of cell proliferation, since at E10-E12 predominantly cell divisions generating precursors occur. Recently it has been shown that the HD of *Pax6* interacts with the hypophosphorylated form of the tumor suppressor gene pRB (retinoblastoma protein) (Cvekl et al., 1999). The retinoblastoma protein forms a complex with E2F in the G1-phase of the cell cycle and upon phosphorylation of pRB, E2F is released and can activate the transcription of Cyclin E, which is required for re-entering the cell cycle. Thus it might be that the HD of the PD-less *Pax6* form interacts with hypophosphorylated pRB and hence inhibits the complex formation with E2F, which could then maybe activate transcription of Cyclin E earlier or more easily, thus the re-entry in the cell cycle would be promoted. This hypothesis is supported by the fact that the PD-less form, although containing HD and TAD and binding to P2 sites in vitro, fails to activate transcription (Mishra et al., 2002). On the other hand one could speculate that the HD depends on the PD in order to activate transcription (Mishra et al., 2002), but it might also be that the PD-less form binds to the DNA and thus blocks as a kind of regulatory molecule HD targets, maybe in a region and time specific manner. PD-less *Pax6* forms were not only identified in the mouse, but also in the quail neuroretina. Interestingly, the PD-less forms (32/33kDa) were only detected in the cytoplasm, while the PD-containing *Pax6* forms (43kDa, 46 kDa and 48 kDa) were detected in the nucleus. However, after transient transfection the PD-less *Pax6* forms were also detected in the nucleus (Carriere et al., 1993).

Further mechanisms involved in the regulation of the time and region-specific role of Pax6 could be posttranslational protein modifications as for example phosphorylation as it has been described for the TAD of zebrafish Pax6, which is phosphorylated at a specific serine residue by the mitogen-activated protein kinases (MAPKs), the extracellular-signal regulated kinase (ERK) and the p38 kinase but not by Jun N-terminal kinase (JNK) in vitro (Mikkola et al., 1999). And also in the quail neuroretina phosphorylation has been described (Carriere et al., 1993). Since phosphorylation is important for the subcellular localisation of proteins, modification of DNA binding and the interaction between TADs of transcription factors with the transcription machinery (Hunter and Karin, 1992), this might be another mechanism to regulate the effects of Pax6 in a region and time-specific manner.

In the quail neuroretina several Pax6 isoforms of different molecular weights (32/33kDa, 43kDa, 46kDa, 48kDa) have been detected, and interestingly the isoforms detected in the nucleus (46kDa and 48kDa) were O-glycosylated, while the unglycosylated forms were only present in the cytoplasm (32/33kDa and 43kDa) (Lefebvre et al., 2002). Thus there seems to a multitude of modification mechanisms that might all influence the region-specific action of Pax6 and might explain the region- and organ-specific different roles of Pax6.

9.7 The influence of the basal cell attachment on neurogenesis and cell proliferation

Not only intrinsic factors, but also extrinsic factors may influence the radial glia lineage and cell proliferation. Radial glia cells, which comprise the majority of proliferating precursor cells at midneurogenesis (Hartfuss et al., 2001) are characterized apico-basal polarity (Huttner and Brand, 1997; Kosodo et al., 2004; Wodarz and Huttner, 2003) and thus receive important extrinsic signals via their apical and basal cell pole that might influence the proliferative behavior or cell differentiation. The apical side of the cell is for example characterized by the presence of prominin-1 (Weigmann et al., 1997) and signaling may occur in the specific prominin domains at the apical cells side (Kosodo et al., 2004). At the basal cell pole of radial glia cells $\alpha 6$ integrin occurs at high concentrations (Wodarz and Huttner, 2003). Recent studies showed that radial glia cells maintain their radial process throughout cell division (reviewed in Fishell and Kriegstein, 2003; Miyata et al., 2001; Noctor et al., 2001). It has been hypothesized that the maintenance of the radial glia endfeet is important for the cells in order to receive signals from the basal side which might influence cell fate decisions (for review

see: Fishell and Kriegstein, 2003), especially since the basement membrane harbors a variety of factors such as fibroblast growth factors (Fgfs). Extracellular Fgfs bind tightly to heparan sulfate proteoglycan (HSPGs) of the extracellular matrix (ECM) (for review see: Dono, 2003). Fgfs are important for the regulation of cell proliferation during cortical development (for review see: Dono, 2003). HSPGs are components of the basement membrane and promote and stabilize the binding of Fgfs to their respective receptors (Schlessinger, 2004). This is of particular interest in regard of the asymmetric inheritance of the radial glia process during cell division, which might play a role for the further cell fate.

9.8 Neurogenesis in absence of basement membrane attachment

The basal influence on radial glia cells was analyzed by means of two different basement membrane mutants, the LN γ 1 mutant (Willem et al., 2002), which is characterized by the detachment of radial glia endfeet at midneurogenesis and the α 6 integrin $^{-/-}$, which lacks a proper basement membrane assembly (Georges-Labouesse et al., 1998). The LN γ 1 mutant displayed in regard of endfeet detachment from the basement membrane a more severe phenotype than the α 6 integrin $^{-/-}$. The neurogenesis seemed normal at E14 in both mutants, where the radial glia processes lack contact to the basement membrane or proper basement membrane assembly. Thus, basement membrane attachment of radial glia endfeet or proper basement membrane assembly at the radial glia endfeet seems not to be important for the rate of neurogenesis. However, neuronal migration seems to be altered in both mouse mutants, as visible in the formation of aberrant neuronal ectopias (Georges-Labouesse et al., 1998; Halfter et al., 2002).

9.9 Basement membrane attachment of radial glia processes and cell proliferation

Especially the presence of growth factors, as for example Fgfs, which act on cell proliferation, and which are captured by the components of the basement membrane (for review see: Dono, 2003; Ornitz, 2000) implies that cell proliferation might be altered when the direct contact of radial glia processes with the BM is lost. However, the quantification of dividing cells at the VS and at abventricular positions per area showed no significant alterations in both basement

membrane mutants LN γ 1 mutant and α 6 integrin $^{-/-}$. One explanation for these results could be that although the endfeet of radial glia cells do not attach at the BM, they nevertheless receive 'basal signals'. The basement membrane in the LN γ 1 mutant forms, but is not properly linked. Nidogen is a linker molecule connecting the laminin sheet with the type IV collagen sheet (for review see: Quondamatteo, 2002), thus lack of the nidogen binding site at the γ 1 chain of laminin leads to improper sheet-linking. Hence it might be even possible that components of the BM enter the parenchyma and supply the basal endfeet of radial glia cells with factors. On the other hand, also in the α 6 integrin $^{-/-}$ no phenotype in regard to cell proliferation has been detected, and in this mutant the basement membrane assembly is affected, thus the matrix that captures the factors that might influence radial glia cells from the basal cell pole, fails to form. Important to mention in this context is that the radial glia endfeet in the α 6 integrin $^{-/-}$ are associated with laminin deposits (Georges-Labouesse et al., 1998) that might be sufficient to deliver the required basal cues, but on the other hand HSGPs and not laminin were shown to play a role in binding Fgfs tightly. In addition, the formation of neuronal ectopias outside the BM and the pia mater in the subarachnoidal space occurred especially in regions where the BM was highly disorganized in the α 6 integrin $^{-/-}$, which might reflect an active degradation process of the BM (Georges-Labouesse et al., 1998). It is also important to mention that the endfeet of neuroepithelial and early radial glia cells are not all detached from the BM at earlier stages in the LN γ 1 mutant (Halfter et al., 2002). Thus the cells could receive at least early during development signals from the BM, even though one would assume that proliferating cells depend not only 'once in their life' on extrinsic signals such as growth factors, but rather during their entire period of proliferation.

Since the glial cells are linked at the apical surface via junctional complexes and their radial processes are spanning the entire width of the cortical wall in order to attach to the basement membrane one could assume that the cell achieves a certain stability that might be required to coordinate the interkinetic nuclear migration and the plane of cell division. The analysis of the interkinetic nuclear migration in the LN γ 1 mutant, showed no alterations. One reason for the lack of a phenotype in regard to the interkinetic nuclear migration could be that this cellular behavior is restricted to the ventricular zone and does not span the entire cortical wall. Obviously the cell contacts at the apical cell pole and in the VZ are sufficient to stabilize the cell and maybe the intracellular anchoring points of the cytoskeleton involved in that process are still sufficient to perform interkinetic nuclear migration properly. Thus, radial glial cells rather require the apical adherens junctions (Vorbrodts and Dobrogowska, 2003), than the basal attachment to coordinate the nuclear translocation. Cells might also receive signals from

the CSF at the apical cell pole, as for example Fgfs (for review see: Dono, 2003) that could influence cell proliferation in general and the interkinetic nuclear migration.

As mentioned above, proliferating cells can divide horizontally, obliquely or perpendicular with respect to the ventricular surface. Based on the findings obtained in *Drosophila* where the apico-basal cell polarity is associated with the plane of cell division and with cell fate (Campos-Ortega, 1993), the question addressed here was whether the loss of the basal cell polarity influences the plane of cell division. However, no changes in the plane of cell division were detected due to the lack of basal attachment and basal polarity in the LN γ 1 mutant, the α 6 integrin $^{-/-}$ and even in a third basement membrane mutant, the perlecan $^{-/-}$ mice. Studies in the ferret cortex showed that horizontal cell divisions are correlated with asymmetric cell divisions giving rise to a precursor cell and a neuron that inherits Notch asymmetrically (Chenn and McConnell, 1995). Thus, the model has been postulated that the plane of cell division is also correlated with cell fate in vertebrates, such that a horizontal cell division is asymmetric giving rise to one neuron and one precursor and perpendicular cell divisions give rise to two identical daughter cells (Chenn and McConnell, 1995). However, a problem with the model of Chenn and McConnell is that only a minority of cell divisions in the neuroepithelium at midneurogenesis occurs horizontally (10-15%), thus there would be too few neurogenic cell divisions. In addition, the mode of cell division should change in mutants characterized by decreased neurogenesis, as for example the Pax6^{Sey} $^{-/-}$ mice, but no changes were detectable in the mode of cell division in Pax6^{Sey} $^{-/-}$ mice (Stricker, unpublished observations). Recent studies showed now that also perpendicular cell divisions with respect to the ventricular surface can be asymmetric due to the inheritance of the apical membrane patch by one of the daughter cells (Kosodo et al., 2004). In addition it has been shown that perpendicular cell divisions give rise to one VZ precursor and one neurogenic SVZ precursor (Noctor et al., 2004).

Apart from the correlation between the plane of cell division and cell fate, it might have been possible that the loss of the basal attachment induces changes in the cytoskeleton that could also influence the orientation of cell division. However, it seems that changes in the cytoskeleton during cell division remain exclusively restricted to the area of cell division and do not involve the entire cytoskeleton, which comprises the width of the entire cortical wall, and since the cell attachment at the apical side was not altered, no changes were obtained.

The only phenotype detected in regard of cell proliferation was the occurrence of ectopic proliferating cell clusters inside the cortical plate of the LN γ 1 mutant that consist of neuronal precursor cells originating from the VZ and persisted during development until E18. The

formation of neuronal ectopias in the LN γ 1 mutant correlates with the defect in reelin signaling (Halfter et al., 2002), but no clear correlation was found between the formation of ectopic proliferating clusters in the cortical plate and altered reelin signaling. Thus it remains unclear how these clusters arise.

In summary, it may be said that the direct contact of radial glia cell endfeet to the basement membrane is not required for the regulation of cell proliferation and neurogenesis. Thus the cells might receive the crucial signals at the apical side.

10 References

- Aaku-Saraste, E., Hellwig, A. and Huttner, W. B.** (1996). Loss of occludin and functional tight junctions, but not ZO-1, during neural tube closure--remodeling of the neuroepithelium prior to neurogenesis. *Dev Biol* **180**, 664-79.
- Alfano, G., Vitiello, C., Caccioppoli, C., Caramico, T., Carola, A., Szego, M. J., McInnes, R. R., Auricchio, A. and Banfi, S.** (2005). Natural antisense transcripts associated with genes involved in eye development. *Hum Mol Genet* **14**, 913-23.
- Assimacopoulos, S., Grove, E. A. and Ragsdale, C. W.** (2003). Identification of a Pax6-dependent epidermal growth factor family signaling source at the lateral edge of the embryonic cerebral cortex. *J Neurosci* **23**, 6399-403.
- Azuma, N., Nishina, S., Yanagisawa, H., Okuyama, T. and Yamada, M.** (1996). PAX6 missense mutation in isolated foveal hypoplasia. *Nat Genet* **13**, 141-2.
- Azuma, N., Tadokoro, K., Asaka, A., Yamada, M., Yamaguchi, Y., Handa, H., Matsushima, S., Watanabe, T., Kohsaka, S., Kida, Y. et al.** (2005). The Pax6 isoform bearing an alternative spliced exon promotes the development of the neural retinal structure. *Hum Mol Genet* **14**, 735-45.
- Bäumer, N., Marquardt, T., Stoykova, A., Spieler, D., Treichel, D., Ashery-Padan, R. and Gruss, P.** (2003). Retinal pigmented epithelium determination requires the redundant activities of Pax2 and Pax6. *Development* **130**, 2903-15.
- Bertrand, N., Castro, D. S. and Guillemot, F.** (2002). Proneural genes and the specification of neural cell types. *Nat Rev Neurosci* **3**, 517-30.
- Bishop, K. M., Goudreau, G. and O'Leary, D. D.** (2000). Regulation of area identity in the mammalian neocortex by Emx2 and Pax6. *Science* **288**, 344-9.
- Bishop, K. M., Rubenstein, J. L. and O'Leary, D. D.** (2002). Distinct actions of Emx1, Emx2, and Pax6 in regulating the specification of areas in the developing neocortex. *J Neurosci* **22**, 7627-38.
- Botzcher, R. T. and Niehrs, C.** (2005). Fibroblast growth factor signaling during early vertebrate development. *Endocr Rev* **26**, 63-77.
- Bottenstein, J. E. and Sato, G. H.** (1979). Growth of a rat neuroblastoma cell line in serum-free supplemented medium. *Proc Natl Acad Sci U S A* **76**, 514-7.
- Bouvard, D., Brakebusch, C., Gustafsson, E., Aszodi, A., Bengtsson, T., Berna, A. and Fassler, R.** (2001). Functional consequences of integrin gene mutations in mice. *Circ Res* **89**, 211-23.
- Briscoe, J., Sussel, L., Serup, P., Hartigan-O'Connor, D., Jessell, T. M., Rubenstein, J. L. and Ericson, J.** (1999). Homeobox gene Nkx2.2 and specification of neuronal identity by graded Sonic hedgehog signalling. *Nature* **398**, 622-7.
- Brittis, P. A., Meiri, K., Dent, E. and Silver, J.** (1995). The earliest patterns of neuronal differentiation and migration in the mammalian central nervous system. *Exp Neurol* **134**, 1-12.
- Bruun, J. A., Thomassen, E. I., Kristiansen, K., Tylden, G., Holm, T., Mikkola, I., Bjorkoy, G. and Johansen, T.** (2005). The third helix of the homeodomain of paired class homeodomain proteins acts as a recognition helix both for DNA and protein interactions. *Nucleic Acids Res* **33**, 2661-75.
- Bulfone, A., Martinez, S., Marigo, V., Campanella, M., Basile, A., Quaderi, N., Gattuso, C., Rubenstein, J. L. and Ballabio, A.** (1999). Expression pattern of the Tbr2 (Eomesodermin) gene during mouse and chick brain development. *Mech Dev* **84**, 133-8.
- Cadigan, K. M. and Nusse, R.** (1997). Wnt signaling: a common theme in animal development. *Genes Dev* **11**, 3286-305.

- Campos-Ortega, J. A.** (1993). Mechanisms of early neurogenesis in *Drosophila melanogaster*. *J Neurobiol* **24**, 1305-27.
- Carriere, C., Plaza, S., Martin, P., Quatannens, B., Bailly, M., Stehelin, D. and Saule, S.** (1993). Characterization of quail Pax-6 (Pax-QNR) proteins expressed in the neuroretina. *Mol Cell Biol* **13**, 7257-66.
- Casarosa, S., Fode, C. and Guillemot, F.** (1999). Mash1 regulates neurogenesis in the ventral telencephalon. *Development* **126**, 525-34.
- Chapouton, P., Gartner, A. and Götz, M.** (1999). The role of Pax6 in restricting cell migration between developing cortex and basal ganglia. *Development* **126**, 5569-79.
- Chauhan, B. K., Yang, Y., Cveklova, K. and Cvekl, A.** (2004). Functional interactions between alternatively spliced forms of Pax6 in crystallin gene regulation and in haploinsufficiency. *Nucleic Acids Res* **32**, 1696-709.
- Chenn, A. and McConnell, S. K.** (1995). Cleavage orientation and the asymmetric inheritance of Notch1 immunoreactivity in mammalian neurogenesis. *Cell* **82**, 631-41.
- Choi, J. S., Park, H. J., Jo, Y. C., Chun, M. H., Chung, J. W., Kim, J. M., Min do, S. and Lee, M. Y.** (2004). Immunohistochemical localization of phospholipase D2 in embryonic rat brain. *Neurosci Lett* **357**, 147-51.
- Costell, M., Gustafsson, E., Aszodi, A., Morgelin, M., Bloch, W., Hunziker, E., Addicks, K., Timpl, R. and Fassler, R.** (1999). Perlecan maintains the integrity of cartilage and some basement membranes. *J Cell Biol* **147**, 1109-22.
- Cvekl, A., Kashanchi, F., Brady, J. N. and Piatigorsky, J.** (1999). Pax-6 interactions with TATA-box-binding protein and retinoblastoma protein. *Invest Ophthalmol Vis Sci* **40**, 1343-50.
- Czerny, T. and Busslinger, M.** (1995). DNA-binding and transactivation properties of Pax-6: three amino acids in the paired domain are responsible for the different sequence recognition of Pax-6 and BSAP (Pax-5). *Mol Cell Biol* **15**, 2858-71.
- Czerny, T., Halder, G., Kloter, U., Souabni, A., Gehring, W. J. and Busslinger, M.** (1999). twin of eyeless, a second Pax-6 gene of *Drosophila*, acts upstream of eyeless in the control of eye development. *Mol Cell* **3**, 297-307.
- Czerny, T., Schaffner, G. and Busslinger, M.** (1993). DNA sequence recognition by Pax proteins: bipartite structure of the paired domain and its binding site. *Genes Dev* **7**, 2048-61.
- de Bergeyck, V., Naerhuyzen, B., Goffinet, A. M. and Lambert de Rouvroit, C.** (1998). A panel of monoclonal antibodies against reelin, the extracellular matrix protein defective in reeler mutant mice. *J Neurosci Methods* **82**, 17-24.
- Dominguez, M., Ferres-Marco, D., Gutierrez-Avino, F. J., Speicher, S. A. and Beneyto, M.** (2004). Growth and specification of the eye are controlled independently by Eyegone and Eyeless in *Drosophila melanogaster*. *Nat Genet* **36**, 31-9.
- Dono, R.** (2003). Fibroblast growth factors as regulators of central nervous system development and function. *Am J Physiol Regul Integr Comp Physiol* **284**, R867-81.
- Engelkamp, D., Rashbass, P., Seawright, A. and van Heyningen, V.** (1999). Role of Pax6 in development of the cerebellar system. *Development* **126**, 3585-96.
- Englund, C., Fink, A., Lau, C., Pham, D., Daza, R. A., Bulfone, A., Kowalczyk, T. and Hevner, R. F.** (2005). Pax6, Tbr2, and Tbr1 are expressed sequentially by radial glia, intermediate progenitor cells, and postmitotic neurons in developing neocortex. *J Neurosci* **25**, 247-51.
- Epstein, J., Cai, J., Glaser, T., Jepeal, L. and Maas, R.** (1994a). Identification of a Pax paired domain recognition sequence and evidence for DNA-dependent conformational changes. *J Biol Chem* **269**, 8355-61.
- Epstein, J. A., Glaser, T., Cai, J., Jepeal, L., Walton, D. S. and Maas, R. L.** (1994b). Two independent and interactive DNA-binding subdomains of the Pax6 paired domain are regulated by alternative splicing. *Genes Dev* **8**, 2022-34.

Ericson, J., Rashbass, P., Schedl, A., Brenner-Morton, S., Kawakami, A., van Heyningen, V., Jessell, T. M. and Briscoe, J. (1997). Pax6 controls progenitor cell identity and neuronal fate in response to graded Shh signaling. *Cell* **90**, 169-80.

Estivill-Torres, G., Pearson, H., van Heyningen, V., Price, D. J. and Rashbass, P. (2002). Pax6 is required to regulate the cell cycle and the rate of progression from symmetrical to asymmetrical division in mammalian cortical progenitors. *Development* **129**, 455-66.

Favor, J., Peters, H., Hermann, T., Schmahl, W., Chatterjee, B., Neuhauser-Klaus, A. and Sandulache, R. (2001). Molecular characterization of Pax6(2Neu) through Pax6(10Neu): an extension of the Pax6 allelic series and the identification of two possible hypomorph alleles in the mouse *Mus musculus*. *Genetics* **159**, 1689-700.

Feng, L., Hatten, M. E. and Heintz, N. (1994). Brain lipid-binding protein (BLBP): a novel signaling system in the developing mammalian CNS. *Neuron* **12**, 895-908.

Fishell, G. and Kriegstein, A. R. (2003). Neurons from radial glia: the consequences of asymmetric inheritance. *Curr Opin Neurobiol* **13**, 34-41.

Ford-Perriss, M., Abud, H. and Murphy, M. (2001). Fibroblast growth factors in the developing central nervous system. *Clin Exp Pharmacol Physiol* **28**, 493-503.

Galipeau, J., Li, H., Paquin, A., Sicilia, F., Karpati, G. and Nalbantoglu, J. (1999). Vesicular stomatitis virus G pseudotyped retrovector mediates effective in vivo suicide gene delivery in experimental brain cancer. *Cancer Res* **59**, 2384-94.

Gambello, M. J., Darling, D. L., Yingling, J., Tanaka, T., Gleeson, J. G. and Wynshaw-Boris, A. (2003). Multiple dose-dependent effects of *Lis1* on cerebral cortical development. *J Neurosci* **23**, 1719-29.

Georges-Labouesse, E., Mark, M., Messaddeq, N. and Gansmuller, A. (1998). Essential role of alpha 6 integrins in cortical and retinal lamination. *Curr Biol* **8**, 983-6.

Gerlach, C., Golding, M., Larue, L., Alison, M. R. and Gerdes, J. (1997). Ki-67 immunoexpression is a robust marker of proliferative cells in the rat. *Lab Invest* **77**, 697-8.

Ghattas, I. R., Sanes, J. R. and Majors, J. E. (1991). The encephalomyocarditis virus internal ribosome entry site allows efficient coexpression of two genes from a recombinant provirus in cultured cells and in embryos. *Mol Cell Biol* **11**, 5848-59.

Götz, M., Stoykova, A. and Gruss, P. (1998). Pax6 controls radial glia differentiation in the cerebral cortex. *Neuron* **21**, 1031-44.

Götz M. and Huttner W.B. (2005). The cell biology of neurogenesis. *Nature Reviews Molecular Cell Biology* **6**, 777-788.

Graus-Porta, D., Blaess, S., Senften, M., Littlewood-Evans, A., Damsky, C., Huang, Z., Orban, P., Klein, R., Schittny, J. C. and Muller, U. (2001). Beta1-class integrins regulate the development of laminae and folia in the cerebral and cerebellar cortex. *Neuron* **31**, 367-79.

Grindley, J. C., Davidson, D. R. and Hill, R. E. (1995). The role of Pax-6 in eye and nasal development. *Development* **121**, 1433-42.

Grindley, J. C., Hargett, L. K., Hill, R. E., Ross, A. and Hogan, B. L. (1997). Disruption of PAX6 function in mice homozygous for the Pax6^{Sey-1Neu} mutation produces abnormalities in the early development and regionalisation of the diencephalon. *Mech Dev* **64**, 111-26.

Guillemot, F., Lo, L. C., Johnson, J. E., Auerbach, A., Anderson, D. J. and Joyner, A. L. (1993). Mammalian achaete-scute homolog 1 is required for the early development of olfactory and autonomic neurons. *Cell* **75**, 463-76.

Hack, M. A., Saghatelyan, A., de Chevigny, A., Pfeifer, A., Ashery-Padan, R., Lledo, P. M. and Götz, M. (2005). Neuronal fate determinants of adult olfactory bulb neurogenesis. *Nat Neurosci*.

Halfter, W., Dong, S., Yip, Y. P., Willem, M. and Mayer, U. (2002). A critical function of the pial basement membrane in cortical histogenesis. *J Neurosci* **22**, 6029-40.

- Hanes, S. D. and Brent, R.** (1989). DNA specificity of the bicoid activator protein is determined by homeodomain recognition helix residue 9. *Cell* **57**, 1275-83.
- Hartfuss, E., Galli, R., Heins, N. and Götz, M.** (2001). Characterization of CNS precursor subtypes and radial glia. *Dev Biol* **229**, 15-30.
- Haubensak, W., Attardo, A., Denk, W. and Huttner, W. B.** (2004). Neurons arise in the basal neuroepithelium of the early mammalian telencephalon: a major site of neurogenesis. *Proc Natl Acad Sci U S A* **101**, 3196-201.
- Haubst, N., Berger, J., Radjendirane, V., Graw, J., Favor, J., Saunders, G. F., Stoykova, A. and Götz, M.** (2004). Molecular dissection of Pax6 function: the specific roles of the paired domain and homeodomain in brain development. *Development* **131**, 6131-40.
- Haydar, T. F., Ang, E., Jr. and Rakic, P.** (2003). Mitotic spindle rotation and mode of cell division in the developing telencephalon. *Proc Natl Acad Sci U S A* **100**, 2890-5.
- Heins, N., Cremisi, F., Malatesta, P., Gangemi, R. M., Corte, G., Price, J., Goudreau, G., Gruss, P. and Götz, M.** (2001). Emx2 promotes symmetric cell divisions and a multipotential fate in precursors from the cerebral cortex. *Mol Cell Neurosci* **18**, 485-502.
- Heins, N., Malatesta, P., Cecconi, F., Nakafuku, M., Tucker, K. L., Hack, M. A., Chapouton, P., Barde, Y. A. and Götz, M.** (2002). Glial cells generate neurons: the role of the transcription factor Pax6. *Nat Neurosci* **5**, 308-15.
- Henzel, M. J., Wei, Y., Mancini, M. A., Van Hooser, A., Ranalli, T., Brinkley, B. R., Bazett-Jones, D. P. and Allis, C. D.** (1997). Mitosis-specific phosphorylation of histone H3 initiates primarily within pericentromeric heterochromatin during G2 and spreads in an ordered fashion coincident with mitotic chromosome condensation. *Chromosoma* **106**, 348-60.
- Hill, R. E., Favor, J., Hogan, B. L., Ton, C. C., Saunders, G. F., Hanson, I. M., Prosser, J., Jordan, T., Hastie, N. D. and van Heyningen, V.** (1991). Mouse small eye results from mutations in a paired-like homeobox-containing gene. *Nature* **354**, 522-5.
- Hirata, T., Nomura, T., Takagi, Y., Sato, Y., Tomioka, N., Fujisawa, H. and Osumi, N.** (2002). Mosaic development of the olfactory cortex with Pax6-dependent and -independent components. *Brain Res Dev Brain Res* **136**, 17-26.
- Hogan, B. L., Hirst, E. M., Horsburgh, G. and Hetherington, C. M.** (1988). Small eye (Sey): a mouse model for the genetic analysis of craniofacial abnormalities. *Development* **103 Suppl**, 115-9.
- Hogan, B. L., Horsburgh, G., Cohen, J., Hetherington, C. M., Fisher, G. and Lyon, M. F.** (1986). Small eyes (Sey): a homozygous lethal mutation on chromosome 2 which affects the differentiation of both lens and nasal placodes in the mouse. *J Embryol Exp Morphol* **97**, 95-110.
- Hunter, T. and Karin, M.** (1992). The regulation of transcription by phosphorylation. *Cell* **70**, 375-87.
- Huttner, W. B. and Brand, M.** (1997). Asymmetric division and polarity of neuroepithelial cells. *Curr Opin Neurobiol* **7**, 29-39.
- Jang, C. C., Chao, J. L., Jones, N., Yao, L. C., Bessarab, D. A., Kuo, Y. M., Jun, S., Desplan, C., Beckendorf, S. K. and Sun, Y. H.** (2003). Two Pax genes, eye gone and eyeless, act cooperatively in promoting Drosophila eye development. *Development* **130**, 2939-51.
- Jessell, T. M.** (2000). Neuronal specification in the spinal cord: inductive signals and transcriptional codes. *Nat Rev Genet* **1**, 20-9.
- Jimenez, D., Garcia, C., de Castro, F., Chedotal, A., Sotelo, C., de Carlos, J. A., Valverde, F. and Lopez-Mascaraque, L.** (2000). Evidence for intrinsic development of olfactory structures in Pax-6 mutant mice. *J Comp Neurol* **428**, 511-26.
- Jun, S. and Desplan, C.** (1996). Cooperative interactions between paired domain and homeodomain. *Development* **122**, 2639-50.

- Jun, S., Wallen, R. V., Goriely, A., Kalionis, B. and Desplan, C.** (1998). Lune/eye gone, a Pax-like protein, uses a partial paired domain and a homeodomain for DNA recognition. *Proc Natl Acad Sci U S A* **95**, 13720-5.
- Kim, A. S., Anderson, S. A., Rubenstein, J. L., Lowenstein, D. H. and Pleasure, S. J.** (2001). Pax-6 regulates expression of SFRP-2 and Wnt-7b in the developing CNS. *J Neurosci* **21**, RC132.
- Kosodo, Y., Roper, K., Haubensak, W., Marzesco, A. M., Corbeil, D. and Huttner, W. B.** (2004). Asymmetric distribution of the apical plasma membrane during neurogenic divisions of mammalian neuroepithelial cells. *Embo J* **23**, 2314-24.
- Kozmik, Z., Daube, M., Frei, E., Norman, B., Kos, L., Dishaw, L. J., Noll, M. and Piatigorsky, J.** (2003). Role of Pax genes in eye evolution: a cnidarian PaxB gene uniting Pax2 and Pax6 functions. *Dev Cell* **5**, 773-85.
- Kurtz, A., Zimmer, A., Schnutgen, F., Bruning, G., Spener, F. and Muller, T.** (1994). The expression pattern of a novel gene encoding brain-fatty acid binding protein correlates with neuronal and glial cell development. *Development* **120**, 2637-49.
- Laird, P. W., Zijderveld, A., Linders, K., Rudnicki, M. A., Jaenisch, R. and Berns, A.** (1991). Simplified mammalian DNA isolation procedure. *Nucleic Acids Res* **19**, 4293.
- Lee, W. P.** (1995). Purification and characterization of tubulin from parental and vincristine-resistant HOB1 lymphoma cells. *Arch Biochem Biophys* **319**, 498-503.
- Lefebvre, T., Planque, N., Leleu, D., Bailly, M., Caillet-Boudin, M. L., Saule, S. and Michalski, J. C.** (2002). O-glycosylation of the nuclear forms of Pax-6 products in quail neuroretina cells. *J Cell Biochem* **85**, 208-18.
- Lumsden, A. and Krumlauf, R.** (1996). Patterning the vertebrate neuraxis. *Science* **274**, 1109-15.
- Malatesta, P., Hack, M. A., Hartfuss, E., Kettenmann, H., Klinkert, W., Kirchhoff, F. and Götz, M.** (2003). Neuronal or glial progeny: regional differences in radial glia fate. *Neuron* **37**, 751-64.
- Malatesta, P., Hartfuss, E. and Götz, M.** (2000). Isolation of radial glial cells by fluorescent-activated cell sorting reveals a neuronal lineage. *Development* **127**, 5253-63.
- Marin, O. and Rubenstein, J. L.** (2003). Cell migration in the forebrain. *Annu Rev Neurosci* **26**, 441-83.
- Marquardt, T., Ashery-Padan, R., Andrejewski, N., Scardigli, R., Guillemot, F. and Gruss, P.** (2001). Pax6 is required for the multipotent state of retinal progenitor cells. *Cell* **105**, 43-55.
- Martinez-Hernandez, A. and Amenta, P. S.** (1983). The basement membrane in pathology. *Lab Invest* **48**, 656-77.
- Mastick, G. S. and Andrews, G. L.** (2001). Pax6 regulates the identity of embryonic diencephalic neurons. *Mol Cell Neurosci* **17**, 190-207.
- Mastick, G. S., Davis, N. M., Andrew, G. L. and Easter, S. S., Jr.** (1997). Pax-6 functions in boundary formation and axon guidance in the embryonic mouse forebrain. *Development* **124**, 1985-97.
- Mikkola, I., Bruun, J. A., Bjorkoy, G., Holm, T. and Johansen, T.** (1999). Phosphorylation of the transactivation domain of Pax6 by extracellular signal-regulated kinase and p38 mitogen-activated protein kinase. *J Biol Chem* **274**, 15115-26.
- Mikkola, I., Bruun, J. A., Holm, T. and Johansen, T.** (2001). Superactivation of Pax6-mediated transactivation from paired domain-binding sites by dna-independent recruitment of different homeodomain proteins. *J Biol Chem* **276**, 4109-18.
- Mishra, R., Gorlov, I. P., Chao, L. Y., Singh, S. and Saunders, G. F.** (2002). PAX6, paired domain influences sequence recognition by the homeodomain. *J Biol Chem* **277**, 49488-94.

- Misson, J. P., Edwards, M. A., Yamamoto, M. and Caviness, V. S., Jr.** (1988). Identification of radial glial cells within the developing murine central nervous system: studies based upon a new immunohistochemical marker. *Brain Res Dev Brain Res* **44**, 95-108.
- Miyata, T., Kawaguchi, A., Okano, H. and Ogawa, M.** (2001). Asymmetric inheritance of radial glial fibers by cortical neurons. *Neuron* **31**, 727-41.
- Miyata, T., Kawaguchi, A., Saito, K., Kawano, M., Muto, T. and Ogawa, M.** (2004). Asymmetric production of surface-dividing and non-surface-dividing cortical progenitor cells. *Development* **131**, 3133-45.
- Morgan, R.** (2004). Conservation of sequence and function in the Pax6 regulatory elements. *Trends Genet* **20**, 283-7.
- Mullen, R. J., Buck, C. R. and Smith, A. M.** (1992). NeuN, a neuronal specific nuclear protein in vertebrates. *Development* **116**, 201-11.
- Muzio, L., DiBenedetto, B., Stoykova, A., Boncinelli, E., Gruss, P. and Mallamaci, A.** (2002). Emx2 and Pax6 control regionalisation of the pre-neuronogenic cortical primordium. *Cereb Cortex* **12**, 129-39.
- Muzio, L. and Mallamaci, A.** (2003). Emx1, emx2 and pax6 in specification, regionalisation and arealization of the cerebral cortex. *Cereb Cortex* **13**, 641-7.
- Nadarajah, B., Brunstrom, J. E., Grutzendler, J., Wong, R. O. and Pearlman, A. L.** (2001). Two modes of radial migration in early development of the cerebral cortex. *Nat Neurosci* **4**, 143-50.
- Nakatomi, H., Kuriu, T., Okabe, S., Yamamoto, S., Hatano, O., Kawahara, N., Tamura, A., Kirino, T. and Nakafuku, M.** (2002). Regeneration of hippocampal pyramidal neurons after ischemic brain injury by recruitment of endogenous neural progenitors. *Cell* **110**, 429-41.
- Nelson, W. J. and Nusse, R.** (2004). Convergence of Wnt, beta-catenin, and cadherin pathways. *Science* **303**, 1483-7.
- Nieto, M., Monuki, E. S., Tang, H., Imitola, J., Haubst, N., Khoury, S. J., Cunningham, J., Götz, M. and Walsh, C. A.** (2004). Expression of Cux-1 and Cux-2 in the subventricular zone and upper layers II-IV of the cerebral cortex. *J Comp Neurol* **479**, 168-80.
- Noctor, S. C., Flint, A. C., Weissman, T. A., Dammerman, R. S. and Kriegstein, A. R.** (2001). Neurons derived from radial glial cells establish radial units in neocortex. *Nature* **409**, 714-20.
- Noctor, S. C., Martinez-Cerdeno, V., Ivic, L. and Kriegstein, A. R.** (2004). Cortical neurons arise in symmetric and asymmetric division zones and migrate through specific phases. *Nat Neurosci* **7**, 136-44.
- Nowakowski, R. S., Lewin, S. B. and Miller, M. W.** (1989). Bromodeoxyuridine immunohistochemical determination of the lengths of the cell cycle and the DNA-synthetic phase for an anatomically defined population. *J Neurocytol* **18**, 311-8.
- Nusse, R.** (2005). Wnt signaling in disease and in development. *Cell Res* **15**, 28-32.
- Ornitz, D. M.** (2000). FGFs, heparan sulfate and FGFRs: complex interactions essential for development. *Bioessays* **22**, 108-12.
- Ory, D. S., Neugeboren, B. A. and Mulligan, R. C.** (1996). A stable human-derived packaging cell line for production of high titer retrovirus/vesicular stomatitis virus G pseudotypes. *Proc Natl Acad Sci U S A* **93**, 11400-6.
- Osumi, N.** (2001). The role of Pax6 in brain patterning. *Tohoku J Exp Med* **193**, 163-74.
- Packard, D. S., Jr., Menzies, R. A. and Skalko, R. G.** (1973). Incorporation of thymidine and its analogue, bromodeoxyuridine, into embryos and maternal tissues of the mouse. *Differentiation* **1**, 397-404.
- Paulsson, M.** (1992). Basement membrane proteins: structure, assembly, and cellular interactions. *Crit Rev Biochem Mol Biol* **27**, 93-127.

- Pear, W. S., Nolan, G. P., Scott, M. L. and Baltimore, D.** (1993). Production of high-titer helper-free retroviruses by transient transfection. *Proc Natl Acad Sci U S A* **90**, 8392-6.
- Percival-Smith, A., Muller, M., Affolter, M. and Gehring, W. J.** (1990). The interaction with DNA of wild-type and mutant fushi tarazu homeodomains. *Embo J* **9**, 3967-74.
- Philips, G. T., Stair, C. N., Young Lee, H., Wroblewski, E., Berberoglu, M. A., Brown, N. L. and Mastick, G. S.** (2005). Precocious retinal neurons: Pax6 controls timing of differentiation and determination of cell type. *Dev Biol* **279**, 308-21.
- Quiring, R., Walldorf, U., Kloter, U. and Gehring, W. J.** (1994). Homology of the eyeless gene of Drosophila to the Small eye gene in mice and Aniridia in humans. *Science* **265**, 785-9.
- Quondamatteo, F.** (2002). Assembly, stability and integrity of basement membranes in vivo. *Histochem J* **34**, 369-81.
- Rubenstein, J. L., Shimamura, K., Martinez, S. and Puelles, L.** (1998). Regionalisation of the prosencephalic neural plate. *Annu Rev Neurosci* **21**, 445-77.
- Scardigli, R., Bäumer, N., Gruss, P., Guillemot, F. and Le Roux, I.** (2003). Direct and concentration-dependent regulation of the proneural gene Neurogenin2 by Pax6. *Development* **130**, 3269-81.
- Schier, A. F. and Gehring, W. J.** (1992). Direct homeodomain-DNA interaction in the autoregulation of the fushi tarazu gene. *Nature* **356**, 804-7.
- Schlessinger, J.** (2004). Common and distinct elements in cellular signaling via EGF and FGF receptors. *Science* **306**, 1506-7.
- Schmahl, W., Knoedlseder, M., Favor, J. and Davidson, D.** (1993). Defects of neuronal migration and the pathogenesis of cortical malformations are associated with Small eye (Sey) in the mouse, a point mutation at the Pax-6-locus. *Acta Neuropathol (Berl)* **86**, 126-35.
- Schneeberger, E. E. and Lynch, R. D.** (2004). The tight junction: a multifunctional complex. *Am J Physiol Cell Physiol* **286**, C1213-28.
- Schwarz, M., Cecconi, F., Bernier, G., Andrejewski, N., Kammandel, B., Wagner, M. and Gruss, P.** (2000). Spatial specification of mammalian eye territories by reciprocal transcriptional repression of Pax2 and Pax6. *Development* **127**, 4325-34.
- Shen, Q., Zhong, W., Jan, Y. N. and Temple, S.** (2002). Asymmetric Numb distribution is critical for asymmetric cell division of mouse cerebral cortical stem cells and neuroblasts. *Development* **129**, 4843-53.
- Sievers, J., Pehlemann, F. W., Gude, S. and Berry, M.** (1994). Meningeal cells organize the superficial glia limitans of the cerebellum and produce components of both the interstitial matrix and the basement membrane. *J Neurocytol* **23**, 135-49.
- Singh, S., Mishra, R., Arango, N. A., Deng, J. M., Behringer, R. R. and Saunders, G. F.** (2002). Iris hypoplasia in mice that lack the alternatively spliced Pax6(5a) isoform. *Proc Natl Acad Sci U S A* **99**, 6812-5.
- Singh, S., Stellrecht, C. M., Tang, H. K. and Saunders, G. F.** (2000). Modulation of PAX6 homeodomain function by the paired domain. *J Biol Chem* **275**, 17306-13.
- Smart, I. H.** (1976). A pilot study of cell production by the ganglionic eminences of the developing mouse brain. *J Anat* **121**, 71-84.
- Sommer, L., Ma, Q. and Anderson, D. J.** (1996). neurogenins, a novel family of atonal-related bHLH transcription factors, are putative mammalian neuronal determination genes that reveal progenitor cell heterogeneity in the developing CNS and PNS. *Mol Cell Neurosci* **8**, 221-41.
- Storck, T., Schulte, S., Hofmann, K. and Stoffel, W.** (1992). Structure, expression, and functional analysis of a Na(+)-dependent glutamate/aspartate transporter from rat brain. *Proc Natl Acad Sci U S A* **89**, 10955-9.
- Stoykova, A., Fritsch, R., Walther, C. and Gruss, P.** (1996). Forebrain patterning defects in Small eye mutant mice. *Development* **122**, 3453-65.

- Stoykova, A., Götz, M., Gruss, P. and Price, J.** (1997). Pax6-dependent regulation of adhesive patterning, R-cadherin expression and boundary formation in developing forebrain. *Development* **124**, 3765-77.
- Stoykova, A. and Gruss, P.** (1994). Roles of Pax-genes in developing and adult brain as suggested by expression patterns. *J Neurosci* **14**, 1395-412.
- Stoykova, A., Hatano, O., Gruss, P. and Götz, M.** (2003). Increase in reelin-positive cells in the marginal zone of Pax6 mutant mouse cortex. *Cereb Cortex* **13**, 560-71.
- Stoykova, A., Treichel, D., Hallonet, M. and Gruss, P.** (2000). Pax6 modulates the dorsoventral patterning of the mammalian telencephalon. *J Neurosci* **20**, 8042-50.
- Takahashi, T., Nowakowski, R. S. and Caviness, V. S., Jr.** (1995). Early ontogeny of the secondary proliferative population of the embryonic murine cerebral wall. *J Neurosci* **15**, 6058-68.
- Takahashi, T., Nowakowski, R. S. and Caviness, V. S., Jr.** (1996). The leaving or Q fraction of the murine cerebral proliferative epithelium: a general model of neocortical neuronogenesis. *J Neurosci* **16**, 6183-96.
- Tanabe, Y. and Jessell, T. M.** (1996). Diversity and pattern in the developing spinal cord. *Science* **274**, 1115-23.
- Tarabykin, V., Stoykova, A., Usman, N. and Gruss, P.** (2001). Cortical upper layer neurons derive from the subventricular zone as indicated by Svet1 gene expression. *Development* **128**, 1983-93.
- Toresson, H., Potter, S. S. and Campbell, K.** (2000). Genetic control of dorsal-ventral identity in the telencephalon: opposing roles for Pax6 and Gsh2. *Development* **127**, 4361-71.
- Treisman, J., Gonczy, P., Vashishtha, M., Harris, E. and Desplan, C.** (1989). A single amino acid can determine the DNA binding specificity of homeodomain proteins. *Cell* **59**, 553-62.
- Tunggal, P., Smyth, N., Paulsson, M. and Ott, M. C.** (2000). Laminins: structure and genetic regulation. *Microsc Res Tech* **51**, 214-27.
- Vitalis, T., Cases, O., Engelkamp, D., Verney, C. and Price, D. J.** (2000). Defect of tyrosine hydroxylase-immunoreactive neurons in the brains of mice lacking the transcription factor Pax6. *J Neurosci* **20**, 6501-16.
- Vorbrodt, A. W. and Dobrogowska, D. H.** (2003). Molecular anatomy of intercellular junctions in brain endothelial and epithelial barriers: electron microscopist's view. *Brain Res Brain Res Rev* **42**, 221-42.
- Walther, C., Guenet, J. L., Simon, D., Deutsch, U., Jostes, B., Goulding, M. D., Plachov, D., Balling, R. and Gruss, P.** (1991). Pax: a murine multigene family of paired box-containing genes. *Genomics* **11**, 424-34.
- Warren, N. and Price, D. J.** (1997). Roles of Pax-6 in murine diencephalic development. *Development* **124**, 1573-82.
- Weigmann, A., Corbeil, D., Hellwig, A. and Huttner, W. B.** (1997). Prominin, a novel microvilli-specific polytopic membrane protein of the apical surface of epithelial cells, is targeted to plasmalemmal protrusions of non-epithelial cells. *Proc Natl Acad Sci U S A* **94**, 12425-30.
- Willem, M., Miosge, N., Halfter, W., Smyth, N., Jannetti, I., Burkhart, A., Timpl, R., Mayer, U.** (2002). The nidogen binding site of laminin g-1 is critically important for kidney and lung development. *Development* **129**, 2711-2722.
- Williams, B. P. and Price, J.** (1995). Evidence for multiple precursor cell types in the embryonic rat cerebral cortex. *Neuron* **14**, 1181-8.
- Williams, B. P., Read, J. and Price, J.** (1991). The generation of neurons and oligodendrocytes from a common precursor cell. *Neuron* **7**, 685-93.
- Wilson, D., Sheng, G., Lecuit, T., Dostatni, N. and Desplan, C.** (1993). Cooperative dimerization of paired class homeo domains on DNA. *Genes Dev* **7**, 2120-34.

- Wodarz, A. and Huttner, W. B.** (2003). Asymmetric cell division during neurogenesis in *Drosophila* and vertebrates. *Mech Dev* **120**, 1297-309.
- Xu, H. E., Rould, M. A., Xu, W., Epstein, J. A., Maas, R. L. and Pabo, C. O.** (1999). Crystal structure of the human Pax6 paired domain-DNA complex reveals specific roles for the linker region and carboxy-terminal subdomain in DNA binding. *Genes Dev* **13**, 1263-75.
- Yun, K., Potter, S. and Rubenstein, J. L.** (2001). Gsh2 and Pax6 play complementary roles in dorsoventral patterning of the mammalian telencephalon. *Development* **128**, 193-205.
- Yurchenco, P. D. and O'Rear, J. J.** (1994). Basement membrane assembly. *Methods Enzymol* **245**, 489-518.
- Zhang, Y. and Emmons, S. W.** (1995). Specification of sense-organ identity by a *Caenorhabditis elegans* Pax-6 homologue. *Nature* **377**, 55-9.
- Zhou, Q., Wang, S. and Anderson, D. J.** (2000). Identification of a novel family of oligodendrocyte lineage-specific basic helix-loop-helix transcription factors. *Neuron* **25**, 331-43.
- Zimmer, C., Tiveron, M. C., Bodmer, R. and Cremer, H.** (2004). Dynamics of Cux2 expression suggests that an early pool of SVZ precursors is fated to become upper cortical layer neurons. *Cereb Cortex* **14**, 1408-20.

11 Thanks and acknowledgements

First, I would like to thank Magdalena Götz for giving me the chance to do this work in her lab. She was an excellent supervisor, always ready for discussions about my work and inspiring for getting new ideas and new ways of thinking. Thank you for supporting me at any time, for the good co-operation, for our publications and also for providing a great scientific environment. Further thank goes also to Barbara Conrad, Paolo Malatesta and Ludger Hengst, the members of my thesis committee. I'm also grateful to Andrea Wizenmann who introduced me patiently in the cloning technique and for answering to any kind of questions. Special thanks goes to Julia von Frowein, a real friend, always ready to help in all possible situations of life and always ready for funny actions outside lab life. I would also like to thank the former lab members, Paolo Malatesta for all the helpful discussions not only about science, but also about the topic how to behave on skis, going downhill; Prisca Chapouton, Nico Heins, Eva Hartfuss, Michael Hack and of course Julia for helping me with questions of the labwork and providing a nice atmosphere, when I started my thesis at the Max-Planck-Institute. Further thank goes to all the new members of the lab, whose number increased actually quite a bit after the move from the MPI to the GSF, for being a very pleasant group. For technical assistance I would like to thank Mucella Öcalan, Marcus Körbs, Andrea Steiner-Mezzadri, Annette Bust, Angelika Waiser and the best Hiwi ever Romy Müller. Thanks also to the former people from the Max-Planck-Institute Jim Chalcraft, Dietmute Bühringer and Karin Brückner from the Histogroup. For the help with the bothering bureaucratic and administrative matters I say thank you to Helga Zepter and Barabara DelGrande. Thanks for reading and correcting the manuscript goes to Magdalena Götz, Prisca Chapouton, Andrea Wizenmann and Julia von Frowein.

Finally, I would like to thank my parents for always supporting me in every regard.

12 Curriculum vitae

Personal data:

20.09.1972 Born in Bernkastel-Kues, Germany.

School:

08/79-07/83 Primary School in Osann-Monzel, Germany.

08/83-06/92 High School, Peter-Wust-Gymnasium in Wittlich, Germany.

06/92 Grade: Abitur

Training and Employment:

09/92-06/94 Training as Biological-technical Assistant (BTA) at Rheinische Akademie e.V. in Cologne, Germany.

09/94 Grade: "Staatlich geprüfte Biologisch-technische Assistentin"

09/94-08/96 Employment as BTA in the Klinikum Großhadern in Munich, Germany.

Study:

11/96-07/01 Study of Biology at Technical University, Munich, Germany.

11/00-07/01 Diploma thesis at the Max-Planck-Institute of Neurobiology, Martinsried (Head: Magdalena Götz). Title of diploma thesis: "Molecular mechanisms of cell cycle regulation in precursor cells in the cerebral cortex: The role of the transcription factor Pax6".

10.07.2001 Diploma of biology (Master of Science), Technical University, Munich, Germany. Award for the best diploma thesis of the faculty of biosciences at the Technical University, Munich.

08/01-10/05 Ph.D. thesis at Max-Planck-Institute of Neurobiology (Group: Neuronal Specification, Head: Magdalena Götz) in Martinsried, Germany and at the GSF, Institute for Stem Cell Research (Head: Magdalena Götz) in Neuherberg, Germany. Title of PhD-thesis: "Cellular and molecular mechanisms regulating cell proliferation during the forebrain development of the mouse".

Publications:

Haubst, N. (2001) Molecular mechanisms of cell cycle regulation in precursor cells of the cerebral cortex: The role of the transcription factor Pax6. Diploma thesis.

Haubst N., Berger J., Radjendirane V., Graw J., Favor J., Saunders G.F., Stoykova A. and M. Götz (2004) Molecular dissection of Pax6 function: the specific roles of the paired and homeodomain in brain development. *Development*. 131: 6131-6140.

Haubst; N., Favor; J. and Götz; M. (2005) The role of Pax6 in the nervous system during development and in adulthood – master control regulator or modular function? *Transcription factors in the Nervous system*. Ed. Gerald Thiel, Wiley-Ch. ISBN 3-527-31285-4. In press.

Nieto M., Monuki E.S., Tang H., Imitola J., Haubst N., Khoury S.J., Cunningham J., Götz M. and Walsh C.A. (2004) Expression of Cux-1 and Cux-2 in the Subventricular Zone and Upper Layers II-IV of the Cerebral Cortex. *The Journal of Comparative Neurology*. 479:168-180.

Graw J., Löster J., Puk O., Münster D., Haubst N., Soewarto D., Fuchs H., Meyer B., Nürnberg P., Pretsch W., Selby P., Favor J., Wolf E. and Hrabé de Angelis M. (2005) Three novel *Pax6* alleles in the mouse leading to the same small-eye phenotype due to different consequences at target promoters. *Investigative Ophthalmology and Visual Science (IVOS-04-1407)*. In press.